**Optimization of pile reinforced slopes using finite element analyses**

by

**I-Hsuan Ho**

A dissertation submitted to the graduate faculty

in partial fulfillment of the requirements for the degree of

DOCTOR OF PHILOSOPHY

Major: Civil Engineering (Geotechnical Engineering)

Program of Study Committee:
Vernon Schaefer
David White
Christopher Williams
Jeramy Ashlock
Thomas Rudolphi

Iowa State University

Ames, Iowa

2009

# TABLE OF CONTENTS

# LIST OF FIGURES

# LIST OF TABLES

# ABSTRACT

Piles have proven to be an effective means of stabilizing active landslides as well as in marginally stable slopes. Many practical empirical design and analysis methods of slope stability and piled-slope stability have been proposed. However, the solutions of analysis and design methods proposed vary due to different analysis methods used and the design methods are poorly understood because the pile-stabilized mechanism is complex. This thesis presents the results of two-dimensional finite element analyses with strength reduction method using the ABAQUS package to validate slope stability analyses of four cases, which are (1) homogeneous slope without foundation, (2) homogeneous slope with foundation, (3) non-homogeneous slope with foundation and (4) non-homogeneous slope with a thin weak layer. The results of unreinforced analyses are validated for each case based on limit equilibrium or finite element analyses in terms of factor of safety. With the results validated, a pile is incorporated in the model and analyzed using coupled analysis, which considers the slope stability and pile response simultaneously. Numerical analyses results based on pile position in the slope, pile head condition, and pile length are used to determine the optimal pile position, suitable pile head condition and appropriate pile length to increase the stability of pile-stabilized slopes. A three-dimensional finite element model of the slope stability is also conducted and the factor of safety found to be higher compared to the results of two-dimensional finite element analysis. The spacing effect of pile is examined in a three-dimensional piled slope model and the factor of safety is found to approach the case without pile when the ratio of spacing to pile diameter is equal or greater than 8.0. An optimal pile spacing of S/D of 4.0 is found. Based on study of the influencing factors in piled slope stability, an optimal design is proposed.

# CHAPTER 1: INTRODUCTION

Piles have proven to be an effective means of stabilizing active landslides as well as in marginally stable slopes. Many successful applications of this technique have been reported by some authors such as De Beer and Wallays (1970), Ito and Matsui (1975), Fukuoka (1977), Chen and Poulos (1995), and Liang and Zeng (2002). In addition, much numerical work has also been done by Cai and Ugai (2000) and Jeong *et al.* (2003). However, the design methods are poorly understood because the pile-stabilized mechanism is complex. Presently, no universal method has been proposed for an analysis of the passive drilled shafts or piles in stabilizing unstable slopes. Consequently, the design in stabilizing piles is often too conservative.

Many empirical and analytical methods of stabilization piles have been proposed by many authors. Basically, these methods can be summarized as three types, (1) Pressure-Based methods, (2) Displacement-based methods, (3) Continuum methods. In early years of design and analytical reinforce slopes, three main concepts have to be involved (Viggiani 1981; Poulos 1995): (1) Evaluate the shear resistance needed to increase the factor of safety, (2) Estimating the maximum shear strength that each pile can provide to stop the failure of

potential unstable, (3) Selection of the type and number of piles, and suitable location of the pile. This concept is based on uncoupled analysis which considers pile response and slope stability separately. The stabilizing pile is regarded as to provide additional resistance to the slope stability. As a result, the design practice for pile-stabilized slopes using limit equilibrium method does not take the soil-pile interaction into consideration (Ito *et al.*, 1979; Poulos, 1995; Lee *et al.* 1991.; Hassiotis *et al.* 1997)

In the numerical analysis of continuum methods, such as finite difference method, finite element method and boundary element method, the pile response and the slope stability are able to be considered simultaneously which is called the coupled analysis. Consequently, the depth of potential slip surface may be changed due to the pile response in the analysis, whereas the fixed failure surface has to be determined in the uncoupled analysis which does not consider the pile response and the slope stability simultaneously. In other words, soil-structure interaction mechanism is taken into consideration in finite element models or other continuum methods.

As previously stated, many numerical modeling and design methods have been established by different authors. The major influencing factors that affect the results of numerical

analysis and the efficiency of piled-slope system are summarized to include (1) selection of constitutive models of soils, (2) size and spacing of piles, (3) location in the slope, (4) conditions of the pile head and bending stiffness of piles, (5) length of the pile into a stable layer.

The optimal pile location in the slope has been proposed by many other researchers. However, the results vary from different analysis methods used by other researchers. Ito *et al*. (1981) thought the best pile location is the middle to upper part of the slope. Hassiotis (1997) concludes that the piles must be placed in the upper part of a slope to reach the maximum factor of safety. Meanwhile, the location also depends upon the steepness of the slopes. The steeper the slopes, the closer to the top of slopes the pile should be placed. Lee *et al*. (1995) summarized that the piles have to be placed either close to the toe or the top of slopes. Lee *et al*. (1995) found that when piles are placed in the middle of slopes, there is little effect on increasing the factor of safety. Cai and Ugai (2000) also reported that the piles have to be placed in the middle of slopes. However, when the same authors applied the modified version of Bishop's method by using Ito-Matsui's equation, they found that the best results can be secured by placing the pile closer to the top. Ausilio *et al*. (2001) used the limit analysis method to find the optimal location of the piles is near the toe. This study presented the piles

close to the toe takes least value of stabilizing force to a desired factor of safety. Meanwhile, this study also shows that piles in the middle to toe are also effective, but higher of the factor of safety required, the smaller of this region is. Jeong *et al*. (2003) used the uncoupled analysis finite element method to predict the maximum factor of safety when the piles are installed a little closer to the top of the slopes, however, in the coupled analysis (2005), the piles are recommended to placed in the middle of the slope, irrespective of pile head conditions. Thus previous studies have not reached a consensus on where piles should be located for maximum beneficial effects to the slope and no universal and consistent solution has been provided.

In the pressured based analysis method, the lateral soil pressure on piles in a row is evaluated based on the equation developed by Ito and Matsui (1975). However, there are some unrealistic assumptions in the model such as the pile is assumed rigid with infinite length and only the soils surrounding piles is in the state of plastic equilibrium which satisfy the Mohr-Coulomb failure criterion. Very few studies recommend an appropriate length of pile. However, from case histories, an empirically defined ratio of the pile length above the slip surface to the entire length of pile around 0.45 to 0.55 can be found.

To provide better definition to the effects of pile position in the slope, pile length, and pile head restrictions, the present study, was undertaken to analyze pile reinforced slopes using the two dimensional elastic-plastic shear strength reduction finite element method with ABAQUS software. The analysis is coupled which considers the pile response and slope stability simultaneously. The pile in each model is assumed elastic, the soil is assumed elastic-plastic which satisfy Mohr-Coulomb yield criterion. Four types of slopes are discussed in this study, homogeneous slope without foundation, homogeneous slope with foundation, non-homogenous slope with foundation and non-homogeneous slope with a thin weak layer, respectively. The factors of safety of the slopes have been validated with other numerical studies and with SLOPE/W, software developed for the slope stability analysis with limit equilibrium theory. Different failure mechanisms due to shear strength ratio between soils in non-homogeneous slopes are also discussed and compared. Numerical evaluations are presented and the major influencing factors which affect the performance of the stabilization pile are discussed. A simplified design method of the stabilization pile is proposed according to the analysis results.

# CHAPTER 2: LITERATURE REVIEW

## 2.1 Introduction

In this chapter, slope stabilization methods are briefly introduced and reviewed. The analysis methods of slope stability are also discussed thereafter. The slope stability reinforced with pile is then mentioned based on piled slope mechanism, analysis methods and influencing factors. The constitutive models of soil often used are also presented herein. The finite element method adopted and software ABAQUS used are both included in the following section.

## 2.2 Slope Stabilization Methods

The logical prevention of all types of landslides may be accomplished by one or more of the following methods: (a) reduction of the activating forces, (b) increasing the resisting forces, and (c) avoidance or elimination of the slide. Reduction of the activating forces typically takes the form of flattening the slope by excavating material from the top of the slope or reduction in the water level in the slope. Resisting forces can be increased by using the following methods: (1) Increasing shear strength by drainage, (2) Removal of weak zones or potential failure zones, (3) Building retaining structures or supports or earth buttresses, (4) Chemical treatment to increase the stability of soil or increase the shear strength of the

ground, and (4) Providing *in situ* reinforcement of the ground. An often used method of *in situ* reinforcement has been the use of piles to stabilize slopes. The use of piles to stabilize a slope is a laterally loaded pile problem in addition to a slope stability problem.

## 2.3 Analysis of Laterally Loaded Piles

In practical use, laterally loaded piles can be termed active and passive. In its simplest terms, an active case is one in which the pile is pushed laterally into the soil and a passive case is one in which the soil is pushed into or around the pile. Most applications of piles are of the active case type and include piles used for supporting a superstructure which applies lateral load on its top and transmits the lateral load to the soil. A passive pile on the other hand has loading applied along the length pile due to the soil moving into the pile, soil movements, and the resulting earth pressures. The use of piles to stabilize slopes is a passive loading case (Reese and Van Impe, 2001).

## 2.4 Slope Stability Analysis Methods

### 2.4.1 Limit Equilibrium Method

Limit equilibrium methods have been the primary method used in estimating the stability of slope for decades. The procedures are based on finding a factor of safety for the slope. The

factor of safety represents the factor by which the shear strength must be reduced so that the reduced strength is just in equilibrium with the shear stress. In other words, when the factor of safety is 1.0, the slope is in a state of limiting equilibrium. The definition of limit equilibrium can be expressed in the form of equation 2.1.

$$\tau = \frac{S}{FS} \tag{2.1}$$

Where s: shear strength of the soil, τ: shear stress in the soil mass.

FS: Factor of Safety

Slopes are usually classified as infinite slopes or finite slopes; an infinite slope mainly indicates a slope with translational failure along a single plane. The ratio of depth of the failure surface to the length of the failure zone is relatively small (<10%). The soil type in this failure is usually granular.

Finite slope failures include plane, circular and noncircular failure surfaces that are so-called rotational failures. These failures occur primarily in cohesive soils. The method of slices is a common method to solve slope stability problem using limit equilibrium methods. This methodology divides a slide mass into several slices and moment and force equilibrium are

summed for the entire sliding mass (Abramson *et. al*, 1995). Numerous methods have been developed and are summarized in the following.

(1) Ordinary Method of Slices: This is one of the simplest methods, which neglects all interslice forces and fails to satisfy the equilibrium for both entire soil mass and individual slices (Abramson *et al.* 2002). This method only satisfies the moment equilibrium. The method is very convenient for hand calculations but less accurate than other procedures of slices (Duncan and Wright 2005).

(2) Bishop's Simplified Method: The interslice shear forces are assumed to be zero by Bishop (1955), leaving the solution overdetermined as horizontal force equilibrium will not be satisfied for one slice. This method satisfies vertical force equilibrium for each slice and overall moment about the center of the circular trial surface.

(3) Janbu's Simplified Method: Similar to Bishop (1955), Janbu (1973) also assumes zero interslice shear forces. This method leads the solution to satisfy vertical force equilibrium and overall horizontal force equilibrium for the entire slice mass. However, the method will not satisfy moment equilibrium conditions. Janbu (1973) proposed a correction factor $f_0$ to account for this incompleteness.

(4) Spencer's Method: Spencer (1967) assumes that the resultant of side forces on each side is at the mid-height of each slice. However, no assumption is made in the inclination of resultants. Therefore, inclination becomes one unknown which is a part of the solution. This method is considered to be more accurate than Bishop's method.

(5) Morgenstern-Price Method: Morgenstern and Price (1965) present a method similar to Spencer's method. However, no assumptions are made on inclination or applied point of resultants and these are considered to be unknowns. This method requires a computer for solving the basic equations.

The Morgenstern-Price method is considered to be the most rigorous limit equilibrium solution; however, the application of the method is quite cumbersome due to its complexity. The simplicity of Bishop's method and the ease of computation of the Bishop, Janbu and Spencer methods make them the most practical limit equilibrium solutions (Duncan and Wright 2005).

### 2.4.2 Finite Element Analysis

The finite element method was first introduced to geotechnical engineering by Clough and Woodward (1967). The finite element method provides great potential to deal with

geotechnical problems due to its ability to model nonlinear stress- strain behavior of materials. Soils are very complex, so linearly elastic behavior is typically not enough to capture the behavior of geotechnical problems. Finite element method has advantages and limitations. The advantage of finite element method is that it can easily capture the characteristics of stress – strain relationships of a soil mass, especially to model complex conditions such as nonlinear stress- strain behavior and non-homogeneous conditions. The limitations are the cost and efficiency of computers, particularly in three- dimensional analyses. A complex computation work has to be completed and it takes some time to compute. For trial and error solutions is time consuming in solving the three-dimensional problems.

The finite element method is capable of modeling the complex and realistic simulation by defining the appropriate initial conditions, stress-strain constitutive relationship, boundary conditions and the loading sequence. Initial conditions such as stresses can be measured or estimated by soil engineering knowledge. Stress-stain relationship determination of materials is most important in finite element analyses. The selection affects the complexity and accuracy of the results. The two characteristics of a material are its elasticity and plasticity. Within elastic models, linear elastic, multilinear elastic and hyperbolic nonlinear elastic

models are available while in more complex models, plastic behavior can be simulated by elastoplastic and elastoviscoplastic constitutive equations.

The selection of a constitutive model for soils in an analysis is associated with the accuracy of the solutions. Soils in their natural state are usually non-homogeneous and anisotropic. Therefore, the behavior of the soil is unlikely to be predicted perfectly. Some simple models such as linear elastic model, multilinear elastic model, hyperbolic elastic model or some elastoplastic models are frequently used to simplify the soil stress-strain relationships and sometimes give good agreement. In the use of elastoplastic models, the characteristics of the soil constitutive model, such as the elasticity, yield function, potential function, and hardening rule are the key factors in determination of a successful model and have to be calibrated by laboratory tests or *in situ* tests.

The linear elastic model is the simplest model, requiring only two parameters (Young's modulus E, and Poisson's ratio, υ). However, this is not a good model to be used in soil material except at low stress and small strain levels. Therefore, elastic–plastic models are usually employed in the soil models. Mohr-Coulomb is the model most frequently used in

soil mechanics. All the most often used constitutive models are discussed in the following section.

### 2.4.3 Strength Reduction Finite Element Method

To obtain a factor of safety for a slope using the finite element method comparable to that found in limit equilibrium methods, the strength reduction method can be used (Zienkiewicz, *et al*., 1975; Ugai, 1989; Matui and San, 1992; Griffiths and Lane, 1999, Chang and Huang, 2004). The strength reduction factor (SRF) is the factor which is divided to bring the slope to the point of failure. In limit equilibrium the factor of safety is defined as

$$FS = \frac{\tau_r}{\tau_d} \tag{2.2}$$

$\tau_r$ : resistant shear stress
$\tau_d$: driving shear stress

In the strength reduction method, the factored shear strength parameters $c_f, \emptyset_f$ are defined as

$$c_f' = c'/SRF \tag{2.3}$$

$$\emptyset_f' = arctan\left(\frac{tan\emptyset'}{SRF}\right) \tag{2.4}$$

Where SRF: strength reduction factor

In applying the Strength Reduction Method in finite element analyses, successive applications of increasing the Strength Reduction Factor are applied to the problem until the solution no longer converges. The lack of convergence is taken as failure of the slope. The value of the largest *SRF* is regarded as equivalent to the *Factor of Safety* in limit equilibrium analysis. In recent years, the strength reduction method has found increasing application of the finite element method (and finite difference methods) to slope stability analyses (Matsui and San, 1992; Griffiths and Lane, 1999, Chang and Huang, 2004). Application of the strength reduction method (SRM) applied to slopes stabilized with piles has been reported by Cai and Ugai (2000); Won *et al*. (2005); and Cheng and Wei, (2009).

### 2.4.4 Definition of Failure

In finite element models, the definition of failure is important, especially in slope stability analysis. Several possible definitions of failure have been proposed including the limiting of the shear stresses on the potential slip surface (Duncan and Dunlop, 1969), nonconvergence solution (Zienkiewicz and Taylor, 1989), or some test of bulging of the slope profile (Snitbhan and Chen, 1976).

### 2.4.5 Advantages of Finite Element Analysis in Slope Stability Analysis

Several well-known advantages of finite element analysis in slope stability are summarized in the following. The main advantages compared to limit equilibrium methods are (Griffiths and Lane, 1999):

(1) No assumptions have to be made regarding the shape or location of failure surfaces

(2) Since there is no concept of slices in the finite element approach there is no need for assumptions about slice side forces. The finite element method satisfies global equilibrium until “failure” is reached.

(3) If soil compressibility data is available, the finite element solution will give information about deformations at the working stress level.

(4) The finite element method is able to monitor progressive failure up to and including overall shear failure.

## 2.5 Analysis Methods of Pile Stabilized Slopes

A number of methods have been proposed to analyze stabilizing piles. The three main categories of analysis have been classified as: (1) pressure based; (2) displacement based; (3) continuum methods (FEM, FD, BEM) (Jeong *et al.* 2003). The pressure based method is based on the estimation of limit lateral soil pressure applied on piles which is discussed in the next section. The displacement based methods involved an uncoupled analysis wherein the pile response which includes shear force at sliding depth, bending moment distribution, pile deflection and soil resistance induced by lateral soil movement will also be discussed in more detail in the next section. Continuum methods which involve coupled analyses will also be presented in the following section.

The general design procedure for stabilizing piles involves the following three main steps (Viggiani 1981; Poulos 1995). (1) Evaluating the total shear force needed to increase the factor of safety of the slope to a desired value; (2) estimating the maximum shear force that each pile can provide to resist the movement of the sliding layer of the slope, (3) selecting the type and number of piles and the most suitable location in the slope (Poulos, 1995).

The factors influencing the performance of a stabilizing pile are (1) pile head restraint, (2) pile stiffness, (3) dimension of pile (3) position and spacing, (4) the length of pile in stable layer, (5) soil properties and movements.(Ang, 2005, Lee *et al*. 2006, Ausilio, *et al.* 2001, Won, *et al.* 2005)

## 2.6 Methodology of Pile-Stabilized Slope System

### 2.6.1 Application of Laterally Loaded Pile Behavior in Slope Stabilization

The stabilizing effect of piles in slopes is due to the passive loading or resistance. The pile acts against the lateral soil moment, which induces bending stresses in the pile. A number of methods have been proposed to assess the pile response to lateral soil movements. Chen and Poulos (1995) propose a plane-strain finite element method for analyzing piles subjected to undergoing soil lateral movement. The analysis assumes a soil movement profile and cycles through equations to obtain the pressure due to the soil-pile interaction. Some two-dimensional (2-D) finite element analyses have been proposed to solve the pile response to the lateral soil movements. (Bransby and Springman 1999, Stewart *et al.*1993, Goh *et al.* 1997). The piled-slope system is shown as Figure 2.1. The top view of the pile arrangement is shown in Figure 2.2. $Z_s/L$ is used to represent the length of pile and the depth of slip

surface. The S/D ratio represents the distance between the center to center and the diameter of pile. The distance of the pile from the toe to the distance between the toe and the crest is given in terms of the ratio $X_p/X$.

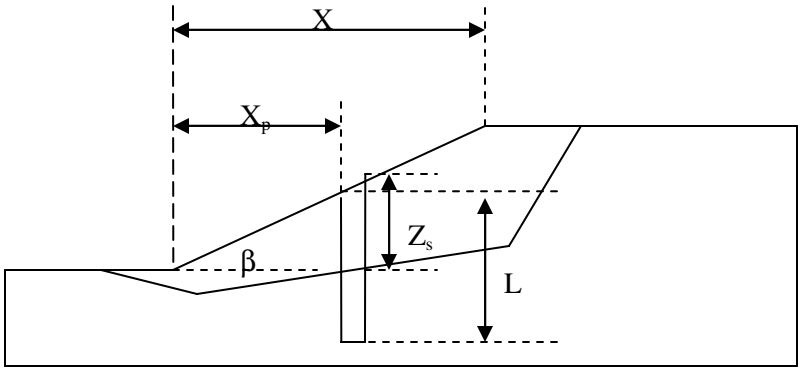


**Figure 2.1 A profile of pile-stabilized system**

Where $Z_s$: the length of pile above slip surface, L: pile length
$X_p$: the distance of pile from the toe, X: the distance between the crest and the toe

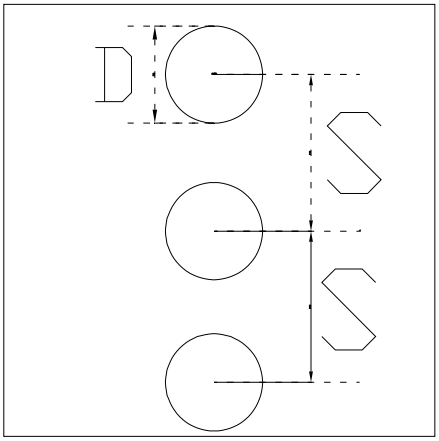


**Figure 2.2 Plane view of pile arrangement**

Where S: the distance between center to center of piles, D: the diameter of pile

### 2.6.2 Optimal Location of Pile in the Slope

Regarding the optimal location of piles within a slope, many studies have been performed such as Ito *et al.* (1979), Hassiotis *et al.* (1997), Lee *et al.* (1995), Cai and Ugai (2000), Ausilio *et al.* (2001) and Nian *et al.* (2008). The concepts of optimal location of piles are discussed in detail below.

Ito *et al.* (1965) determined that piles placed in the middle of the slope could provide the maximum required shear force without taking soil-pile interaction into consideration. Hassiotis *et al.* (1997) also concluded that the appropriate location of pile is in the upper middle part of the slope, and that when the slope is steeper, piles have to be placed closer to the top. Lee *et al.* (1995) discussed the effect of pile location within the slopes in three difference cases, (a) homogeneous, (b) two-layer inhomogeneous soil slope that the upper soft layer is underlain by a stiff layer, and (c) two-layer inhomogeneous soil slope that the upper stiff layer is underlain by a soft layer, respectively. In a homogeneous slope, the authors use dimensionless unit and pile-slope improvement ratio to investigate the effect of the pile location, it was found that piles placed at the toe or crest lead to a higher improvement ratio than piles placed in the middle portion of the slope. In a two-layer

inhomogeneous cohesive soil slope, two conditions were discussed, case 1; an upper soft layer is underlain by a stiff layer and case 2; the lower soft layer is overlain by a stiff layer. The results are quite different. In upper soft underlain by stiff layer, the position is recommended between the middle to the crest of the slope regardless of free head pile or fixed head pile head conditions. In the case of the soft layer overlain by stiff layer, the result is similar to the pile location in the homogeneous slope; the piles are recommended to be placed at either the toe or close to the crest of the slope. Cai and Ugai (2000) compared the results obtained by using shear strength reduction finite element methods and Bishop's simplified methods. The conclusions are also different, in the finite element analysis, the optimal location of pile was recommended in the middle of the slope. In Bishop's simplified method, the largest factor of safety of pile-reinforced slope will occur in the upper middle part of the slope. That is the same conclusion made by Hassiotis *et al*. (1997). Ausilio *et al*. (2001) used the kinematic approach of limit analysis to analyze the stability of slopes reinforced with piles. The improvement ratio of the factor of safety in a piled slope was found to be the largest when the pile is placed at the toe, where the stabilizing force needed to increase the safety factor to the desired value takes a minimum value. Nian *et al.* (2008) investigated the location of piles against landslides in non-homogeneous and anisotropic soils

and concluded that the most suitable location of piles is near the toe because the minimum stabilizing force is required to increase the piled-slope to a desired factor of safety. A summary of the optimal pile position is shown in Table 2.1.

**Table 2.1 Summary of recommended optimal pile position**

| Reference | Soil type | Failure type | Recommended location | Case histories or analytical model | Comments |
|---|---|---|---|---|---|
| Ito *et al.* (1979) | Cohesive soil | Circular | Middle | Pressure based method | Infinite pile length and rigid pile |
| Poulos (1995) | Clay, Claystone and Silt stone | Circular | Middle | Highway 23, Newcastle AU Use program ERCAP derive from Ito & Matui's Equation | Analyzed the response of pile placed in the middle |
| Hassiots *et al.* (1997) | Cohesive soils | Circular | Upper to top | Friction circle method incorporate the reaction force derived from plasticity | Plane Strain conditions |
| Lee *et al.* (1995) | Purely Cohesive slope | Circular | Toe and Crest | Uncoupled formulation<br>Pile response-boundary element<br>Slope stability –simplified<br>Bishop slip circle approach | Different soil distributions govern the optimal pile location |
| Lee *et al.* (1995) | Upper soft<br>lower stiff | Circular | Between middle and Crest | | |
| Lee *et al.* (1995) | Upper Stiff<br>lower soft | Circular | Toe and crest | | |
| Cai and Ugai (2000) | c=10 kPa<br>$\phi$=20º | Circular | Middle | 3-D Shear Reduction finite element method | Compared different pile head conditions<br>Hinged pile condition is recommended |
| Cai and Ugai (2000) | c=10 kPa<br>$\phi$=20º | Circular | Top | Modified Bishop Method | Did not consider the influence of pile head conditions |

**Table 2.1 Summary of recommended optimal pile position (continued)**

| Reference | Soil type | Failure type | Recommended location | Case histories or analytical model | Comments |
|---|---|---|---|---|---|
| Ausilio (2001) | c=4.7 kPa<br>$\phi$ =25º | Circular | Toe | Kinematic approach limit Analysis | |
| Nian *et al.* (2008) | Anisotropic and non-homogeneous | Log-spiral | Toe | Kinematic Limit analysis combined with strength reduction method | |
| Joeng *et al.* (2003) | $\gamma$=20.0 kN/m$^3$,<br>c=10kPa<br>$\phi$=20˚ | Circular | Middle | ABAQUS Finite element modeling | Uncoupled analysis |

Table 2.1 Summary of recommended optimal pile position (continued)

### 2.6.3 Limit Equilibrium Method

The Limit equilibrium method for analyzing slope stability has been proposed by many researchers in the past decades. In practical design, the limit equilibrium method is used most often in analysis due to its simplicity. The basic concept to determine the factor of safety is as shown in equation 2.5. This equation is based on the resisting moment $M_r$ of the soil, and the driving moment, $M_d$ of the sliding mass. After placing a reinforcing pile in an unstable slope, the pile is considered to provide an additional resistance and will increase the overall resistance. In the calculation, a limiting resistance force per unit width, $F_r$ which is provided at the sliding surface by reinforcing pile is added to the internal forces of the intersecting slice. The additional resistance provided by the pile is included in the equilibrium equations to satisfy the static equilibrium. The resisting moment by the pile, $M_p$ can be determined. The equation of the factor of safety can be written as equation 2.6.

$$F_S = \frac{M_r}{M_d} \tag{2.5}$$

$$F_s = \frac{M_r + M_p}{M_d} \tag{2.6}$$

However, the present design for pile-stabilized slopes using limit equilibrium methods is unable to take the pile-soil interaction into account. The piles are assumed to only provide the reinforcing resistance. (Ito *et al.* 1979, Poulos, 1995; Lee *et al.* 1995; Hassiotis *et al.* 1997). Accordingly, the major disadvantages of using this approach are summarized as (1) the assumptions are too simple, (2) soil-structure interaction mechanisms are not considered.

### 2.6.4 Limit Analyses - Upper Bound and Lower Bound

Limit analysis is the method which takes advantage of the lower bound and upper bound theorems of plasticity to obtain rigorous bounds on the true solution of a stability problem. Limit analysis solutions are rigorous in that the stress field associated with a lower bound solution is in equilibrium with imposed loads at the boundaries of the soil mass, and the velocity field associated with the upper bound solution is compatible with imposed velocities. Therefore, lower bounds imply equilibrium while upper bounds imply collapse. A range of solutions is defined between the upper bound and lower bound solutions. The plastic soil behavior can be assumed perfectly plastic, either obeying an associated flow rule or a non-associated flow rule. The difficulties of this method are to find the appropriate stress field, velocity field and optimal solutions giving the highest possible lower bound solution

and the lowest possible upper bound solution. However, the finite element method can also be applied to overcome the difficulties in limit analyses.

Ausilio *et al.* (2001) used the kinematic approach of limit analysis to analyze the slope reinforced with piles. The slope without stabilizing piles has to be considered first to determine both the factor of safety and the location of the potential slip surface. Then the slope stabilized with piles is analyzed. Due to the presence of the pile in the model, force and moment are assumed to be applied on the pile at the depth of slip surfaces. The response of pile can be calculated and the factor of safety of the slope incorporating piles is obtained. Nian *et al.* (2008) also used the kinematic approach of limit analysis combined with a strength reduction technique to analyze the slope stability of anisotropic and non-homogeneous slopes reinforced with piles. Similar to Asuilio *et al.* (2001), the slope stability without stabilizing with piles is analyzed to determine the factor of safety and the potential slip surface of the slope, then a slope reinforced with a row of piles is analyzed. Therefore, the exerted force and moment provided by the pile to give a desired factor of safety can be determined.

### 2.6.5 Coupled Analysis of Pile-Stabilized Slope

The pile response and the slope stability are considered simultaneously in a coupled analysis. Continuum methods are capable of treating coupled analyses. In finite element and finite difference methods, local equilibrium is satisfied everywhere in the entire model, however, in the limit equilibrium method, only global equilibrium for the sliding mass is considered (Won *et al*. 2005). A limit analysis method presented by Ausilio *et al*. (2001) considered the coupling effect on the piled stabilization problem. Nian *et al*. (2008) used the kinematic approach of limit analysis to analyze the slope stability of anisotropic and non-homogeneous slope reinforced with piles. In these so called coupled analyses, the slip surface in the analysis always changes due to the presence of the stabilizing piles.

### 2.6.6 Uncoupled Analysis of Pile-Stabilized Slope

The pile-soil interaction mechanism is complicated and still unclear, with many researchers proposing different analysis approaches. In the pile-stabilized slope system, the pile is regarded as the passive case due to the lateral soil movement. Therefore, how the pile installation interferes with the depth of the slip surface is usually unclear. Previous studies have assumed the depth of the slip surface or determined the location of the slip surface in

the slope stability analysis, then considered the pile response after placing the pile. In other words, the pile response and the slope stability are considered separately. Therefore, the pile installed will not change the location of the slip surface. This analysis can be classified as one of two types, one is the pressure based method and the other one is the displacement based method. The pressure based methods are proposed by De Beer and Wallays (1970), Ito and Matsui (1981), Hassiotis *et al*. (1997). While displacement based methods are presented by Viggiani (1981), Hull *et al*. (1991), Poulos (1995), Lee *et al.* (1995), Chow (1996) and Jeong *et al.* (2003).

Hull *et al.* (1991) identified four types of failure modes of the pile response due to the lateral soil movement at different sliding depths for a fixed length of pile. These four types of failure modes are summarized as:

(1) Flow model: The sliding surface is relatively shallow compared to the pile length so that the sliding soil just passes around the pile as shown in Figure 2.3a.

(2) Intermediate failure mode: the depth of sliding surface is between the flow and the short pile modes, where the soil strength in both the unstable and stable soil is fully mobilized along the pile length which is shown in Figure 2.3b.

(3) Short pile failure mode: when the sliding surface is deeper, the same length of the pile is strong enough to resist the bending moment and the shear forces induced by the lateral soil movement as shown in Figure 2.3c.

(4) Long pile failure mode: One or more locations along the pile are found to reach the yield moment and the plastic hinges have been developed. This failure mode occurs in the pile which is shown in Figure 2.3d.

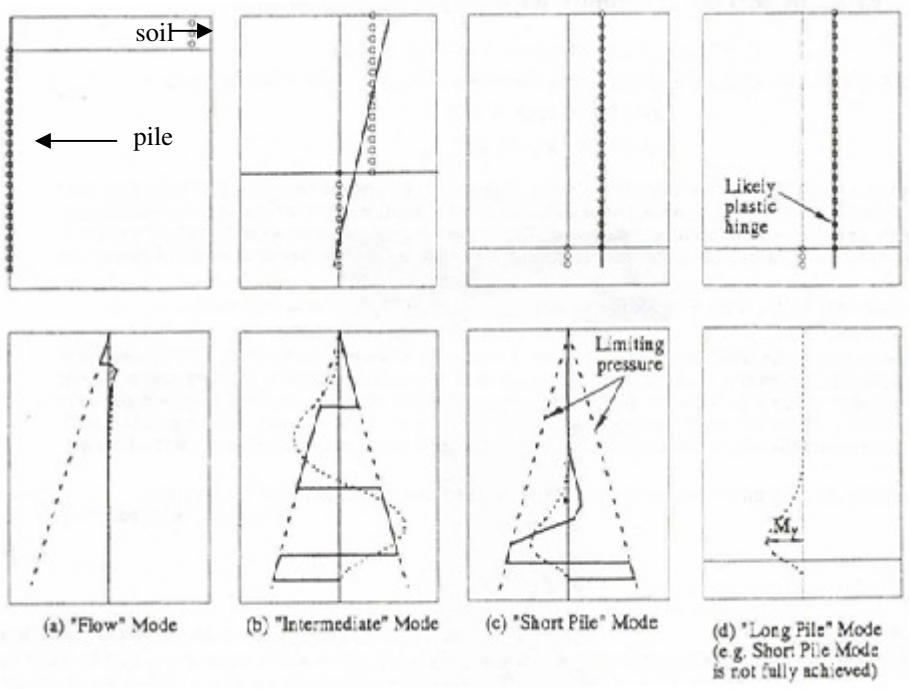


**Figure 2.3 Relative displacements between the pile and the soil and the corresponding distributions of bending moment, distributed load and limiting pressure with depth generated due to different failure modes: a) flow mode, b) intermediate mode, c) short pile mode, and d) long pile mode. (from Hull *et al.* 1991)**

### 2.6.7 Pressure Based Method

This method is based on the analysis of the passive pile subjected to the lateral soil pressure. The lateral pressure applied on the pile is based on plastic state theory developed by Ito and Matsui (1975). The equation to estimate the pressure acting on the pile, q is derived as the follows. The plan view of soil plastic deformation is shown in Figure 2.4 to illustrate the following equations.

$$p(z)=A_c\left[\frac{1}{N_\phi\tan\phi}\left\{\exp\left(\frac{D_1-D_2}{D_2}N_\phi\tan\phi\tan\left(\frac{\pi}{8}+\frac{\phi}{4}\right)\right)-2N_\phi^{1/2}\tan\phi-1\right\}+\frac{2\tan\phi+2N_\phi^{1/2}+N_\phi^{-1/2}}{N_\phi^{1/2}\tan\phi+N_\phi-1}\right]-c\left\{D_1\frac{2\tan\phi+2N_\phi^{\frac{1}{2}}+N_\phi^{-1/2}}{N_\phi^{1/2}\tan\phi+N_\phi-1}-2D_2N_\phi^{\frac{1}{2}}\right\}$$

$$+\frac{\tau_z}{N_\phi}\left\{D_1\left(\frac{D_1}{D_2}\right)^{N_\phi^{1/2}}\exp\left(\frac{D_1-D_2}{D_2}N_\phi\tan\phi\tan\left(\frac{\pi}{8}+\frac{\phi}{4}\right)\right)-D_2\right\} \qquad (2.7)$$

$$p(z)=c\left\{D_1(3\log\frac{D_1}{D_2}+\frac{D_1-D_2}{D_2}\tan\frac{\pi}{8})-2(D_1-D_2)\right\}+\gamma_z(D_1-D_2) \qquad (2.8)$$

Where, $N_\phi$ : $\tan^2(\pi/4+\phi/2)$,

$D_1$: the center to center interval in a row,
$D_2$: the clear interval between piles,
C: cohesion of soils
$\phi$: the angle of internal friction of soil,
$\gamma$: the unit weight of soil
z: the arbitrary depth from the ground surface.

To estimate the pressure acting on the pile from the moving soil is very important to determine the pile response. In the analysis of the single passive pile, the values of the ultimate soil pressure are in the range of 9 to $12S_u$ for cohesive soils. Broms (1964a) suggests 0 from the ground surface to $9S_u$ at the depth of 1.5 times the pile diameter. Chen and Poulos (1994) argue that $9S_u$ is appropriate. Viggiani (1981) proposes 2.8 to $4S_u$ as acceptable. Poulos (1995) proposes $2S_u$ from the ground surface to $9S_u$ at a depth of 3.5 times of the pile width. Chen (1994) uses $11.7S_u$ as the limiting soil pressure on the pile. Bransby and Springman (1999) use $11.75S_u$. Randolph and Houlsby (1984) propose that $p_y$ is $10.5S_u$. Reese (1984) suggests the smaller of two equations, $p_y = \left(3 + \frac{\gamma z}{c_u} + \frac{0.5z}{d}\right) c_u and\ p_y = 9c_u$. For cohesionless soils, Broms (1964 b) proposes $3\sigma_p$ as the ultimate soil pressure applied on pile, Where $\sigma_p$ is the pressure applied on the pile.

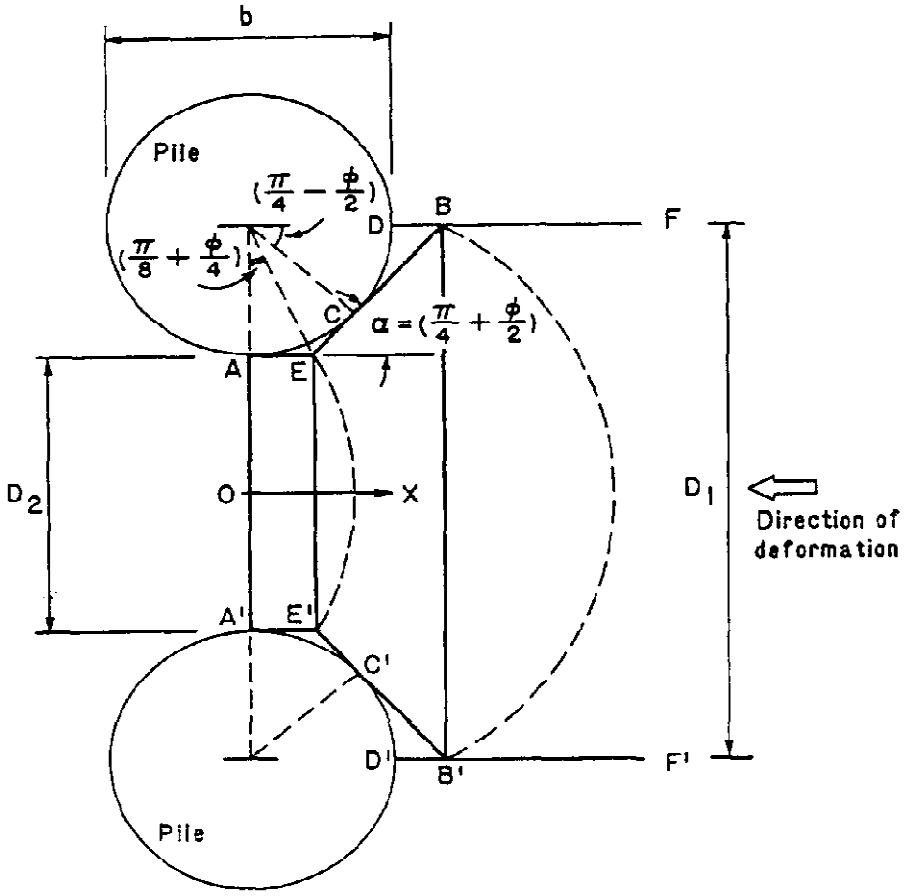


**Figure 2.4 Plastically deforming ground around stabilizing piles**
**[after Ito and Matsui (1975)]**

### 2.6.8 Displacement Based Method

This method considers the relative displacement between the soil and pile. The soil movement can be measured directly from inclinometer data or calculated using the finite element approach. Poulos (1973) developed a computer program PALLAS by using the simplified boundary element method, Hull *et al.* (1991) developed a microcomputer-based

program with the ability to model the pile head and tip loading by using a modified nonlinear boundary element approach. Cai *et al.* (2003) used a subgrade reaction solution for the response of flexible piles in landslides where the influence of the laterally linear soil movement of the sliding layer on the pile was considered. The soil was modeled as an elastic continuum or a set of springs. A nonlinear pile-soil interface element with the ability to represent a hardening or softening plastic response prior to reaching an ultimate state was incorporated. The incremental analysis can solve the pile-soil interaction problem for increasing soil movements up to and beyond the state at which full pile-soil interface strength has been mobilized. Four modes of failure were defined in the program, (1) flow mode: flow of the slide past an intact pile, (2) intermediate mode: rotation of the pile with the soil at failure along the full length of the pile, (3) short pile mode: translation of the pile with the sliding soil, resulting in failure of the supporting soil, (4) long pile mode: the maximum bending moment in the pile reaches the yield moment of the pile before complete development of the other three modes. The long pile mode can be associated with the other three modes. The soil movement was treated on a case by case basis on the pile rotation near its top. The p-y method is versatile and provides a practical means for design, as suggested 30 years ago (McClelland & Focht, 1958; Reese & Matlock, 1956). Two developments made

the method possible: the digital computer for solving the nonlinear, fourth order differential equation for a beam-column and remote-reading strain gauges for obtaining p-y curves from experiment. The fourth order differential equation 2.9 for the beam column on a foundation was derived by Hetenyi (1946).

$$EI\frac{\partial^4 y}{dx^4} + Q\frac{\partial^2 y}{\partial x^2} - p + w = 0 \qquad (2.9)$$

Where:
Q=axial load on the pile,
y=lateral deflection of the pile at a point x along the length of the pile,
p=soil reaction per unit length,
EI=flexural rigidity, and
w=distributed load along the length of the pile.

In potential slides, based on the movement of the soil, the relative displacement between the pile and the soil has is taken into consideration. The p-y method has been verified as a rational method for large deformation problems. Therefore, free-field soil movement is included in soil-pile interaction analysis. The modified equation is as shown in Eq. 2.10, where the relative displacement is incorporated.

$$EI\frac{d^4 y}{dx^4} + Q\frac{d^2 y}{dx^2} - k(y - y_s) + w = 0 \qquad (2.10)$$

Where $y_s$=free-field soil movement at a particular depth.
y : the deflection of pile.

Numerical methods such as boundary element method (PALLAS, Poulos 1997), finite element method (ABAQUS, Jeong *et al*. 2003, Pan *et al.* 2002) and finite difference method (LPILE, Reese, 1996, FLAC 3D, Won, *et al.,* 2005) computer programs have been developed to solve this differential equation. By solving this fourth order differential equation, five solutions are obtained. The solutions and the physical meaning are shown in Figure 2.5, pile deflection, slope, bending moment, shear force and soil resistance on the pile at a particular depth, respectively. The lateral displacement of the pile is related to the pile bending stiffness and the horizontal soil-pile interaction stresses. The numerical analysis indicates that the pile head conditions and bending stiffness can influence the stability of the slope stability with piles. However, in limit equilibrium method, the influence of pile head conditions and stiffness of the pile cannot be incorporated into the analysis. The pile-soil interaction mechanism and analytical model based on displacement-based method is illustrated in Figure 2.6.

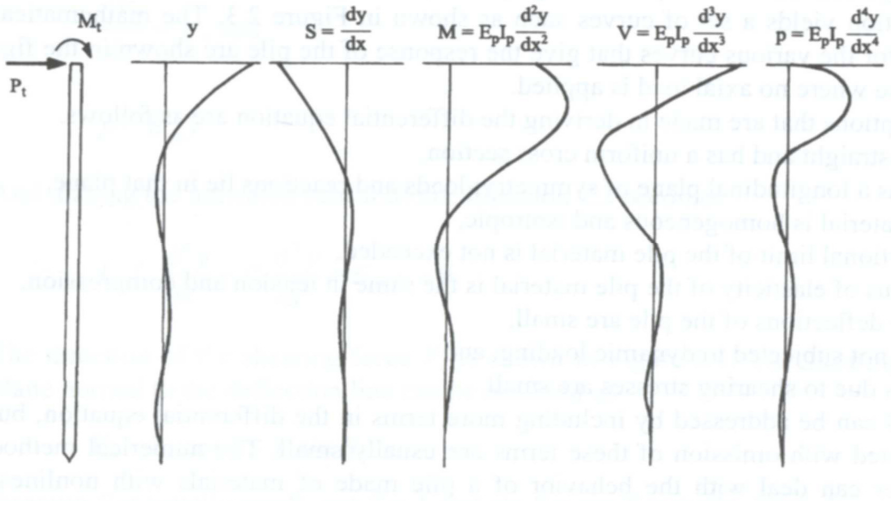


**Figure 2.5 Form of the results obtained from a complete solution (From Reese and Van Impe, 2001)**

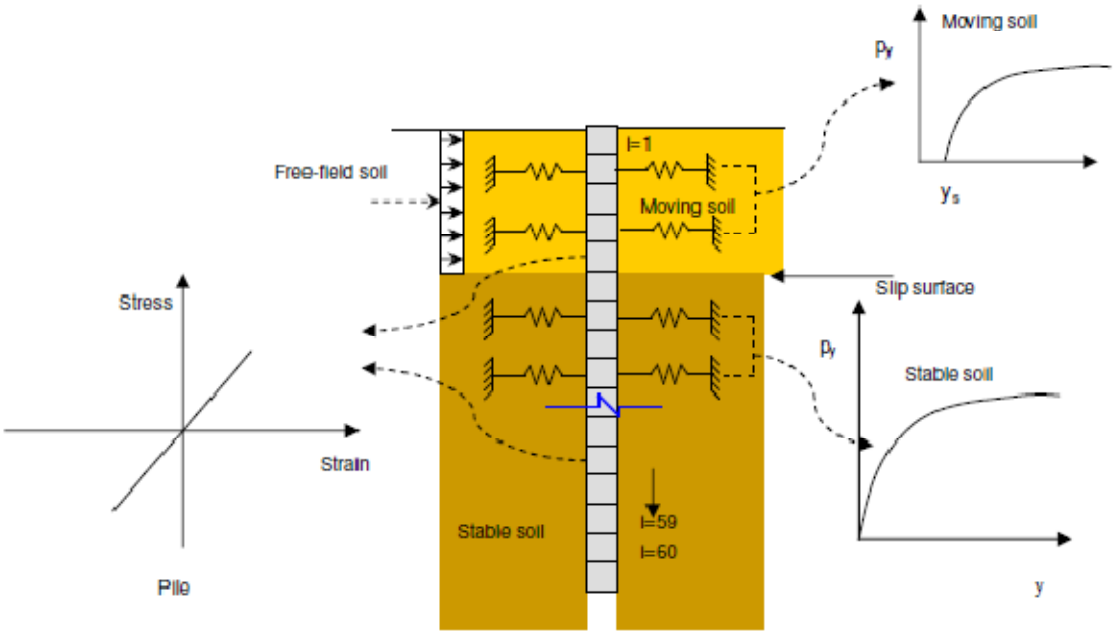


**Figure 2.6 The 2-D analytical model used to study the behavior of pile in stabilizing slopes**

### 2.6.9 Continuum Method

In pile-stabilized slope problems, limit equilibrium methods are used most often. However, pile-soil interaction cannot be incorporated in the analysis. Piles in limit equilibrium analyses are considered to supply the additional resistance against the sliding portion. In addition, the advantages of the finite element approach in solving slope stability problems are (1) the location or depth of slip surface is not required to be assumed in advance. Slip surface can be determined using the plastic shear strains in the soil mass. (2) Unlike the limit equilibrium method, there is no need to assume the interslice forces. (3) The deformation of a slope in working stress can be obtained if the reliable information of soil compressibility is provided, (4) instead of giving the global failure in limit equilibrium method, a local failure or initial failure location can be found, therefore, progressive failure can be also modeled in finite element analyses.

Some methods have been proposed for analyzing the response of single piles and group piles under the lateral loading from horizontal soil movement. Either finite element method (Carter 1982; Broms *et al.* 1987; Springman 1989; Stewart *et al.* 1993; Chen and Poulos, 1994; Goh *et al.* 1997, Cai and Ugai, 2000; Jeong *et al.,* 2003), finite difference method (Poulos and

Davies 1980; Brandshaug, 2001 FLAC, Chen and Martin 2002 FLAC) or boundary element method (Hull *et al.* 1991, Chen and Poulos, 1997) was used.

A couple of piled-slope 2-D or 3-D models using finite element methods have been developed in the past few years. Cai and Ugai (2000) used the 3D strength reduction finite element method to solve the homogeneous slope reinforced with pile problem. Chen and Martin (2002) used the finite difference analysis package, FLAC, to evaluate the pile-soil interaction mechanism. Jeong *et al.* (2003) used the 3D finite element program ABAQUS to investigate the stability of a slope reinforced with piles. Goh *et al.* (1997) presented a simplified numerical method for analyzing the response of single piles to lateral soil movements. In their method, the pile is modeled with beam elements and the pile-soil interaction is modeled with the hyperbolic soil springs. A simplified finite element approach that can account for non-homogeneous soil strength conditions, pile stiffness, and pile fixity is used. A computer program BCPILE (1995), was developed using the resulting numerical procedures.

## 2.7 Influencing Factors on Pile Stabilized Slope

The factors which affect the efficiency of the stabilizing pile in design are summarized as the pile length, diameter and spacing of the pile (S/D), stiffness of the pile (EI), location of a pile placed in the slope, depth of the potential slip surface, pile length below the slip surface, pile head conditions and soil properties according to previous studies. To investigate the relationship between the influencing factors and slope stability reinforced with piles, the numerical analysis done previously will be reviewed and compared to the results using the finite element methods in ABAQUS in this study.

### 2.7.1 Soil Constitutive Model

The Mohr-Coulomb failure criterion is the most widely used soil model in numerical analyses. Elasto-plastic criteria with Mohr-Coulomb failure criterion is used (Chen and Martin, 2002; Chae *et al.*, 2004), isotropic-elastic model associated with Mohr-Coulomb failure criterion is employed in the soil model built in ABAQUS software (Jeong *et al*. 2003). The elastic continuum (Springman, 1989) is also used to simulate the soil behavior due to its simplicity. The elastic-perfectly plastic soil model associated with Mohr-Coulomb failure criteria in the study used the finite difference program FLAC (Brandshaug, 2001).

### 2.7.2 Pile-Soil Interface

Chen and Martin (2002) investigated the mechanics of the mobilization of the resistance from the passive pile due to the lateral soil movement in terms of the arching effect. The effect of the roughness between soil and pile are examined first. Interface elements allow the computation of normal and shear stresses on the pile interface. To simulate a perfectly smooth interface between the soil, a normal stiffness and shear stiffness without cohesive and frictional strength is modeled while an undrained shear strength is selected as $5c_u$ to represent a perfectly rough pile surface. An elastic spring stiffness was used to model the pile-soil interaction between pile and soil (Broms *et al.* 1987; Goh *et al.* 1997). Jeong *et al.* (2003) modeled the interface using 2-D quadratic 4-node elements with zero thickness which can only transfer shear forces. Therefore, these elements are completely defined by the geometry and a friction coefficient, $\eta$. A limiting displacement of 5mm was assumed for full mobilization of the skin friction as suggested by Broms (1979).

### 2.7.3 Pile Model

Piles are usually assumed as elastic members in the numerical models. Elastic beam elements are most often used in numerical modeling (Goh, *et al.* 1997, Cai and Ugai, 2000,

Brandshaug, 2001, Jeong *et al.,* 2003, Chae *et al.* 2004). Viggiani (1981) discussed soil failure modes due to lateral soil moment towards the pile if the pile is rigid or contains plastic hinges. Three failure modes are discussed for the rigid pile case and the pile with plastic hinges.

### 2.7.4 Pile Head Condition

The pile head condition is considered as one of the important influencing factors affecting the performance of the stabilizing pile in pile –slope systems. Four possible pile head conditions are introduced and used (Cai and Ugai, 2000): (1) free head: both displacement and rotation are allowed; (2) unrotated head: displacement is allowed but rotation is not allowed; (3) hinged head: rotation is allowed, but displacement is not allowed; (4) fixed head: neither displacement nor rotation is allowed. Free head and fixed pile cap cases are discussed in Chae's study (2004). Three types of pile head conditions are used in this analysis, free head, unrotated head and hinged head, respectively. Ito and Matsui (1975) used the approach which assumed the pile is rigid and of infinite length. However, the assumptions cannot represent the actual pile conditions in the field which are of finite length and flexible. Finite element analysis results of four types of pile head conditions are compared by Cai and Ugai (2000).

Fixed and free head piles were adopted in the study of Hull, *et al.* (1991). The four pile head conditions are illustrated in Figure 2.7.

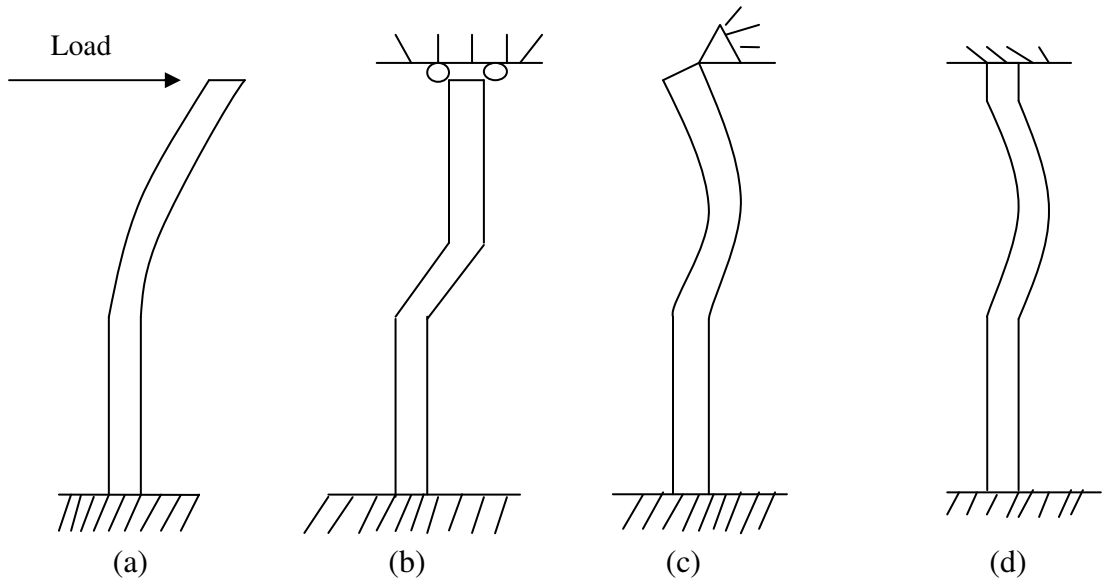


**Figure 2.7 Deformation of three types of pile head restriction in numerical modeling, (a) free-head, (b) unrotated head, (c) hinged head, (d) fixed head**

### 2.7.5 Lateral Soil Movement Profile

In previous studies, soil movements were often assumed uniform in the moving slides or the data were directly obtained from inclinometers. The soil movement leads to the pressure applied on the pile and the pile response depends upon the nature amount of soil movement. Profiles of soil movement were observed or assumed by different authors in their analyses. The shapes of the soil movement against the piles assumed or observed in previous studies using numerical analysis are summarized in the following and shown in Figure 2.8.

a) Uniform soil movements: Lee *et al.* (1995), Poulos (1995), Chen and Poulos (1997), Jeong *et al.* (2003), Ang, (2005),

b) Linear soil movements: Chen and Poulos (1997).

c) Trapezoidal: Chow (1996), Goh *et al.* (1997).

d) Hyperbolic: Cai and Ugai (2003).

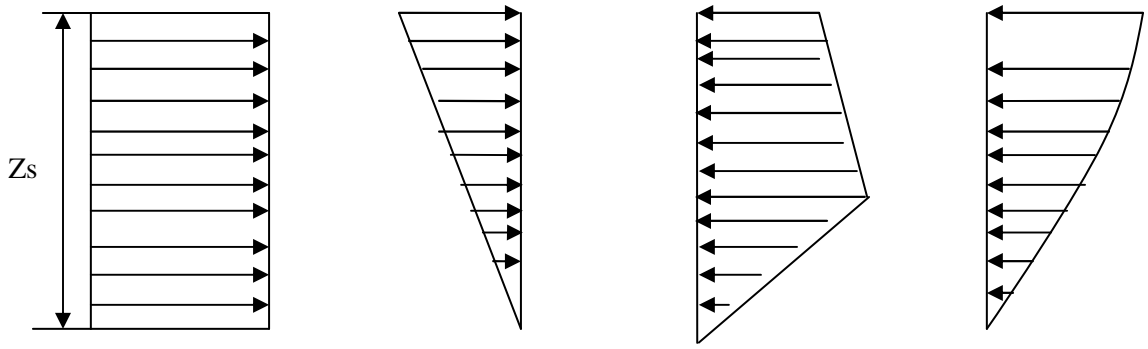


$Z_s$: Depth of slip surface

(a) (b) (c) (d)

**Figure 2.8 Shapes of soil deformation profiles (a) uniform, (b) linear, (c) trapezoidal, (d) hyperbolic shape.**

## 2.8 Constitutive Model of Soil

In finite element analysis, selection of an appropriate model is very important to make the results more accurate. A number of soil constitutive models have been proposed in past decades, including elastic model and elastic-plastic model. To capture real soil behavior, elastic-plastic models are adopted most frequently. The Mohr-Coulomb failure criterion with associated and non-associated flow rules is used most often. However, a shortcoming is the inability to predict the dilatancy of the actual soils. Therefore, in the following sections, several noted elastic-plastic soil models which may be used in this study are introduced in detail to compare against available models used in finite element analysis.

### 2.8.1 Elastic Soil Model

The linear-elastic model is the simplest model; only two parameters (Young's modulus E, and Poisson's ratio, υ) are needed. However, this model is not accurate for soils except at low stress and strain levels. As a result, some nonlinearly elastic models such as the Bi-linear model, K-G model, Hyperbolic model, Small strain stiffness model, Puzrin and Burland model were proposed by different authors.

### 2.8.2 Elastic-Plastic Soil Models

In addition to linearly elastic and nonlinearly elastic models, many elastic-plastic models were also proposed for materials including simple elastic-plastic models such as Tresca, von Mises, Mohr-Coulomb, Drucker-Prager models. Other advanced elastic-plastic models such as Lade's double hardening model, Bounding surface formulation of soil plasticity, MIT soil models, Bubble models, Al-Tabbaa and Wood model were also proposed. Due to the computational improvements based on these numerical methods such as finite difference method, finite element method, boundary element method and discrete element method, the difficulties and the cost to deal with these non-linear problems have been reduced suprisingly.

In the elastic-plastic model, four ingredients have to be characterized; (1) elastic properties, (2) yield function and surface, (3) plastic potential function and surface, and (4) hardening rule. Some elastic-plastic models used in soil mechanics most frequently are summarized in the following.

The most important part of a plasticity model is how to simulate the behavior in the plastic strain after yielding. Before yielding, the mechanical behavior is assumed to be elastic. After yielding, the behavior is captured by different plastic failure criteria. Generally speaking, a yield function can be expressed mathematically as.

$$f(\sigma_{ij}) = 0 \quad \text{Yeild} \tag{2.11}$$

$$f(\sigma_{ij}) < 0 \quad \text{Elastic State} \tag{2.12}$$

At present, two types of failure criterion can be discussed based on the properties of the material; hydrostatic-pressure-independent materials and hydrostatic pressure dependent materials. The former type of material are often called frictionless materials and the latter are

called frictional materials. Geologic materials such as soils, rocks and concrete belong to the frictional materials category. Mohr-Coulomb and Drucker-Prager are the typical failure criteria in this group. These are simple linear elastic perfectly plastic models often used in soils and other frictional materials and are discussed in the following sections.

### 2.8.3 Mohr-Coulomb Criterion

Mohr's failure criterion is an elastic-perfectly plastic model characterized by the stress-stain relationship like the one shown in Figure 2.9. The Mohr-Coulomb failure criterion is based on the assumption that the maximum shear stress is the decisive measure of yielding. The critical shear stress is not a constant but a function of the normal stress σ,

$$|\tau| = h(\sigma) \tag{2.13}$$

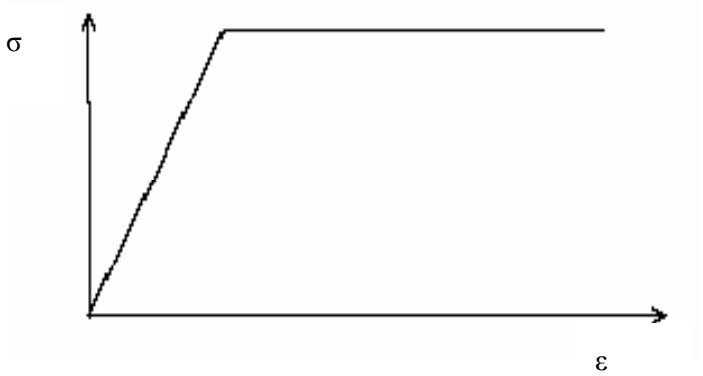


**Figure 2.9 Elastic-perfectly plastic stress-strain behavior**

The expression of Mohr envelope is a straight line, the equation of which is known as Coulomb's equation which can be expressed mathematically in the form,

$$|\tau| = c + \sigma \tan \emptyset \tag{2.14}$$

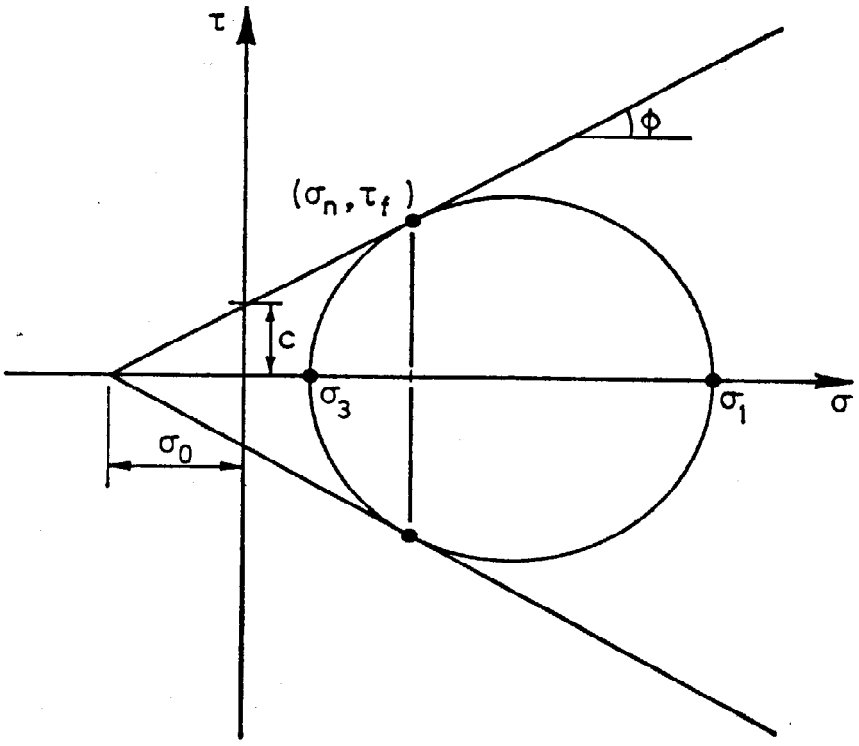


**Figure 2.10 Mohr's circle and Mohr-Coulomb Failure envelope**

Five input parameters which are Young's modulus (E) and Poisson's ratio (ν) for soil elasticity, ϕ and c for soil plasticity and φ as an angle of dilatancy are involved in the

Mohr-Coulomb model. Using the Mohr's circle of stress as shown in Figure 2.10, In terms of equation 2.14, Mohr-Coulomb criterion for $\sigma_1 \geq \sigma_2 \geq \sigma_3$ can be written mathematically as

$$\frac{1}{2}(\sigma_1 - \sigma_3)\cos\emptyset = c - \left[\frac{1}{2}(\sigma_1 + \sigma_3) + \frac{\sigma_1 - \sigma_3}{2}\sin\emptyset\right]\tan\emptyset \qquad (2.15)$$

Equation 2.15 is called the Mohr-Coulomb failure criterion and is adopted as the yield function in the form:

$$F(\{\sigma'\},\{k\}) = \frac{1}{2}(\sigma_1 - \sigma_3)\cos\emptyset - c - \left[\frac{1}{2}(\sigma_1 + \sigma_3) + \frac{\sigma_1 - \sigma_3}{2}\sin\emptyset\right]\tan\emptyset = 0 \qquad (2.16)$$

For use in three-dimensional analysis, the Mohr-Coulomb criterion can be expressed as

$$\sigma_1 \frac{1-\sin\emptyset}{2c\cos\emptyset} - \sigma_3 \frac{1+\sin\emptyset}{2c\cos\emptyset} = 1 \qquad (2.17)$$

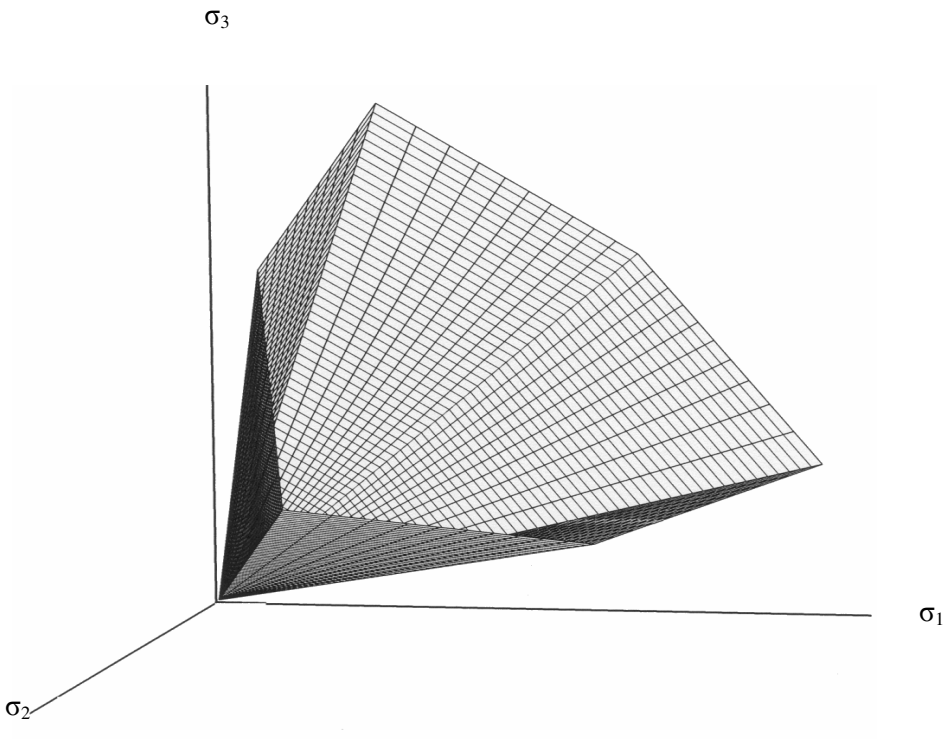


**Figure 2.11 Yield surface of Mohr-Coulomb criterion in principal stress space**

The yield surface in the principal stress space is shown in Figure 2.11.

Where $\sigma_1$ and $\sigma_3$ are major and minor principal stresses, respectively. The equation also indicates that Mohr Coulomb failure criterion is independent of the intermediate principal stress $\sigma_2$. ($\sigma_1 \geq \sigma_2 \geq \sigma_3$).

In terms of stress invariants, the equation of Mohr-Coulomb criteria can be derived as

$$f(I_1, J_2, \theta) = \frac{1}{3} I_1 \sin\emptyset + \sqrt{J_2}\sin\left(\theta + \frac{\pi}{3}\right) + \frac{\sqrt{J_2}}{\sqrt{3}}\cos\left(\theta + \frac{\pi}{3}\right)\sin\emptyset - c\cos\emptyset = 0 \qquad (2.18)$$

Where $I_1 = \sigma_1 + \sigma_2 + \sigma_3$, first invariant of the stress tensor

$J_2 = s_1 + s_2 + s_3$, second invariant of stress deviator tensor, $\quad s_i = \sigma_i - \frac{1}{3} I_1, i = 1,2,3$

In terms of the stress invariants $p'$, $J$ and θ in the deviatoric plane in principal stress space. The yield function 2.18 can be rewritten as equation 2.19.

$$f(p', J, \theta) = J - \left(\frac{c'}{\tan \varphi'} + p'\right) g(\theta) \tag{2.19}$$

Where $g(\theta) = \frac{\sin \emptyset'}{\cos \theta + \frac{\sin \theta \sin \emptyset'}{\sqrt{3}}}$

$$p' = \frac{1}{3}(\sigma_1' + \sigma_2' + \sigma_3')$$

$$J_2 = \frac{1}{\sqrt{6}} \sqrt{(\sigma_1' - \sigma_2')^2 + (\sigma_2' - \sigma_3')^2 + (\sigma_3' - \sigma_1')^2}$$

The Mohr-Coulomb model is assumed to be perfectly plastic without a hardening or softening law. To describe the plastic part of a model, a potential function g is required. If the yield function f and the potential function g coincide, the flow rule is termed associated. Figure 2.12 compares the shape of failure surfaces of Drucker-Prager and Mohr-Coulomb failure surfaces in the deviatoric plane. Figure 2.13 shows the shape of yield surfaces of Drucker-Prager and Mohr-Coulomb failure criteria in principal stress space.

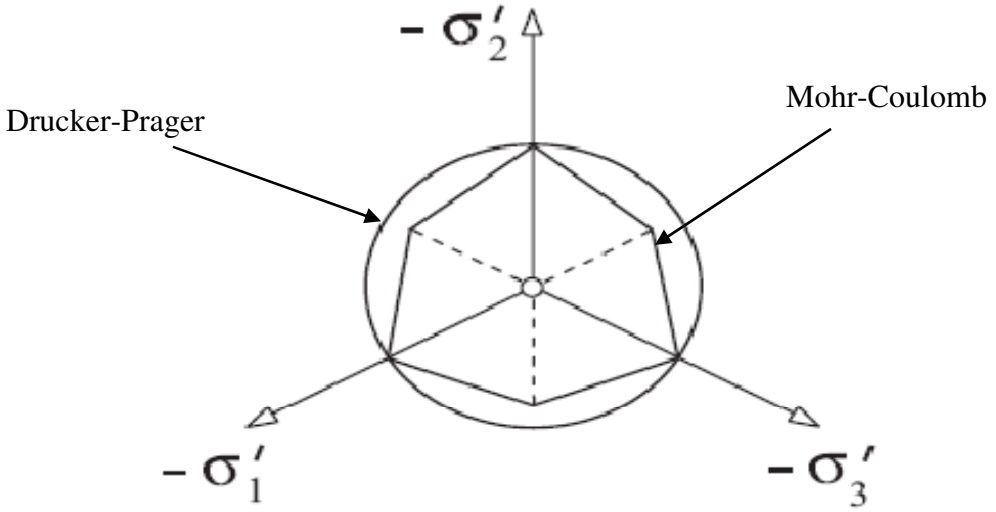


**Figure 2.12 The Drucker-Prager and Mohr-Coulomb failure surfaces in deviatoric plane.**

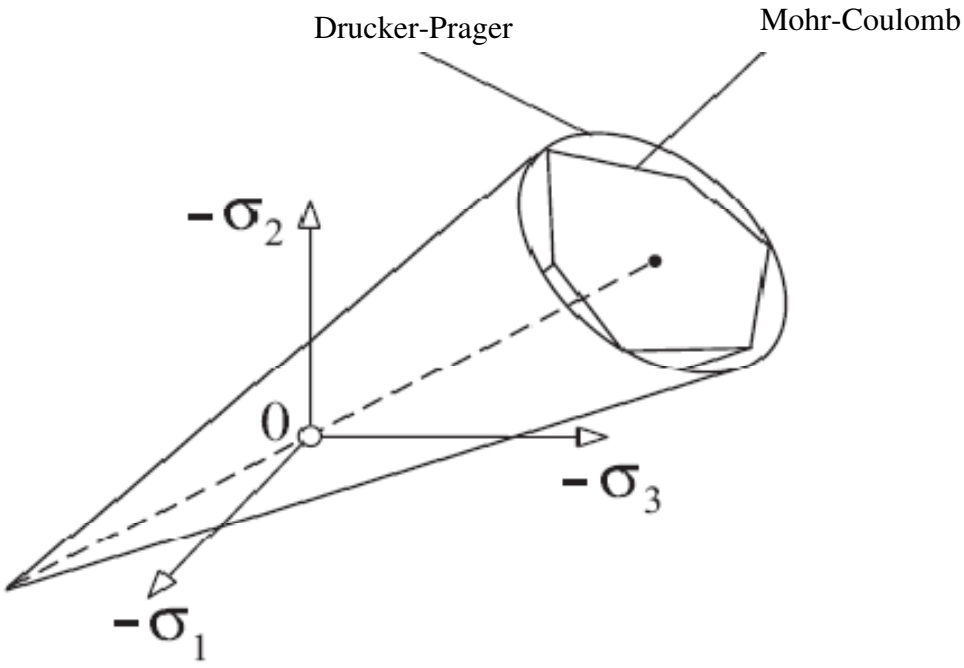


**Figure 2.13 The Drucker-Prager cone and Mohr-Coulomb pyramid matched along the compressive meridian in principal stress space.**

## 2.9 Flow Rule-Plastic Potential Function

To describe the stress-strain behavior after yielding in the elastic-plastic material, the direction and magnitude of the plastic strain has to be defined. The flow rule concept is introduced to define a plastic potential function g in analogy with ideal fluid-flow problems. If the yield function f and potential function coincide (f=g), the flow rule is termed as associated. If the f≠g, the flow rule is termed as non-associated. When the flow rule is said to be associated, the yield surface has the same shape as the plastic potential surface. The incremental plastic strain vector is normal to the yield surface and the normality condition is said to apply.

Flow rules are important in constitutive modeling of a material because they govern dilatancy which has a significant influence on volume changes and strength. The plastic strain increment vector $d\varepsilon_{ij}^{p}$, that is (1) the ratio among the component, (2) the magnitudes against the stress increment $d\sigma_{ij}$. The flow rule is defined as.

$$d\varepsilon_{ij}^{P} = d\lambda \frac{dg}{d\sigma_{ij}} \tag{2.20}$$

$d\lambda$ is a non-negative scalar function that varies throughout the plastic loading history. The gradient vector $dg/d\sigma_{ij}$ represents the direction of the plastic strain increment of $d\varepsilon_{ij}^{p}$.

Therefore, when the flow rule is termed associated, the plastic potential surface has the same shape as the yield surface g =f, therefore the flow rule can also be written as

$$d\varepsilon_{ij}^{P} = d\lambda \frac{df}{d\sigma_{ij}} \tag{2.21}$$

In this case, the plastic strain develops along the normal to the current loading surface.

In geotechnical engineering, both associated and non-associated flow rules in plasticity constitutive models are commonly used.

In the Mohr-Coulomb failure criterion, either associated or non-associated flow rules could be adopted. For non-associated flow, the plastic potential function can be rewritten as equation 2.22 by taking the similar form of equation 2.19 and replacing ϕ with φ.

$$P(J_2, p', \theta) = J_2 - \left(a_{pp} + p'\right) g_{pp}(\theta) = 0 \tag{2.22}$$

$$g_{pp}(\theta) = \frac{\sin\varphi}{\cos\theta + \frac{\sin\theta \sin\varphi}{\sqrt{3}}} \tag{2.23}$$

Where φ is the dilation angle

If φ=ϕ, the form of potential equation is the same as equation (f=g), giving the associated condition.

## 2.10 Hardening Rule

A yielding surface changes its current configuration during the loading process so that the stress point always lies on it. There are an infinite number of yield surfaces that meet this condition, and it is not a simple matter to determine the loading surfaces. The rules governing the evolution of a loading surface are called hardening rules. Several hardening rules have been proposed for use in plasticity analysis. The response of a material after initial yielding can differ depending upon the employed hardening rules, such as the isotropic hardening, kinematic hardening and mixed hardening rules.

The Mohr-Coulomb model is assumed to be perfectly plastic after yielding. Therefore, there is no hardening and softening law required. Several soil models have been propsed, each model has its advantage, disadvantage, limitations and applicable soil type. The comparison of each soil constitutive model is tabulated in Table 2.2.

**Table 2.2 Comparisons of soil failure criterion**

| Soil model | Advantage | Disadvantage | Model calibration | Soil type |
|---|---|---|---|---|
| Mohr-Coulomb | Control over the shape in deviatoric plane.<br>Finite element method is compatible to deal with conventional soil mechanics.<br>Simple and easy for application in limit analysis procedures.<br>Often used in planar problems. | Program has to deal with the corners of the yield and plastic potential surface which imply singularity in the corners. | Triaxial compression and triaxial extension tests. | Cohesive and cohesionless soils |
| Drucker-Prager | Overcomes the corner problem which leads to singularity in Mohr-Coulomb Model.<br>Both yield an strength are dependent on the intermediate principal stress, $\sigma_2$. | Very little experimental data available to accurately quantify the effect of intermediate stress. | True triaxial test or hollow cylinder device. | Cohesive soils and cohesionless soils |
| Modified Cam Clay | Good for model the behavior of soil hardening and softening.<br>Most conveniently described in terms of the strain response to changes in effective stress.<br>Able to predict response in all regions of strain space. | Not all changes in stress are allowable | Triaxial compression or extension tests | Cohesive soils |

**Table 2.2 Comparisons of soil failure criterion (continued)**

| Soil model | Advantage | Disadvantage | Model calibration | Soil type |
|---|---|---|---|---|
| Drucker-Prager Cap Model | Simple to compare to other work-hardening plasticity models.<br>The use of associated flow rule reduces computer storage requirements because it makes the matrix symmetric. | The deviatoric plane in principal stress is circular which results in equal strength predictions for both triaxial compression and extension.<br>The model hints it is more accurate to predict the isotropic response. than the anisotropic behavior.<br>The expansion and contraction of the cap are controlled by the same hardening rule. | Drained isotropic or uniaxial compression test to indentify the cap hardening characteristics.<br>Drained or undrained triaxial tests to identify Drucker-Prager shear surface. | Cohesive soils |
| Lade Cap Model | The use of non-associated flow rule allows accurate representation of the observed plastic volumetric response of sands. | Due to the use of nonassociated flow, nonsymmetric system of equations need to be solved which require a large demand on computational capacity. | Isotropic compression, triaxial compression and extension test. | Cohesionless soils |

## 2.11 Three-Dimensional Finite Element Analysis

Three-dimensional finite element model applied in the slope stability analysis has been used more than thirty years, according to Duncan (1996), the factor of safety for three dimensional analysis is greater than the factor of safety from the two-dimensional analysis. Only few studies indicated the factor of safety for two dimensional is greater than the results from three dimensional models which have been regarded as inaccurate analyses such as the studies by Hovland (1977), Chen and Chameau (1983) and Seed *et al.* (1990). Azzouz and Baligh (1978) indicated the use of the Ordinary Method in three dimensional analyses is inadequate by assuming zero normal stress applied on vertical surfaces. Also, in the research of Seed et al. (1990) was found all conditions of equilibrium cannot be satisfied in 2-D and 3-D analyses. Hutchinson and Sharma (1985) also pointed out that 2-D and 3-D analyses should give the same factor of safety on cohesionless soils because the slip surface is a shallow plane and parallel to the surface of the slope. Azzouz *et al*. (1981), also found that if the 3-D effects are ignored in the analyses to back calculate shear strengths, the results from back calculation will be too high. Griffiths (2007) compared the results of analysis on 2-D slope and 3-D slope, the 3-D analysis is found to possess a higher factor of safety. When the width in the third direction is increasing, the analysis tends to the plane strain solution which is close to

the result from 2-D analysis. Therefore, the boundary condition assumptions are significant in three dimensional analyses due to the side forces are not readily justified. The solutions from 3-D analyses will tend to the plain strain solution for the ratio of width and slope height close or greater than 10.

The three-dimensional finite element analyses are also widely used in the slope stability of pile-stabilized slopes, or the pile behavior due to lateral soil movement. In three-dimensional models, more influencing factors regarding the pile installation such as the spacing and arching effect can be further identified. Miao *et al.* (2006) investigated the passive pile response subjected to the lateral soil movement. The analyses indicate that the behavior of the pile is significantly influenced by the pile flexibility, the magnitude of soil movement, the pile head boundary conditions, the shape of the soil movement profile and the thickness of the moving soil mass. Ang (2005) investigated the load transfer mechanism in slopes reinforced with the piles by using three-dimensional ABAQUS finite element technique. The flexible piles used for evaluating the mobilized and limit loads on piles are recommended. Jeong *et al.* (2003) used the uncoupled finite element analysis approach to study on the slope/pile system induced by the lateral soil movement. The results predicted that the highest safety factor occurs when the pile is placed closer to the top of the slopes and the factor of

safety of pile-stabilized slope decreases with the pile spacing increases. Cai and Ugai (2000) also proposed a three-dimensional elasto-plastic shear strength reduction finite element method to study the effect of pile position, spacing, pile head conditions and bending stiffness of pile on the slope stability of pile-stabilized slope. The pile response in terms of deflection, shear force, moment and soil resistance are investigated based on the different pile spacing. The results present the pile spacing decreases, the piles more like a continuous barrier and the soil arching effect becomes more significant, so the soil does not reach the limit state until the soil deforms greatly.

### 2.12 ABAQUS Finite Element Program

ABAQUS is a powerful commercial finite element program. It has been widely used in the mechanical industry such as automobile, aircraft, power plant and so forth. The application in Civil engineering is getting popular nowadays. The package is capable of solving three dimensional models and good at solving nonlinear behavior of materials. There are a number of built-in plastic models of soil such as Mohr-Coulomb, Cap, Drucker-Prager Cam-Clay model, structural materials, interface properties for use. User also can easily define the particular model develop by their own. ABAQUS/CAE utilize CAD mode for users to draw the modeling and define material properties, element type selection, interaction properties,

boundary and initial conditions definition and calculation stages. The 2-D and 3-D models can be constructed in ABAQUS/CAE. ABAQUS was used to conduct the 2-D and 3-D piled-slope finite element analyses this study. The coupled analysis with strength reduction method is associated with this finite element analysis.

# CHAPTER 3: A REVIEW OF CASE HISTORIES OF STABILIZING PILE IN SLOPE REMEDIATION

## 3.1 Introduction

Piles have been widely used in the remediation of slopes and have been proven to be an efficient means. In Japan, timber piles have been used against landslides over 100 years ago (Fukuoka, 1977). The installation of piles as a stabilization element has been applied successfully without disturbing the equilibrium of the slope. However the mechanism of pile-soil interaction is very complex and is still unclear. Although limit equilibrium and finite element numerical methods have been applied to the problem, no universal method has been accepted. As a result, case histories can provide an engineer empirical and general ideas in preliminary design for a stabilizing pile. This chapter summarizes a number of case histories worldwide. The advantages and disadvantages of using stabilizing piles are compared. The advantages can make design more efficient in terms of time, cost and safety. Conversely, the disadvantages could be avoided in design and selection. Furthermore, case histories also provide a good database for numerical studies. Based on these case studies, with appropriate selection of parameters in numerical analysis such as properties of materials including piles and soil and constitutive models and reasonable boundary conditions of numerical models, a

successful simulation can be obtained. The successful simulation of the pile-slope system is helpful to develop a better design method in stabilizing piles due to the influencing factors of stabilizing piles such as the pile head restraint, pile stiffness, dimension of the pile, position and spacing, the length of pile in a stable layer, soil properties, and movements. Meanwhile, the pile-soil interaction mechanism will be further explored with these case studies.

### 3.2 Review of Case Histories

A number of case histories are listed in Table 3.1. Based on the influencing factors of slopes reinforced with piles, the case histories are summarized and discussed below.

A successful stabilizing pile can be discussed in three parts. First, the characteristics of slopes, such as the dimension, depth of the slip surface, and geometry of the slope are reviewed. Second, the properties of a pile are discussed. In this part, steel and concrete are the primary materials of the stabilizing piles. They can be further divided into bored concrete piles, drilled shafts, steel pipe piles, steel box piles and so on. Both steel and concrete piles have some limitations on construction and will be discussed. Third, the properties of soils affecting the response of the stabilizing piles are discussed. In other words, the strength parameters of soils in slopes and soil movement play important roles in the performance of piled-slope system due to soil-structure interaction.

The parameters of all influential factors of stabilizing piles and the lessons from case histories are discussed in the following sections.

**Table 3.1 Case histories of slope reinforced with piles**

| Case | Type of size | Soil type | Pile type | Length and S/D | $X_p/X$ | Slope failure type | Pile head | $Z_s/L$ |
|---|---|---|---|---|---|---|---|---|
| Heyman (1965) | 4m High Embankment | Sand, peat clay underlain by sand | Steel Box t=6mm 300*300mm | 12.5m | 0 | 15mm @ 12 m from the toe, 30mm @ toe | NA | NA |
| Leussink and Wenz (1969) | Embankment | Clay, $C_u$=15 kPa | 0.85 m steel square box | 30m | NA | Hyperbolic soil movement with 0.5 m maximum | Hinge to restrained head | |
| Bigot *et al.* (1977) | Embankment | NA | Steel tube pile D=926 mm t=15 mm | L=24m, | NA | Hyperbolic soil movement with 0.18 m maximum | Free | 0.63 |
| Stewart (1992) | Embankment | 0.5m surface sand, 18 m kaolin, 6m dense sand | 0.4m*0.4m Square pile | 22.5m | NA | Hyperbolic, Maximum 0.15m | Free | 0.8 |
| Polous (1990) | Bypass in Newcastle β=26.6 | 1.5-2.0 m thick high plasticity clay relatively stiff | Bored concrete pile D=1.2 m, | L=9m S/D=2~4 | 0.5 | Uniform soil movement Circular slip surface | Free | 0.5 |
| Fukumoto (1975) | Landslide in Niigata, Japan | Coefficient of subgrade reaction $K_h$ = 5 MPa (sliding layer) $K_h$= 8 MPa(stable layer) | Steel pipe pile D=318.5 mm. t=6.9mm | L=24 m S/D=12.5 | NA | Linear | Free | 0.5 |

**Table 3.1 Case histories of slope reinforced with piles (continued)**

| Case | Type of size | Soil type | Pile type | Length and S/D | $X_p/X$ | Slope failure type | Pile head | $Z_s/L$ |
|---|---|---|---|---|---|---|---|---|
| Fukumoto (1975) | Landslide in Niigata, Japan | Coefficient of subgrade reaction $K_h$<br>$K_h$ = 5 MPa (sliding layer)<br>$K_h$=15 MPa(stable layer) | Steel pipe pile<br>D=318.5 mm.<br>t=6.9mm | L=17m | NA | Linear soil movement | Free | 0.48 |
| Fukumoto (1975) | Landslide in Kamimoku, Japan | Coefficient of subgrade reaction Kh<br>Kh = 5 MPa (sliding layer)<br>Kh=8 MPa(stable layer) | Steel pipe pile<br>D=318.5mm.<br>t=6.9mm | L=14m<br>S/D=12.5 | | Linear soil movement | Free | 0.47 |
| Fukumoto (1976) | Landslide in Kamimoku, Japan | Coefficient of subgrade reaction Kh<br>$K_h$ = 5 MPa (sliding layer)<br>$K_h$=8 MPa(stable layer) | Steel pipe pile<br>D=318.5mm.<br>t=6.9mm | L=10m | ~0 and ~1.0 | | Free | 0.4 |
| Fukumoto (1972) | Landslide in Katamachi, Japan | Clay, $S_u$=30kPa<br>Clay, $S_u$=50kPa | Reinforced Concrete<br>D=0.3m<br>t=60mm | L=13m | | Planar sliding | Free | 0.55 |
| Esu and D' Elia (1974) | Active landslide | Clay, $C_u$=40 kPa linearly from 0 at surface to 80 kPa to the tip | Reinforced Concrete<br>D=0.79m | L=30m | | Planar sliding surface | Free | 0.25 |

**Table 3.1 Case histories of slope reinforced with piles (continued)**

| Case | Type of size | Soil type | Pile type | Length and S/D | $X_p/X$ | Slope failure type | Pile head | $Z_s/L$ |
|---|---|---|---|---|---|---|---|---|
| De Beer and Wallays (1) | Embankment Zelzate in Belgium | | Steel pipe pile D=0.9m, t=15mm | 28m | | Linear (Triangular) | Hinged | 0.63 |
| De Beer and Wallays (2) | Zelzate in Belgium | | Reinforced Concrete D=0.6m | 23.2m | | Linear (Triangular) | Hinged | 0.75 |
| Carrubba *et al.* (1989) | Sicily, Italy | Clay, $C_u$=30 kPa | Reinforced Concrete D=1.2m | 22m | | Uniform soil movement, | | 0.43 |
| Kalteziotis (1993) | Sliding slope | Lacustrine deposits | Steel pipe piles (two rows) D=1.03m, t=18mm S = 2.5m | L=12m S/D=2.5 | | Triangular soil movement | | 0.5 |
| Chow (1996) | Athens, Greece | $C_u$=100 kPa above, $C_u$=356 kPa below | Concrete Bored Piles D= 1m, S=2.5m | L=12m S/D=2.5 | | Uniform soil movement Planar sliding surface | | 0.33 |
| McClelland and Cox (1976) | River Delta Seashore structure | Clay, $C_u$=24 kPa | Steel tube Pile D=0.76m, t=7mm | Embedded seafloor 45m | NA | Uniform soil movement, Planar sliding | Free | 0.52 |

**Table 3.1 Case histories of slope reinforced with piles (continued)**

| Case | Type of size | Soil type | Pile type | Length and S/D | $X_p/X$ | Slope failure type | Pile head | $Z_s/L$ |
|---|---|---|---|---|---|---|---|---|
| Mc Clelland and Cox (1976) | Mississippi River | Clay, $C_u$=24 kPa | Steel tube Pile D=1.22m, t= 19mm | 120m | | Uniform soil movement | Fixed | 0.08 |
| Davies *et al.* 2000 | M25 Highway London, UK β=11°~15 200m*40m | Gault ($C_u$=100 kPa) Residual Gault ($C_u$=50 kPa) | Steel pipe D=1.0m S=2.5m | 16m S/D=2.5 | =1/3 | Uniform 38 mm | Free | 0.5 |
| Fukuoka (1977) | Kanogawa Dam 250m*125 m β=26.5° | | Steel pipe pile filled with concrete D=458 mm t=9mm | | ~0 | | | |
| Fukuoka (1977) | Hokuriku Expressway β=26.5° | | Steel pipe pile and steel H pile D=0.6m | 20m | ~0 | | | |
| Fukuoka (1977) | Niigata Prefecture 130m * 40m β=12.4° | Clay and silt Weathered mudstone | Steel pipe D=318.5mm, t= 6.9mm D=318.5mm, t= 10.3 mm | 20m | ~0 | Planar | Free | 0.25 |

**Table 3.1 Case histories of slope reinforced with piles (continued)**

| Case | Type of size | Soil type | Pile type | Length and S/D | $X_p/X$ | Slope failure type | Pile head | $Z_s/L$ |
|---|---|---|---|---|---|---|---|---|
| Robert Liang (2002) | Pomeroy Landslide, USA | Soil-rock interface properties c=3.4 kPa, ϕ=16.5 | Drilled shafts D=1.22m S=2.44m | Rock-socket length of 2m | ~0 | Planar | Free | 0.6 |
| Yamin (2007) | State Route 152 at Jefferson County, OH 280*35 ft β=10° | | drilled shafts D=1.07m S=2.14m | Rock-socket 6.1 m L=13.7 S/D=2 | 0.5 | Uniform to hyperbolic | Free | 0.55 |
| Yamin (2007) | WAS-7 site, OH, USA 1093ft*100 ft β=5.2° | Colluvium Alluvium Residuum Soft Rock | Drilled Shafts D=1.22m S=3.66m | Rock-socket 3 m L=12 m S/D=3 | 0.5 | Uniform to hyperbolic | Free | 0.75 |
| Yamin (2007) | State Route 376 Muskingum River 152ft* 50 ft β=18° | | Drilled Shafts D=1.22m S=2.44m | Rock-socket 6m L=13.3m S/D=2 | | Uniform to hyperbolic | Free | 0.55 |

Table 3.1 Case histories of slope reinforced with piles (continued)

**Table 3.1 Case histories of slope reinforced with piles (continued)**

| Case | Type of size | Soil type | Pile type | Length and S/D | $X_p/X$ | Slope failure type | Pile head | $Z_s/L$ |
|---|---|---|---|---|---|---|---|---|
| Polysou *et al.* (1998) | Landslide<br>Beatton River Highway, Canada<br>β=10°<br>200m*305m<br>15-20m | NA | Steel tube piles<br>D=1-1.5 m<br>t=19-25 mm<br>S=1.54 m | L=24m | 0.5 | Planar | Free | 0.46 |
| Ito *et al.* (1981) | Landslide<br>65m*95m<br>β=25° | Clay ($\gamma$=16.2 kN/m$^3$, c=9.8 kN/m$^2$, $\phi$'=5) | Steel pipe<br>D=711.2mm<br>t=22mm | L=5m<br>S/D=2.5 | 1/3 | Planar sliding surface | Unrotated | 0.6 |

## 3.3 Characteristics of Slope

### 3.3.1 Dimension of Slopes

Generally speaking, the dimensions of slopes vary from case to case and can be small as an embankment of a highway or as large as a large landslide. Reviewing the cases shown in Table 3.1 reveals slopes ranging from a four meter high embankment (Heyman 1965) to the largest being a 250 meter long 125 meter high embankment at the Kanogawa Dam in Japan (Fukuoka, 1977). In the case of the M25 highway, UK (Davies, *et al.* 2000), the landslide with 200 meters long and 25 meters high, the slope angle is estimated between 11~15˚. The slope failure mobilized over 90,000 $m^3$ of material (Davies, *et al.* 2000). Fukuoka (1977) discusses a slope 130m by 40m with a 12.4˚ slope angle. Generally speaking, the angle of the failed slope is small. The dimension of a slope determines the number of piles and the number of rows of piles to be used. In Fukumoto (1977), two rows of piles have been built in different locations. Each row has 95 and 100 piles, respectively. In the Hokuriku Expressway, Japan (Fukuoka, 1977) landslide, 4 rows of piles have been used to stabilize a huge landslide. Yamin (2007) presents three cases in Ohio with one row of drilled shafts installed individually, their dimensions are 60m by 7.6m, 200 ft by 60 ft and 70 ft by 40 ft, respectively.

### 3.3.2 Depth and Type of Slip Surfaces

The depth of the slip surface relates to the length of pile to be used to stabilize the slope. In most landslide cases, the slip surfaces range from 8 to 12 m and the type of the slip surface is usually non-circular or planar. The case in the Mississippi River Delta (Lee *et al*. 1991), the slip surface reached about 23.5 m. As a result, the length of pile is usually taken about two times the depth of the slip surface since the soil below the slip surface is usually regarded as a stable layer or stiff layer. The ratio $Z_s/L$ ($Z_s$: depth of slip surface, L: the length of pile) presents the percentage of portion of pile in the stable layer and in the unstable layer. The ratio in many case histories is selected as around 0.5 (Polous, 1995; Fukumoto, 1975; Carrubba *et al.*, 1989; Davies *et al*., 2000). Accordingly, the length of piles depends on the depth of slip surface. For an ideal design, maximum bending moment and maximum soil resistance should occur in the stable layer so that both pile and stable soil can provide sufficient resistance. The presence of stabilizing piles could also change the depth of slip surface due to the coupled effect between pile and soil. In the landslide cases in Japan (Fukumoto, 1975), the ratio of $Z_s/L$ ranging from 0.48 to 0.55 was adopted. Two cases presented by Yamin (2007) use 0.55 as the ratio of $Z_s/L$, the other one uses about 0.75. All three cases studied by Yamin (2007) have soft rock overlain by soil, in these cases, the length

socketed into the bedrock is significant in stabilizing the slope and the interface of soil-rock can be regarded as the slip surfaces. In the case presented by Esu and Elia (1974), the ratio of $Z_s/L$ is 0.25. In the Mississippi River offshore structure case, the long pile made the ratio $Z_s/L$ is as small as 0.08, which is called flow mode failure according to the definition by Hull *et al.* (1981).

### 3.3.3 Lateral Soil Movement

The lateral soil movement in these cases was measured using inclinometers. In Stewart (1992), the shape of soil movement from ground surface to slip surface was found to be hyperbolic and the maximum soil movement is 15cm on the ground surface. In the case in Sicily, Italy (Carrubba *et al.* 1989), the profile of soil movement is uniform from the ground to the slip surface. In the M25 Highway, UK (Davies *et al*. 2000), the soil movement is also uniform from inclinometer data, and the amount of soil movement after 19 months is about 38 mm. The case reported by Heyman (1965), the soil movement was measured larger at the toe compared to the soil movement in the middle. Yamin (2002) observed the soil movement by installing the inclinometer along with a drilled shaft is initially uniform below the ground surface but becomes a hyperbolic shape in the long run. In these pile-slope cases, the relative

soil movement between soil and piles is more important in investigating the pile-soil interaction mechanism based on the displacement-based method which the depth of the slip surface has to be pre-defined. The pressure applied to the piles is due to the lateral soil movement. To investigate the relative movement between the soil and pile is more important to research than the pile-soil interaction mechanism. The typical shape of the soil movement can be classified as (1) uniform, (2) linear, (3) trapezoidal, or (4) hyperbolic (see Figure 2.7).

## 3.4 Properties of Piles

The properties of piles include the pile type, pile length, diameter, spacing and the location where the piles are placed.

### 3.4.1 Pile Type

In stabilizing landslides and preventing the slope movement, both concrete and steel piles have been used. The types of pile include steel pipe pile, steel box pile, concrete pile, and drilled shaft. The row and length of piles depends upon the dimension of the slope in the cross section and the depth of slip surfaces. The number of piles used depends on the width of the slope. The diameter depends on the shear force and bending moment to be provided that is related to the area and bending stiffness EI. The maximum shear force in a pile is

typically found at the depth of the slip surface. The area of a pile in cross section affects the shear stress distribution in the pile. The moment of inertia of a pile cross section depends on the diameter and the thickness if steel tube piles are used. A larger bending stiffness can reduce the deformation of pile due to moving slides. The spacing depends on the required factor of safety which is typically promoted by incorporating the arching effect (Chen and Martin, 2003). The group effect in a sandy soil is more significant than other soil types and has to been taken into consideration in the numerical analysis (Liang, 2003). In the past, timber piles were first to be used in slope stabilization, concrete piles were brought to be used thereafter. Then steel piles were used for the same purpose. The importance of the pile materials is to provide sufficient strength to resist the shear force, bending moment and the deformation due to the lateral soil movement. So, the strength modulus of the material and the moment of inertia of a cross section determine the key factors of a single pile to be used. In addition, the constructability of a pile has also to be taken into account. Driven piles, cast in place piles or drilled shaft are suitable.

### 3.4.2 Length Effect

According to the case histories, most of the length of piles is between 12 to 24m, the ratio of depth to the length ($Z_s$/L) is around 0.5. In other words, the length of the pile above the slip surface is equivalent to the length in the stable layer. The length effect of the pile depends on the $Z_s$/L ratio. There is no absolutely appropriate pile length to be used because it is dependent on the dimension of the slope and the depth of potential slip surface. In some special cases, such as the offshore pile foundation in Mississippi River Delta (Lee *et al*. 1991), the piles used in both cases are long piles, with lengths of 45m and 120m of steel tube. The $Z_s$/L is relatively small which is only 0.083, however, it is not an often used method to stabilize slopes.

### 3.4.3 Diameter Effect

The diameter of piles can be discussed according to the materials used and workability. In concrete piles, the diameter is more flexible to design. It can be a cast-in-place pile or a driven pile. The diameter of cast–in-place concrete piles is usually larger. From the cases listed in Table 3.1, regardless of concrete piles and steel piles, the diameter ranges from 0.3m to 1.2m. In the field, an engineer may care more about the ratio S/D (S: spacing between

piles from center to center, D: diameter of piles) so that the number of piles can be determined.

### 3.4.4 Spacing Effect

The spacing of piles is very important to a row of stabilizing piles. In the case histories listed in Table 3.1, the ratio S/D ranges between 2 and 3. The stress applied on each pile and the factor of safety can be increased depending on the spacing of the piles in a row or the spacing between the pile rows. In a sandy soil, the arching effect is also related to the spacing of piles (Tien, 1990). Usually, the effect of spacing depends on the ratio of space between center and center of piles to the diameter of piles S/D (Tien, 1990). In Kalterziotis (1993) and Chow (1996), the ratio of S/D is around 2.5 in clayey soils. The threshold ratio of S/D is between 3.0 (Cox, *et al.* 1983) and 5.0 (Shibata *et al.* 1989). Liang (2002) found the arching effect becomes most pronounced at S/D=2.0 in sandy slopes and 1.5 in clayey slopes when drilled shafts are installed. When S/D is larger than 8.0, there is no arching effect and each shaft behaves like a single shaft.

### 3.4.5 Location of Piles

The pile location is also one of the more important influencing factors the pile stabilization. However, few cases indicated the location of pile where piles were placed. Most cases use one row of piles in a certain location in a slope. However, some cases use two rows of piles in different locations, respectively in different time series. The case in Fukumoto's paper (1976), one row of piles were installed close to the toe then another row of piles were installed close to the crest one year after. The three cases discussed in Fukuoka's paper (1977), the piles were basically installed around the toe. Polous (1999) presented a case in Newcastle, Australia, where the location of pile is in the middle portion of the slope. Davies *et al.* (2000) indicated the pile location is one-third away from the toe in the slope in M25 Highway, UK. Yamin (2007) also studies two cases with drilled shafts which are placed in the middle portion of the both slopes. Ito *et al.* (1981) shows the location of piles in this landslide case is one-third away from the toe. The landslide along the Beatton River Highway in Canada (Polysou *et al*., 1998) has the pile position in the middle portion of the slope.

### 3.5 Soil Properties

In the evaluation of a landslide, strength parameters of the soil, the cohesion and internal friction angle are controlling factors of the slope stability. In addition, the soil movement will affect the response of stabilizing piles no matter the shape of soil movement profile or the amount of soil movement. From these cited cases, stabilizing piles were used to deal with clayey soil in most cases and usually weak soils overlaid the stronger soils. Or, the residual is soil underlain by the rock. The clay of a failed mass usually has a low cohesion and a low internal friction angle. The failure surfaces are usually non-circular or planar failure surfaces.

### 3.6 Implications of Case Histories

The case histories provide experiences and based on the information, the engineers can make preliminary design decisions. The implications of using stabilizing piles are summarized based on the length of pile, properties of pile material, size, spacing, pile location, soil properties and so on. From these cases histories, experience may provide good solutions to stabilize the slopes using a similar design. However, the successful application of case histories proves the slope reinforced with piles is an efficient approach was used.

The stability of pile-stabilized slopes depends on the geometry of slopes, properties of piles and soil properties. However, the only factor which engineers can control is the properties of the piles and design. The geometry of the slopes and the properties of soils are not easily controlled and generally must be accepted as is.

The implications of the case histories thus only focus on the pile design. However, the successful design of a pile is still relevant to the external conditions given from the geometry of the slopes and soil properties. As discussed previously, an adequate pile design selects the strength of materials, length, diameter, spacing, number and location of the piles in a slope.

In the characteristics of pile materials, the properties of pile section such as Young's modulus of concrete and steel is not able to change and the types can be selected are limited due to the limitations of the materials.

In length of piles, most of the case histories used a ratio of depth of slip surface to the length of pile ($Z_s/L$) close to 0.5 or less. This ratio is very reasonable because the approach can make the maximum bending moment and shear force to occur in stable soil by installing more than 50% of the pile in the stiff layer. According to the coupled numerical analysis between soil and pile interaction presented by Won *et al.* (2005), the potential slip surface

may go deeper when the stabilizing pile is inserted. Therefore, if the design ratio is slightly less than 0.5, or about 0.45, the potential slip surface will go deeper to make the ratio at around 0.5. When the ratio $Z_s$/L is around 0.5, according to the definition by Lee *et al.* (1991), the failure mode of a pile is called an intermediate mode. In this failure mode, the maximum bending moment will occur in the pile in the stable layer. As long as the maximum bending moment falls in the stable layer, the design of material strength and diameter or cross section of piles can be determined accordingly.

In most of the cases, the diameter has to be considered together with the spacing. Accordingly, a ratio of distance between center to center of two piles to diameter, S/D, is more important than the diameter of pile. When this ratio is greater than 4.0, the group effect and the arching effect does not have to be considered and a single pile behavior can be assumed adequately. However, the phenomenon of arching effect is still not fully understood and the necessary requirements for soil arching to occur is not easy to quantify and is generally regarded as contributing to the capacity of the piled-slope system. As for the pile location, some of these papers propose the adequate location is the middle of the slope, while others thought the location near the toe is most reasonable. However, the initial or potentially initial failure in a slope is different from case to case, the adequate location may change.

According to Fukuoka (1977), the construction of a pile may be started from the location where the displacement velocity is the lowest or from the parts which the acting load on the piles is the smallest which depends on the soil type. In overconsolidated soils, the failure starts from the toe, so putting piles at toe is more beneficial.

Although the case histories provide valuable information, the listed case histories are often lacking in practical details. For example, the pile position is not included in most of the case histories. In some cases, pile head conditions are not clear either. In other cases, the depth of the slip surface was not detailed. Consequently, with the limited information, the further numerical work can be performed to integrate all the required information in design. With the results of numerical analysis, back calculation and models can be calibrated with available data.

### 3.7 Summary and Conclusions

The case studies presented in this paper provide good insight on the design of stabilizing piles due to lateral soil movement of slope failures. However, the case studies discussed generally lacked sufficient information on all aspects of a successful design. Based on the

review of the case histories, several conclusions and suggestions are made in the following subsection.

### 3.7.1 Conclusions

(1) Piles have proven to be successfully applied in stabilizing slopes and increasing the factor of safety of a failing slope or a potential failure slope.

(2) Both reinforced concrete piles and steel pipe piles or combination piles have been selected to be used in slope stabilization. Besides considering the type of piles, other factors, such as workability, cost and transportation of piles also have to be considered.

(3) The ratio of the slip surface to the length of pile, $Z_s/L$ most likely should range between 0.45-0.50. If the ratio is too small, not only could the failure mode be changed, but a waste in material and an uneconomical design may result. If the ratio is too large, it could lead to the maximum bending moment falling in the part of pile in the sliding layer. This is not favorable in design and will lower the efficiency by increasing the factor of safety of a slope.

(4) The group effect of stabilizing piles is pronounced when S/D is small which is usually smaller than 3.0, when the S/D is larger than 8.0, the group effect is not significant and the pile behaves like a single pile.

(5) In most of the case histories, the slip surfaces are non-circular or planar. However, in the slope stability analysis, whether using the traditional limit equilibrium method or continuum numerical methods, the potential slip surfaces are usually circular. Thus, before performing a numerical analysis for design purposes, a site investigation and soil properties have to be fully understood. Otherwise, the error between practice and numerical modeling can be large.

# CHAPTER 4: HOMOGENEOUS SLOPE WITHOUT FOUNDATION

## 4.1 Introduction

This chapter presents analyses of the case of a homogeneous slope without a foundation. The unreinforced case is reviewed first, followed by an analysis of the case reinforced with piles in a two-dimensional model. The case is first described, with factors of safety of the unreinforced slope compared to solutions by Griffiths and Lane (1999) and Rocscience (2004). Piles are then introduced into the case, analyses conducted and the results discussed.

## 4.2 Case Description

In this case, the geometry of a homogeneous slope without foundation, is shown in Figure 4.1. This case follows that analyzed by Griffiths and Lane (1999) and Rocscience (2004) as a benchmark case to study the applicability of finite element analyses to slope stability. The slope and the proportion of the dimensions are also shown in Figure 4.1. The slope angle is 2H:1V or 26.56˚. The soil properties of this slope are listed in Table 4.1. For the analyses conducted herein, the height of the slope, H, is set at 40 m. To validate the results of analyses, the internal friction angle of the soil is 20˚, $c/\gamma H$ is set as 0.05, Young's Modulus, E is $10^5$ kPa, and Poisson's ratio is 0.3, as used by Griffiths and Lane (1999) and Rocscience (2004).

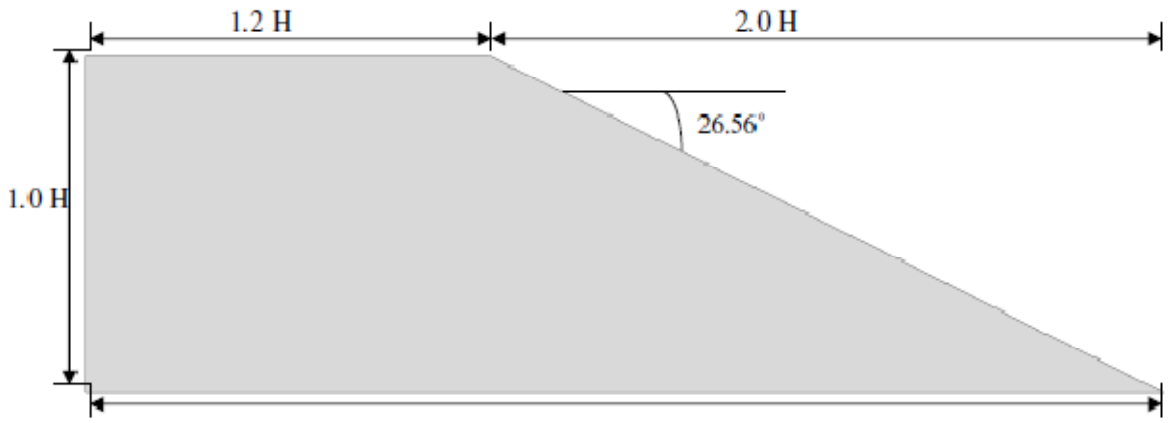


**Figure 4.1 Homogeneous slope without foundation**

**Table 4.1 Slope dimension and material properties**

| E ($kN/m^2$) | $\phi$ (°) | $\gamma$ ($kN/m^3$) | $\nu$ | C ($kN/m^2$) | H (m) |
|---|---|---|---|---|---|
| 100000 | 20 | 20 | 0.3 | 40 | 40 |

### 4.3 Unreinforced Slope Stability Analysis

The factor of safety in slope stability analyses can be determined by limit equilibrium, finite difference or finite element methods (Duncan 1996). As discussed in the literature review, the limit equilibrium method is a well known method for determining the factor of safety of a slope. For finite element and finite difference methods, the Strength Reduction Method (SRM) can be used to find the factor of safety of a slope. For the cases studied herein, the factor of safety of the slope found using the limit equilibrium methods in SLOPE/W

(Geoslope, 2004) and the finite element method using ABAQUS (2009). The slope shown in Figure 4-1 has been previously analyzed by Griffiths and Lane (1999) and Rocscience (2004). For validation purposes of the programs used in this study, slope stability analyses of the slope were conducted. The slope conditions for the limit equilibrium analyses are those shown in Figure 4.1. For the finite element analyses, the mesh shown in Figure 4.2 was used. The element type in this model is selected as a 6-node triangular and 8-node quadrilateral with reduced integration, respectively. The elastic-perfectly plastic Mohr-Coulomb failure criterion is used in the soil model. The dilation angle of the soil is selected as 0°, so the plastic potential of the soil constitutive model is non-associated flow. The factor of safety (FS) of the homogeneous slope is defined as the maximum value of strength reduction factor (SRF) which brought the slope failure by using strength reduction technique. (Griffiths and Lane, 1999).

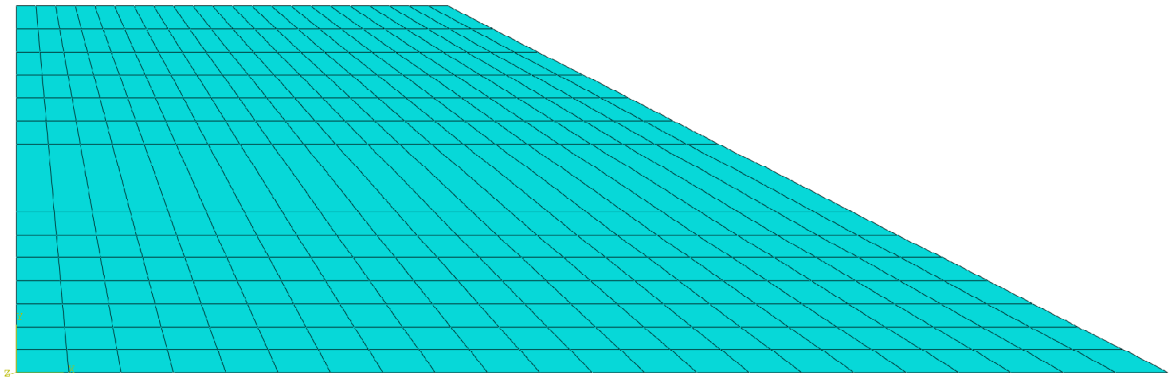

**Figure 4.2 Mesh of finite element model (ABAQUS)**

### 4.3.1 Results Validation and Comparisons

The factor of safety of this case is based on limit equilibrium analyses using the Bishop Simplified method as has been reported as 1.38 (Rocscience 2004) and as 1.40 using the Bishop and Morgenstern charts (Griffiths and Lane 1999). This slope was analyzed using the limit equilibrium computer program SLOPE/W (Geoslope 2004). The failure modes are shown in Figures 4.3 and 4.4, with resulting factors of safety of 1.386 and 1.383, respectively for general failure and toe failure. These values compare very favorably with those of Rocsicence (2004) and the chart solution of Bishop and Morgenstern (1960). SLOPE/W uses a variety of limit equilibrium methods to find the factor of safety of the slope. The complete results are shown in Table 4.2. The Morgenstern-Price method is generally regarded as the

most accurate limit equilibrium method and thus the factor of safety of slope can be regarded as 1.38. Thus the results found in this study compare favorably with those found by others.

Factors of safety for this case using finite element analyses with the SRM have been conducted by Griffiths and Lane (1999) and Rocscience (2004). The results are shown in Table 4.3 when using 8-node quadrilateral elements. It can be seen that the values of 1.4 and 1.42 are slightly higher than the Bishop factor of safety of 1.38. This case was analyzed using ABAQUS and the SRM with 8 node quadrilateral elements, resulting in a factor of safety of 1.38. The deformed mesh and plastic strain contours are shown in Figure 4.5. The undeformed mesh with contours of plastic strain contours are shown in Figure 4.6 and it can be seen that the failure surface compares very well with the failure surface from limit equilibrium methods (Figures 4.3 and 4.4).

To further compare the results or errors that may be caused due to the selection of different types of elements, 3-node and 6-node triangular elements and 4-node and 8-node quadrilateral elements were also used to determine the factors of safety. This follows the use of these elements by Rocscience (2004). The results are shown in Table 4.4 for Griffiths and Lane (1999), Rocscience (2004) and this study. It can be seen that using three noded

triangular elements provides factors of safety higher than the accepted value of 1.38, as does the Rocsciece result for a four-node quadrilateral element. This is attributed to the lower order and fewer integration points per element. When higher order elements with more integration points are used, T6 and Q8 elements, the results compare more favorably with the value of 1.38. The differences between the Griffiths and Lane, Rocscience and ABAQUS results are small, yet measureable; however, the reasons for the differences have not been determined. These results do indicate that the factor of safety of slopes can be accurately determined using finite element analyses and the SRM using T6 and Q8 elements. Such elements have been adopted for the remainder of the ABAQUS analyses in this study.

**Table 4.2 Results of numerical analysis in slope stability, homogeneous slope**

| Method | Janbu | Bishop | Spencer | GLE | Ordinary | Morgenstern-Price |
|---|---|---|---|---|---|---|
| **Toe** | 1.298 | 1.383 | 1.382 | 1.385 | 1.318 | 1.385 |
| **Slope** | 1.302 | 1.386 | 1.376 | 1.373 | 1.317 | 1.373 |

**Table 4.3 Factor of Safety (SRF) using different methods**

| Bishop | Griffiths | Rocscience Inc. | ABAQUS |
|---|---|---|---|
| 1.38 | 1.4 | 1.42 | 1.38 |

**Table 4.4 Comparisons of results from different element types in finite element analyses**

| Program | T3 | T6 | Q4 | Q8 |
|---|---|---|---|---|
| **Griffiths and Lane (1999)** | | | | 1.4 |
| **Rocscience (2004)** | 1.51 | 1.39 | 1.47 | 1.42 |
| **ABAQUS** | 1.70 | 1.39 | 1.37 | 1.38 |

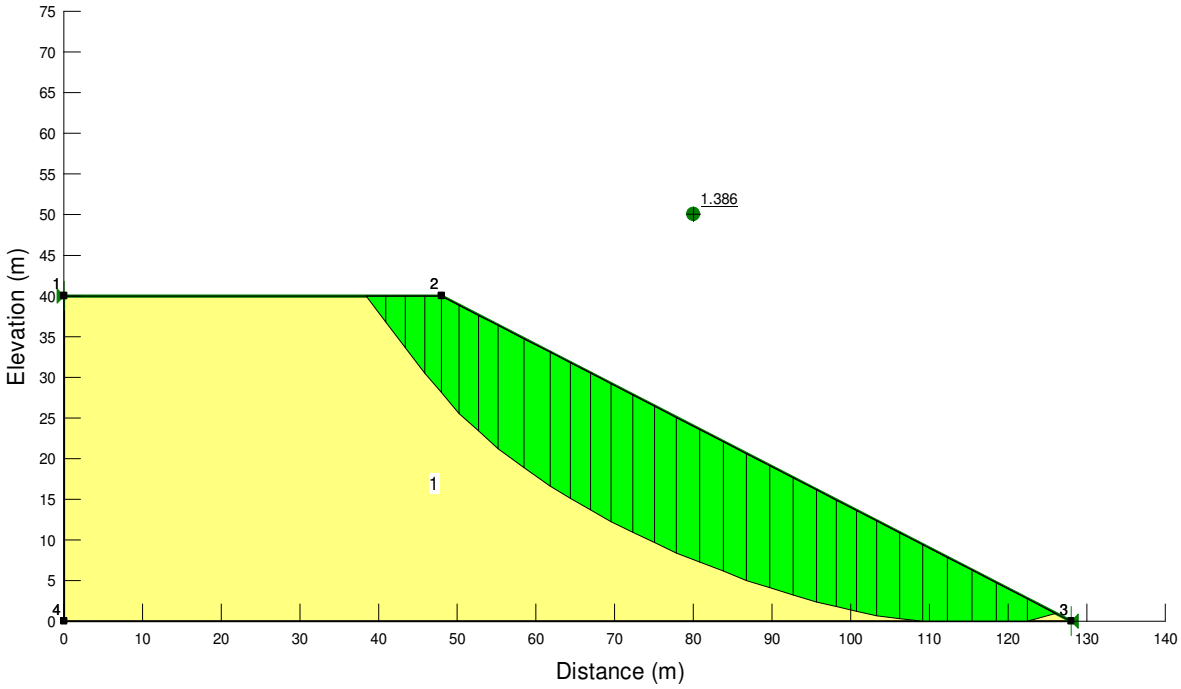


**Figure 4.3 Analysis using SLOPE/W (Bishop method)–slope failure, FS=1.386**

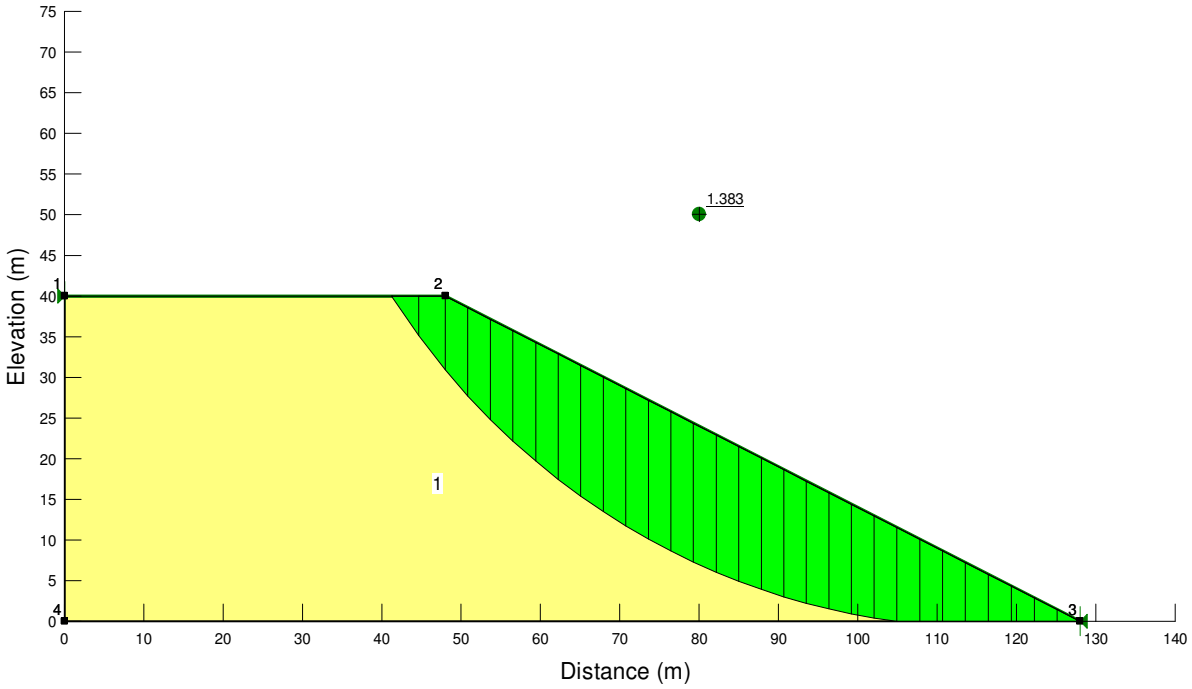


**Figure 4.4 Analysis using SLOPE/W (Bishop method)–toe failure, FS=1.383**

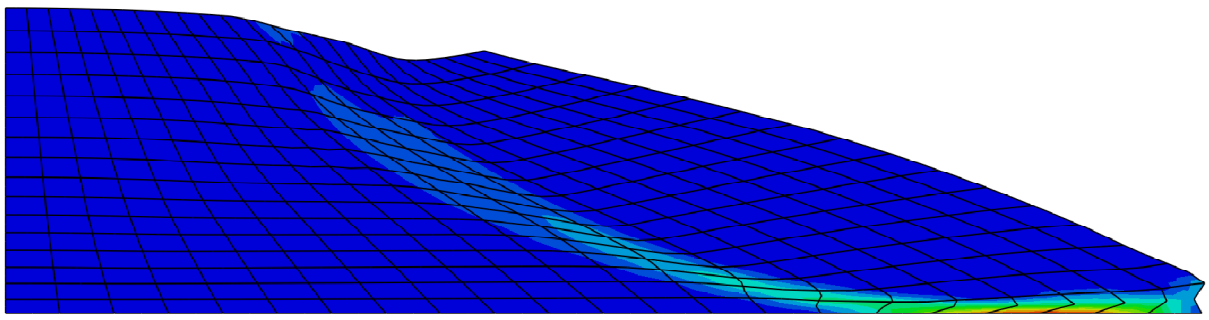

**Figure 4.5 Deformed mesh and plastic strain contour of slope (FS=1.38)**

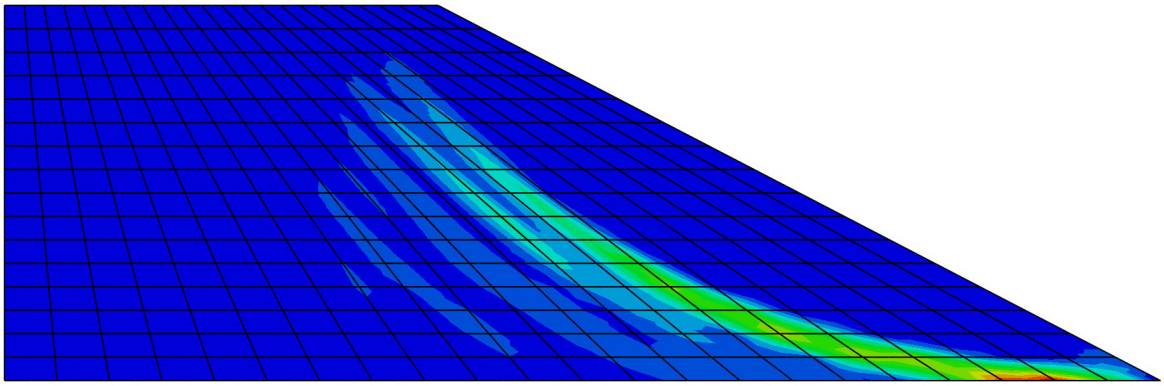

**Figure 4.6 Undeformed mesh and contour of plastic strain in ABAQUS (FS=1.38)**

## 4.4 Analysis of Slope Stability Using Piles

This section is including the pile stabilization case description, the analyses based on the pile location, pile length and the pile head condition.

### 4.4.1 Pile Stabilization Case Description

Reinforcement of a slope using piles can be achieved by inserting a pile along to the slope to a selected depth. Figure 4.7 shows this case with a pile inserted into the slope. The length of the pile is represented by L and the distance $X_p$ represents the location of the pile from the toe of the slope. X represents the horizontal length of the slope from the toe to the crest, thus the ratio $X_p/X$ represents the relative location of the pile to the toe and the crest.

The pile is assumed to be an elastic media. The pile is simulated as an elastic material with 2-D plane stress element, 8 nodes with reduced integration. The Young's modulus (E) of the piles is 60000 MPa and Poisson's ratio (ν) is 0.2. The initial length of pile is assumed as 19m, which represents about one-half the slope height. Based on the limit equilibrium analyses, the failure surface at mid-slope is about 15m deep. Due to the geometry constraints in this particular case, the amount of pile in the stable zone is less than generally desired based on the case history review.

The soil material properties are taken to be the same as the unreinforced case, as shown in Table 4.1. To present the improvement of pile installed, an improvement ratio $N_{pi}$ in terms of percentage is defined and used herein. The definition of improvement ratio, $N_{pi}$ is as follows:

$$N_{pi} = \frac{F_p - F_s}{F_s} * 100\% \quad (4.1)$$

Here $F_p$ is minimum factor of safety of pile-slope system, $F_s$ is the minimum factor of safety of the slope stability problem without piles.

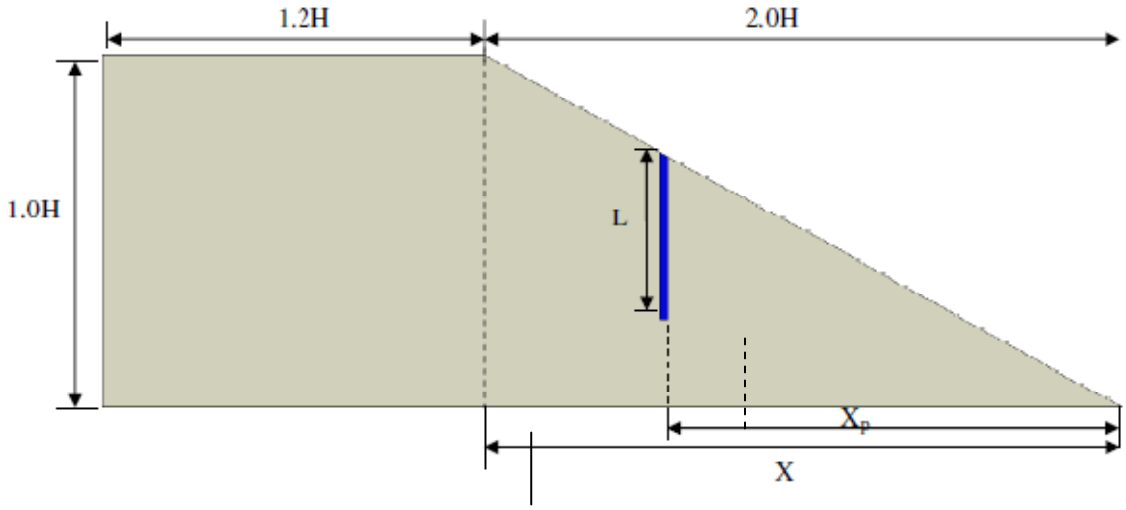


**Figure 4.7 Homogeneous slope reinforced with a pile**

In this study, the pile response and slope stability are considered simultaneously, which is the so called 'coupled analysis'. In numerical modeling of the piled slope system, the parameters of materials, the failure criteria, and pile-soil interaction properties have to be designated appropriately. The selection of element type of the pile is a 2-D plane stress, 8-node with reduced integration element, while the soil elements are 2-D plane strain, 8-node with reduced integration quadrilateral elements. The meshed model is shown in Figure 4.8. The property of interface element between pile and soil is assumed zero-thickness which can only transfer shear stress across the surfaces when a compressive normal pressure (p') is applied

on it. The pile soil friction coefficient, η, is 0.3, which is based on $\eta = \tan(\delta)$, where δ is friction angle between pile and surrounding soil.

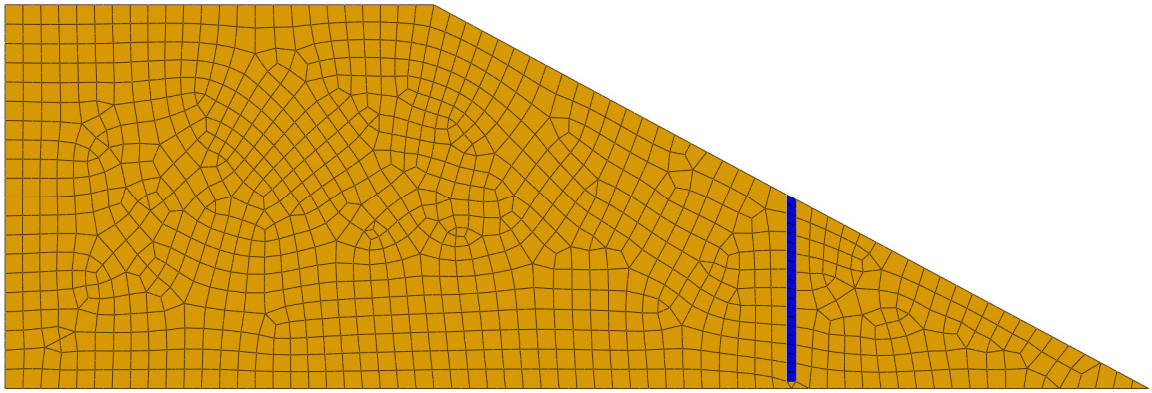

**Figure 4.8 Mesh of piled-slope system**

Analysis results for the optimal location of the pile, length of pile and failure mechanisms, and pile head conditions are presented below.

### 4.4.2 Optimal Pile Location

The results from finite element analysis using the strength reduction technique in terms of pile location are plotted in Figure 4.9. Both free and fixed pile head conditions were analyzed, resulting in the two curves shown and compared in Figure 4.9. The improvement rate in terms of the ratio $N_{pi}$ is presented in Figure 4.10. The ratio $X_p/X$ is used to represent the position of pile in terms of slope dimension. $X_p/X = 0$ means the position of the pile is at the

toe and $X_p/X$ indicates the position is at the crest of the slope. For the free pile head condition, the highest factor of safety of 1.77 occurs when the pile placed in the middle of the slope ($X_p/X=0.5$). The corresponding improvement rate ($N_{pi}$) is 28.3%. If the pile is placed close to the toe ($X_p/X=0.25$), the factor of safety is 1.55 and the ratio $N_{pi}$ is 12.3%. If the pile is placed at the crest ($X_p/X=1.0$), the factor of safety is 1.40 and $N_{pi}$ is only 1.45%, which is the lowest among all locations. When the fixed head condition is applied to the pile, the factor of safety when the pile is placed in the middle portion is 1.85, and the corresponding improvement rate ($N_{pi}$) is 34%. The factor of safety induced either at the toe or crest is consistent to the value obtained from the case due to free pile head. These results show that the optimal pile location is near the middle of the slope. Additionally, the fixed head condition provides a slight advantage over the free head condition in the middle of the slope, but no advantage occurs at the toe or the crest.

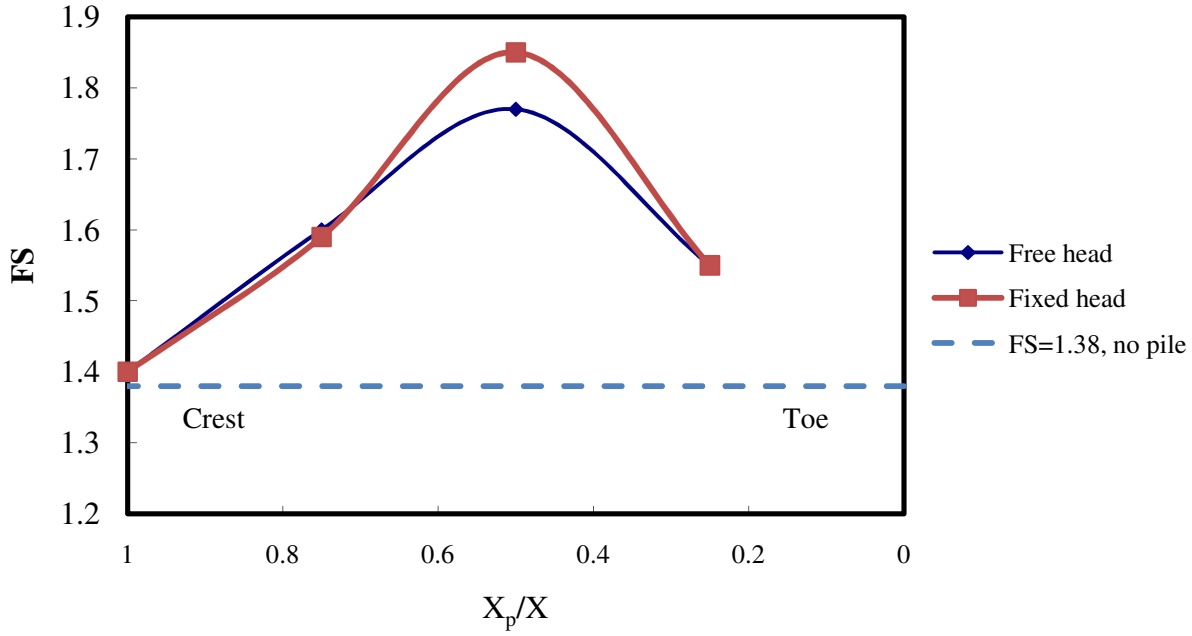


**Figure 4.9 Factor of safety versus $X_p/X$**

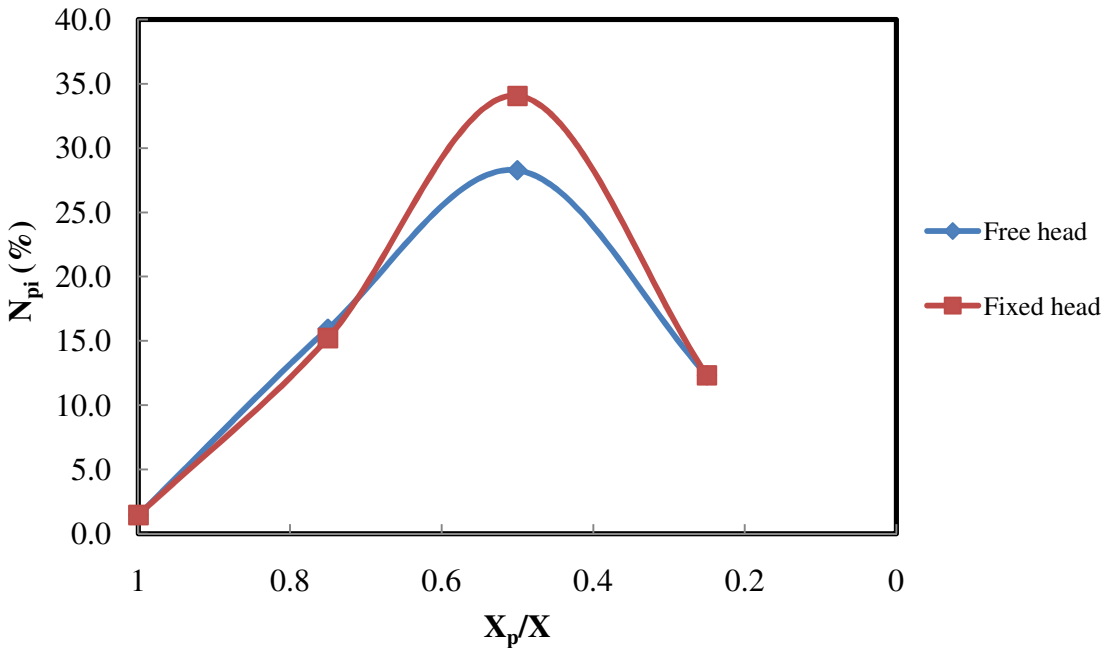


**Figure 4.10 $N_{pi}$ versus $X_p/X$**

### 4.4.3 Length of Pile

To study the effect of pile length, various lengths of piles were analyzed at the optimal pile location of $X_p/X = 0.5$. In terms of pile length, length of pile in this numerical analysis is the only variable based on the optimal location of pile concluded in this study. The pile length above the potential slip surface $L_z$ was found to be 15m based on the plastic strain contours shown in Figures 4.5 and 4.6. The results of numerical analysis are summarized in Table 4.5, which shows the factors of safety as the pile length is varied. Figures 4.11 and 4.12 show the highest factor of safety is developed when the pile length is between 10 and 15m. In Figure 4.11, the factor of safety of both free and fixed head pile are consistent if the length of pile is between 10 and 15m. When the pile is longer than 15 meters, the factor of safety contributed by the free head pile decreases slightly and that of the fixed head pile does not change. Due to the geometry constraints of the slope in this case (without a foundation), the ratio of $L_z/L$ is difficult to determine because the potential slip surface will be close and tangent to the firm base.

The contours of plastic strain with the various pile lengths are shown in Figures 4.13 to 4.18. These figures show the failure mechanisms that result when the various length piles are

inserted into the slope. In Figures 4.13 and 4.14, an 8 m length pile was modeled resulting in a factor of safety of 1.82 compared to the unreinforced case of 1.38 for both the free-head and fixed-head conditions. Because of the geometry constraints (no foundation) the failure surface in the reinforced and the reinforced case both go to the bottom of the slope, thus the pile does not affect the failure mechanism, but does lead to an increase in the factor of safety of the slope. The failure mechanism for a pile length of 10 m and fixed head conditions is shown in Figure 4.15. The resulting factor of safety of the slope is 1.83 and as shown in Figure 4.15, the failure surface now occurs at upslope of the pile indicating that the pile has altered the location of the failure surface from the base of the slope. The free-head case resulted in a similar failure mechanisms and an identical factor of safety. Additional cases were conducted using pile lengths of 15, 17 and 19 meters. All resulted in similar failure mechanisms with the failure surface forced upslope from the pile and the factors of safety shown in Table 4.5. The failure mechanism for a length of 17m and fixed head conditions is shown in Figure 4.16. As can be seen in Table 4.5 and Figure 4.11, the factor of safety of the fixed-head and the free-head conditions are the same until the pile length is greater than 15m, at which point the fixed head condition provides a slightly larger factor of safety.

**Table 4.5 Factor of safety of pile-stabilized slope based on length of pile**

| $X_p/X=0.5$ | | | | | | |
|---|---|---|---|---|---|---|
| **Pile length, L (m)** | **8** | **10** | **13** | **15** | **17** | **19** |
| **$L_z/L$ ($L_z$=15m)** | | | | 1.00 | 0.88 | 0.79 |
| **FS** | 1.82 | 1.83 | 1.83 | 1.83 | 1.78 | 1.77 |
| **$N_{pi}$ (%)** | 32.85 | 33.58 | 33.58 | 33.58 | 29.93 | 29.20 |
| **FS** | 1.82 | 1.83 | 1.83 | 1.83 | 1.83 | 1.85 |
| **$N_{pi}$ (%) (fixed head)** | 32.85 | 33.58 | 33.58 | 33.58 | 33.58 | 35.04 |

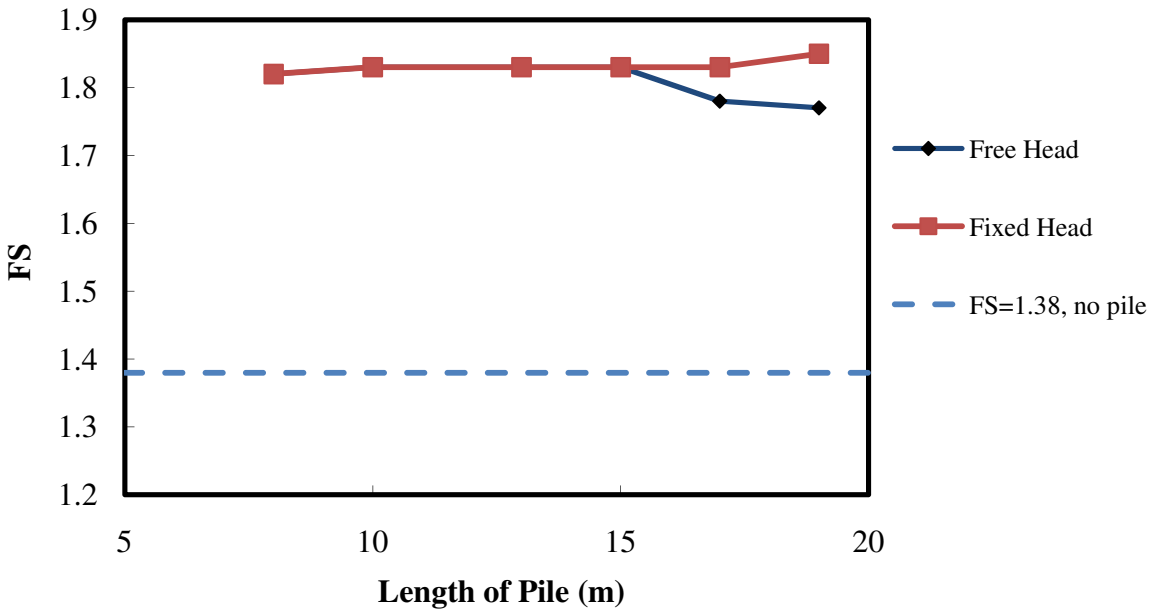


**Figure 4.11 Factor of safety versus Length of Pile**

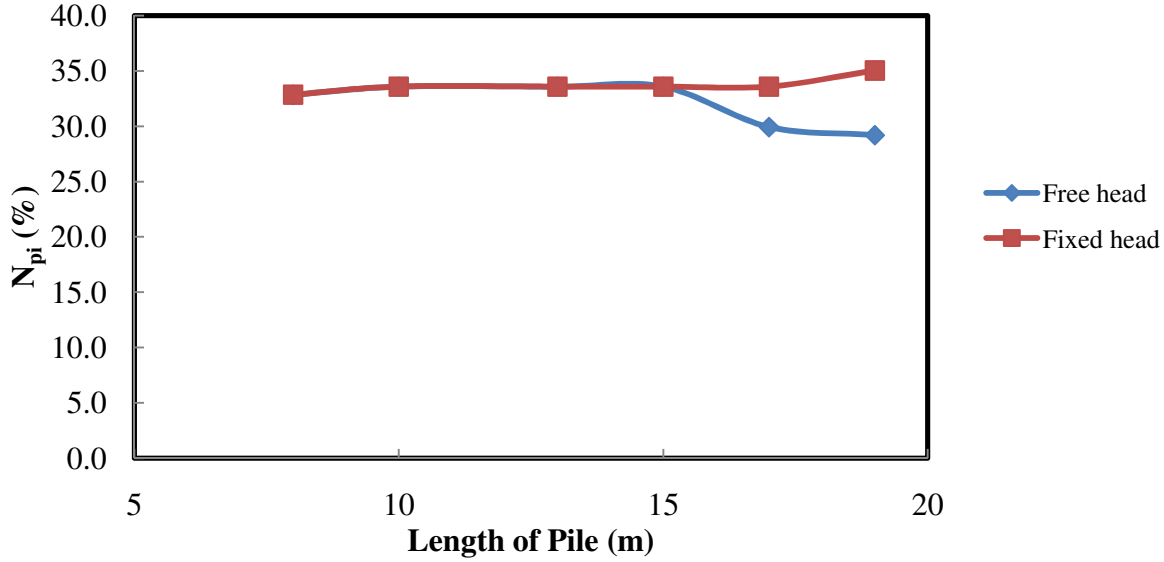


**Figure 4.12 $N_{pi}$ versus Length of Pile (Fixed head and Free head conditions)**

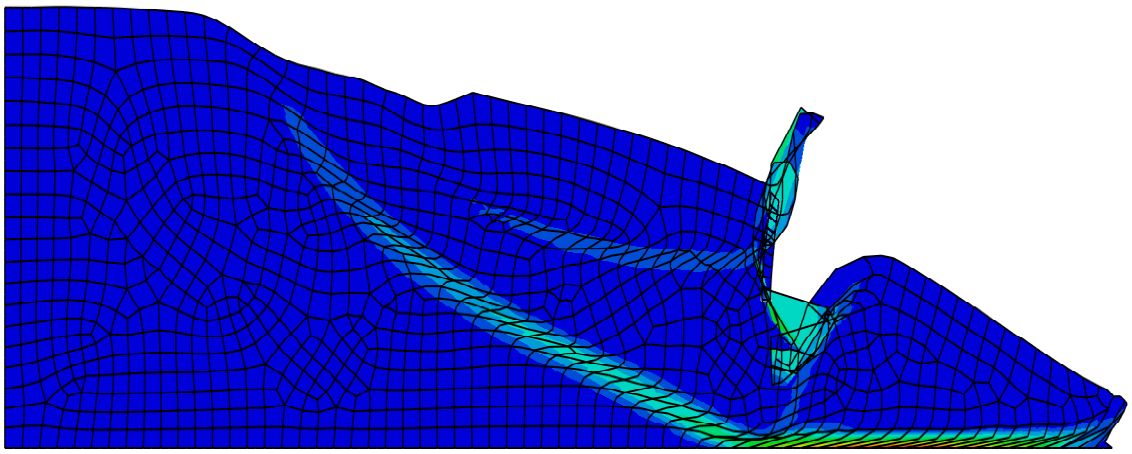

**Figure 4.13 The contour of plastic shear strain of slope with pile (L=8m, D=1m), free head, FS=1.82**

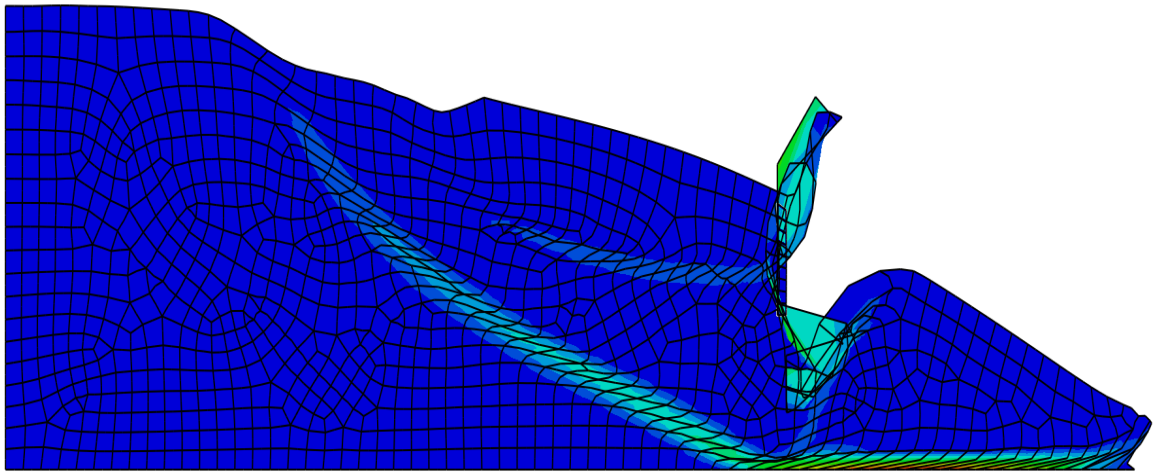

**Figure 4.14 The contour of plastic shear strain of slope with pile (L=8m, D=1m), fixed head, FS=1.82**

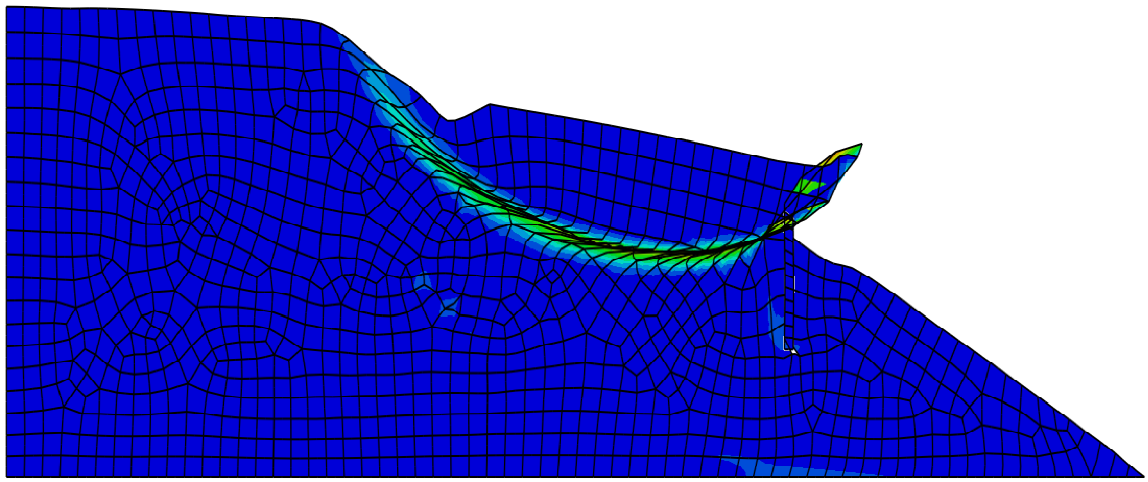

**Figure 4.15 The contour of plastic shear strain of slope with pile (L=10m, D=1m), fixed head, FS=1.83**

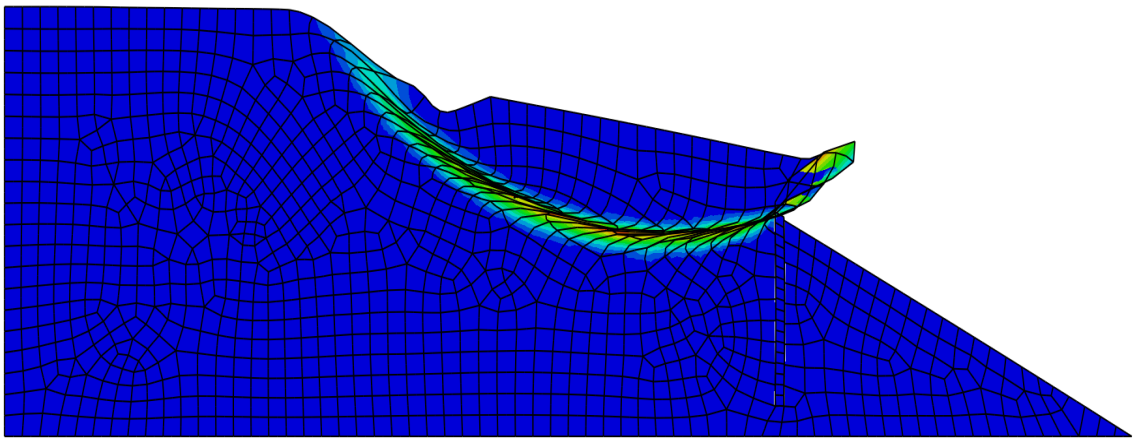

**Figure 4.16 The contour of plastic shear strain of slope with pile (L=17m, D=1m), fixed head, FS=1.83**

### 4.4.4 Pile Head Condition

Pile head conditions are also regarded as one of the important factors affecting the performance of stabilizing piles. In Figures 4.9 and 4.10, the pile with fixed head contributes a higher factor of safety than a free head pile if the pile placed in the middle of the slope. In other positions of the slope investigated, the factors of safety are almost the same regardless of pile head condition.

In terms of pile length, the results compared in Figures 4.11 and 4.12, the factor of safety is shown to be identical when the length of pile between 10 and 15m. When the pile is longer

than 15 m, the fixed head pile still leads the factor of safety on slope stability at around 1.83 which is pretty similar for the entire length with the same pile head condition. While the factor of safety of slope contributed by pile with free head condition slightly decreases. Therefore, when the pile is longer than 15 m, the fixed head pile is slightly more advantageous than the free head pile.

### 4.5 Discussion of Results

From the results summarized in Table 4.4, the factor of safety of the slope analyzed using finite element method with ABAQUS software are comparable with all of the studies by Griffiths and Lane (1999), Rocscience (2004) and limit equilibrium methods which assume the slip surface through the toe. Except for the Ordinary Method of Slices, the results of other limit equilibrium methods are very close. However, Ordinary Method of Slices has been regarded as a less accurate method in slope stability analysis (Duncan 1996). Therefore, a factor of safety of 1.38 for the unreinforced slope is a reliable value in this case.

Using the finite element method with the strength reduction technique, the factors influencing of stabilizing piles, namely optimal pile location, length of pile, and pile head conditions are investigated. The analysis results show that a pile placed in the middle of the

slope gives rise to the highest factor of safety. This is because the pile stops the movement of soil upslope and utilizes the soil response downslope. The results shown in Figure 4.9 illustrate the optimal location for the pile to be in the middle position resulting in the factor of safety 1.77 for free head pile and 1.85 for fixe head pile, which is the largest in the slope.

In terms of pile length, a pile length between 8 and 15m gives rise to the largest factor of safety and the optimal improvement in slope stability for the free head pile. If the pile head is restricted as fixed, a pile length between 8 and 15m is identical to the case with free pile head. When the pile is longer, a pile with a fixed head increases the factor of safety slightly but the pile with free head decreases a little bit.

When the pile is longer (>15m) , the factor of safety difference between free pile head and fixed pile head is obvious as shown in Figures 4.9 and 4.10. This is because the larger displacement occurs on the top to resist the slope failure. Therefore, restricting the pile head as a fixed type can result in the change of failure mechanism and location of slip surface. However, if the pile is shorter (L < 15m which is depth of potential slip surface), the pile head does not have much displacement in free pile head case and both the free pile head and fixed pile head lead to a similar failure mechanism.

## 4.6 Summary and Conclusions

The two-dimensional shear strength reduction finite element method is conducted using ABAQUS to investigate the homogeneous slope without foundation reinforced with a single pile. The pile-soil interaction and coupled analysis have been considered in the numerical study. Based on the effect of pile position, length of pile, pile head conditions, several conclusions can be made and is summarized as follows.

(1) The pile placed in the middle of the slope has been found to be the optimal pile location in homogeneous slope reinforced with the pile. The factor of safety is 1.77 when pile is placed in the middle for free pile head case, and 1.85 for fixed pile head case.

(2) The fixed head pile in terms of length does not show to be more advantageous than a free pile head condition. In this case, the pile length equal or shorter than 15m shows the identical improvement rate which is close to the highest factor of safety that can be reached regardless of pile head condition.

(3) Most previous studies have not taken the pile length into consideration. Obviously, pile length is an important influencing factor in piled slope system. Previous studies often adopted the pile length to be the same as the height of slope and in light of the

results here, this is unreasonable. In this case, if the pile is long enough, the difference on slope stability improvement will be presented. If the effect of pile length is not taken account, it may mislead the designer in that the fixed pile head condition usually provides more improvement on the slope stability of piled slope system.

(4) Using this case as an example, which is a homogeneous 2H:1V slope with a height of 40 m, the optimal pile design length is between 13 and 15 meters. Use of a longer pile does not increase the factor of safety more than a 15m length and would result in an uneconomical design.

# CHAPTER 5: HOMOGENEOUS SLOPE WITH FOUNDATION

## 5.1 Introduction

This chapter presents the case of a homogeneous slope and foundation. The chapter contents include a case description, slope analysis of the unreinforced slope using limit equilibrium and finite element methods, and analysis of the reinforced slope using finite element methods. The slope incorporating the pile is analyzed based on location, length and pile head conditions. The results are presented and discussed herein and summary and conclusions are made.

## 5.2 Case Description

In this case, a 2H:1V slope is underlain by a 0.5H thickness of foundation. The geometry of this case is shown as Figure 5.1. The unreinforced version of this slope has been analyzed by Griffiths and Lane (1999) and Rocscience (2004). Other properties and geometry of the slope are listed in Table 5.1

**Table 5.1 Slope dimension and material properties**

| E ($kN/m^2$) | $\phi$ (º) | $\gamma$ ($kN/m^3$) | $\nu$ | C ($kN/m^2$) | H (m) |
|---|---|---|---|---|---|
| 100000 | 20 | 20 | 0.3 | 40 | 40 |

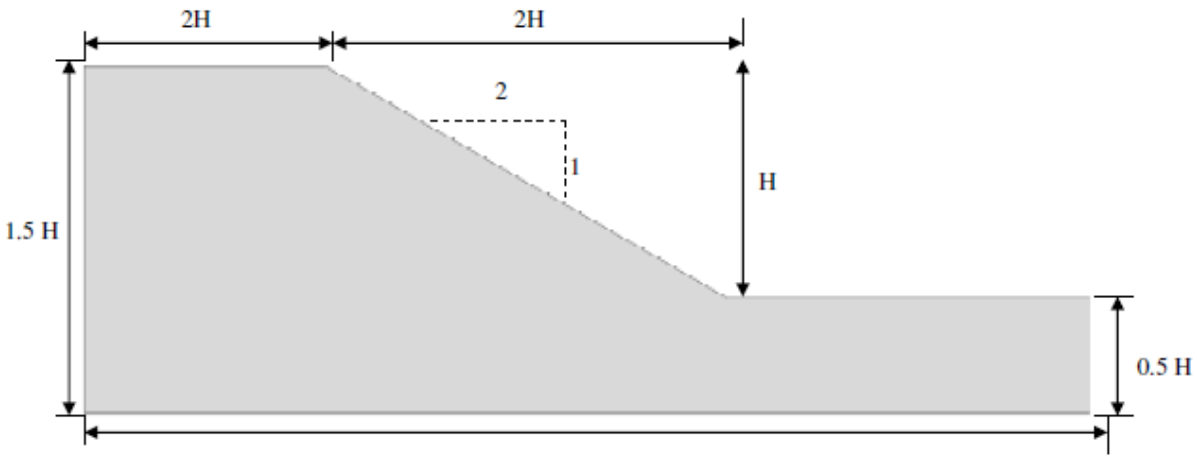


**Figure 5.1 Homogeneous slope with a foundation (D=1.5)**

### 5.3 Unreinforced Slope Stability Analysis

The geometry shown in Figure 5.1 was analyzed for slope stability with an overall height of 60m, thus the slope height was 40m and the foundation depth was 20m. The resulting factors of safety using limit equilibrium methods are shown in Table 5.2. Except for the Janbu's method, the factor of safety is indicated to be 1.37. Figures 5.2 and 5.3 show the results of circular and log spiral failure surfaces, respectively. Both of these two figures indicate that the critical failure surfaces pass through the toe of the slope, dipping down into the foundation materials.

This case was also analyzed using the finite element method. Based on the earlier results of the homogeneous slope, the element type was selected to be the 2-D plane strain, 8-node, quadrilateral element with reduced integration (4 Gauss-points for each element). The well known elastic-perfectly plastic Mohr-Coulomb failure criterion is adopted. Both quadrilateral and triangular elements were used in the analyses, with the respective meshes shown in Figures 5.4 and 5.5.

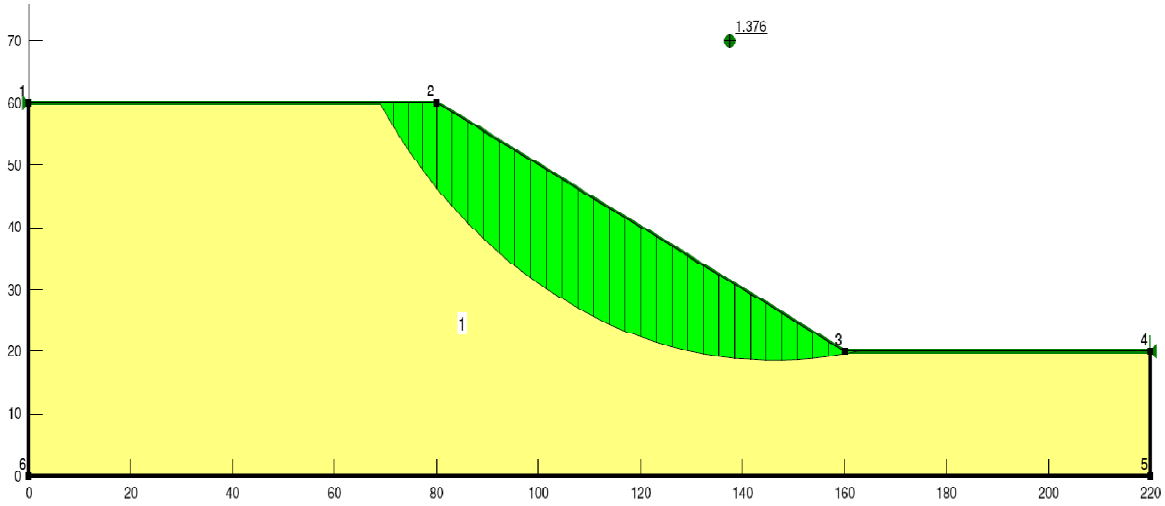


**Figure 5.2 The slope stability analysis using SLOPE/W (Bishop, circular slip surface)**

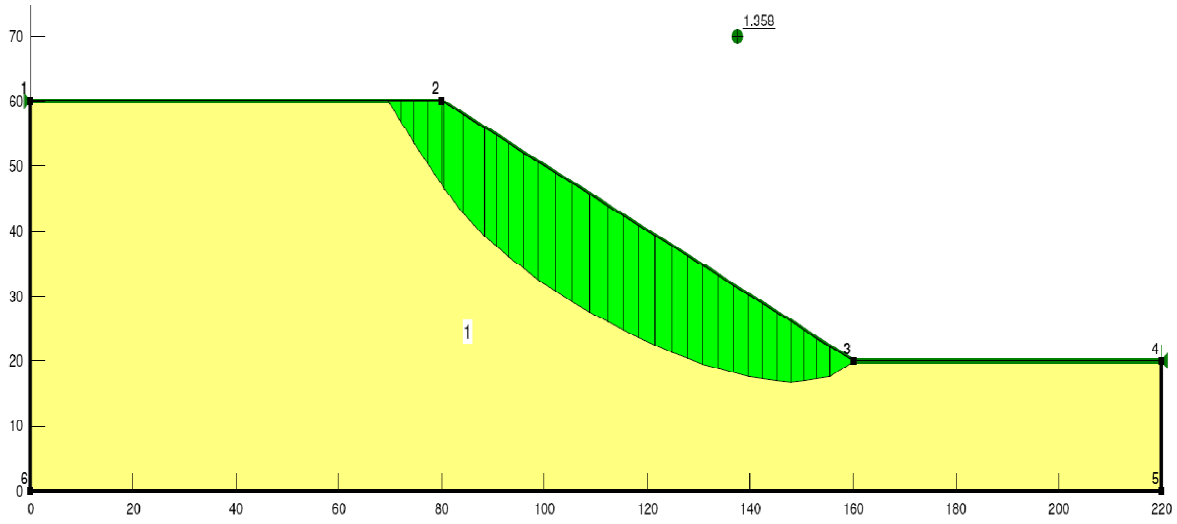


**Figure 5.3 The slope stability analysis using SLOPE/W (Bishop, log spiral surface)**

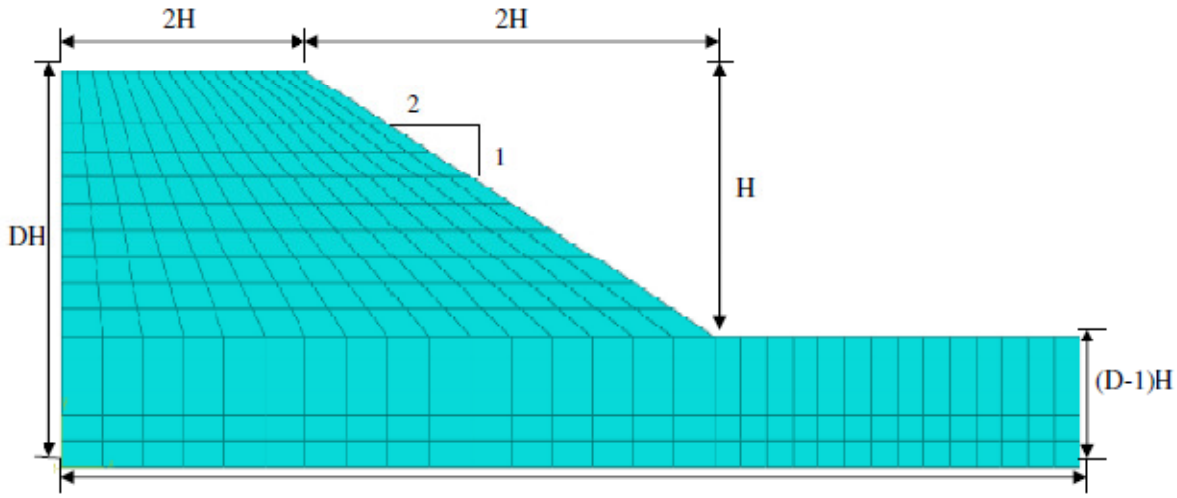


**Figure 5.4 Quadrilateral mesh of finite element model (ABAQUS)**

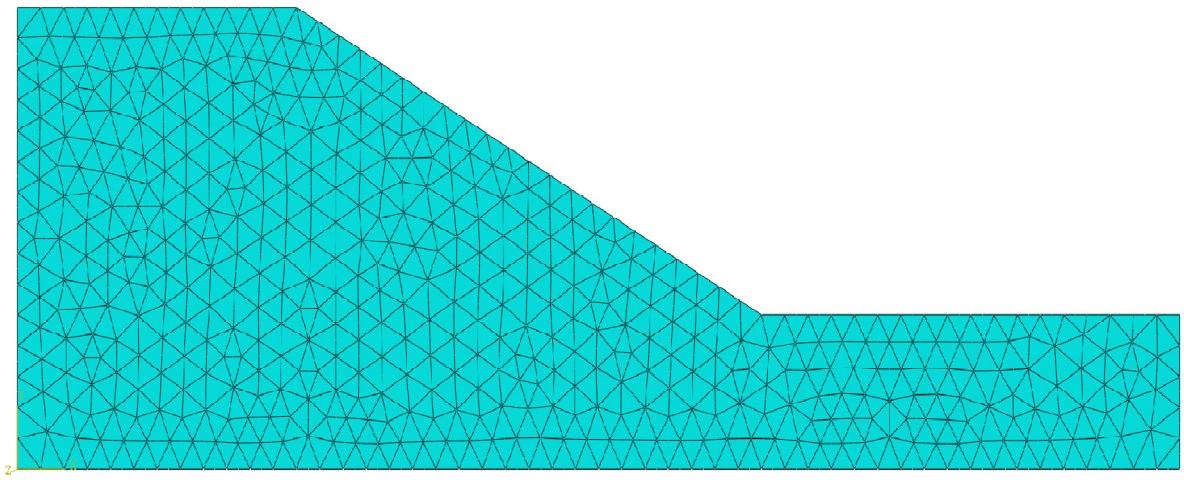

**Figure 5.5 Triangular mesh of finite element model (ABAQUS)**

The plastic strain contours in undeformed and deformed meshes in finite element analyses using ABAQUS are shown in Figure 5.6 and 5.7, respectively. The factor of safety is found to be 1.36 in this case using Q8 elements. If the mesh is changed to T6, the factor of safety is found to be 1.39. The results are summarized in Table 5.3, which includes the finite element results of Griffiths and Lane (1999). Griffiths and Lane (1999) found the factor of safety of this slope to be 1.37, similar to the 1.36 value found using ABAQUS.

In the following sections, the slope reinforced with piles is analyzed and discussed. The geometry and properties of material will follow the example in Griffiths and Lane (1999).

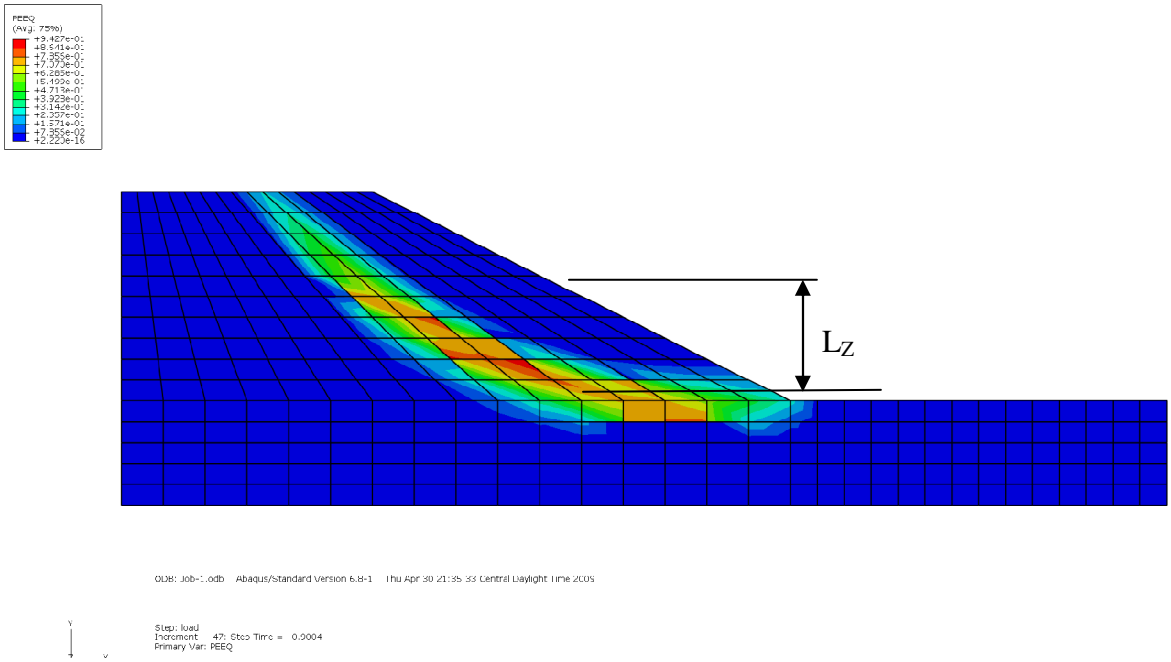


**Figure 5.6 The undeformed modeling of slope with foundation in finite element analysis, H=40m, D=1.5**

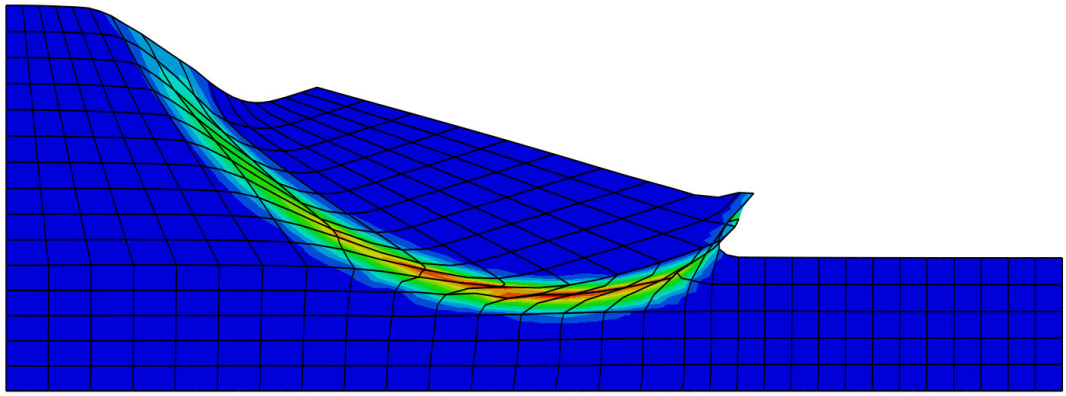

**Figure 5.7 The deformed modeling of slope stability analysis in finite element model, H=40m, D=1.5**

**Table 5.2 Results of limit equilibrium methods using SLOPE/W in slope**

| Method | Bishop | Spencer | GLE | Morgenstern-Price |
|---|---|---|---|---|
| **Circular** | 1.376 | 1.373 | 1.378 | 1.373 |
| **Log-spiral** | 1.361 | 1.363 | 1.348 | 1.348 |

**Table 5.3 Comparison of FE results of Griffiths and Lane and ABAQUS in slope stability, homogeneous slope with foundation**

| Program | Griffiths and Lane | ABAQUS |
|---|---|---|
| Element T6 | NA | 1.39 |
| Element Q8 | 1.37 | 1.36 |

## 5.4 Analysis of Slope Stability Using Piles

This section includes the pile stabilization case description, finite element analysis, optimal pile location, length of pile, and pile head condition based on the homogeneous slope reinforced with the pile.

### 5.4.1 Pile Stabilization Case Description

The pile used to stabilize the homogeneous slope with a foundation is investigated in this case to find the optimal location of pile, the length of pile and the pile head conditions. The

effect of location on the slope is investigated at six locations from the toe to the crest of the slope. The position is expressed in terms of $X_p/X$ with 0, 0.125, 0.25, 0.5, 0.75 and 1.0, respectively. The nomenclature symbols used for the slope analysis are shown in Figure 5.8. The length of pile to determine the optimal location is defaulted as 20 meters long which is the distance of the height in the middle portion of the slope to the base of the slope. To investigate the impact of the pile head conditions, the pile head conditions are assumed free and fixed. To present the improvement of pile installed, an improvement ratio $N_{pi}$ in terms of percentage is used herein. The definition of improvement ratio, $N_{pi}$ is defined as follows:

$$N_{pi} = \frac{F_p - F_s}{F_s} * 100\% \quad (5.1)$$

where $F_p$ is minimum factor of safety of piled-slope system, $F_s$ is the minimum factor of safety of the slope stability problem without pile.

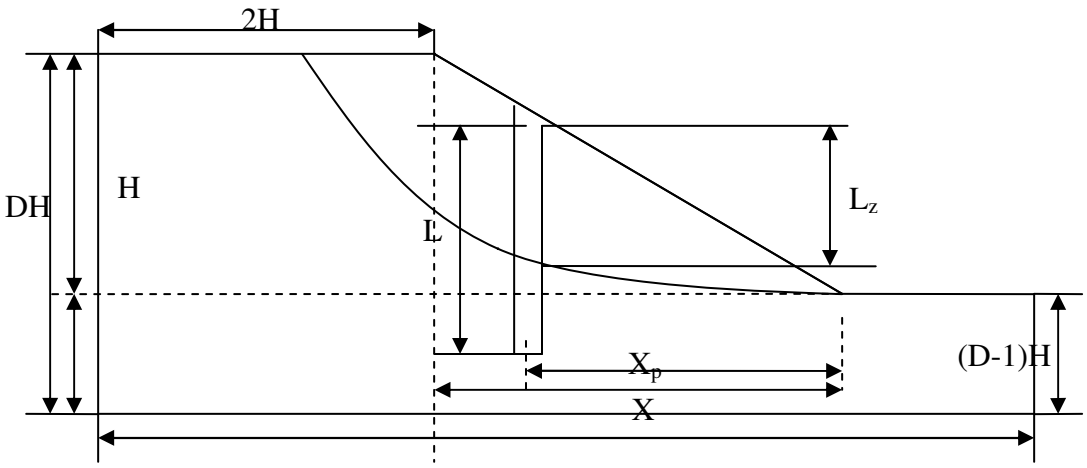


**Figure 5.8 The piled-slope system in homogeneous slope with foundation.**

Where $X_p$ : The distance of pile between centerline to the toe.
X: The distance between the toe and the crest.
$L_z$ : pile length above potential slip surface

In the piled slope system of finite element modeling, the parameters of materials, failure criteria and pile-soil interaction properties have to been applied appropriately in the analysis. The pile is assumed as an elastic media with material properties of pile assumed as Young's modulus (E) 60000 MPa, and Poisson's ratio (ν) 0.2, respectively. The selection of element to simulate the pile is a 2-D plane stress, 8- node with reduced integration element, and the soil is selected as 2-D plane strain, 8-node with reduced integration quadrilateral element. The mesh model including the pile is shown in Figure 5.9. The property of interface element

between pile and soil is assumed zero-thickness which can only transfer shear stress across the surfaces when a compressive normal pressure (p') it is applied. The pile soil friction coefficient, $\eta$ is 0.3 which is based on $\eta = \tan(\delta)$, where $\delta$ is friction angle between pile and surrounding soil.

### 5.4.2 Optimal Pile Location

The factors of safety of stabilized slopes are different if the locations of piles are different. The results of different pile head conditions in terms of pile locations are plotted and compared in Figures 5.10 and 5.11. The ratio of $X_p/X=0$ indicates the pile is placed at the toe and $X_p/X=1.0$ means the position of pile is on the crest. The factor of safety of the slope in the unreinforced case is 1.36. The factor of safety increases from 1.36 to 1.39 if the pile is placed at the toe. With moving the pile from the toe to the middle portion of the slope, the factor of safety increases until the position is at the middle of the slope; here the factor of safety is found to be 1.9 for the fixed head conditions. The factor of safety is 1.86 for the free pile head condition. When the pile is moved from the middle portion of the slope toward the crest, the factor of safety decreases from the highest values back to the value of 1.38, which is very close to the value in the unreinforced analysis. At both the crest and toe in a slope, the

improvement in the factor of safety by the free and fixed head conditions is identical. The factors of safety on both the toe and crest are only slightly higher than the unreinforced slope. In terms of improvement rate in percentage, $N_{pi}$, the distribution and comparison of improvement rate versus the pile location are based on the free and fixed pile head is shown in Figure 5.11. Due to the slope direction of the crest on left and toe on right in the model, these figures follow from left to right. The left number is 1.0 to indicate the pile location is at the crest in corresponding to Figure 5.9. Similarly, the number on the right 0 means the pile is placed at the toe.

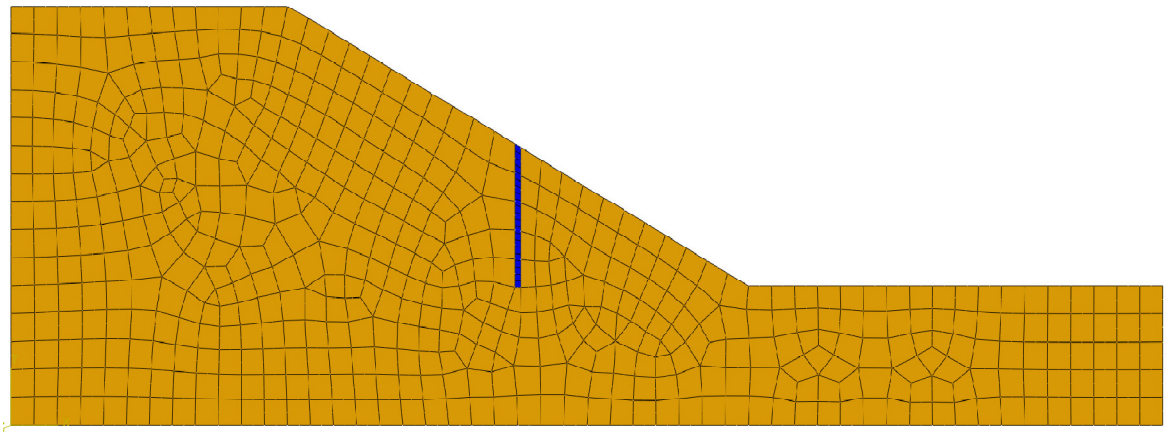

**Figure 5.9 Mesh of pile-slope system**

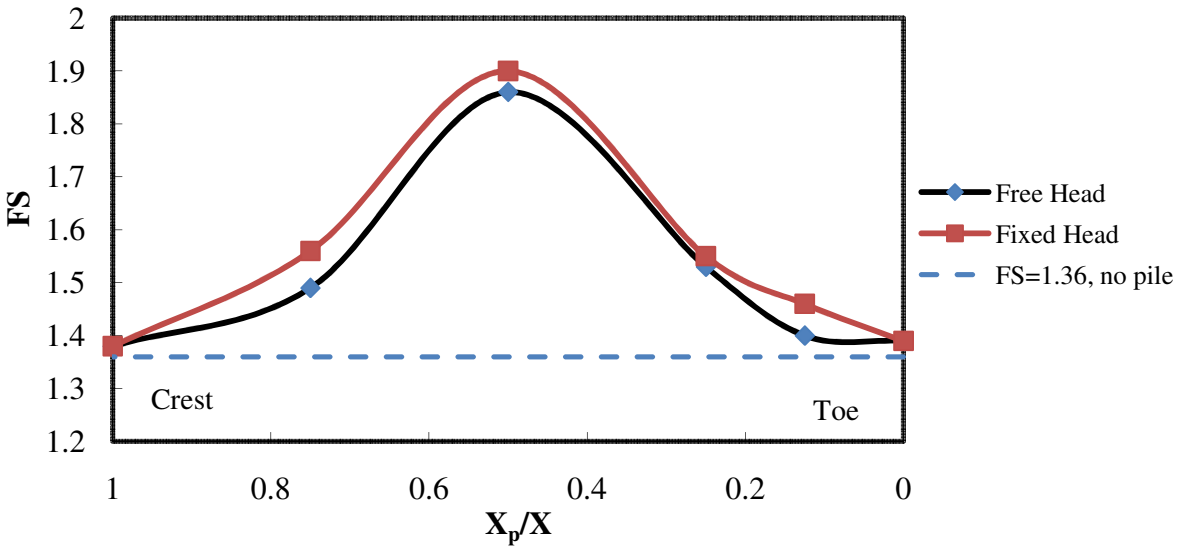


**Figure 5.10 Factor of safety versus $X_p/X$ (L=20m)**

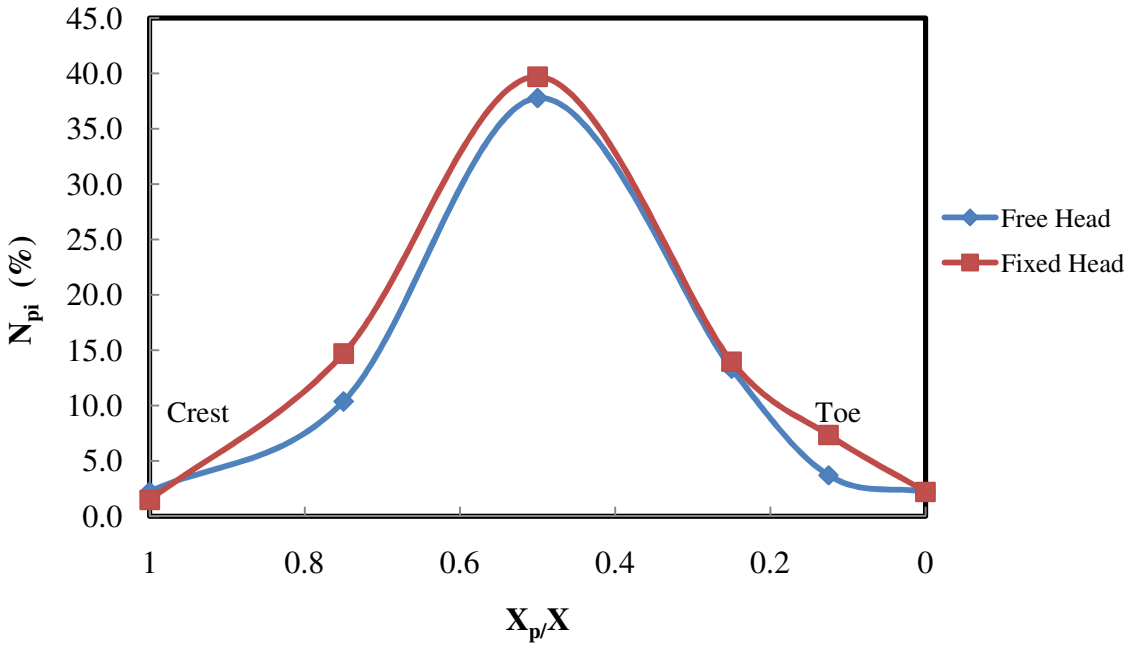


**Figure 5.11 $N_{pi}$ versus $X_p/X$ (L=20m)**

### 5.4.3 Length of Pile

The factors of safety in the analyses of finite element method based on pile length are shown in Figure 5.12. The relationship of improvement rate, $N_{pi}$ and the length of pile is plotted in Figure 5.13. The results of numerical analysis are summarized in Table 5.4 The contour of the numerical analysis of the slope stability in ABAQUS in the undeformed model which indicates the potential slip surface of unreinforced slope is shown in Figure 5.6. The potential slip surface is circular and slightly through foundation in the deformed finite element model is shown in Figure 5.7. With the presence of the pile in the slope, the failure mechanism changes and the highest factor of safety occurs when the pile is placed in the middle portion of the slope in previous analysis of optimal pile location determination.

Based on the length of pile, the result indicates the pile length from 12m to 23m leads to the maximum factors of safety which are around 1.9. The pile length is actually not a good scheme for design since the length of pile may be different on a case by case basis depending upon the dimension of the slope or the depth of the slip surface. For the convenience to evaluate the relationships between the factors of safety and the length of pile or the improvement rate, $N_{pi}$ and the length of pile, a dimensionless ratio $L_z/L$ is used. $L_z$ is defined

as the depth of potential slip surface in unreinforced slope stability analysis. The potential slip surface in finite element analysis usually can be determined based on the plastic strain contour in the numerical model. L is the true length of the pile. Due to the previous conclusion regarding the optimal pile location, the middle portion of the slope is determined as the optimal pile location in a slope. Therefore, the factor of safety based on the length of pile is only analyzed in the middle portion of the slope.

In Figure 5.6, the depth of potential slip surface ($L_z$) in the middle of the slope is estimated approximately as 16m deep. Therefore, $L_z$=16m is selected in this case. The corresponding length of the pile and the ratio $L_z$/L is summarized in Table 5.4. The reason why a potential slip surface has to be determined using the unreinforced case is the analysis is the so called coupled analysis in finite element analysis. In a coupled analysis, the slip surface may change due to the presence of the pile in the slope. Figures 5.14 and 5.15 shows if the pile is shorter than the depth of the potential slip surface, the potential slip surface will go through the deeper position. The presence of pile changes the depth of the potential slip surface to a deeper position in the coupled finite element analysis. In this condition, the factor of safety will be relatively higher. If the length of the pile is 16m, the slip surface is divided into two

portions as shown in Figures 5.16 and 5. 17 based on the free and fixed pile head conditions. The failure mechanism also changes to a shallow slip surface above the pile.

Figures 5.18 and 5.19 present the case of L=20m which is right at the height of the slope in the middle portion of the slope. The failure type shows the upper portion if the slope is inclined to fail. In terms of the ratio $L_z/L$, when $L_z/L$ is less than 0.64 which means the length of pile is larger than 25 m, the factor of safety starts to decrease if the pile head condition is free versus fixed. If the ratio of $L_z/L$ is greater than 0.7, between 0.7 to 1.0, the factor of safety is around 1.86. Figures 5.20 and 5.21 show that the pile length of 30m and factor of safety of 1.87, respectively for free head and fixed condition which is longer than the depth of the slip surface gives rise to the factor of safety 1.79. The potential failure surface is at upper portion of the pile and quite shallow upslope from the pile in both cases. The pile shows the lowest improvement rate ($N_{pi}$) when the ratio $L_z/L$=0.46, the corresponding length of the pile is 35m and the factor of safety is only 1.53. The failure type of the piled slope is shown in Figure 5.22 when the pile head is free, and the lower portion of the slope is inclined to fail. In terms of improvement ratio, $N_{pi}$ in this case, the rate of improvement is 12.5%. For the 35m long pile and fixed head conditions, the plastic strain contours are shown in Figure 5.23 where it can be seen that the fixed head pile contains the soil material upslope and the

failure mechanism is a slope failure below the pile (FS=1.88). Thus, with long piles, the failure mechanism changes from the upslope of the pile to downslope of the pile.

Based on the changing length of pile, the highest rate of improvement is found to be around 37% when the pile length is between 12m and 23m. The pile tip is restricted as fixed tip in this analysis. Figures 5.14, 5.16, 5.18, 5.20 and 5.22 present different failure contours due to the length of the pile ranges from 10, 16, 20, 30 and 35m, respectively. They exhibit the different failure mechanisms due to pile length effect. All of these piles in the models are all assumed to be free heads.

If the pile head is fixed, the factor of safety does not change surprisingly with the change of pile length. The factor of safety ranges between 1.82 to 1.9, and the corresponding rate of improvement is between 33.8% and 39.7%. In terms of $L_z/L$, when $L_z/L$ is lower than 0.64, the factor of safety contributed by the fixed head pile obviously better than free head. The possible failure mechanisms due to fixed head pile conditions analyzed in ABAQUS are shown in Figures 5.15, 5.17, 5.19, 5.21 and 5.23, respectively.

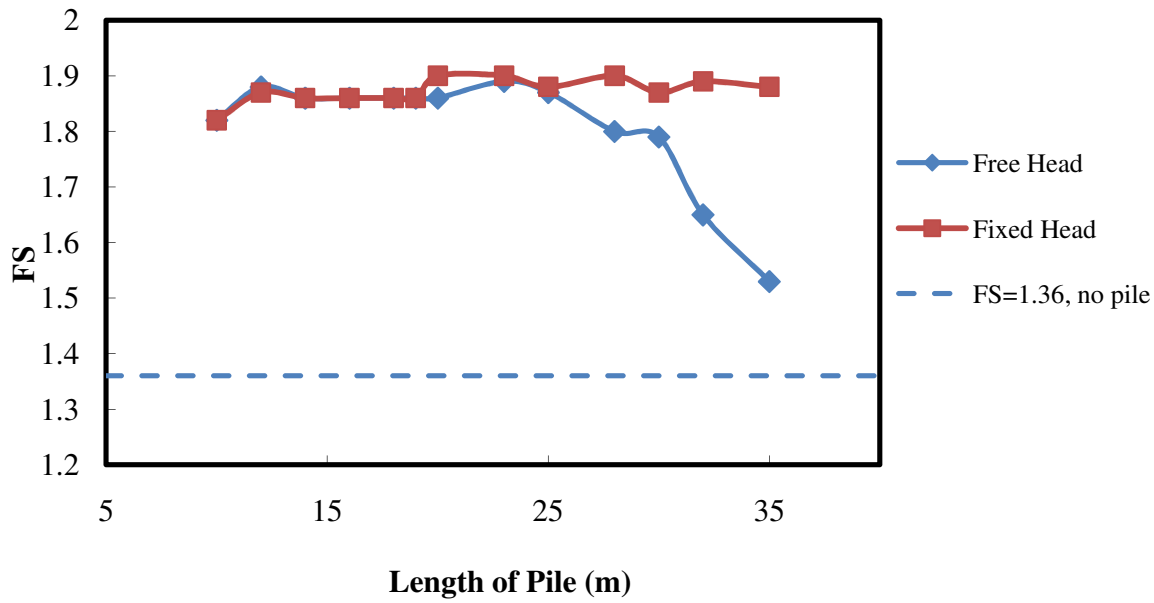


**Figure 5.12 Factor of safety versus Length of Pile**

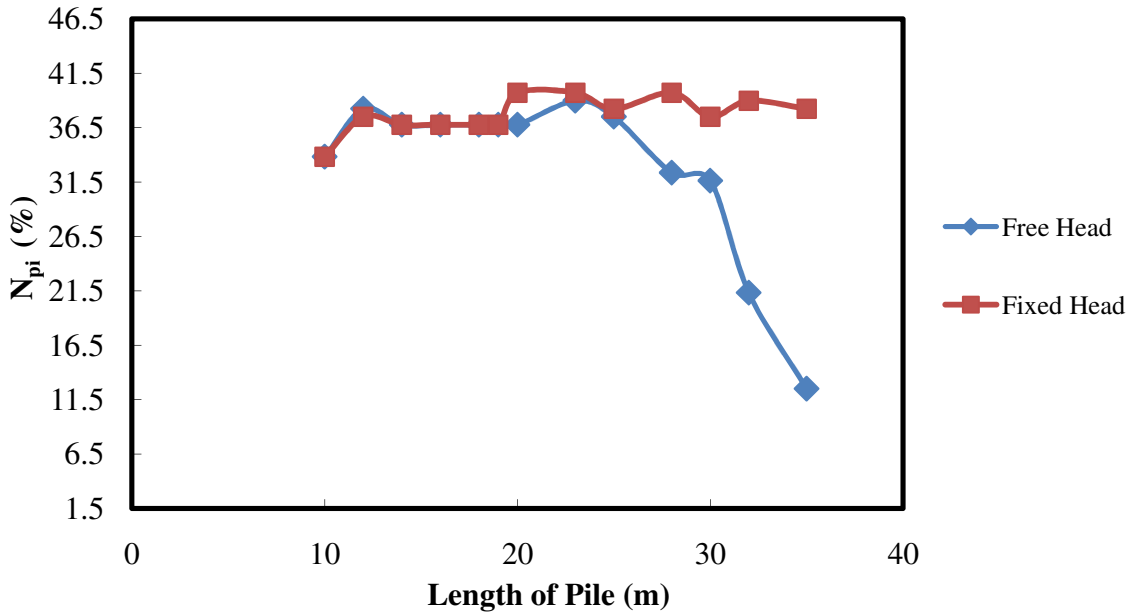


**Figure 5.13 $N_{pi}$ versus Length of Pile**

**Table 5.4 Factor of safety of pile-stabilized slope based on length of pile**

$X_p/X=0.5$

| Pile length, L (m) | 10 | 12 | 14 | 16 | 18 | 19 | 20 | 23 | 25 | 28 | 30 | 32 | 35 |
|---|---|---|---|---|---|---|---|---|---|---|---|---|---|
| $L_z/L$ ($L_z$=16m) | | | | 1.00 | 0.89 | 0.84 | 0.80 | 0.70 | 0.64 | 0.57 | 0.53 | 0.5 | 0.46 |
| FS (free head) | 1.82 | 1.88 | 1.86 | 1.86 | 1.86 | 1.86 | 1.86 | 1.89 | 1.87 | 1.80 | 1.79 | 1.65 | 1.53 |
| $N_p$ (%) | 33.82 | 38.24 | 36.76 | 36.74 | 36.76 | 36.76 | 36.76 | 38.97 | 37.50 | 32.35 | 31.62 | 21.32 | 12.50 |
| FS | 1.85 | 1.87 | 1.86 | 1.86 | 1.86 | 1.87 | 1.90 | 1.90 | 1.88 | 1.90 | 1.87 | 1.89 | 1.88 |
| $N_p$ (%) (fixed head) | 33.82 | 37.5 | 36.76 | 36.76 | 36.76 | 36.76 | 39.71 | 39.71 | 38.24 | 39.71 | 37.5 | 38.97 | 38.24 |

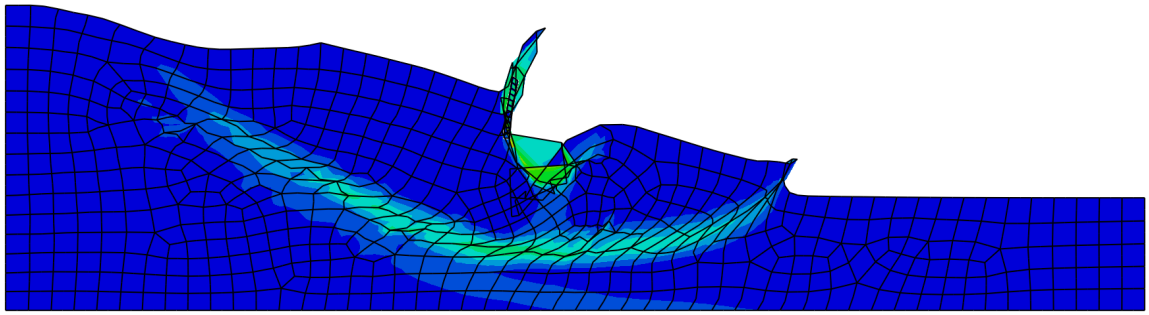

**Figure 5.14 The plastic strain contour of slope failure with stabilizing pile (L=10m), FS=1.82, free head**

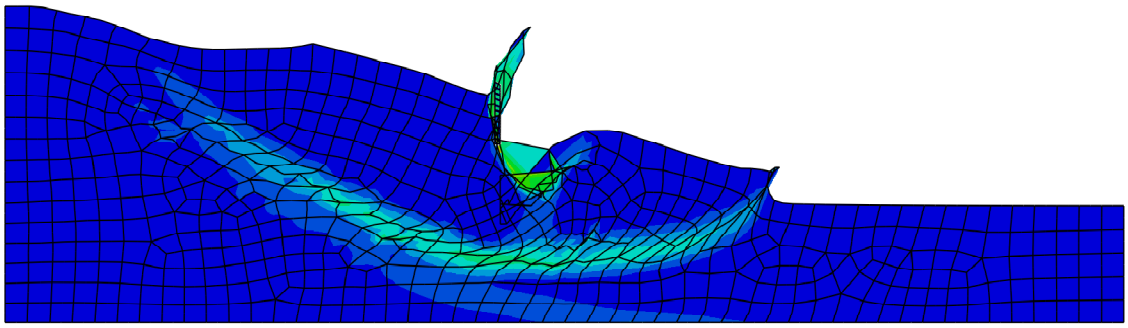

**Figure 5.15 The plastic strain contour of slope failure with stabilizing pile (L=10m), FS=1.85, fixed head**

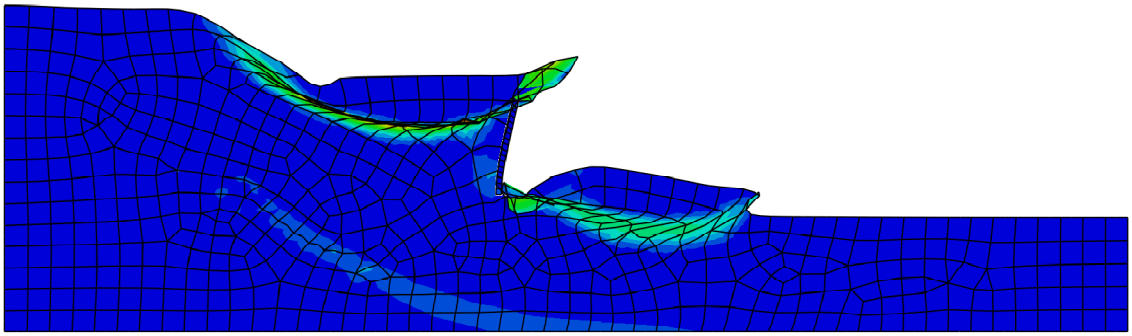

**Figure 5.16 The plastic strain contour of slope failure with stabilizing pile (L=16m), FS=1.86, free head**

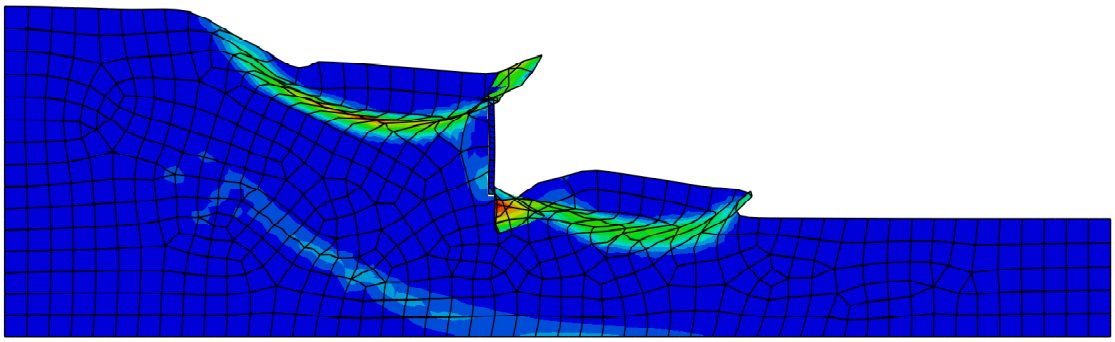

**Figure 5.17 The plastic strain contour of slope failure with stabilizing pile (L=16m), FS=1.86, fixed head**

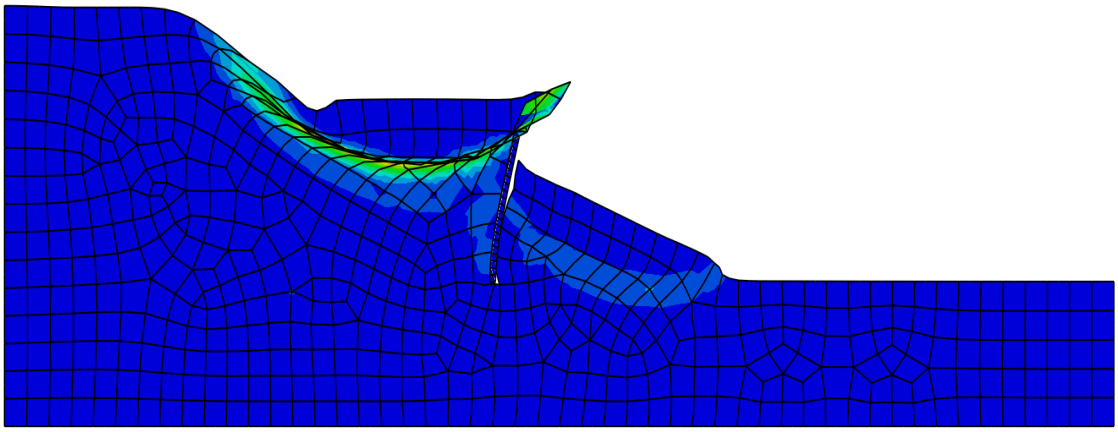

**Figure 5.18 The plastic strain contour of slope failure with stabilizing pile (L=20m), FS=1.86, free head**

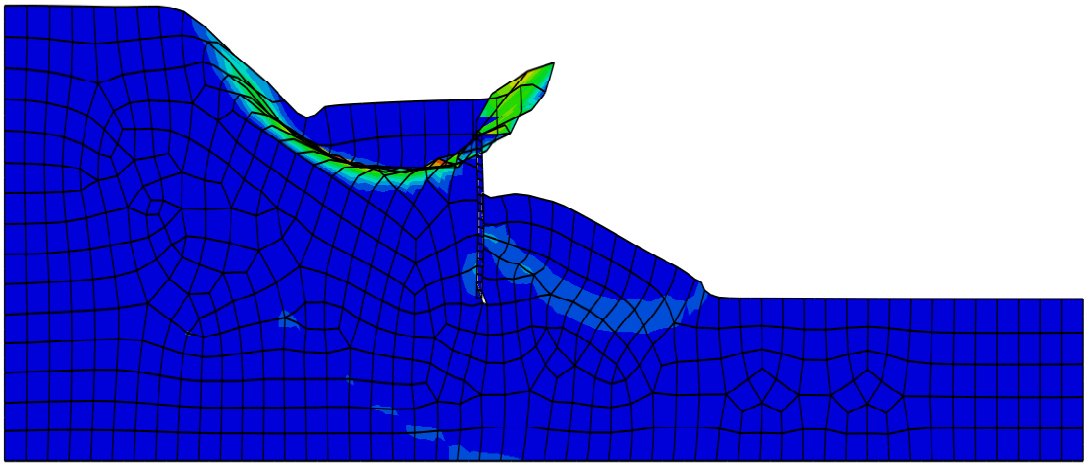

**Figure 5.19 The plastic strain contour of slope failure with stabilizing pile (L=20m), FS=1.90, fixed head**

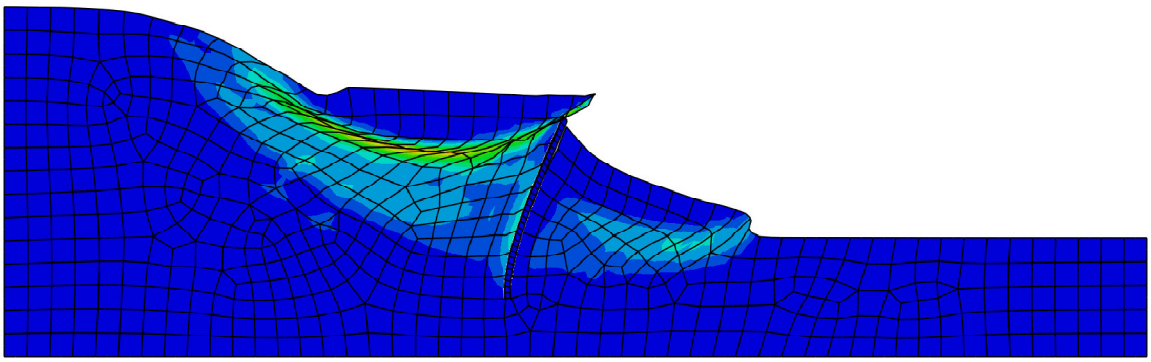

**Figure 5.20 The plastic strain contour of slope failure with stabilizing pile (L= 30m), FS=1.79, free head**

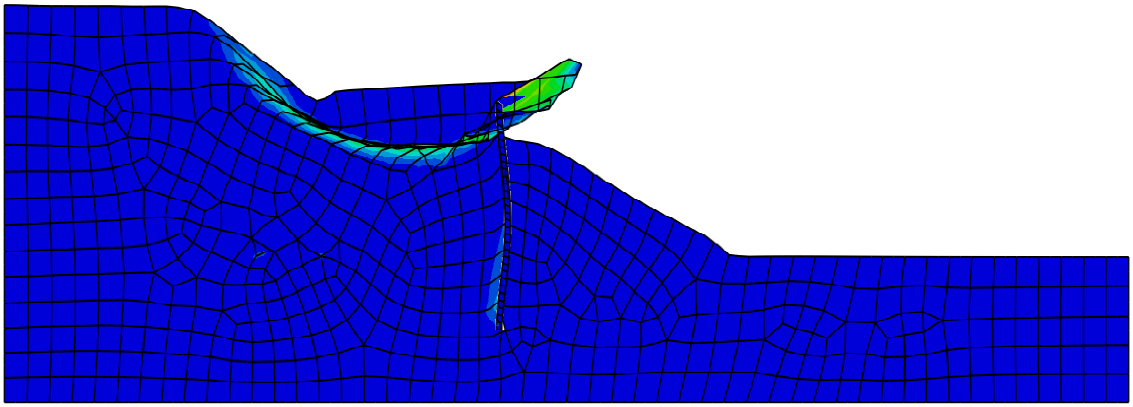

**Figure 5.21 The plastic strain contour of slope failure with stabilizing pile (L= 30m), FS=1.87, fixed head**

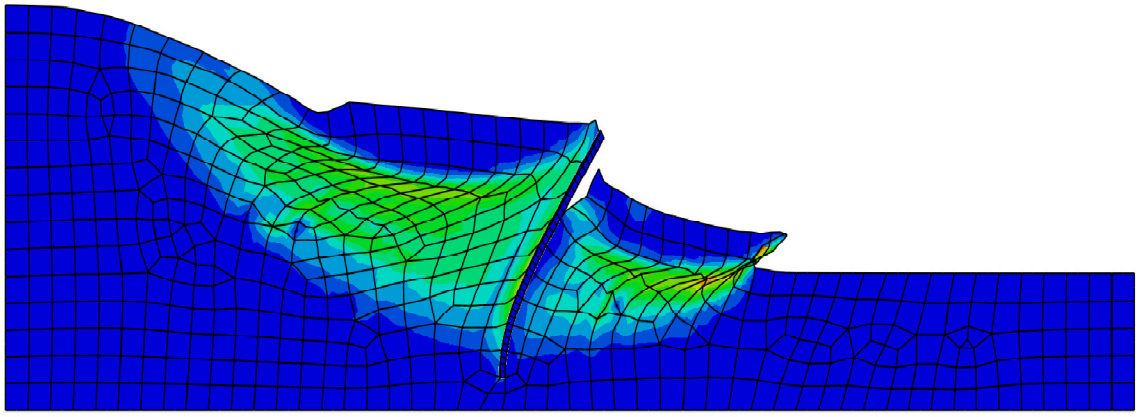

**Figure 5.22 The plastic strain contour of slope failure with stabilizing pile (L= 35m), FS=1.53, free head**

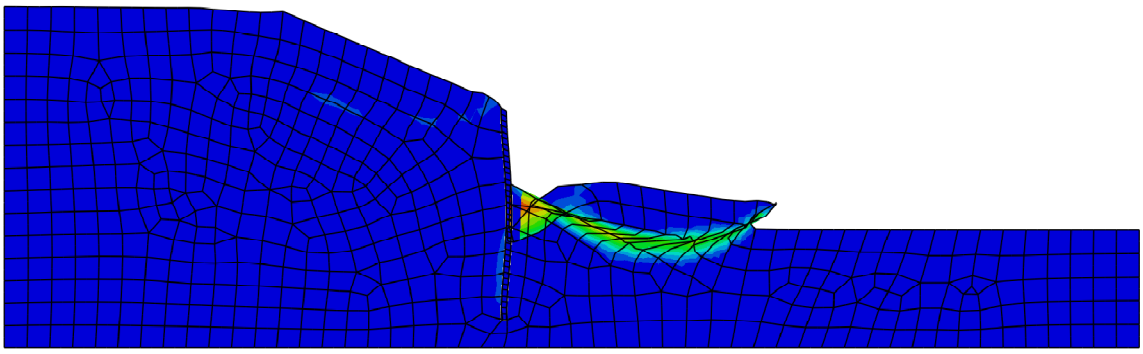

**Figure 5.23 The plastic strain contour of slope failure with stabilizing pile (L= 35m), FS=1.88, fixed head**

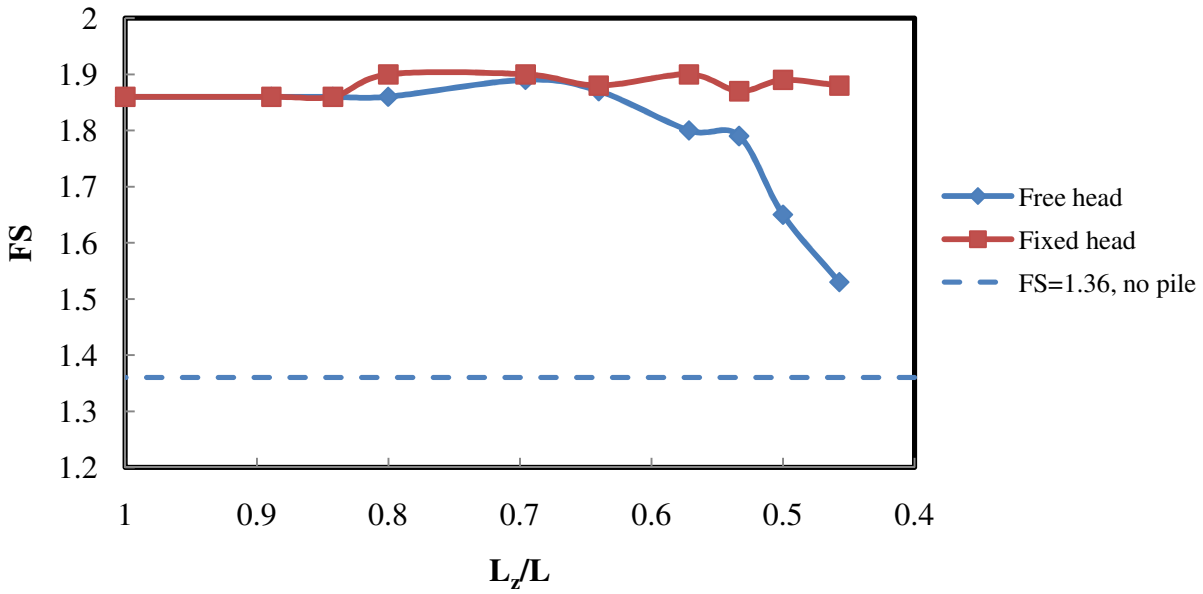


**Figure 5.24 Factor of safety versus $L_z/L$**

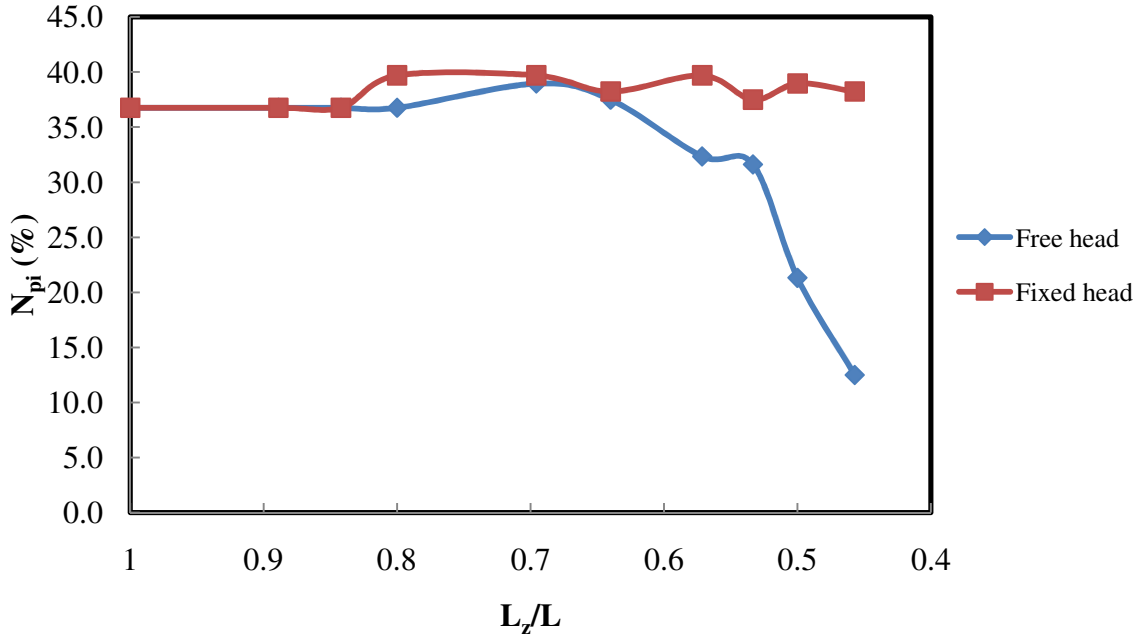


**Figure 5.25 $N_{pi}$ versus $L_z/L$**

### 5.4.4 Pile Head Condition

The pile head condition is considered as one of the important factors to affect the performance of the stabilizing pile. In the analysis, different pile head conditions exhibit different factor of safety in different locations as shown in Figure 5.10. In terms of $N_{pi}$ the results are plotted in Figure 5.11 which has been discussed in the previous section. Moreover, the pile head condition can also change the failure mechanism (see Figure 5.22 and 5.23). The results of numerical analysis show that the fixed head condition leads to a slightly higher factor of safety than the free pile head condition does. In both ends, at the toe and the crest, the factors of safety are nearly at the same value. In other words, the fixed pile head does not improve much stability in both the toe and the crest of the slopes in terms of factor of safety. Comparing the contours of plastic strain in Figures 5.14 and 5.15 (L=10m), the similar failure type occurs regardless of the pile head condition, and the potential slip surface goes through the deeper portion of the slope. In Figures 5.16 and 5.17 (L=16m), the failure types are also similar, both soil upslope and downslope will fail simultaneously. In Figures 5.18 and 5.19 (L=20m), the pile with fixed head has less effect on the soil downslope with slightly higher factor of safety than free pile head condition does. From Figures 5.20 and 5.21 (L=30m), the effect is similar to Figures 5.18 and 5.19, the fixed pile head can lower the soil

movement downslope. However, in Figures 5.22 and 5.23 (L=35m), the fixed pile head has different failure mechanism from free head condition of pile. The fixed head pile can stop the movement upslope while the slope failure occurs down slope with a higher stability than free head pile stabilization in terms of the factor of safety.

## 5.5 Discussion of Results

When the slope is reinforced with a pile, the optimal pile location is found to be in the middle portion of the slope regardless of pile head conditions, the factor of safety is improved by 36.8 % compared to the value in an unreinforced slope stability. The 36.8% of the improvement rate $N_{pi}$ is based on the length of pile 20m if the free pile head condition is applied. A slightly higher factor of safety is obtained if a fixed head pile condition is applied. The reason is that if the pile is placed in the middle portion of the slope, the strength of the soil-pile interface is sufficiently mobilized by the fact that the pressure is acting on the piles (Cai and Ugai, 2000). In Figure 5.6, the middle portion of the slope was found to have largest plastic strain in the unreinforced slope. Therefore, the pile placed in the middle portion of the slope to reduce the soil movement is quite reasonable. A pile length between 10 to 25m leads to the optimal factor of safety; beyond 25m, the factor of safety starts to decrease if the pile

head condition is free which is shown in Figure 5.12. In terms of the ratio $L_z/L$, below 0.64 will lead to the decrease of the factor of safety if the pile has a free pile head. The numerical results are summarized in Table 5.4 and the trend is plotted in Figure 5.24. However, the results indicate the factor of safety does not change surprisingly if the fixed pile head condition is applied.

Meanwhile, the failure type is different in a short pile as compared to a long pile which has been illustrated previously. The failure types can be classified as four, greater circular failure plane, both upper and lower with smaller circular plane failure, upper portion failure and lower portion failure observed in the finite element analysis using ABAQUS with the length changes from short to long as shown in Figures 5.14, 5.16, 5.18, 5.20 and 5.22, respectively. If the pile head condition is fixed, the classification of failure types is similar, which are shown as Figures 5.15, 5.17, 5.19, 5.21 and 5.23, respectively. The results also show if the pile is longer, the pile head condition is important for stabilizing the slope. Comparing Figures 5.22 and 5.23, in Figure 5.22, the pile head is free, the soil upslope has larger soil movement due to the more flexible of pile. Figure 5.23 presents the pile head is restricted to fixed, the soil movement upslope is lowered and the least factor of safety occurs at the

downslope soil to the toe. In terms of factor of safety, the stability contributed by a fixed head pile is more than a free head pile.

In the free pile head case, when the pile is shorter than the potential slip surface in unreinforced case, the pile head does not have much displacement on pile head to stop the slope failure. This is because the failure surface is deeper than the length of pile. However, when the pile is longer than the depth of potential slip surface, the pile has to deform more on the top to prevent the slope failure. That is why when the pile is shorter, there is no much difference in improvement of the factor of safety regardless of the pile head is fixed or not. The pile head condition cannot change the failure mechanism in shorter pile cases. However, the longer pile has much difference on the factor of safety with different pile head conditions due to different failure mechanisms induced.

In Figures 5.10 and 5.11, the pile with fixed head condition does not contribute more on stabilization at both crest and toe. In the middle portion, a fixed head pile gives rise to a higher factor of safety on slope stability than free pile head does. In other words, a fixed pile head is not always a better option in designing a slope stabilizing pile. Therefore, the pile has to be designed to make use of pile-soil interaction to increase higher safety on slope stability.

Free head pile design in the proper length can make good use of the pile-soil interaction mechanism to increase slope stability particularly when the pile length less than 25m or $L_z/L$ greater than 0.64 which is presented in Figures 5.25 and 5.26, respectively. A free head pile in a shorter pile case can be pushed into the soil to increase to a higher factor of safety. However, in long pile cases, a fixed pile head can be used to hold large soil masses upslope. That is why the failure portion may occur in the lower portion of the slope not in upper portion when pile length is 35m as shown in Figure 5.23.

The failure portion transits from the large circular to the upper portion then to the lower portion in the slope if the pile length changes from short to long. Figures 5.14 to 5.23 are used to compare the difference. In the finite element coupled analysis, the depth of slip surface is affected by the length of pile. The failure mechanism is also affected by pile head condition.

## 5.6 Summary and Conclusions

The numerical results of slope stability and slope reinforced with the pile in homogeneous slope with foundation case are presented above. Based on the slope stability analysis, slope reinforced with the pile based on optimal pile location, pile length and pile head restriction

have been incorporated into finite element analysis and discussed. Several conclusions and recommendations can be made in design of the stabilizing pile for this case.

### 5.6.1 Conclusions

(1) In a homogeneous slope with a foundation, the optimal pile location is in the middle portion of the slope, in terms of the factor of safety, the pile placed in the middle portion of the slope leads to highest factor of safety regardless of the pile head condition.

(2) Based on the length of pile, a $L_z/L$ ratio between 0.64 and 1.0 which is defined in this study gives rise to the highest factor of safety. In previous studies, a few researchers have discussed the suitable length of pile in stabilization. However, in terms of design, it is necessarily to provide the appropriate length of a pile, to assume an infinite length of pile is apparently unreasonable and not realistic. The length of pile used is related to the dimension of the slope.

(3) In pile head conditions, fixed or free head conditions make no difference in terms of the factor of safety when the pile is shorter. In this study, a $L_z/L$ ratio greater than 0.64,

corresponding to the pile length is 25m based on the depth of the potential slip surface in this 40m high slope is 16m deep. However, a longer pile with a $L_z/L$ ratio less than 0.64, the pile with fixed head provides a higher factor of safety than the free head does. However, compared to other length of pile in fixed pile head cases, the factors of safety are quite similar. It is around 1.88 on average, but the factor of safety decreases in the longer pile case when the pile head condition is free.

(4) The fixed pile head does not always provide the stabilizing pile a better remediation in slope stability. It depends on the depth of potential slip surface and the length of the pile used.

(5) The fixed pile head condition is able to increase stability when the failure mechanism can be changed and be different from the failure mechanism caused by a free pile head condition. In other words, if the failure type cannot be changed due to the change of pile head condition, the slope stability will not increase.

### 5.6.2 Recommendations

(1) In viewpoint of design, the pile has to be placed in the middle portion of the slope to reach the highest factor of safety compared to other locations in the slope.

(2) The pile length cannot be either too short nor too long, the appropriate length is between a $L_z/L$ ratio of 0.6 to 1.00. $L_z$ is the depth of potential slip surface in a unreinforced slope that is related to the dimension of a homogeneous slope with foundation.

(3) In terms of the dimensions of a homogeneous slope, a relatively long pile should be avoided since the higher factor of safety cannot be gained by adding length to the pile. In terms of pile head conditions, even the relatively long pile with a fixed head condition does not reach a higher factor of safety compared to a shorter one. Therefore, in this case, an appropriate length of pile between the ratios of 0.6 to 1.00 with a free head is recommended.

# CHAPTER 6: NON-HOMOGENEOUS SLOPE WITH FOUNDATION

## 6.1 Introduction

This chapter presents the case of a slope with a underlying foundation with different soil properties resulting in a non-homogeneous slope based on soil properties. The contents of this chapter include a case description, analysis of the unreinforced slope using limit equilibrium methods and finite element methods, and the analysis of the reinforced slope using finite element methods. The effect of the pile reinforcement is analyzed on the basis of pile location, pile length, and pile head conditions. Results of these analyses are presented herein along with discussion of the results and summary and conclusions.

## 6.2 Case Description

Following the case presented in Chapter 5, a similar geometry of the slope is used such as the same dimensions and the slope angle. This case presents the analysis of the slope stability of the non-homogeneous slope which has different shear strength in the slope and in the foundation. The geometry of the non-homogeneous slope is presented in Figure 6.1. The slope model consists of two materials, $C_{u1}$ and $C_{u2}$, representing the undrained shear strength of the slope and the foundation, respectively. The material properties are summarized in

Table 6.1. In Table 6.1, the undrained shear strength is $C_{u1}$. $C_{u1}/\gamma H$ , an non dimensional ratio, is assumed to be 0.25 following the example in the paper of Griffiths and Lane (1999) for the reason to validate the results of accuracy of stability analysis in ABAQUS. The different $C_{u2}$ values to be adopted are based on the ratio of $C_{u2}/C_{u1,}$ and ratios of 0.5, 1.0, 1.5 and 2.0 are used in the numerical analyses. Note that a $C_{u2}/C_{u1}$ ratio of one produces a homogeneous solution, similar to the case studied in Chapter 5; however, in this chapter the thickness of the foundation is twice that in Chapter 5.

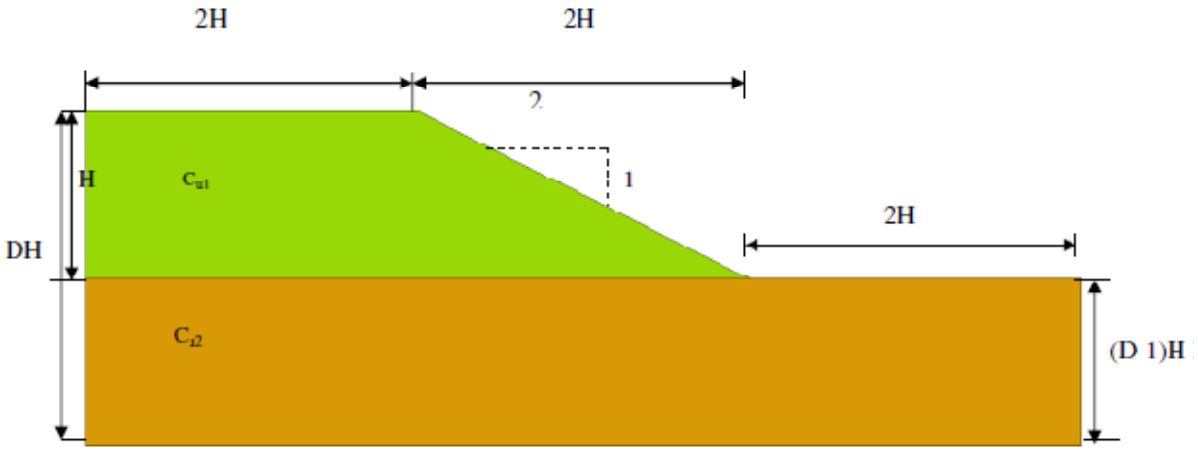


**Figure 6.1 Geometry of Non-homogeneous slope with foundation. (D=2.0)**

**Table 6.1 Slope dimension and material properties**

| E ($kN/m^2$) | $\phi$ (°) | $\gamma$ ($kN/m^3$) | $\upsilon$ | $C_{u1}$ ($kN/m^2$) | H (m) |
|---|---|---|---|---|---|
| 100000 | 0 | 20 | 0.4 | 200 | 40 |

### 6.3 Unreinforced Slope Stability Analysis

The geometry shown in Figure 6.1 was analyzed for slope stability. The slope has an inclination of 2H:1V, with an overall height of 80m, thus the slope height was 40m and the underlying foundation is 40m thick. The analysis using limit equilibrium methods and finite element method are shown and the results are compared herein. Two types of meshes are used in the finite element analysis in ABAQUS, triangular and quadrilateral elements, respectively. The selection of element types are 2-D plain strain elements with reduced integration and the geometry order is quadratic. Therefore, there are six nodes (3 Gauss-points for each element) in each element of triangular element and eight nodes (4 Gauss-points for each element) in each element of quadrilateral element. T6 and Q8 are used to represent the element type of six nodes and eight nodes, respectively. The slope model meshed with T6 element is shown in Figure 6.2 and the model meshed with Q8 element is shown in Figure 6.3. The slope stability analysis using finite element method in ABAQUS and limit

equilibrium methods in SLOPE/W are discussed herein based on the different strength ratios ($C_{u2}/C_{u1}$) of slope soil and foundation soil.

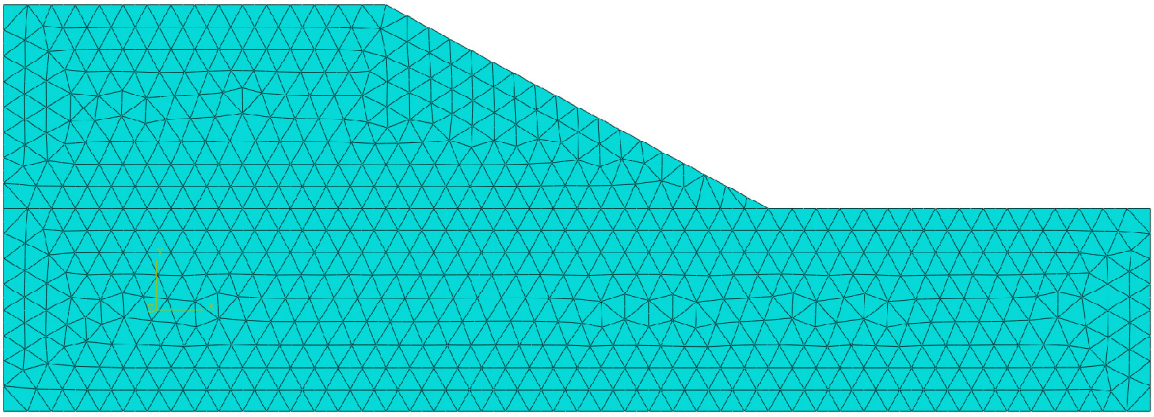

**Figure 6.2 Mesh with T6 element in the slope model**

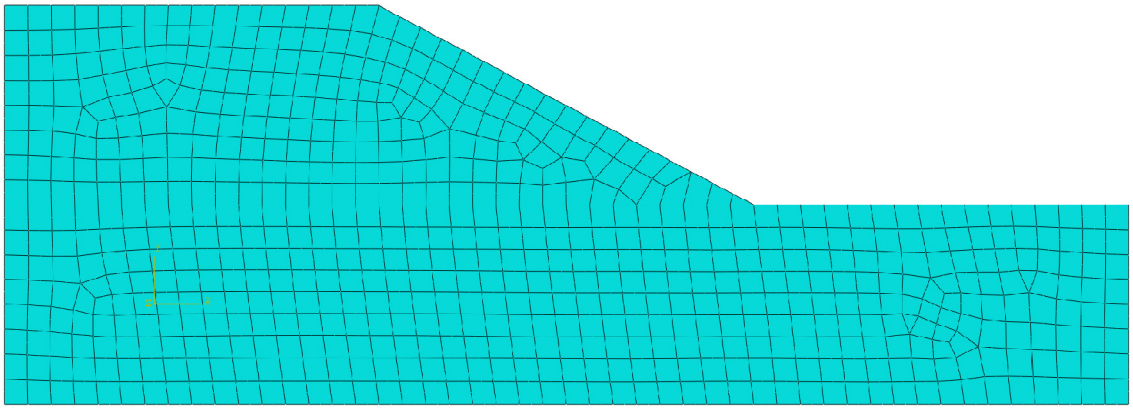

**Figure 6.3 Mesh with Q8 element in the slope model**

The four strength ratios ($C_{u2}/C_{u1}$) of slope soil and foundation soil are adopted in the finite element analysis and limit equilibrium methods are shown in the following based on $C_{u2}/C_{u1}$=0.5, 1.0, 1.5 and 2.0, respectively.

### 6.3.1 $C_{u2}/C_{u1}$=0.5

The resulting factors of safety using SLOPE/W and ABAQUS with $C_{u2}/C_{u1}$ =0.5 are summarized in Table 6.2. The finite element analysis using T6 and Q8 elements have the same results on factor of safety of slope stability analysis. Compared to the results using limit equilibrium methods, the values using ABAQUS make good agreement with the results using these noted methods. The factor of safety is approximately 0.88 reported by Griffiths and Lane (1999). The circular slip surface resulting from the limit equilibrium method using SLOPE/W is shown in Figure 6.4. The plastic strain contour shown in Figure 6.5 using ABAQUS indicates the potential slip surface where the maximum plastic stain occurs in the slope. The potential slip surface goes through the base and shape is circular which is similar to the result shown in Figure 6.4. Looking at the two figures and the factors of safety in Table 6.2, the limit equilibrium and finite element methods provide similar factors of safety and failure mechanisms.

**Table 6.2 Results of numerical analysis in slope stability, $C_{u2}/C_{u1}$=0.5**

| Method | Janbu | Bishop | Spencer | GLE | Ordinary | M-P* | ABAQUS(T6) | ABAQUS(Q8) |
|---|---|---|---|---|---|---|---|---|
| **Circular** | 0.893 | 0.876 | 0.876 | 0.876 | 0.876 | 0.876 | 0.88 | 0.88 |

* Morgenstern and Price

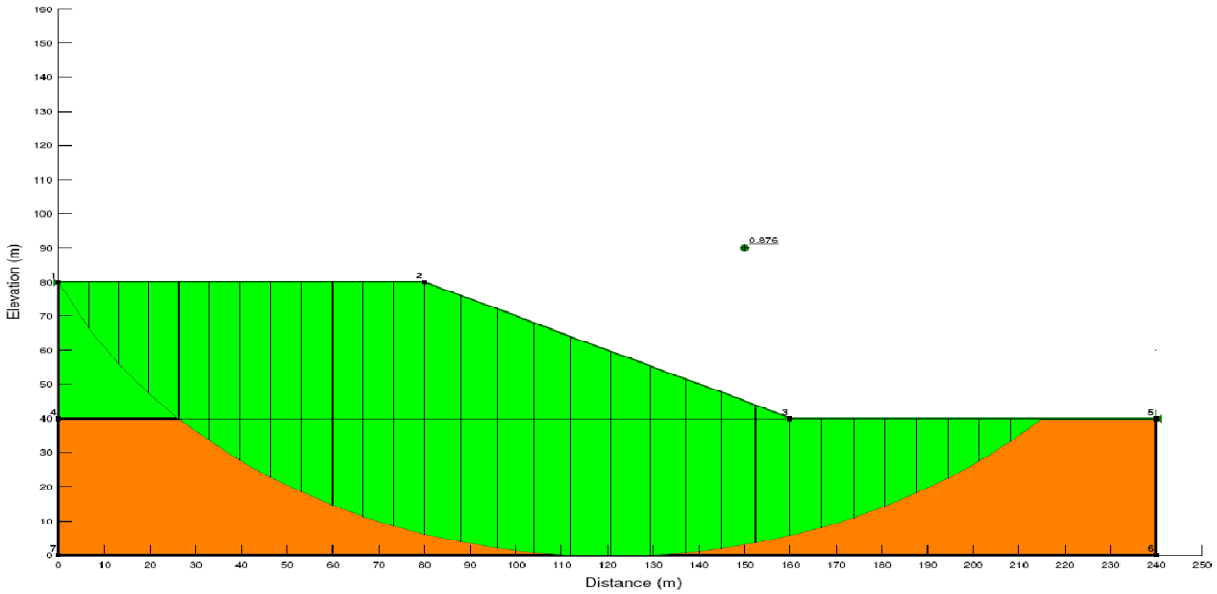


**Figure 6.4 SLOPE/W analysis on slope stability with circular slip surface ($C_{u2}/C_{u1}$=0.5)**

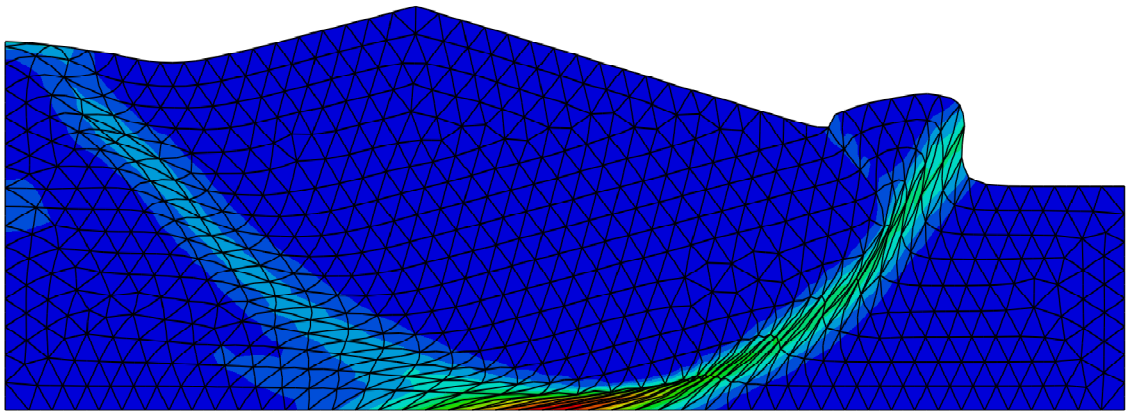

**Figure 6.5 The plastic strain contour with $C_{u2}/C_{u1}$=0.5, FS=0.88 (T6 element)**

### 6.3.2 $C_{u2}/C_{u1}$=1.0

The factors of safety resulting from analyses with $C_{u2}/C_{u1}$ =1.0 are summarized in Table 6.3. The case is actually a homogeneous slope condition, similar to that in Chapter 5, but herein the foundation is twice as thick as that analyzed in Chapter 5. However, in this analysis the case is regarded as the special case of non-homogeneous slope with the same shear strength of soil in both slope and foundation. The factor of safety of the slope using finite element makes good agreement with from most of the limit equilibrium methods except for Janbu's solution. The reasons for Janbu's lower factor of safety were not readily apparent. The results of slope stability analysis using ABAQUS are slightly higher than limit equilibrium, 1.50 with T6 element, 1.49 with Q8 element. The plastic strain contour is shown in Figure 6.6 which indicates the location of the potential slip surface based on the location with maximum shear strain. The potential slip surface shown in Figure 6.6 is a base failure tangent to the firm base; similar results were obtained using the limit equilibrium methods.

**Table 6.3 Results of numerical analysis in slope stability, $C_{u2}/C_{u1}$=1.0**

| Method | Janbu | Bishop | Spencer | GLE | Ordinary | M-P | ABAQUS(T6) | ABAQUS(Q8) |
|---|---|---|---|---|---|---|---|---|
| **Circular** | 1.408 | 1.477 | 1.477 | 1.477 | 1.477 | 1.477 | 1.50 | 1.49 |

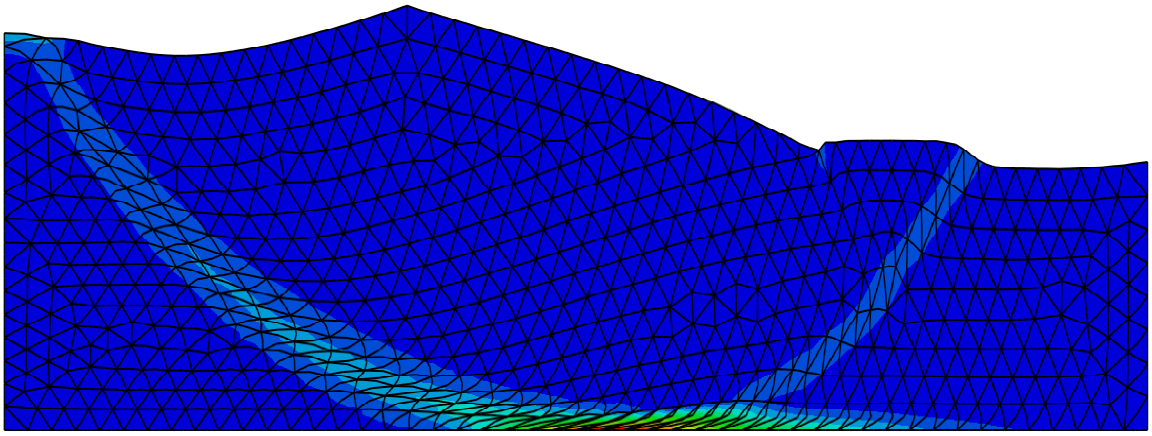

**Figure 6.6 The plastic strain contour with $C_{u2}/C_{u1}$=1.0, FS=1.50 (T6 element)**

### 6.3.3 $C_{u2}/C_{u1}$=1.5

Continuing to increase the shear strength of the soil in the foundation, the resulting factors of safety with $C_{u2}/C_{u1}$ =1.5 using limit equilibrium methods using SLOPE/W and finite element methods using ABAQUS are summarized in Table 6.4. The majority of the limit equilibrium methods provide a factor of safety for this case of 2.078, except for the Janbu's method. The reason for the discrepancy in Janbu's results with the other limit equilibrium methods is unclear. The analyses using T6 and Q8 elements provide similar factors of safety, which are 2.09 and 2.08 respectively. Griffiths and Lane (1999) found a factor of safety for this slope of

2.10 using finite element methods. The failure mechanism using T6 elements is shown in Figure 6.7. Two potential slip surfaces emerge, one is a circular surface at the base of the foundation and the other is a planar surface through the toe of the slope. These surfaces formed simultaneously in the analyses and which is a weaker surface cannot be ascertained. These results match the failure surfaces found by Griffiths and Lane (1999) for this particular case

**Table 6.4 Results of numerical analysis in slope stability, $C_{u2}/C_{u1}$=1.5**

| Method | Janbu | Bishop | Spencer | GLE | Ordinary | M-P | ABAQUS(T6) | ABAQUS(Q8) |
|---|---|---|---|---|---|---|---|---|
| **Circular** | 1.915 | 2.078 | 2.078 | 2.078 | 2.078 | 2.078 | 2.09 | 2.08 |

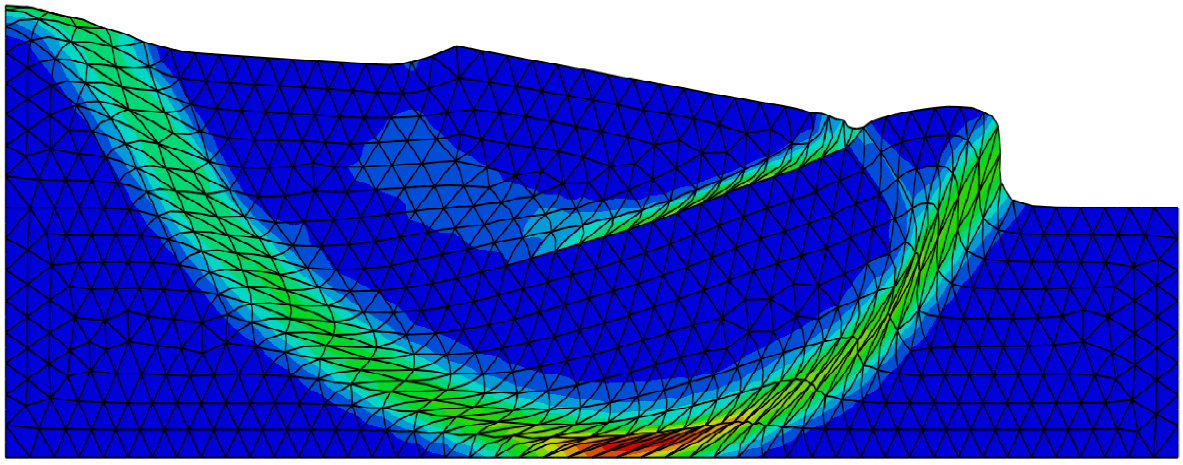

**Figure 6.7 The plastic strain contour with $C_{u2}/C_{u1}$=1.5, FS=2.09 (T6 element)**

### 6.3.4 $C_{u2}/C_{u1}$=2.0

If the strength ratio, $C_{u2}/C_{u1}$ rises up to 2.0, the resulting factors of safety are summarized in Table 6.5. The analyses performed with T6 and Q8 elements have very close results on factor of safety of 2.18 and 2.17, respectively. Comparing these results to the results using limit equilibrium methods based on the similar failure type analysis (toe failure), the values are both higher in finite element analysis than in limit equilibrium analyses, 2.17 to 2.12. The plastic strain contour in finite element analysis using ABAQUS is shown in Figure 6.8. The potential slip surface in terms of maximum plastic strain found in finite element analysis occurs at the toe on the slope not through the foundation. The limit equilibrium method provides another failure mechanism for this case, in which the slip surface passes to the bottom of the foundation soils and results are lower factors of safety as shown in Table 6.5. However, in finite element analyses, the failure surface is not preassumed, thus, there is no result to be compared with those in limit equilibrium methods. Thus the finite element method and the limit equilibrium method diverge on their results for this case. The finite element would predict that the failure surface passes through the toe of the slope and not into the foundation soils. The finite element results make intuitive sense in that the when the foundation soils are twice as strong as the slope soils, there would not be an expectation that

a failure surface would necessarily move into the foundation. These finite element slope stability results agree with those presented by Griffiths and Lane (1999).

In Figure 6.9, the relationship of factor of safety and $C_{u2}/C_{u1}$ is presented. The trend of curve in the plot shows when $C_{u2}/C_{u1}$ is at or exceeds 1.5, and the factor of safety increase is very limited, which is identical to the results by Griffiths and Lane (1999). The results of slope stability analysis using ABAQUS with the T6 and T8 elements give rise to very close solutions and trend (see Figure 6.10)

**Table 6.5 Results of numerical analysis in slope stability, $C_{u2}/C_{u1}$=2.0**

| Method | Janbu | Bishop | Spencer | GLE | Ordinary | M-P | ABAQUS(T6) | ABAQUS(Q8) |
|---|---|---|---|---|---|---|---|---|
| **Slope** | 2.083 | 2.125 | 2.125 | 2.125 | 2.125 | 2.125 | 2.18 | 2.17 |
| **Base** | 1.940 | 1.977 | 1.969 | 1.967 | 2.017 | 1.997 | NA | NA |

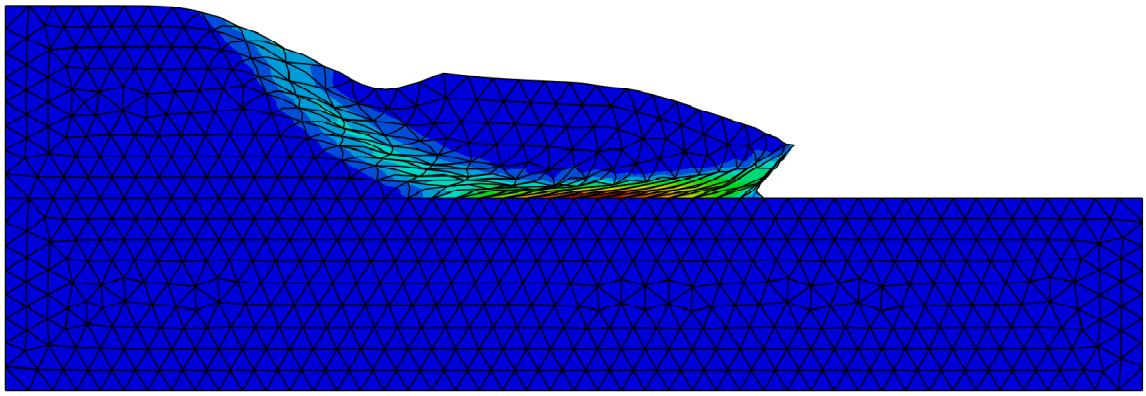

**Figure 6.8 The plastic strain contour with $C_{u2}/C_{u1}$=2.0, FS=2.18 (T6 element)**

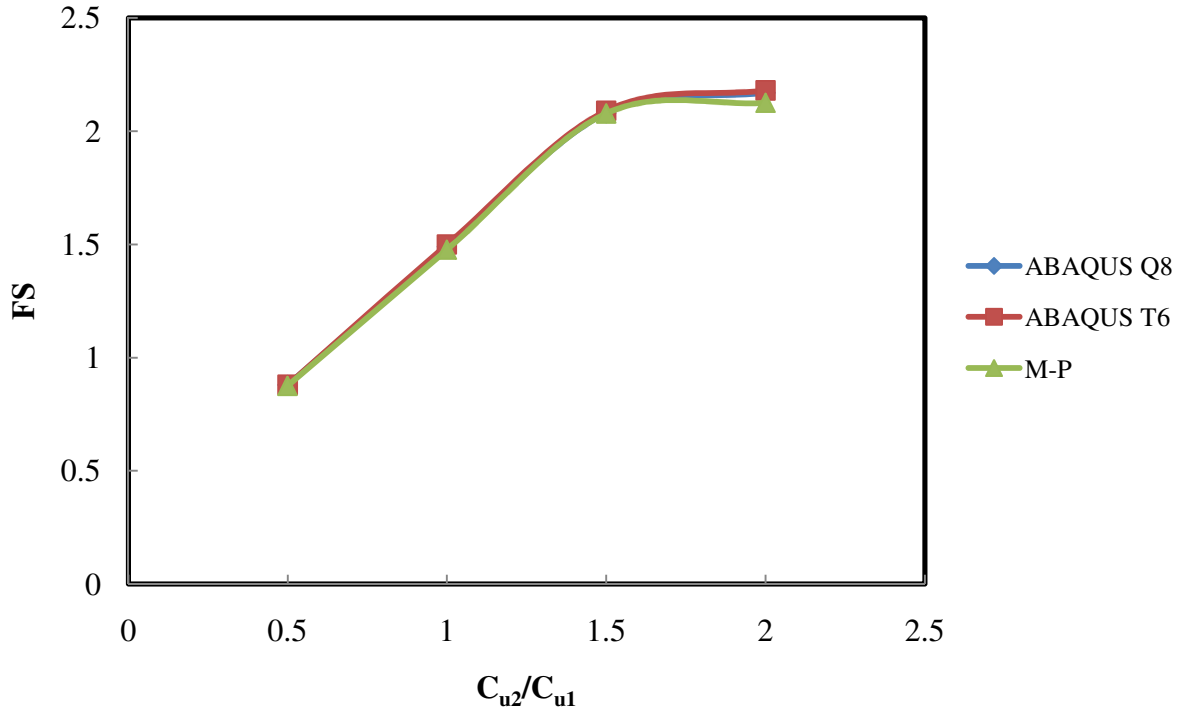


**Figure 6.9 Factor of safety versus $C_{u2}/C_{u1}$, non homogeneous slope with foundation**

## 6.4 Analysis of Slope Stability Using Piles

This section includes the pile stabilization case description, finite element analysis, optimal pile location, length of pile, and pile head condition based on the non homogeneous slope stabilized with the reinforced pile.

### 6.4.1 Pile Stabilization Case Description

A pile is used to stabilize the non-homogeneous slope with different undrained shear strength in the slope and underlying foundation. The analysis is to determine the optimal pile location, appropriate pile head condition and acceptable pile length in a slope. The geometry of the slope reinforced with pile in this case is shown as Figure 6.10. The regions in Figure 6.10 marked with different colors are to represent the different soil shear strength. The soils in this case are assumed undrained. Therefore, the undrained shear strength in the slope portion is assigned as $C_{u1}$, and the soil in the underlain foundation is assigned as $C_{u2}$. $C_{u1}$ is determined by the ratio $C_{u1}/\gamma H=0.25$, and $C_{u2}$ is obtained according to the assumption of the ratio $C_{u2}/C_{u1}$. The ratios of strength, $C_{u2}/C_{u1}$ are used as 0.5, 1.0, 1.5 and 2.0. The results of the analyses are discussed herein.

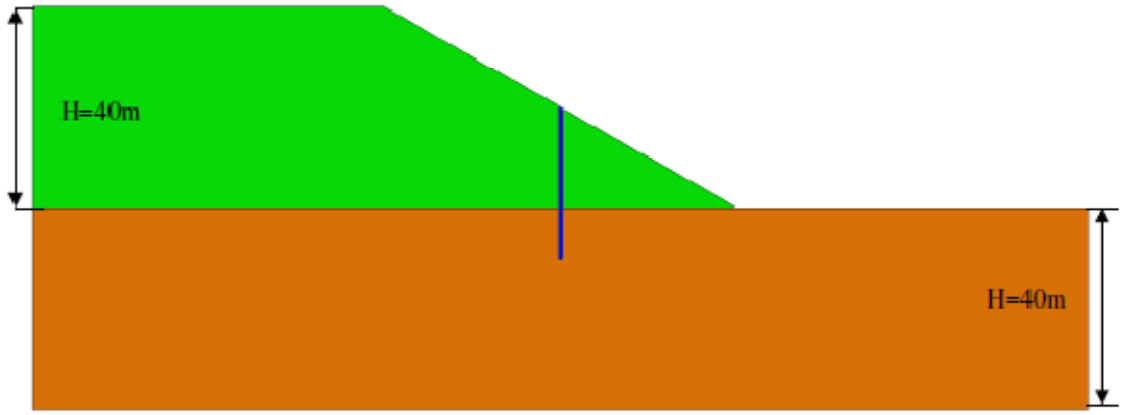


**Figure 6.10 Piled-Slope System model in ABAQUS ($X_p/X$=0.5, L=30m)**

### 6.4.2 Finite Element Analysis

In finite element analysis, the soil properties are used the same to the slope stability analysis in this case which have been summarized in Table 6.1 based on the strength of slope ($C_{u1}$). $C_{u2}/C_{u1}$=0.5, 1.0, 1.5 and 2.0 used for analysis. The pile is assumed as an elastic media 20m long, and the elastic material properties of the pile are Young's modulus (E) =60000 MPa, and Poisson's ratio (ν)=0.2, respectively. The selection of element type on pile is a 2-D plane stress, 8- node with reduced integration element, and the soil is selected as 2-D plane strain, 8-node with reduced integration quadrilateral element. The property of interface element between pile and soil is assumed zero-thickness which can only transfer shear stress across the surfaces when a compressive normal pressure (p') applies on it. The pile-soil friction coefficient, η is 0.30 which is based on η=tan(δ), where δ is friction angle between pile and

surrounding soil. To present the improvement of slope stability after pile is inserted, an improvement ratio $N_{pi}$ in terms of percentage is used herein. The definition of improvement ratio, $N_{pi}$ is defined as follows:

$$N_{pi} = \frac{F_p - F_s}{F_s} * 100\% \quad (6.1)$$

Where $F_p$ is minimum factor of safety of piled-slope system, $F_s$ is the minimum factor of safety of the unreinforced slope stability problem.

### 6.4.3 Optimal Pile Location

Following the slope stability analyzed in previous sections, the slope incorporates the pile in the analysis is classified as four types based on the ratio $C_{u2}/C_{u1}$. The $C_{u2}/C_{u1}$ =0.5, 1.0, 1.5 and 2.0 are discussed respectively. The relationship between the factor of safety and the position ratios $X_p/X$ are presented in the following Figures.

#### 6.4.3.1 $C_{u2}/C_{u1}$=0.5

In this case, the undrained shear strength of the soil in the foundation is weaker than the soil in the slope. As discussed previously, the resulting factor of safety before the pile installed is 0.88 using ABAQUS. The pile used to determine the optimal pile location is assumed as 20m

long. The highest factor of safety is found to be 1.13 when pile is installed in the middle portion of the slope and pile head is free. In both ends, toe and crest, the factors of safety are 0.98 and 0.95, respectively. The factors of safety at both ends are still lower than 1.0 after the pile is installed. If the pile head is restricted as fixed, the highest factor of safety occurs when the pile is placed at $X_p/X=0.25$ of the slope which is the quarter distance from the toe between the crest and the toe. The resulting factor of safety is found to be 1.20. The two curves in terms of the pile location and factor of safety resulted are plotted and compared in the slope in Figure 6.11. Thus the placement of a pile in a weak foundation case provides for improvement of the factor of safety only when the pile is placed away from the crest or toe. The largest increase in factor of safety occurs at the quarter point from the toe, and reaches a value of about 1.2.

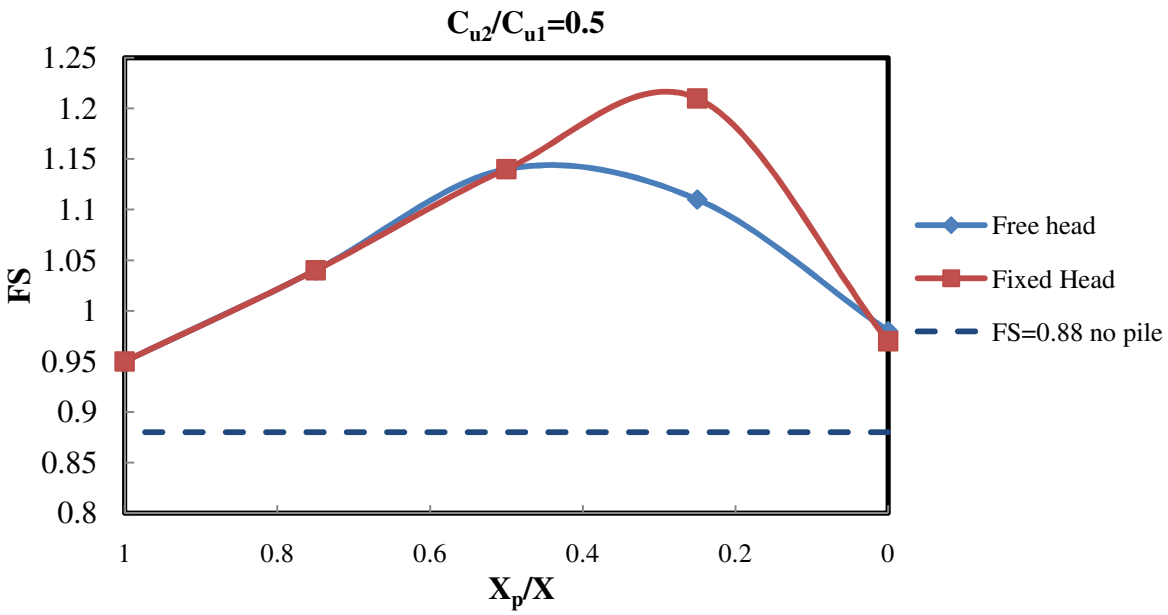


**Figure 6.11 Factor of safety versus $X_p/X$, $C_{u2}/C_{u1}$=0.5**

### 6.4.3.2 $C_{u2}/C_{u1}$=1.0

The case with $C_{u2}/C_{u1}$=1.0 is actually a homogeneous slope, the same undrained shear strength of soils in the slope and foundation which has been discussed in Chapter 5, but with a deeper foundation soil. The failure mechanism has been discussed in this Chapter as well. However, the different thickness in the foundation can lead to a different factor of safety in the analysis. In this case, the highest factor of safety resulted in the middle portion of the slope are found to be 1.88 and 1.92 with respect to free and fixed pile head condition, respectively, as shown in Figure 6.12 . Meanwhile, the lowest factors of safety resulted in the

finite element analysis for the pile with both head conditions occur when the pile is placed at the toe of the slope. The second lowest factors of safety occur in the crest of the slope. The relationship between the factor of safety and $X_p/X$ in the finite element analysis for pile with both free and fixed head conditions is shown and compared in Figure 6.12.

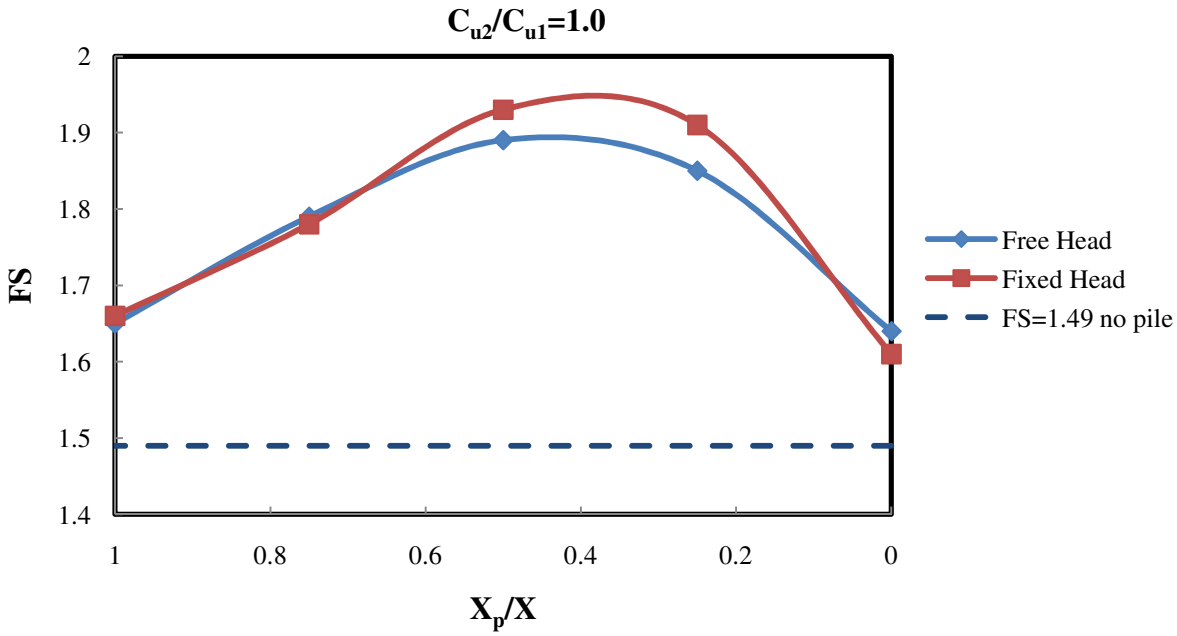


**Figure 6.12 Factor of safety versus $X_p/X$, $C_{u2}/C_{u1}$=1.0**

### 6.4.3.3 $C_{u2}/C_{u1}$=1.5

If the strength ratio of the slope and foundation, $C_{u2}/C_{u1}$=1.5, the undrained shear strength of soil in foundation is stronger than the soil in the slope. Refer to the slope stability analysis,

Figure 6.7 shows the potential slip surfaces may occur in two places at the same time. In this case, the relationship between the factor of and the pile location ratio, $X_p/X$ are very similar in the finite element analysis using ABAQUS for both pile head conditions and the results are shown in Figure 6.14. The highest factor of safety will still occur in the middle portion of the slope with the same value of 2.55 in the analysis for pile with both head conditions.

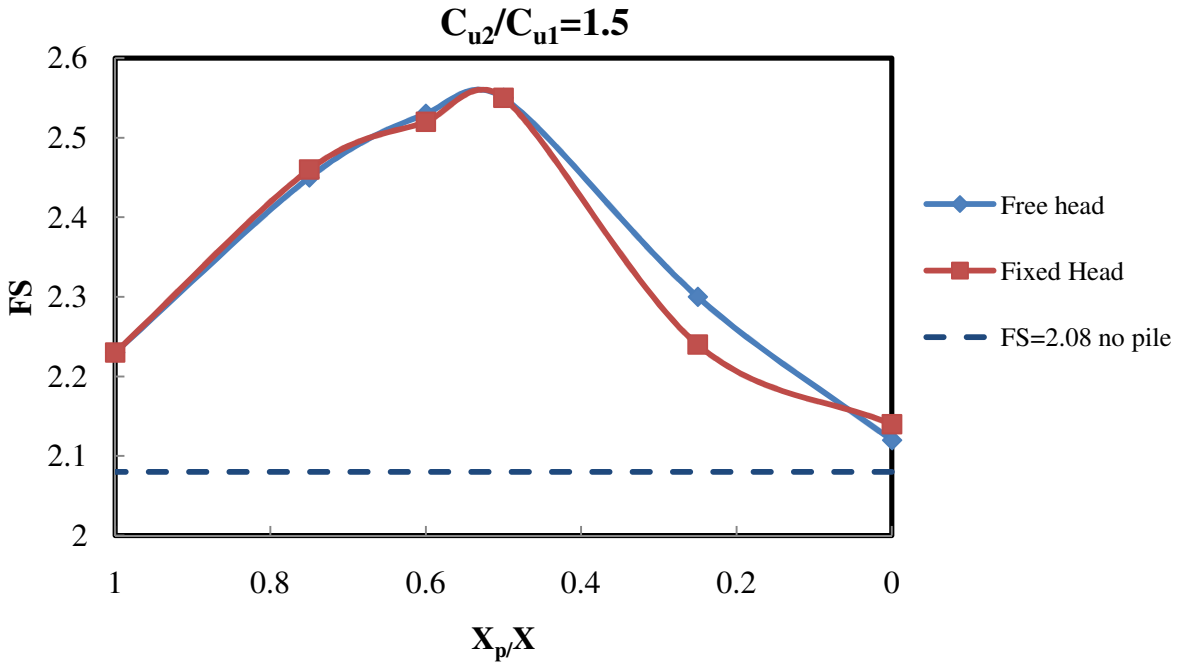


**Figure 6.13 Factor of safety versus $X_p/X$, $C_{u2}/C_{u1}$=1.5**

### 6.4.3.4 $C_{u2}/C_{u1}$=2.0

In this case, the undrained shear strength of the soil in the foundation is much stronger than the strength of soil in the slope. The case is similar to the case with the firm foundation or the

example case given in Chapter 4. The result of slope stability analysis presented previously shows the failure occurs in the slope, not through the foundation. Thus, the resulting factor of safety depends on the undrained shear strength of the soil in the slope (see Figure 6.8). The peak value of factor of safety is 3.15 which resulted when the pile is placed in the middle portion of the slope and the lowest value occurs when the pile is placed at the toe. The results of the pile with both free and fixed head condition are plotted in Figure 6.14. Both curves show the results are almost identical for the pile with free and fixed condition in Figure 6.14, respectively. The factor of safety resulted in both pile conditions are almost the identical along the entire location of the slope. The result shows that the stabilizing pile can just contribute slightly higher factor of safety on the slope stability of the piled slope.

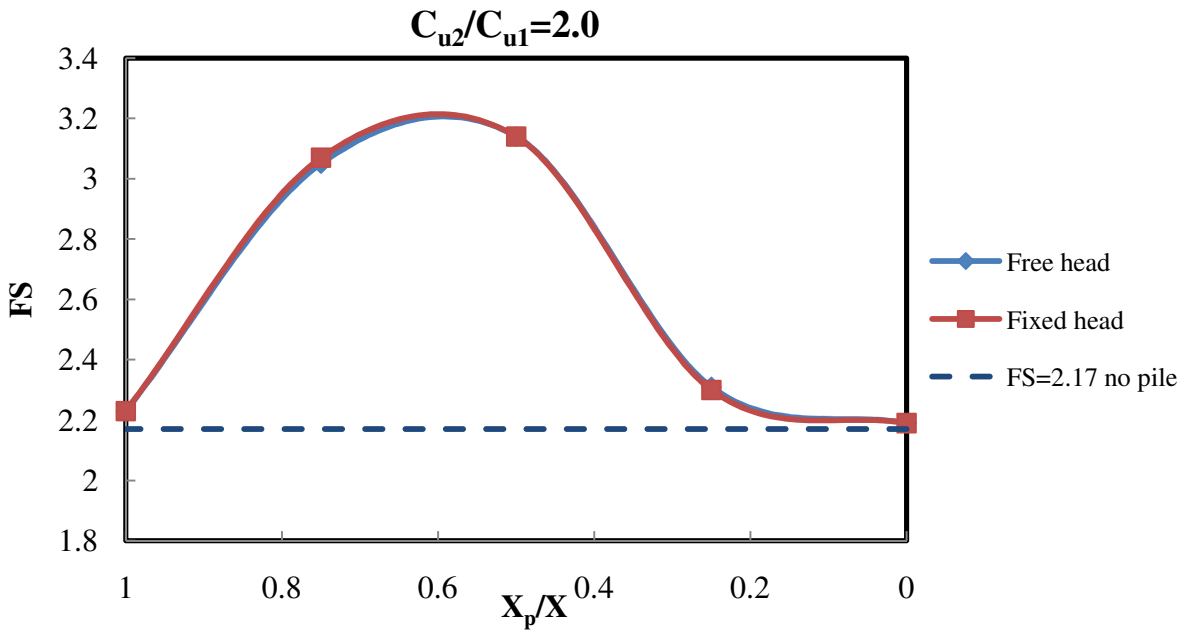


**Figure 6.14 Factor of safety versus $X_p/X$, $C_{u2}/C_{u1}$=2.0**

### 6.4.4 Length of Pile

The effect of the pile length in this case will also be classified into four sub-sections to discuss according to the strength ratio $C_{u2}/C_{u1}$ which is 0.5, 1.0, 1.5 and 2.0, respectively. According to the definition of $L_z/L$, the potential slip surface in homogeneous slope with foundation is 16 m deep in the unreinforced slope stability analysis by locating the surface with the maximum plastic strain. The $L_z$ is the depth of potential slip surface which based on the contour of the largest plastic shear strain. The reason to select a potential slip surface is the same as which mentioned previously in Chapters 4 and 5. The potential slip surface may

change in the so called coupled analysis due to the presence of the stabilizing pile. Unlike in the so called uncoupled analysis, the depth of slip surface has to be assumed or determined based on slope stability analysis. It is more difficult to determine a slip surface and compare to the depth of pile installation in this coupled analysis. The L, the true length of the pile, is selected from 10m which is the half of the middle height of the slope with is 40m high. In previous section, the optimal pile location has been determined in the middle portion of the slope, therefore, the height of the slope in the middle portion is 20m, the half of the height to be used as the least length of pile in the finite element analysis.

#### 6.4.4.1 $C_{u2}/C_{u1}=0.5$

Basically, the factor of safety rises along with the increase of the pile length in the analysis of the $C_{u2}/C_{u1}=0.5$. Figure 6.15 presents the correlation of the factor of safety and the length of pile. The results of finite element analysis using ABAQUS are summarized in Table 6.6. Figure 6.16 shows the improvement rate ($N_{pi}$) of the slope stability using pile to stabilize. Figure 6.17 presents the factor of safety versus $L_z/L$ and Figure 6.18 shows the factor of safety of slope stability improved using stabilizing pile in terms of $L_z/L$. In addition, in Figure 6.11, the results indicate the highest factor of safety occurs at the position, $X_p/X=0.25$

when pile head is restricted as fixed. Therefore, based on this position, the analyses are also performed in terms of pile length and the results are also compared in Figures 6.15 to 6.18. In a certain range of the pile length, the result does show the advantages. However, based on the depth of slip face at $X_p/X=0.25$, the resulting factor of safety using 10m of stabilizing pile in terms of $L_z/L$ is lower than the value resulted when the pile is place in the middle portion of the slope which is shown in Figures 6.17 and 6.18. The results of finite element analysis are summarized in Table 6.7. Due to the different depth of slip surface in these two locations, the $L_z$ is determined as 10m at the location of $X_p/X=0.25$, while at $X_p/X=0.5$, $L_z$ is located as 16m depth.

**Table 6.6 Factor of safety of the pile-stabilized slope based on the length of pile, $C_{u2}/C_{u1}$=0.5, $X_p/X$=0.5**

| $X_p/X$=0.5 | | | | | | | | | | | | | |
|---|---|---|---|---|---|---|---|---|---|---|---|---|---|
| Pile length, L (m) | 10 | 12 | 14 | 16 | 18 | 19 | 20 | 23 | 25 | 28 | 30 | 32 | 35 |
| $L_z/L$ ($L_z$=16m) | | | | 1.00 | 0.89 | 0.84 | 0.80 | 0.70 | 0.64 | 0.57 | 0.53 | 0.5 | 0.46 |
| FS | 1.00 | 1.03 | 1.05 | 1.08 | 1.11 | 1.13 | 1.14 | 1.17 | 1.22 | 1.29 | 1.30 | 1.34 | 1.37 |
| $N_{pi}$ (%) | 13.64 | 17.05 | 19.32 | 22.73 | 26.14 | 28.41 | 29.55 | 32.95 | 38.64 | 46.59 | 47.73 | 52.27 | 55.68 |
| FS | 1.00 | 1.03 | 1.05 | 1.08 | 1.11 | 1.13 | 1.14 | 1.15 | 1.24 | 1.29 | 1.31 | 1.39 | 1.47 |
| $N_{pi}$ (%) (fixed head) | 13.64 | 17.05 | 19.32 | 22.73 | 26.14 | 28.41 | 29.55 | 37.50 | 40.91 | 46.59 | 48.86 | 57.95 | 67.05 |

**Table 6.7 Factor of safety of the pile-stabilized slope based on the length of pile, $C_{u2}/C_{u1}$=0.5, $X_p/X$=0.25**

| Position $X_p/X$=0.25 | | | | | | | | | | |
|---|---|---|---|---|---|---|---|---|---|---|
| Pile length, L (m) | 18 | 20 | 22 | 24 | 26 | 28 | 30 | 32 | 34 | 35 |
| $L_z/L$ ($L_z$=10 m) | 0.556 | 0.5 | 0.455 | 0.417 | 0.385 | 0.357 | 0.333 | 0.313 | 0.294 | 0.286 |
| FS (fixed head) | 1.17 | 1.21 | 1.23 | 1.27 | 1.29 | 1.33 | 1.33 | 1.34 | 1.35 | 1.35 |
| $N_{pi}$ (%) | 32.95 | 37.50 | 39.77 | 44.32 | 46.59 | 51.14 | 51.14 | 52.27 | 53.41 | 53.41 |

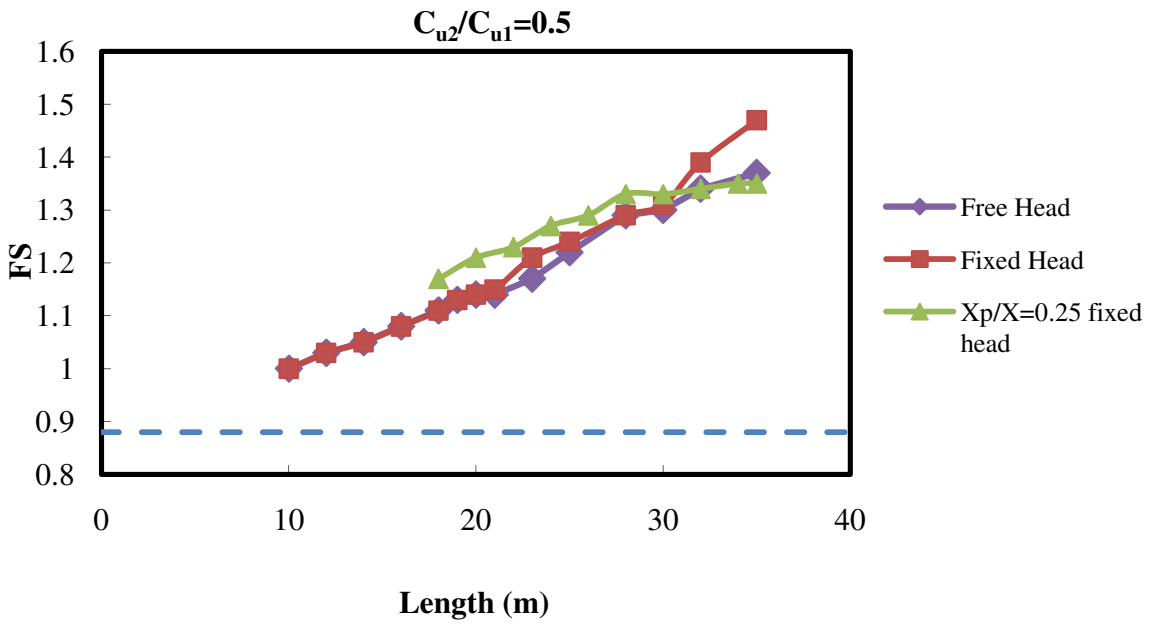


**Figure 6.15 Factor of safety versus Length of pile in non-homogeneous slope with foundation, $C_{u2}/C_{u1}$=0.5**

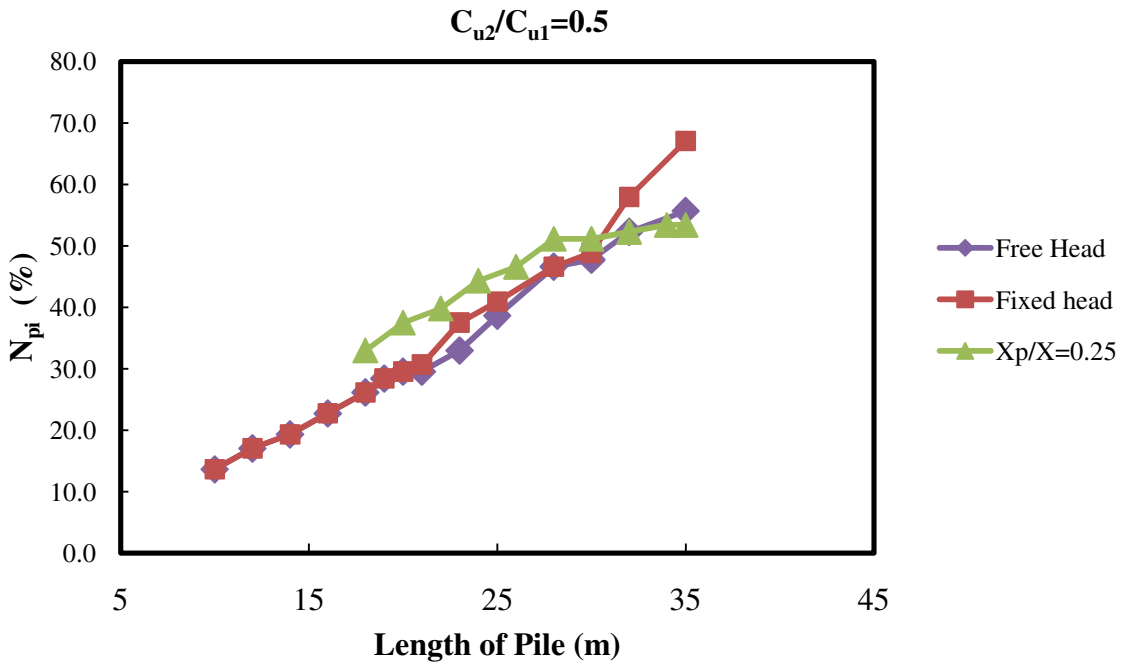


**Figure 6.16 $N_{pi}$ versus Length of Pile**

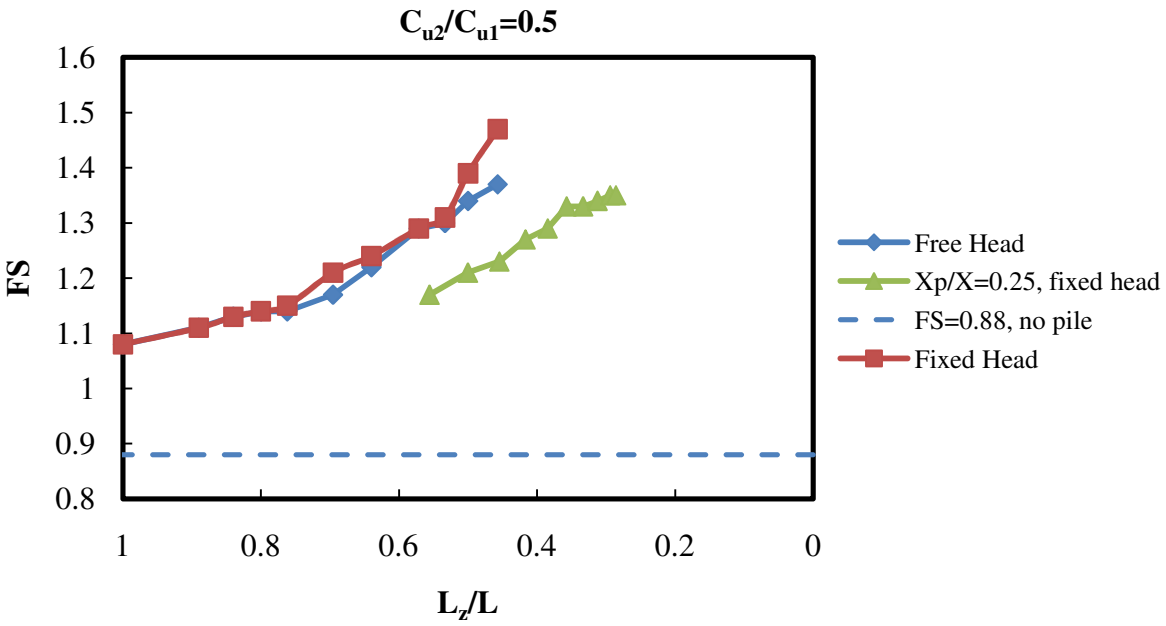


**Figure 6.17 Factor of safety versus $L_z/L$, $C_{u2}/C_{u1}$=0.5**

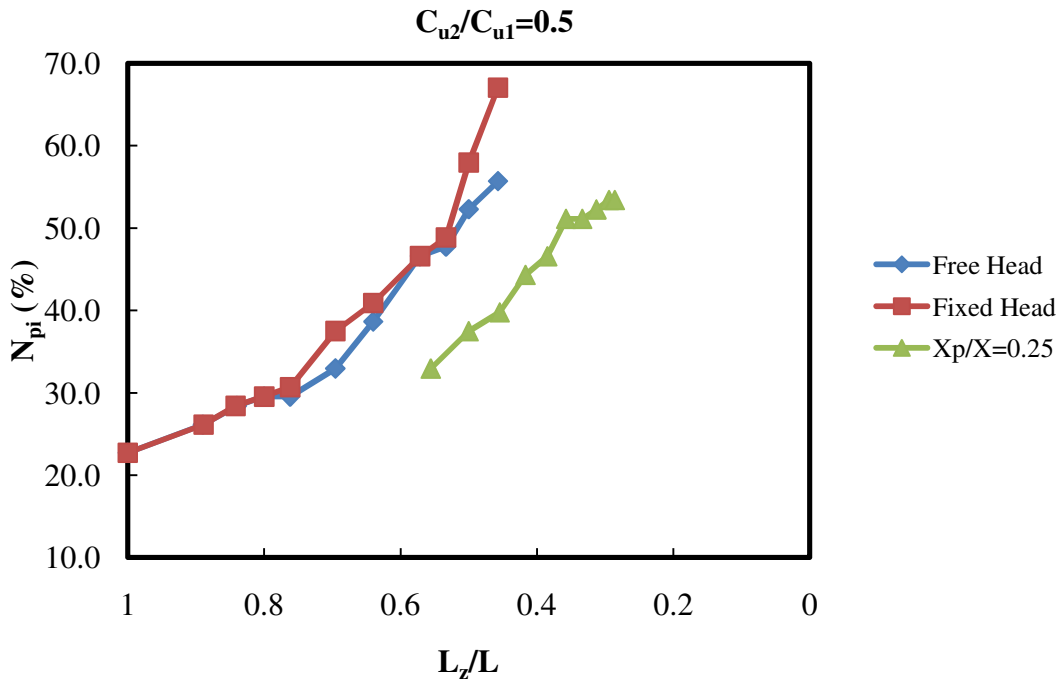


**Figure 6.18 $N_{pi}$ versus $L_z/L$, $C_{u2}/C_{u1}$=0.5**

### 6.4.4.2 $C_{u2}/C_{u1}=1.0$

The resulting factor of safety increases along with the increase of the pile length when $C_{u2}/C_{u1}=1.0$. The results of analysis are summarized in Table 6.8. Figure 6.19 presents the correlation of the factor of safety and the length of pile. Because the factor of safety the slope stability analysis is 1.49, the results of the slope reinforced with pile compared to the unreinforced slope are shown in Figure 6.19. In this Figure, the factor of safety increases from 1.64 to 2.2 for fixed head pile condition, but, for the free head pile condition, the factor of safety increases to about 2.2, and stops increasing after. Figure 6.20 shows the results in terms of improvement ratio $N_{pi}$. The improvement ratio increases from 10% to 48 % for free head pile, and 10% to nearly 70% for fixed head pile, respectively. Figure 6.21 presents the factor of safety versus $L_z/L$ and Figure 6.22 shows the factor of safety of the slope stability improved using the pile in terms of $L_z/L$. Both Figures 6.20 and 6.22 present the comparison of the results for pile with free and fixed head condition in terms of the improvement ratio, $N_{pi}$, respectively. The result shows the improvement ratio of the slope stability of the piled slope increases with the increase of the pile length.

**Table 6.8 Factor of safety of the pile-stabilized slope based on the length of pile, $C_{u2}/C_{u1}$=1.0**

| $X_p/X$=0.5 | | | | | | | | | | | | | |
|---|---|---|---|---|---|---|---|---|---|---|---|---|---|
| Pile length, L (m) | 10 | 12 | 14 | 16 | 18 | 19 | 20 | 23 | 25 | 28 | 30 | 32 | 35 |
| $L_x/L$ ($L_x$=16m) | | | | 1.00 | 0.89 | 0.84 | 0.80 | 0.70 | 0.64 | 0.57 | 0.53 | 0.5 | 0.46 |
| FS | 1.64 | 1.67 | 1.73 | 1.78 | 1.84 | 1.87 | 1.89 | 2.03 | 2.06 | 2.16 | 2.14 | 2.21 | 2.2 |
| $N_{pi}$ (%) | 10.07 | 12.08 | 16.11 | 19.46 | 23.49 | 25.50 | 25.85 | 35.24 | 38.26 | 44.97 | 43.62 | 48.32 | 47.65 |
| FS | 1.64 | 1.68 | 1.73 | 1.78 | 1.84 | 1.87 | 1.93 | 2.04 | 2.07 | 2.19 | 2.27 | 2.36 | 2.49 |
| $N_{pi}$ (%) (fixed head) | 10.07 | 12.75 | 16.11 | 19.46 | 23.49 | 25.50 | 29.53 | 35.91 | 38.93 | 46.98 | 52.35 | 58.39 | 67.11 |

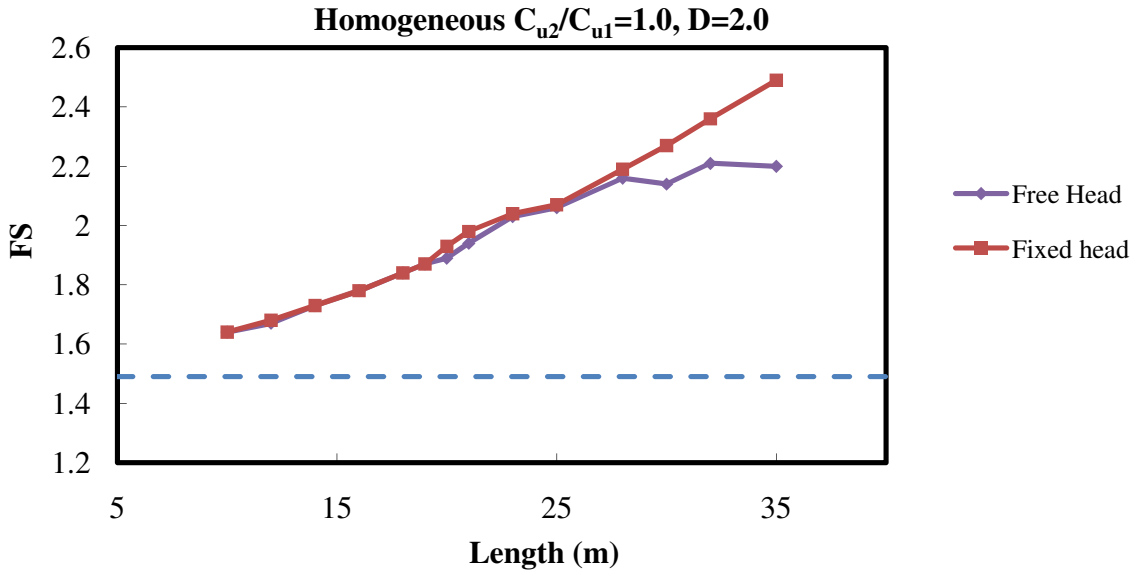


**Figure 6.19 Factor of safety versus Length of pile in non-homogeneous slope with foundation, $C_{u2}/C_{u1}$=1.0**

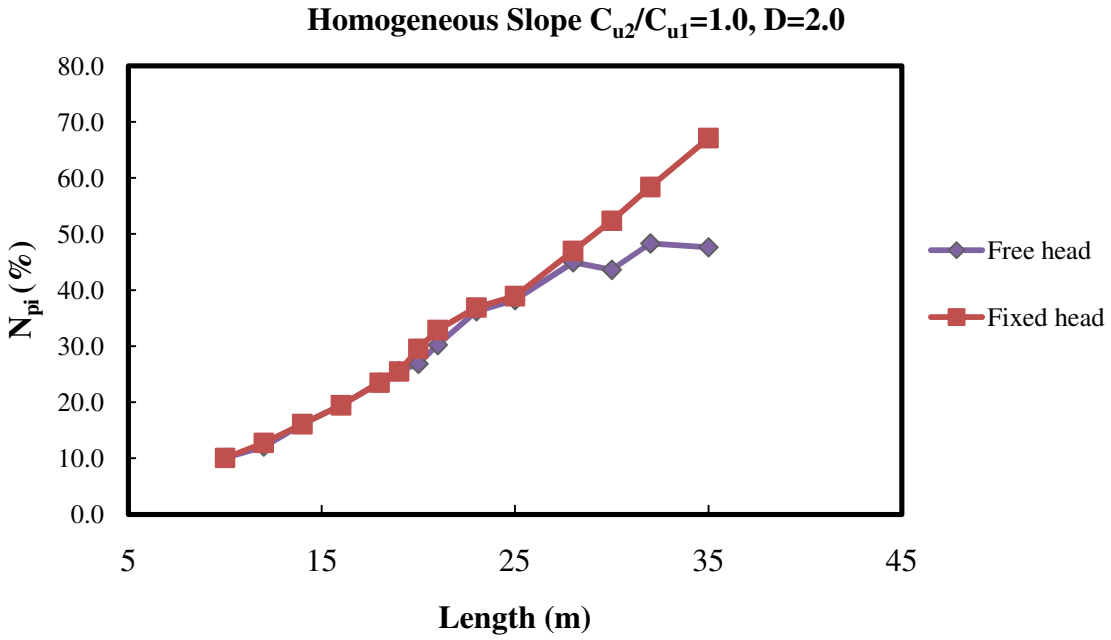


**Figure 6.20 $N_{pi}$ versus Length of Pile, $C_{u2}/C_{u1}$=1.0**

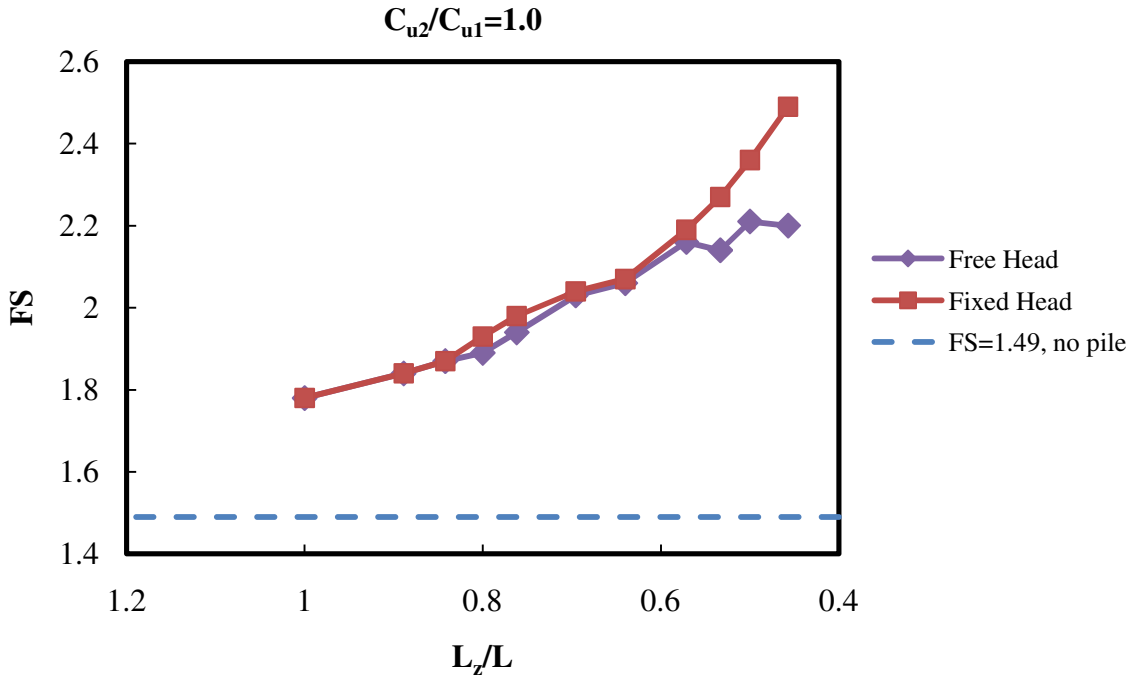


**Figure 6.21 Factor of safety versus $L_z/L$, $C_{u2}/C_{u1}$=1.0**

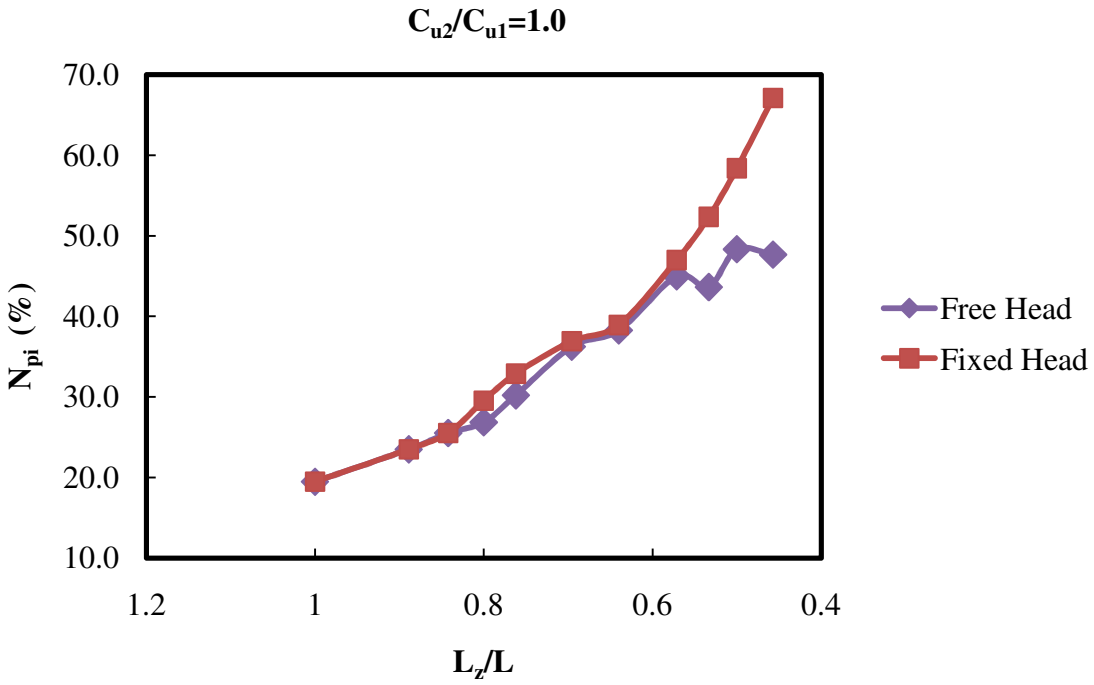


**Figure 6.22 $N_{pi}$ versus $L_z/L$, $C_{u2}/C_{u1}$=1.0**

### 6.4.4.3 $C_{u2}/C_{u1}$=1.5

The resulting factors of safety are summarized in Table 6.9 for the case with the strength ratio, $C_{u2}/C_{u1}$=1.5. Figure 6.23 presents the correlation of the factor of safety and the length of the pile. The factor of safety of the slope reinforced with the pile increases with the increase of the pile length. The factor of safety in the slope stability analysis of unreinforced slope is 2.08, the dash line in Figures 6.23 and 6.25 show the comparisons between the slope stability reinforced with pile or unreinforced slope. The results presented in Figure 6.23 show

the factor of safety increases from 2.25 to around 3.05. Figure 6.24 shows the improvement rate ($N_{pi}$) of the piled-slope stability. To confirm the optimal pile location does not occur in any other location along the slope, the finite element analysis in terms of pile length based on $X_p/X=0.6$ is conducted. The result is also included in the following figures. The improvement rate ($N_{pi}$) increases from 8% to 47 %. Figure 6.25 presents the factor of safety versus $L_z/L$ and Figure 6.26 shows the factor of safety in the stability analysis of the slope reinforced with pile improved from pile because of the different length ratios, $L_z/L$. Both Figure 6.25 and Figure 6.26 present the comparison of the analysis results for the pile with free and fixed head condition. The results also show the improvement of the slope stability in piled slope increase by increasing the length of the pile.

**Table 6.9 Factor of safety of the pile-stabilized slope based on the length of pile, $C_{u2}/C_{u1}$=1.5**

| $X_p/X$=0.5 | | | | | | | | | | | | | |
|---|---|---|---|---|---|---|---|---|---|---|---|---|---|
| Pile length, L (m) | 10 | 12 | 14 | 16 | 18 | 19 | 20 | 23 | 25 | 28 | 30 | 32 | 35 |
| $L_r/L$ ($L_r$=10m) | | | | 1.00 | 0.89 | 0.84 | 0.80 | 0.70 | 0.64 | 0.57 | 0.53 | 0.5 | 0.46 |
| FS | 2.25 | 2.30 | 2.36 | 2.42 | 2.49 | 2.53 | 2.49 | 2.73 | 2.78 | 2.92 | 3.00 | 3.07 | 3.06 |
| $N_{pi}$ (%) | 8.17 | 10.58 | 13.46 | 16.35 | 19.71 | 21.63 | 19.71 | 26.92 | 33.65 | 40.38 | 44.23 | 47.60 | 47.12 |
| FS | 2.25 | 2.29 | 2.35 | 2.41 | 2.47 | 2.50 | 2.50 | 2.74 | 2.78 | 2.95 | 3.04 | 3.11 | 3.24 |
| $N_{pi}$ (%) (fixed head) | 8.17 | 10.10 | 12.98 | 15.87 | 18.75 | 20.19 | 20.19 | 31.73 | 33.65 | 41.83 | 46.15 | 49.52 | 56.25 |

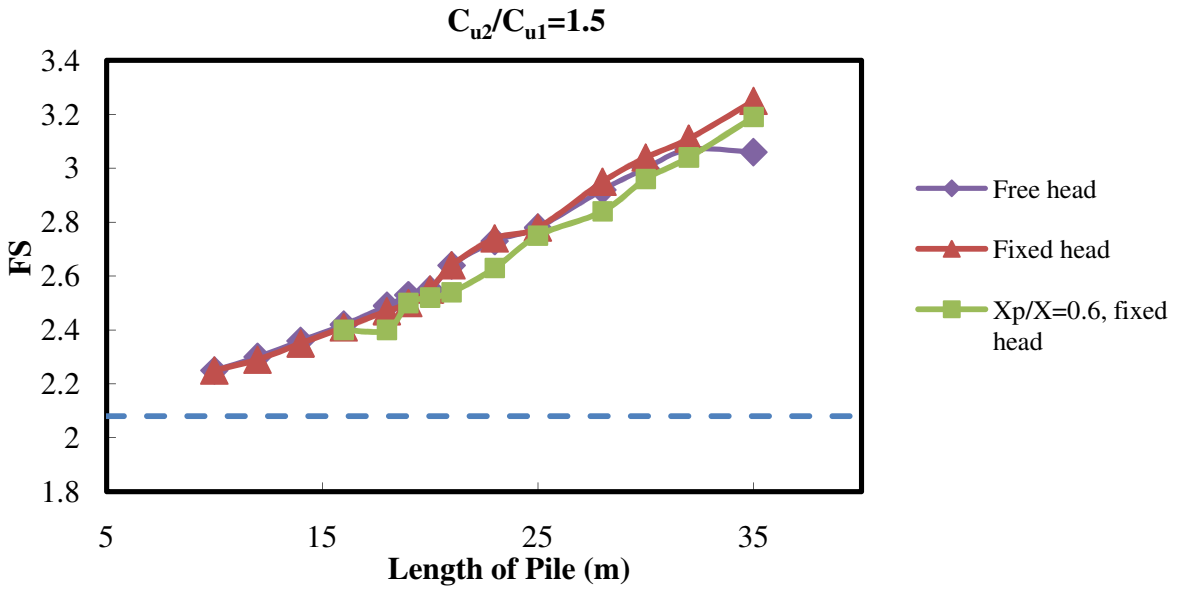


**Figure 6.23 Factor of safety versus length of pile in non-homogeneous slope with foundation, $C_{u2}/C_{u1}$=1.5**

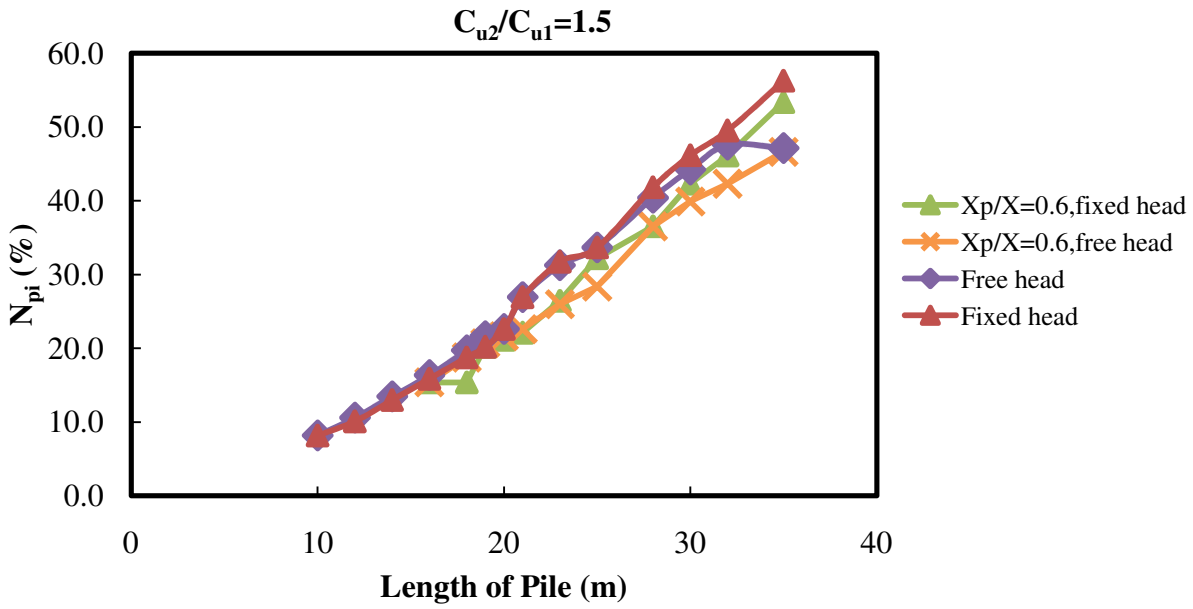


**Figure 6.24 $N_{pi}$ versus Length of Pile**

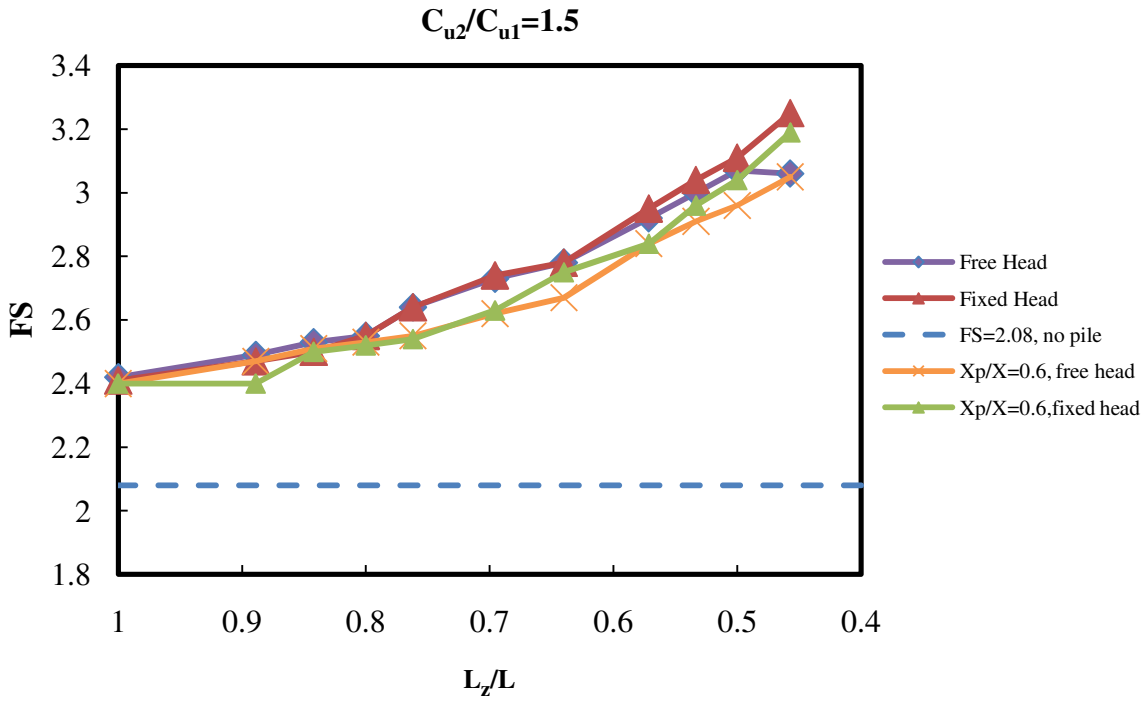


**Figure 6.25 Factor of safety versus $L_z/L$, $C_{u2}/C_{u1}$=1.5**

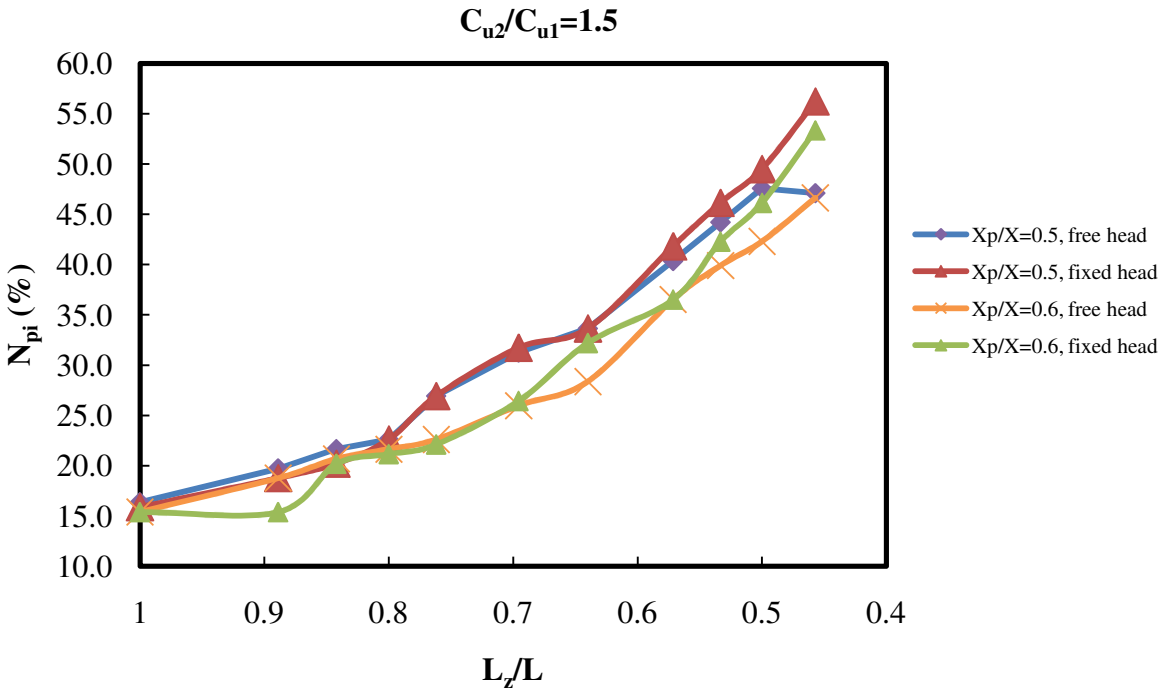


**Figure 6.26 $N_{pi}$ versus $L_z/L$, $C_{u2}/C_{u1}$=1.5**

#### 6.4.4.4 $C_{u2}/C_{u1}$=2.0

In this case, the undrained shear strength of the soil in the foundation becomes double of the soil in the slope. The numerical results are summarized in Table 6.10. Figure 6.27 presents the correlation of the factor of safety and the length of pile. The factor of safety increases in the early portion of the curve, then slightly decreases when the pile length reaches 23m for free head pile, however in the fixed head pile, the factor of safety keeps slightly increasing. The corresponding ratio of $L_z/L$ is 0.7. Because the factor of safety in the slope stability analysis is 2.17, the dashed line plotted in Figure 6.27 can be used to compare the factor of

safety increases. The results presented in Figure 6.27 show the lowest factor of safety is 2.84, and the highest value is 3.32. Figure 6.28 shows the improvement ratio ($N_{pi}$) of the piled-slope stability. The trend of the improvement ratio, $N_{pi}$ , showing the lowest value is 30.88%, and the highest value is 53.0 %. Figure 6.29 presents the factor of safety versus $L_z/L$ and Figure 6.30 shows the factor of safety of the slope stability improved due to the change of the ratio, $L_z/L$.

**Table 6.10 Factor of safety of the pile-stabilized slope based on the length of pile, $C_{u2}/C_{u1}$=2.0**

| $X_p/X$=0.5 | | | | | | | | | | | | | |
|---|---|---|---|---|---|---|---|---|---|---|---|---|---|
| **Pile length, L (m)** | 10 | 12 | 14 | 16 | 18 | 19 | 20 | 23 | 25 | 28 | 30 | 32 | 35 |
| **$L_z/L$ ($L_z$=16m)** | | | | 1.00 | 0.89 | 0.84 | 0.80 | 0.70 | 0.64 | 0.57 | 0.53 | 0.5 | 0.46 |
| **FS** | 2.84 | 2.9 | 3.01 | 3.04 | 3.1 | 3.14 | 3.15 | 3.3 | 3.32 | 3.32 | 3.3 | 3.29 | 3.27 |
| **$N_{pi}$ (%)** | 30.88 | 33.64 | 38.71 | 40.09 | 42.86 | 44.70 | 45.16 | 52.07 | 53.00 | 53.00 | 52.07 | 51.61 | 50.69 |
| **FS** | 2.84 | 2.89 | 3.01 | 3.02 | 3.08 | 3.11 | 3.15 | 3.33 | 3.31 | 3.34 | 3.36 | 3.36 | 3.39 |
| **$N_{pi}$ (%) (fixed head)** | 30.88 | 33.18 | 38.71 | 39.17 | 41.94 | 43.32 | 45.16 | 53.46 | 52.53 | 53.92 | 54.84 | 54.84 | 56.22 |

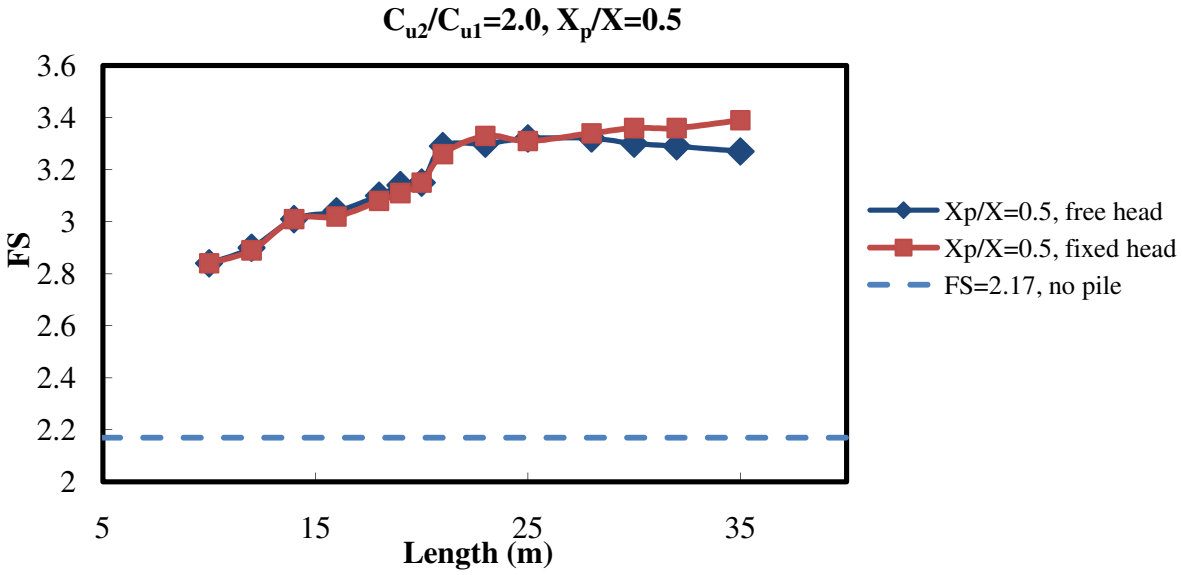


**Figure 6.27 Factor of safety versus length of pile in non-homogeneous slope with foundation, $C_{u2}/C_{u1}$=2.0**

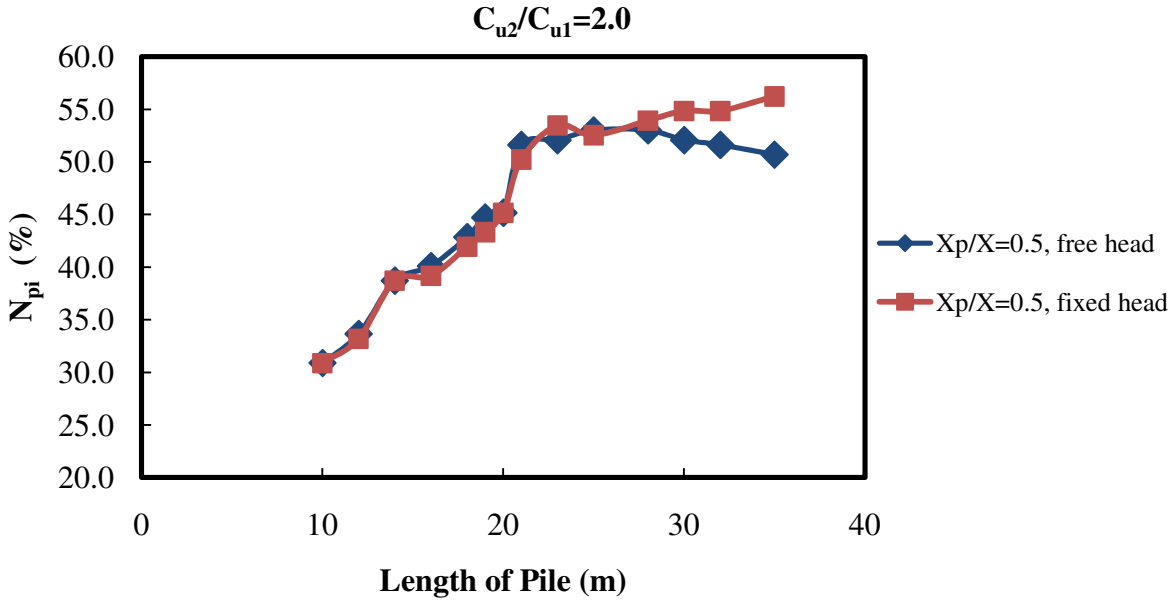


**Figure 6.28 $N_{pi}$ versus Length of Pile, $X_p/X$=0.5**

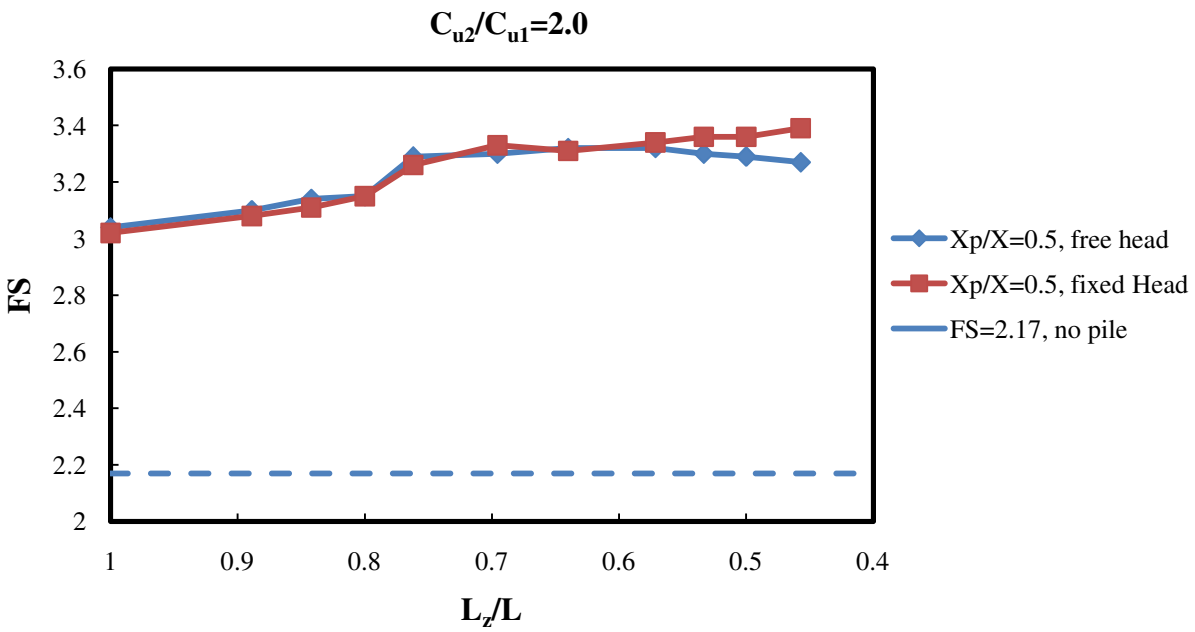


**Figure 6.29 Factor of safety versus $L_z/L$, $C_{u2}/C_{u1}$=2.0**

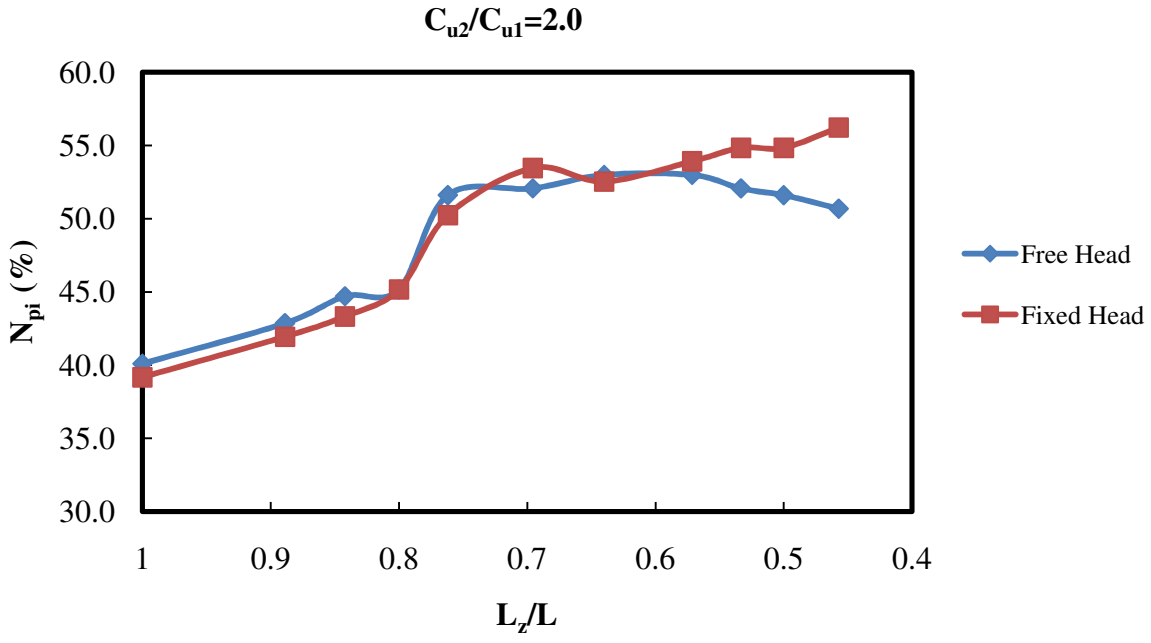


**Figure 6.30 $N_{pi}$ versus $L_z/L$, $C_{u2}/C_{u1}$=2.0**

To summarize the overall results due to the different ratios, $C_{u2}/C_{u1}$, 0.5, 1.0, 1.5 and 2.0, Figure 6.31 presents the comparison of the overall resulting factors of safety in the analysis of different strength ratios of the slope for the pile with free head condition. Undoubtedly, the highest factors of safety occur if the strength ratio of the slope, $C_{u2}/C_{u1}$=2.0 which slope with a firm foundation and the lowest factor of safety occurs when $C_{u2}/C_{u1}$=0.5 which slope with a weaker foundation. In terms of the improvement ratio, $N_{pi}$, the factor of safety of the cases with $C_{u2}/C_{u1}$=0.5, 1.0 and 1.5 increase when the pile length increases. In addition, the rates of improvement are very close as shown in Figure 6.32 except for the slope with $C_{u2}/C_{u1}$=2.0. However, if the $C_{u2}/C_{u1}$=2.0, the improvement ratio ($N_{pi}$) will reach the highest value when the pile is as long as 23 m long and slightly decreases after the length of pile over 23m. Based on the ratio, $L_z/L$ defined in this study, Figures 6.33 and 6.34 show the comparisons of the factor of safety and the improvement ratio ($N_{pi}$) of the pile-reinforced slopes with different strength ratios, respectively.

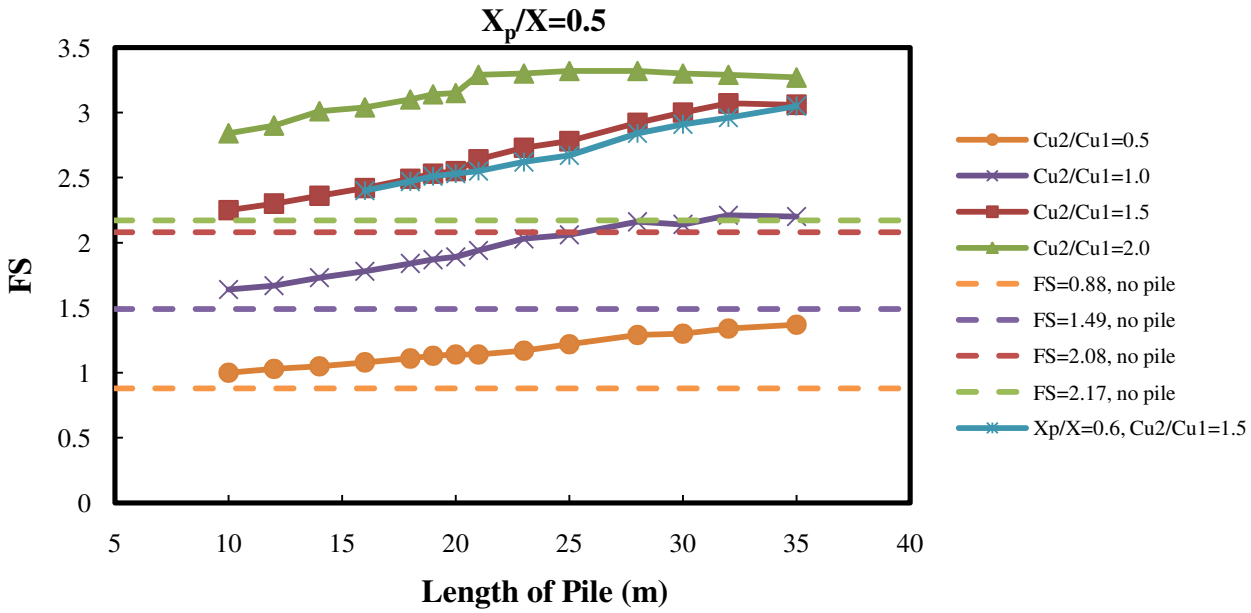


**Figure 6.31 Factor of safety versus Length of pile in non homogeneous slope with foundation, free head**

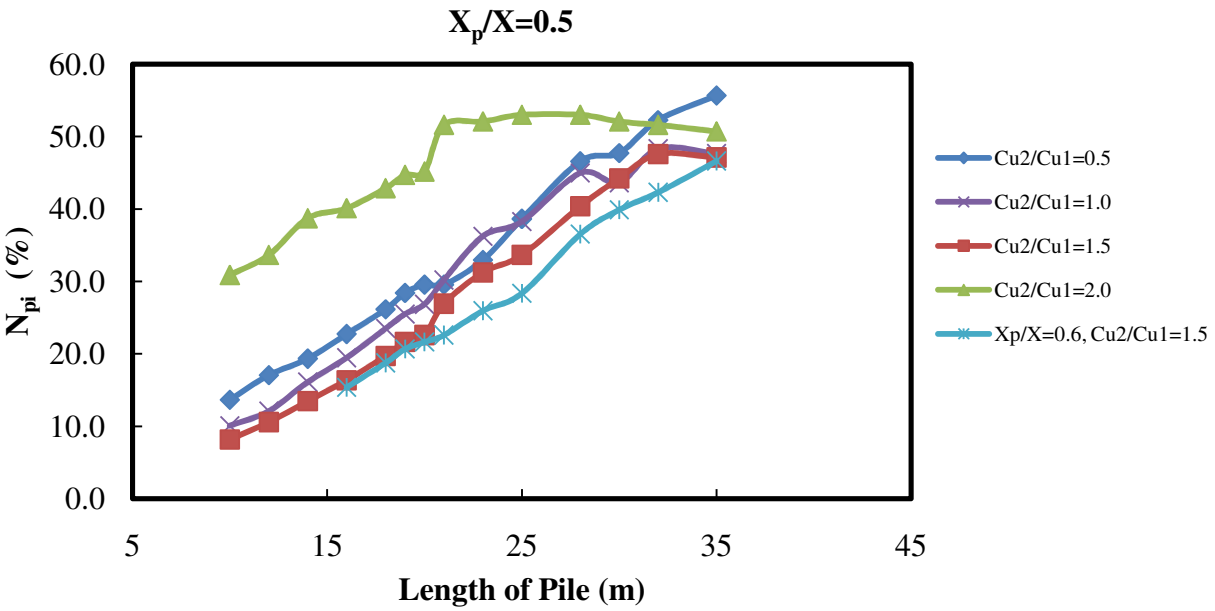


**Figure 6.32 $N_{pi}$ versus Length of Pile, free head**

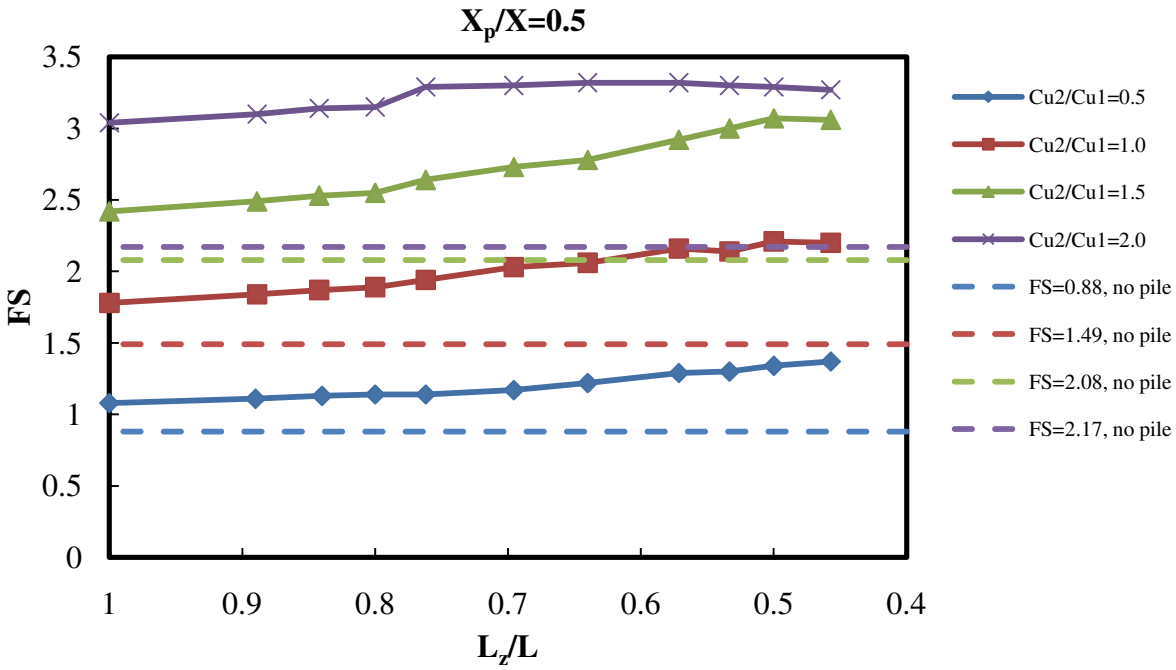


**Figure 6.33 Factor of safety versus $L_z/L$, free head**

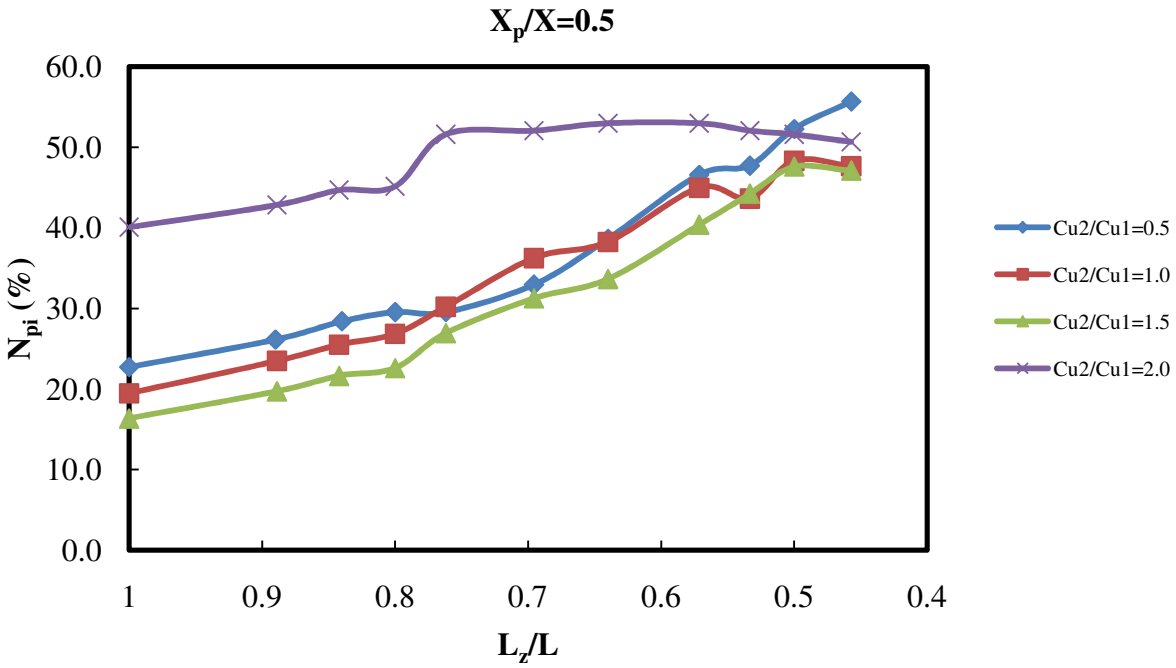


**Figure 6.34 $N_{pi}$ versus $L_z/L$, free head**

### 6.4.5 Pile Head Condition

The results of the finite element analysis with different pile head conditions in different locations of the slope can be referred to Figures 6.11 to 14. Figures 6.11 and 6.12 show that the improvement ratio ($N_{pi}$) of the slope stability varies due to the different pile head condition is applied. In both cases of the free and fixed head pile, the ratio $C_{u2}/C_{u1}$=0.5 and 1.0, indicate the pile with fixed head condition contribute slightly higher factor of safety than free head pile does. However, Figures 6.13 and 6.14 indicate that both cases of the strength ratios on slopes, $C_{u2}/C_{u1}$=1.5 and 2.0, the resulting factors of safety are nearly identical on both fixed and free pile head condition applied, respectively.

Figures 6.15 to 6.30 show the impact of the pile length on the slope stability of the piled slope due to the different pile head condition in terms of the factor of safety and the improvement rate ($N_{pi}$) respectively. In these four cases ($C_{u2}/C_{u1}$=0.5, 1.0, 1.5 and 2.0), the results show the fixed pile head condition works better when the pile is long enough. These figures indicate the fixed pile head condition give rise to a higher factor of safety than free head pile when the length of the pile is around or longer than 30 m. To normalize the length using the ratio of $L_z/L$ defined in this study, refer to Figures 6.18, 22, 26 and 30; when the

ratio ($L_z/L$) is less than 0.6, the fixed pile head leads to higher factors of safety than free pile head does on the improvement of the slope stability.

For the pile with fixed head condition, Figure 6.35 presents the comparison of the overall resulting factors of safety in the analysis of different strength ratios, $C_{u2}/_{Cu1}$. Similarly, the highest factors of safety resulted if the strength ratio of the slope, $C_{u2}/C_{u1}$=2.0, as the case with free head pile. The factors of safety resulted are very close if the strength ratios ($C_{u2}/C_{u1}$) of the slope are 1.0 and 1.5. In terms of the improvement ratio, $N_{pi}$, the factor of safety of the cases with $C_{u2}/C_{u1}$=0.5, 1.0 and 1.5 increase when the pile length increases. In addition, the rates of improvement are very close as shown in Figure 6.36 except for the slope with $C_{u2}/C_{u1}$=2.0. When $C_{u2}/C_{u1}$=2.0, the resulting improvement ratio ($N_{pi}$) compared to the other three cases ($C_{u2}/C_{u1}$=0.5, 1.0 and 1.5) is higher if the pile length is at or shorter than 30m. Based on the length ratio, $L_z/L$, Figures 6.37 presents the correlation of the factor of safety and the length ratio $L_z/L$ and Figure 6.38 shows the comparison of the improvement ratio ($N_{pi}$) of the pile-reinforced slopes with different length ratios of $L_z/L$. The improvement ratio, $N_{pi}$,is higher in the case with $C_{u2}/C_{u1}$=2.0 than the other three cases with $C_{u2}/C_{u1}$=0.5, 1.0 and 1.5 when the length ratios, $L_z/L$ are greater than 0.53.

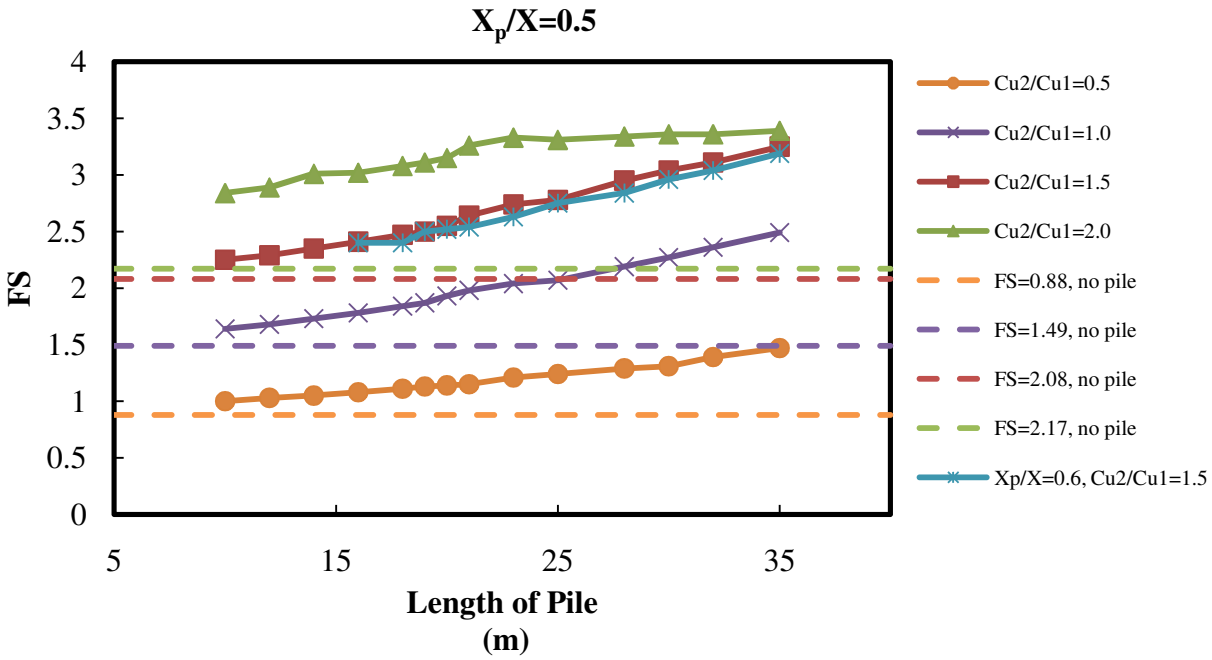


**Figure 6.35 Factor of safety versus Length of Pile in non-homogeneous slope with foundation, fixed head**

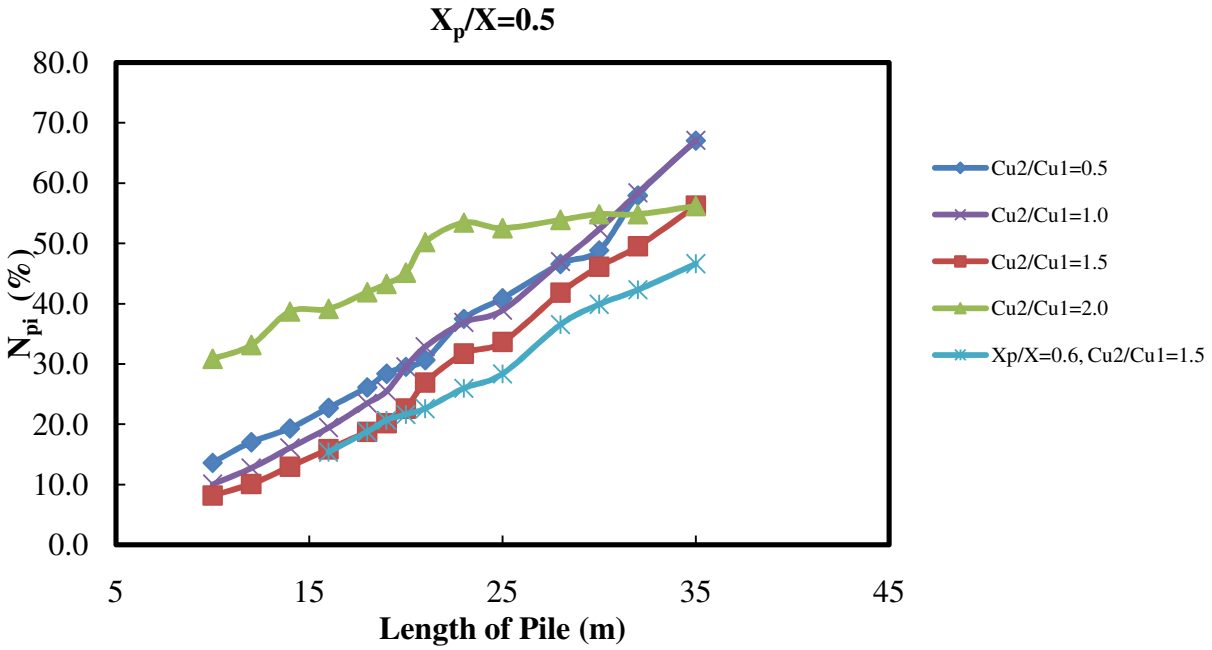


**Figure 6.36 $N_{pi}$ versus Length of Pile, fixed head**

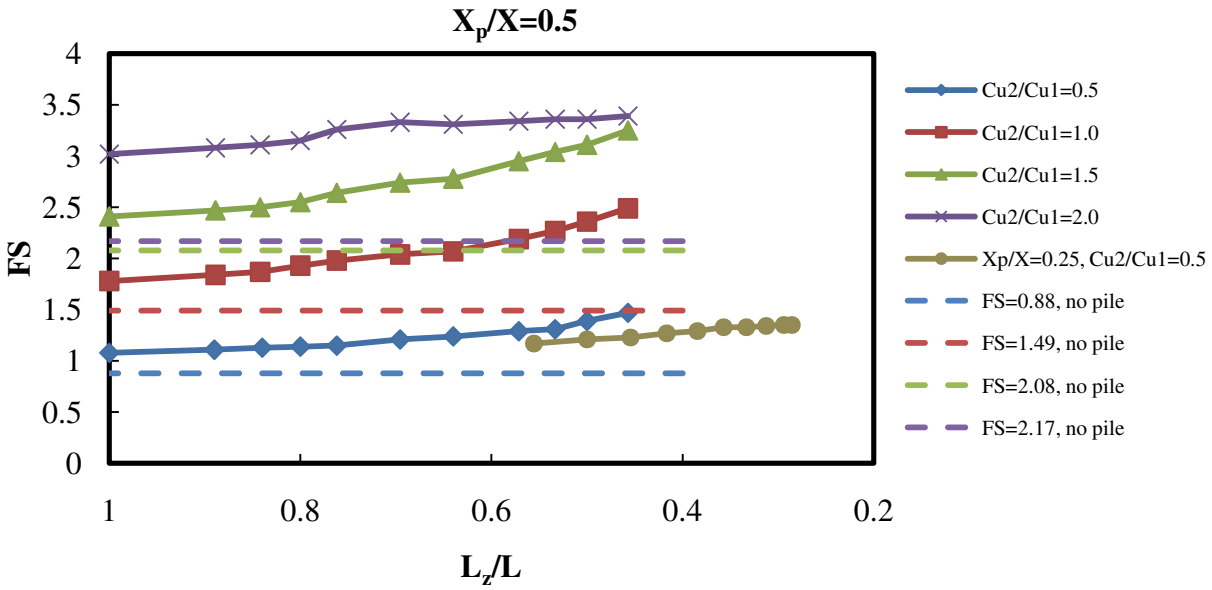


**Figure 6.37 Factor of safety versus $L_z/L$, fixed head**

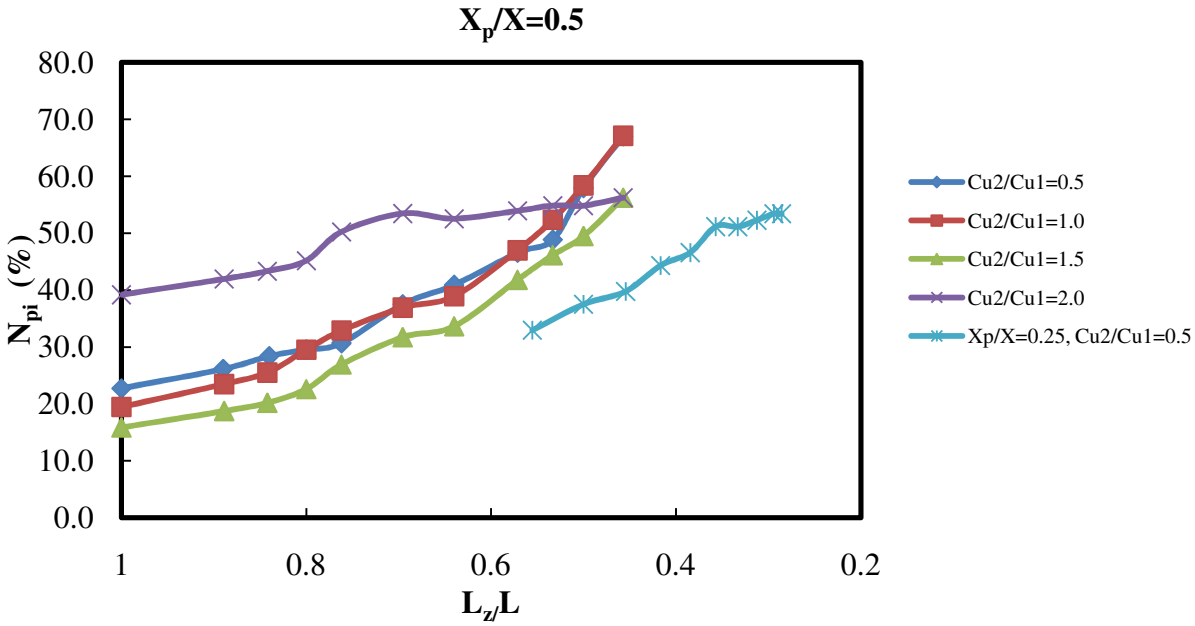


**Figure 6.38 $N_{pi}$ versus $L_z/L$, fixed head**

## 6.5 Discussion of Results

The discussions on results based on slope stability analysis, the optimal pile location, the effect of pile length and the pile head condition are made in following.

### 6.5.1 Slope Stability Analysis

Slope stability analyses on slopes with different strength ratios, four different strength ratios $C_{u2}/C_{u1}$=0.5, 1.0, 1.5 and 2.0, have been conducted using finite element methods and the results are discussed herein. When $C_{u2}/C_{u1}$=0.5, the undrained shear strength of soil in the foundation is weaker than the soil in the slope. Therefore, the failure mechanism of the slope depends on the foundation. The failure mode of the slope is the base failure as shown in Figure 6.4. The factor of safety is 0.88, less than 1.0. Thus under these conditions, this slope would fail unless reinforced by some means. The results of finite element analysis using ABAQUS provide good agreement with the results of limit equilibrium methods using SLOPE/W which assumes the potential slip surface is circular. The resulting factors of safety between limit equilibrium and finite element methods are quite close. The results are also in agreement to those of Griffiths and Lane (1999).

When the $C_{u2}/C_{u1}$=1.0, Figure 6.5 shows the slip surface is still at the base. $C_{u2}/C_{u1}$=1.0 is regarded as the special case of non-homogeneous slope case. Comparing the results of finite element analysis to the values of the homogeneous slope with foundation in Chapter 5, the potential slip surface is in different location. In Chapter 5, the thickness of the foundation is only half height of the slop (D=1.5), in this case, the thickness of the foundation is the same to the height of the slope (D=2.0). When D=1.5, the potential slip surface occurs within the slope with a lower factor of safety, while when D=2.0, the potential slip surface forms circularly through the bottom of the foundation with a higher factor of safety. Base on the similar failure surface assumed in the limit equilibrium analysis, the results also make very good agreement on both finite element analysis and conventional limit equilibrium analysis using ABAQUS and SLOPE/W, respectively.

If the ratio, $C_{u2}/C_{u1}$=1.5, slip surfaces form in two locations simultaneously, one is along the boundary of slope and foundation, the other one is the great circle through the bottom of the foundation. Both slip surfaces dominate the failure mechanism of the slope stability. The soil of the foundation is 50% stronger than the soil in the slope portion. The results are interesting since the results observed in $C_{u2}/C_{u1}$, the potential slip surface passes through the foundation. But in this case, two slip surfaces occur in the slope stability analysis.

If the ratio, $C_{u2}/C_{u1}$ rises up to 2.0, the shear strength of the foundation soil is much stronger than the soil in the slope. In this case, the foundation is relatively firm, so the slip surface as shown in Figure 6.9 will occur circularly along the boundary between slope and foundation which failure occur at the toe, not through the foundation. Only the soil in the slope dominates the failure mechanism of the slope. In this condition, the resulting factor of safety is the highest among these cases. The slope stability increases along with the increase of the ratio $C_{u2}/C_{u1}$. This case has similar failure mechanism with the case which is a homogeneous slope without a foundation discussed in Chapter 4 and the slip surface is tangent to the firm base.

### 6.5.2 Optimal Pile Location

Comparing the results of analyses from four different strength ratio ($C_{u2}/C_{u1}$) cases, the middle portion of the slope was found as the optimal location where pile should be placed when the pile head condition is free. In fixed pile head cases, only when the $C_{u2}/C_{u1}$=0.5, the optimal pile location does not occur in the middle portion, the other three cases $C_{u2}/C_{u1}$=1.0, 1.5 and 2.0, the optimal location of pile is still in the middle portion. Although the pile was found to perform better when placed at $X_p/X$=0.25 for the $C_{u2}/C_{u1}$ = 0.5, however, it is only

with a certain length. In Figure 6.15, if the pile length is longer than 30 m in this case, the pile place at the middle with fixed head will still have better performance than the pile placed at $X_p/X=0.25$. In the other cases, the shear strength of the pile-soil interface can be sufficiently mobilized due to large relative soil movement occurring between pile and soil in the middle portion of the slope, the optimal pile location therefore is determined as the middle portion of the slope. Also, the reason why the fixed pile does not contribute more stability to the slope is the pile in these cases does not really change the failure mechanism from free pile head condition (Figures 6.39 and 6.40). The potential slip surface still goes through the bottom of the base.

In the case of $C_{u2}/C_{u1}=1.5$, to insure the optimal pile location is not at the other location, $X_p/X=0.6$ is also investigated, the result shows the factor of safety using 20m long pile is lower than the value resulted when pile placed in the middle portion of the slope.

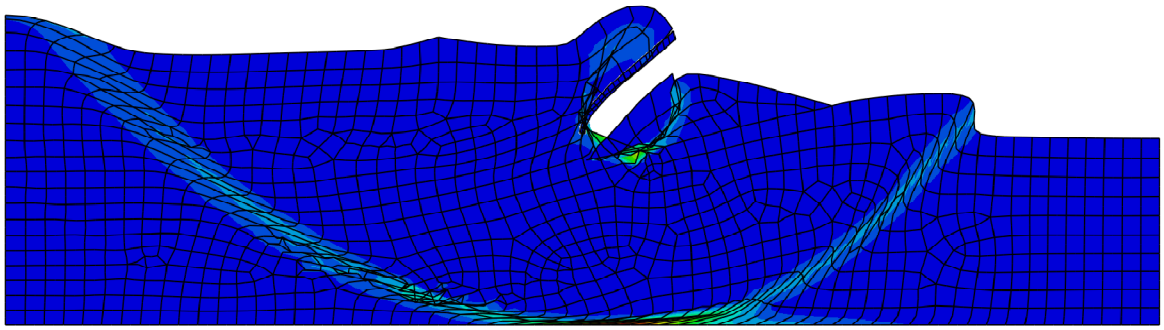

**Figure 6.39 The contour of plastic shear strain of slope (L=20m, D=1m), FS=3.15, free pile head**

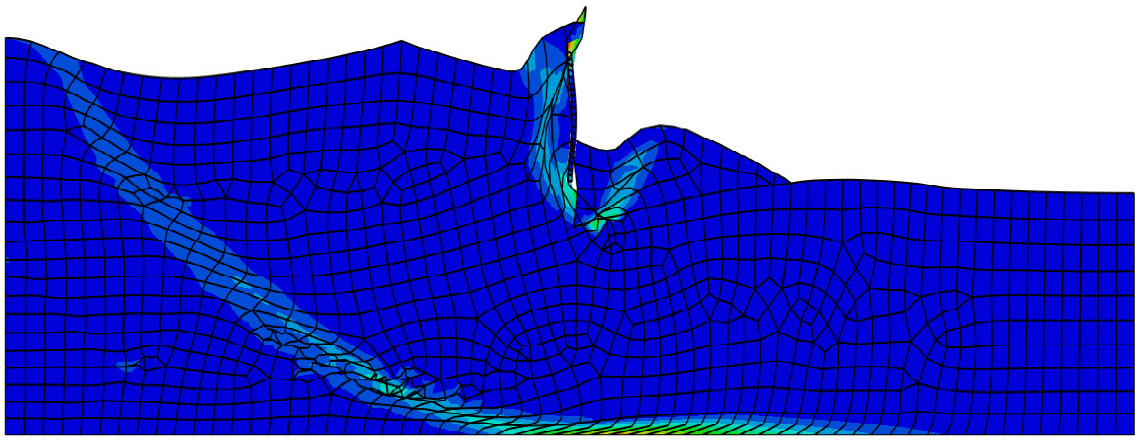

**Figure 6.40 The contour of plastic shear strain of slope (L=20m, D=1m), FS=3.15, fixed pile head**

### 6.5.3 Effect of Pile Length

In terms of the pile length, and comparing Figures 6.34 and 6.38, the longer pile is found to give rise to higher factors of safety on the piled-slope stability regardless of pile head

conditions except for the case, $C_{u2}/C_{u1}$=2.0. If $C_{u2}/C_{u1}$=2.0, the factor of safety increases with the pile length increases in the early portion, when $L_z/L$ less than 0.7, the factor of safety improved remains constant regardless of pile head conditions applied. In previous studies, the pile was usually assumed as an infinite length (Ito *et al.*, 1975), or the same height to the slope and foundation (Jeong *et al*., 2003). Obviously, a pile too short cannot really change very much on the failure mechanism of the slope reinforced with the pile, so the contribution on the slope stability is little.

However, if the pile is longer, the pile-soil interaction mechanism can be mobilized due to the flexible pile movement. Particularly, in the case of the slope with the ratio, $C_{u2}/C_{u1}$=2.0, the failure surface occurs on the slope only when the pile is longer than the original depth of slip surface in unreinforced slope, the failure mechanism and depth of slip surface may be changed, the factor of safety thus increases due to the change on the failure mechanism. However, the shorter pile may not reach the desired factor of safety on the slope reinforced with the pile, and a long pile may be uneconomical in design. To normalize the length of pile results, the ratio $L_z/L$ is developed to be the reference of pile length in describing a pile length in a slope. In the case with $C_{u2}/C_{u1}$=2.0, the length ratio $L_z/L$ less than 0.75 can be determined from Figure 6.31. As for the other cases, the ratios, $C_{u2}/C_{u1}$=0.5, 1.0, 1.5, the

required $L_z/L$ depends on the desired factor of safety in a reinforced slope and Figures 6.31 and Figure 6.35 can be referred to for the suitable length of the stabilizing pile with free and fixed pile head condition, respectively.

According to the optimal pile location concluded above, when the strength ratio $C_{u2}/C_{u1}=0.5$, the optimal pile location seems to occur at $X_p/X=0.25$ if the pile head is fixed. However, the result is based on the pile length 20 m. To further investigate in terms of pile length, the factor of safety of the slope stability is higher if the pile is shorter than 30 m for pile placed at $X_p/X=0.25$ compared to the pile placed in the middle portion of the slope with fixed head condition. However, when the pile is longer than 30 m, the pile placed in the middle portion of the slope with fixed head will lead to a higher factor of safety on slope stability compared to the position with $X_p/X=0.25$. Based on the $L_z/L$ ratio (see Figure 6.17), the pile placed in the middle portion of the slope regardless of pile head conditions always provide higher factors of safety in the slope stability. However, this is because the different $L_z$ determined in the middle portion of the slope from the $L_z$ at $X_p/X=0.25$ of the slope.

### 6.5.4 Pile Head Condition

The contribution of pile head condition in terms of location has been discussed previously. With the increase of ratio $C_{u2}/C_{u1}$, the effect of pile head condition becomes less (Figures 6.11 to 6.14).

Based on the pile length and comparing Figures 6.15, 19, 23 and 27, there are no large differences between the factor of safety improved using reinforced pile with fixed or free head condition when pile is short. In these four cases ($C_{u2}/C_{u1}$=0.5, 1.0, 1.5 and 2.0), only when the pile is longer, the pile with fixed head can lead to a larger factor of safety than the free head pile does. Figures 6.17, 21, 25 and 29 show the relationship between the factor of safety and the length ratio, $L_z/L$ due to both pile head conditions. Figure 6.17 shows if the $L_z/L$ less than 0.53, the fixed head pile generates a larger factor of safety in the slope stability. Also, compared to the pile with fixed head installed at $X_p/X$=0.25, the factor of safety is always lower than the pile placed in the middle portion of the slope in terms of the ratio, $L_z/L$. Figure 6.21 indicates when the $L_z/L$ less than 0.57, fixed head pile will contribute more factor of safety on the slope stability. Similarly, Figures 6.25 and 6.29 show the $L_z/L$ less than 0.53 and 0.57 respectively, has the same situation. There are two reasons why the fixed head pile

does not possess the advantages of the free head pile: first, the failure mechanism is not changed due to the presence of a shorter pile and second, the pile-soil interaction mechanism is not fully mobilized in shorter piles with both pile head conditions.

## 6.6 Summary and Conclusions

The results of finite element analysis using ABAQUS in the non-homogeneous slope with foundation are presented in this Chapter. Based on the discussion of the results of the optimal pile location, the effect of pile length and the pile head condition in pile-stabilized slope, several conclusions and suggestions can be made as follows.

### 6.6.1 Conclusions

(1) The slope stability analysis indicates the higher factor of safety is obtained when the homogeneous slope has a thicker foundation. Also, the failure types are different. The result of homogeneous slope presented in Chapter 5 with thinner (D=1.5) foundation shows the potential failure surface is in the slope. However, the failure type shown in this chapter that slope has thicker foundation (D=2.0) is base failure. The potential slip surface is circular and goes through the bottom of the foundation.

(2) The optimal pile location is found to be the middle portion of the slope regardless of the strength ratio $C_{u2}/C_{u1}$ when the pile with free head. If the pile head is restricted as fixed, the highest factor of safety still occurs in the middle portion when $C_{u2}/C_{u1}$=1.0, 1.5 and 2.0. But the optimal pile location will occur in the position of $X_p/X$=0.25 when $C_{u2}/C_{u1}$=0.5. Thus when the underlying foundation soils are weaker than the soils in the slope, the pile should be moved closer to the toe when using fixed head piles.

(3) Basically, both pile head conditions result in the increase of the factor of safety along with the increase of the pile length in this non-homogeneous slope with an underlying foundation. However, when the strength ratio $C_{u2}/C_{u1}$=2.0, the factor of safety nearly remains constant with the increase of the pile length if pile head is free.

(4) When the ratios $C_{u2}/C_{u1}$=0.5 and 1.0, the fixed pile head condition lead to higher factors of safety in the slope stability analysis when the pile is placed in the quarter and the middle portion of the slope, respectively. If the $C_{u2}/C_{u1}$=1.5 and 2.0, there is no difference between fixed pile head and free pile head in any location of the slope.

(5) If the $C_{u2}/C_{u1}$=0.5, the optimal location occurs when the pile placed at $X_p/X$=0.25 based on pile length 20 m. The pile shorter than 30 m in this case will lead to larger

factors of safety. If the desired factor of safety is larger, the longer pile (>30m) placed in the middle portion is necessary. The corresponding $L_z/L$ in the middle portion is 0.53 or lower. However, if the desired factor of safety between 1.2 to 1.33 is acceptable, pile can be placed at position of $X_p/X$=0.25 with $L_z/L$=0.33 or above, which $L_z$= 10m is found in this location.

(6) When the ratio of $L_z/L$ less than 0.57, the pile with fixed head will lead to a higher factor of safety than free head pile do regardless of strength ratio $C_{u2}/C_{u1}$. The results show the pile with fixed head does not make many benefits on slope stability improvement.

### 6.6.2 Recommendations

(1) In the non-homogeneous slope with foundation underlain, regardless of the strength ratio ($C_{u2}/C_{u1}$) between two layers, the optimal pile location is the middle portion of the slope when the pile head condition is free. If the fixed pile head condition has to be used, middle portion is the optimal location except $C_{u2}/C_{u1}$=0.5. When $C_{u2}/C_{u1}$=0.5,

the fixed pile head location should be the quarter distance of the slope length away from the toe.

(2) The $L_z/L$ =0.75 is recommended to be adopted if $C_{u2}/C_{u1}$=2.0; for other ratios it depends upon the desired factor of safety in the design because the factor of safety rises with the increase of the pile length.

(3) For the non-homogeneous case, a pile with fixed head condition is not recommended, since the fixed pile head does not provide benefit in improvement of slope stability over the free head pile. A slight benefit is shown when the pile is long. However, the pile too long is not appropriate and is uneconomical. The desired factor of safety can be reached when adopting an appropriate ratio provided in this study.

# CHAPTER 7: NON-HOMOGENEOUS SLOPE WITH FOUNDATION -THIN LAYER

## 7.1 Introduction

This chapter presents the case of a non-homogeneous slope with a thin weak layer. The contents of this chapter include the case description of the slope, the analysis of the unreinforced slope with different strength ratios between thin weak layer and surrounding soil, analysis of reinforced slope stability using piles, discussion of the results of numerical analysis, and summary and conclusions are made.

## 7.2 Case Description

This case involves a slope with a weak thin layer and follows a slope analyzed by Griffiths and Lane (1999). The geometry of the slope is shown in Figure 7.1. The slope with a thin layer can be classified into three cases with different strength ratios to discuss the slope stability between thin layer and surrounding soil. $C_{u2}$ is the undrained shear strength of the weak layer, and $C_{u1}$ is the undrained shear strength of soil of the slope. In this study, internal friction angle of soil is assumed to be 0º in undrained cases (Griffith and Lane, 1999) and $C_{u2}$ is assumed smaller than $C_{u1}$. The $C_{u1}/\gamma H$ ratio is taken as 0.25 which is the same ratio presented in the paper by Griffiths and Lane (1999). H is defaulted as 20 m high. The soil

properties of the slope are listed in Table 7.1. The Young's modulus (E) and Poisson's ratio (ν) of both soils are defaulted as $10^5$ kPa and 0.4. Ratios of the undrained shear strength of $C_{u2}/C_{u1}$=0.2, 0.6 and 1.0 are analyzed in slope stability analysis and discussed in this study, respectively

**Table 7.1 Soil properties of the slope**

| $C_{u1}$ ($N/m^2$) | Φ (°) | γ ($kN/m^3$) | $C_{u2}$ ($N/m^2$) $C_{u2}/C_{u1}$=1.0 | $C_{u2}$ ($N/m^2$) $C_{u2}/C_{u1}$=0.6 | $C_{u2}$ ($N/m^2$) $C_{u2}/C_{u1}$=0.2 |
|---|---|---|---|---|---|
| 100000 | 0.1 | 20 | 100000 | 60000 | 20000 |

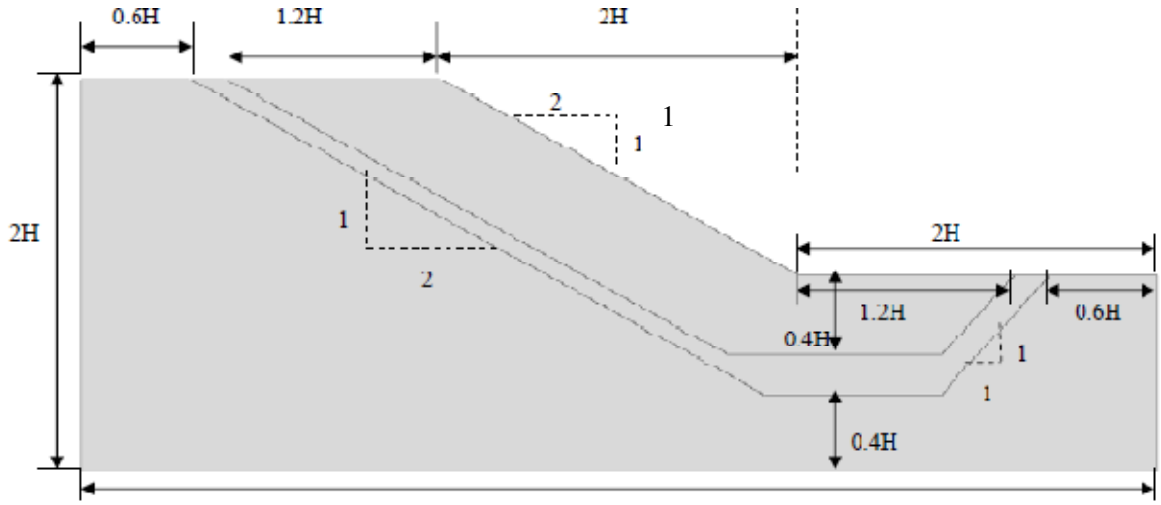


**Figure 7.1 Non-homogeneous slope with thin layer (ABAQUS)**

## 7.3 Unreinforced Slope Stability Analysis

The unreinforced slope is shown as Figure 7.1. In the unreinforced cases, the strength ratios $C_{u2}/C_{u1}$ =1.0, 0.6 and 0.2 are analyzed using finite element methods in ABAQUS. This slope is modeled with 2-D plane strain, 8-node quadrilateral element with reduced integration (four Gauss-integration points). The Young's modulus (E) and Poisson's ratio (υ) of both soils are defaulted as $10^5$ kPa and 0.4, respectively. The elastic-perfectly plastic Mohr-Coulomb failure criterion is also applied to be the constitutive model of the soil which is also adopted in Griffiths and Lane's study (1999). The factors of safety of finite element analysis using these three strength ratios are analyzed and discussed herein. The mesh and element type are shown in Figure 7.2.

### 7.3.1 $C_{u2}/C_{u1}$=1.0

The strength ratio $C_{u2}/C_{u1}$=1.0 is analyzed using the finite element method in ABAQUS. This case is actually a homogeneous slope with a foundation (D=2, which is defined in Chapter 6). The factor of safety of the slope stability analysis is 1.49 and governed by the circular base failure mechanism as shown in Figure 7.3.

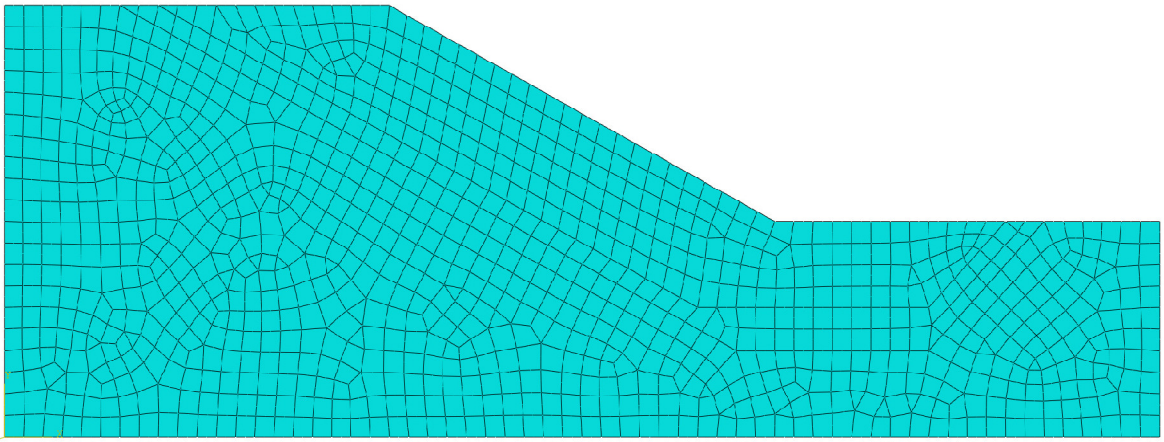

**Figure 7.2 Mesh of the non-homogeneous with thin layer (ABAQUS)**

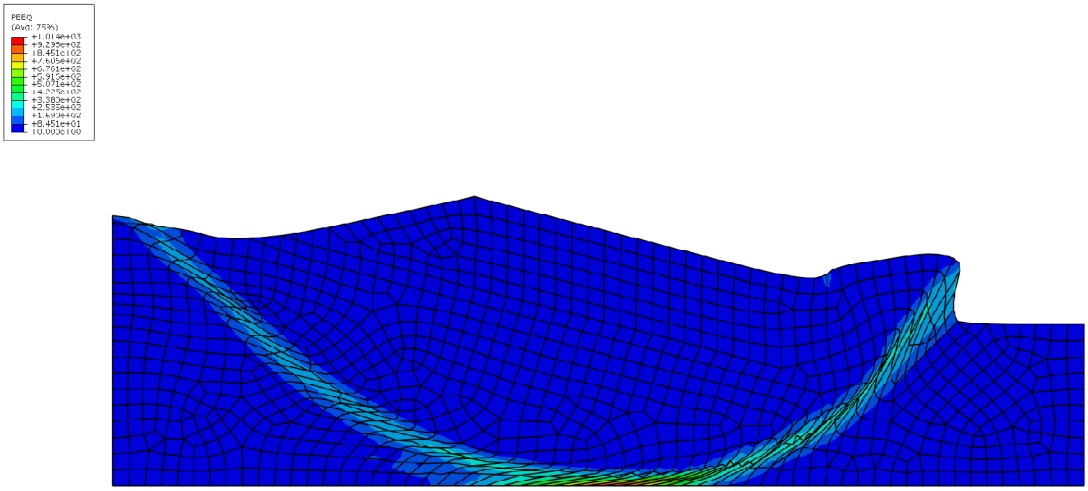

**Figure 7.3 Slope failure mechanism when $C_{u2}/C_{u1}$=1.0**

### 7.3.2 $C_{u2}/C_{u1}$=0.6

In the case of the strength ratio $C_{u2}/C_{u1}$=0.6, both circular and non-circular failure mechanisms governed by the thin weak layer dominate the slope stability. The factor of safety is given as 1.40 in finite element analysis using ABAQUS with strength reduction

technique. The failure contour which indicates the maximum plastic shear strain in a slope and failure mechanism is shown in Figure 7.4.

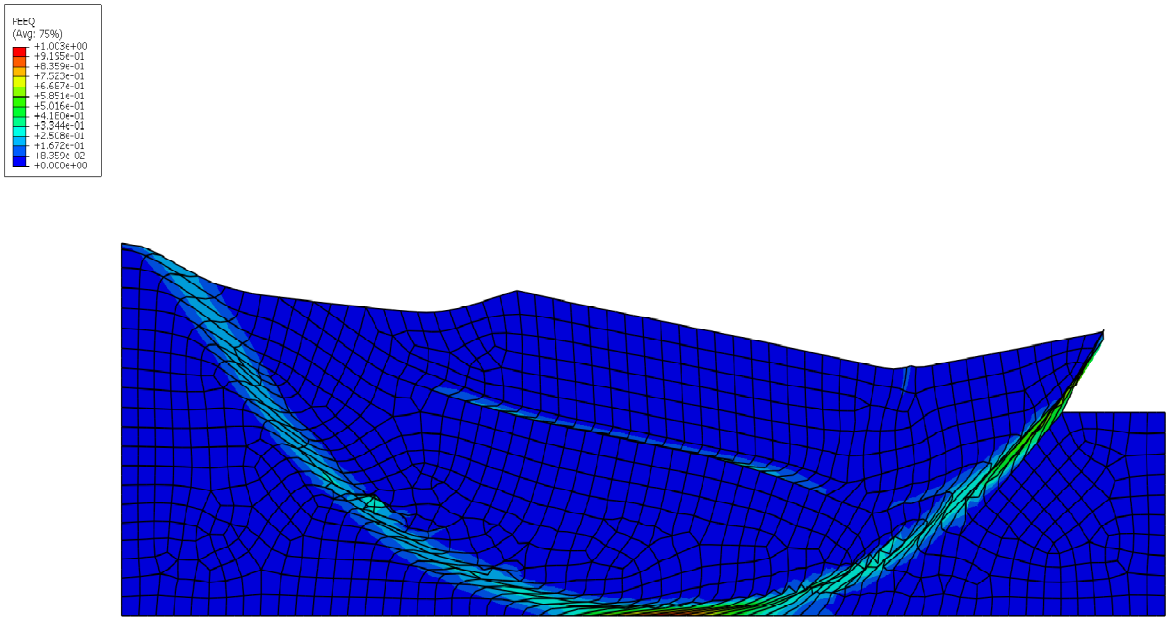


**Figure 7.4 Slope failure mechanism when $C_{u2}/C_{u1}$=0.6**

### 7.3.3 $C_{u2}/C_{u1}$=0.2

In this case of the $C_{u2}/C_{u1}$=0.2, the undrained shear strength of the soil in the thin layer is relatively low compared to the surrounding soil. The thin weak layer governs the slope failure mechanism when the shear strength in the thin layer is low. The factor of safety in this

case is 0.59 using finite element method with strength reduction technique. The failure mechanism is shown in Figure 7.5. The failure occurs above the sliding surface.

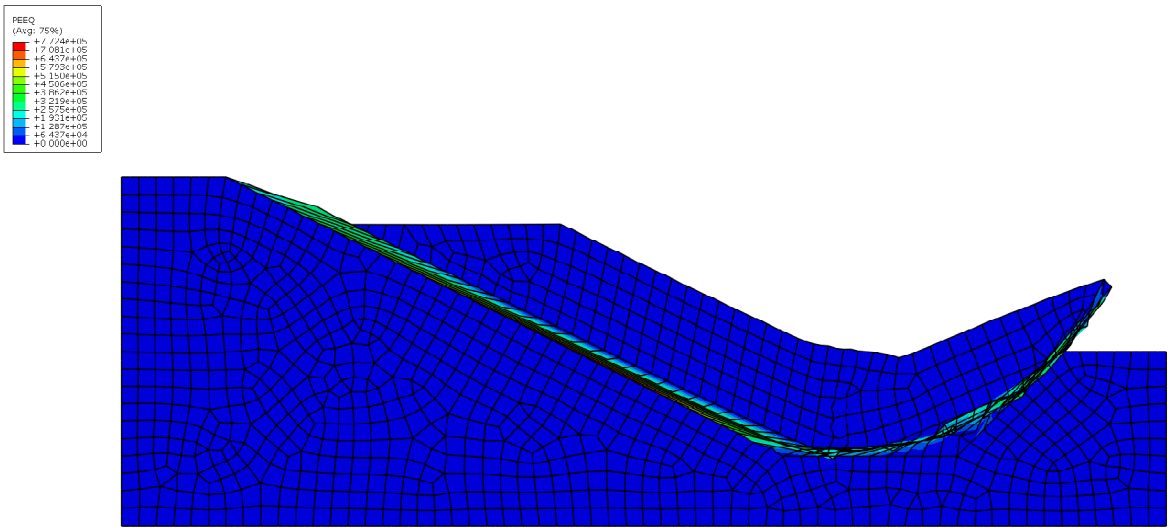


**Figure 7.5 Slope failure mechanism when $C_{u2}/C_{u1}$=0.2**

## 7.4 Results Validation and Comparisons

The results of finite element analysis using ABAQUS with 2-D model are summarized in Table 7.2. These analyses based on different strength ratios, $C_{u2}/C_{u1}$ and the $C_{u2}/C_{u1}$ ranges from 0.2 to 1.0 with 0.2 increment. The relationship between the factor of safety and the strength ratio $C_{u2}/C_{u1}$ is shown in Figure 7.6. Compared to the results of finite element analysis with strength reduction technique in the example used by Griffiths and Lane (1999), the same $C_{u1}/\gamma H$=0.25 is adopted, Figure 7.6 shows the both results of slope stability analysis

using different strength ratios make good agreement. For a homogeneous slope ($C_{u2}/C_{u1}$=1.0), Taylor's solution is 1.47 as stated in Griffiths and Lane's study. As described by Griffiths and Lane (1999), the strength of the thin weak layer was gradually reduced, an apparent change in the failure mechanism is observed. The change of the failure mechanism is identical in this study as well as in Griffiths and Lane's study.

When the ratio, $C_{u2}/C_{u1}$=1.0, the failure occurs at base and the failure plane is circular failure which is tangent to the firm base which is the so called base failure in this study. If the ratio of $C_{u2}/C_{u1}$=0.6, the failure mechanism is governed by both base circular failure and a non-circular failure which occurs at the thin weak layer. This failure mechanism is described as the transition between the circular mechanism and non-circular mechanism governed by the thin weak layer. If the ratio of $C_{u2}/C_{u1}$ is 0.2, the failure mechanism is governed by the thin weak layer only. In this condition with the relatively low strength ratio between the soil of thin weak layer and the surrounding soil, if the traditional limit equilibrium method is used, the factor of safety could be overestimated because the assumption of the failure surface will not be in the thin weak layer. Thus, the failure mechanism in the lower $C_{u2}/C_{u1}$ using limit equilibrium methods is the circular failure surface still goes through the base rather than just

occurs in the thin weak layer. The factor of safety of the slope stability analysis by assuming the failure surface through the base will be larger and thus relatively unconservative.

**Table 7.2 Factor of safety versus $C_{u2}/C_{u1}$**

| $C_{u2}/C_{u1}$ | 0.2 | 0.4 | 0.6 | 0.8 | 1.0 |
|---|---|---|---|---|---|
| ABAQUS | 0.59 | 1.03 | 1.40 | 1.45 | 1.49 |
| Griffiths (1999) | 0.60 | 1.05 | 1.40 | 1.44 | 1.46 |

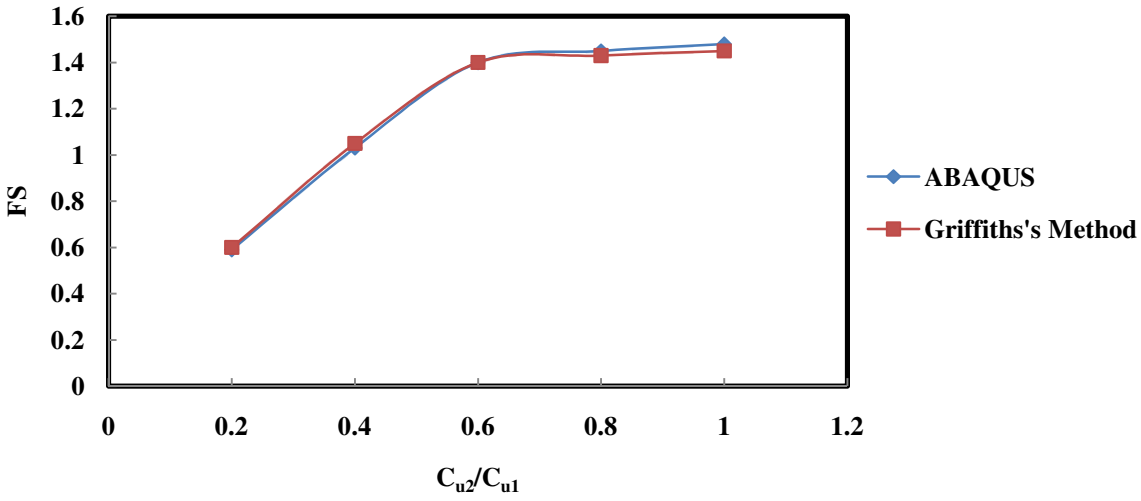


**Figure 7.6 Factor of safety versus strength ratio of two types of soils**

## 7.5 Analysis of Slope Stability Using Piles

The pile is incorporated into the finite element analysis using ABAQUS with strength reduction method. This section includes the pile stabilization case description, finite element analysis, optimal pile location, length of pile, and pile head condition based on the non

homogeneous slope stabilized with the reinforced pile. In addition, a three dimensional finite element model is used to compare the difference on the results between 2-D and 3-D models.

### 7.5.1 Pile Stabilization Case Description

The geometry of the slope containing a weak thin layer, reinforced with pile is shown in Figure 7.7. The height of the slope, H is defaulted as 20m. The thickness of the thin weak layer is 4m with the same inclination 2H:1 V as the slope. Soils are assumed undrained condition, so, the undrained shear strength in the slope portion is assigned as $C_{u1}$, and the soil in the thin layer is assigned as $C_{u2}$. $C_{u1}$ is determined by the ratio $C_{u1}/\gamma H=0.25$, and $C_{u2}$ is obtained according to the assumptions of the ratio $C_{u2}/C_{u1}$ which is summarized in Table 7.1. $L_z$ is the pile length above the thin layer or the depth of the potential slip surface which determined from the unreinforced slope stability analysis mentioned in the previous section. The $L_z$ is 12.5m and L is assumed to be 19m for the purpose of finding the optimal pile location in this case. The position of the pile is designated by the distance of the pile from the toe of the slope, $X_p$. $X_p/X$ is the ratio normalized to indicate the position of the pile away from the toe and $L_z/L$ is the normalized ratio to represent the relative length of the pile.

2 H

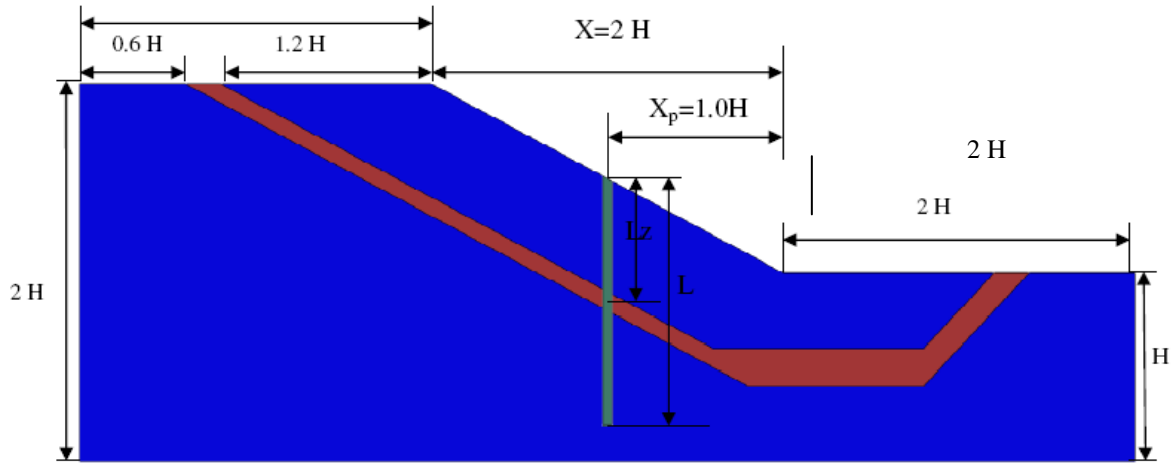


**Figure 7.7 Pile-slope system model in ABAQUS ($X_p$/X=0.50, L=20m)**

In the finite element analysis using ABAQUS, the pile is modeled as an elastic beam with Young's modulus (E) 6000=MPa, and Poisson's ratio (υ)=0.2, respectively. The interaction property between soil and pile is frictional with coefficient 0.3. The properties of soil are summarized in Table 7.1. The Young's modulus and Poisson's ratio are defaulted as $10^5$ kPa and 0.4, respectively. The selection of element type applied on pile media is a 2-D plane stress, 8- node with reduced integration element (4 Gauss integration points per element).while the soil is selected as a 2-D plane strain, 8-node with reduced integration quadrilateral element. The meshed model is as shown in Figure 7.8. The selection of element type is free quadrilateral-dominated due to the geometry limitation in the finite element

model using ABAQUS. Therefore, the mesh shape in somewhere is irregular which is as shown in Figure 7.8. The property of interface element between pile and soil is assumed zero-thickness which can only transfer shear stress across the surfaces when a compressive normal pressure (p') applies on it. The pile soil friction coefficient, η is 0.3, which is explained in Chapter 6.

Based on the three different failure mechanisms which are defined in the previous section (base circular, non-circular and both) regarding slope stability analysis, five conditions are studied on the stabilizing pile incorporated into the finite element model herein with the ratios $C_{u2}/C_{u1}$= 1.0, 0.8, 0.6, 0.4 and 0.2, respectively.

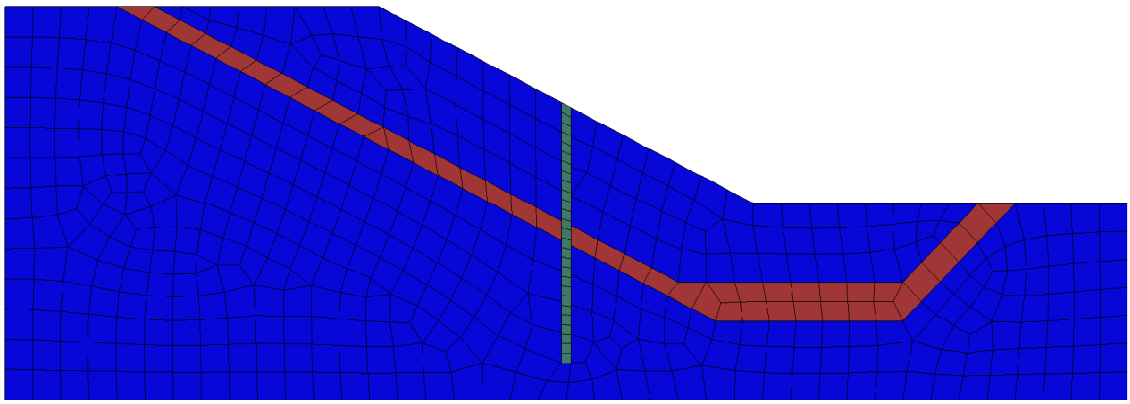

**Figure 7.8 Mesh of finite element model (ABAQUS)**

### 7.5.2 Optimal Pile Location

The optimal pile location is determined by dividing the slope into five sections from toe to crest. $X_p/X$ from 0 to 1 with 0.25 increment represents the relative location away from the toe. In slope stability analysis discussed previously, different strength ratio $C_{u2}/C_{u1}$ induces different failure mechanism. Therefore, in piled-slope system, $C_{u2}/C_{u1}$=0.2, 0.4, 0.6, 0.8 and 1.0 are discussed respectively. For convenience, the figures below use a reversed scale to represent the slope failure direction which is from left to right. $X_p/X$ =1.0 is the crest on the left and $X_p/X$ = 0 is the toe on the right.

#### 7.5.2.1 $C_{u2}/C_{u1}$=0.2

In Figure 7.9, the result shows the curve due to different location is bell shape regardless of pile head condition (free or fixed). The peak value occurs when the pile is placed in the middle portion of the slope and the factor of safety is 1.63 for both pile head conditions. Figure 7.10 indicates the improvement rate ($N_{pi}$) of slope stability which is defined in the previous section. The lowest improvement ($N_{pi}$) rate 18.64% occurs at the crest and the highest 176.27 % is in the middle portion of the slope regardless of the pile head conditions

(free or fixed). The improvement rate at the toe is 37.3% for free head pile and 52.5% for fixed head pile which can be seen in Figure 7.10.

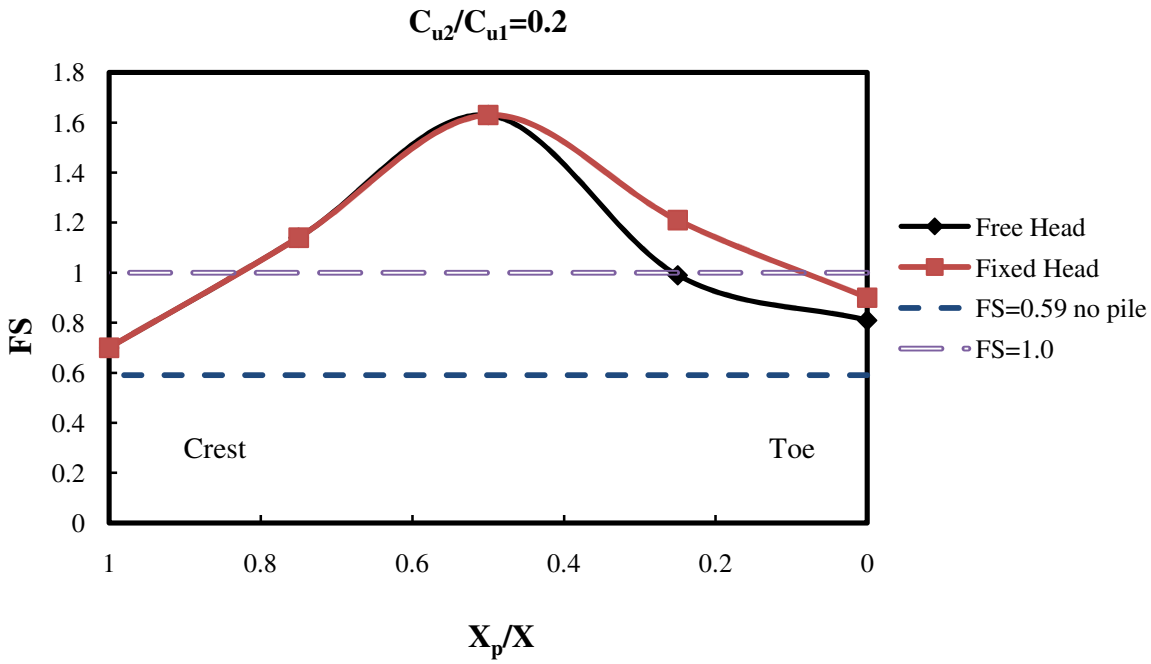


**Figure 7.9 Factor of safety versus $X_p/X$ ($C_{u2}/C_{u1}$=0.2)**

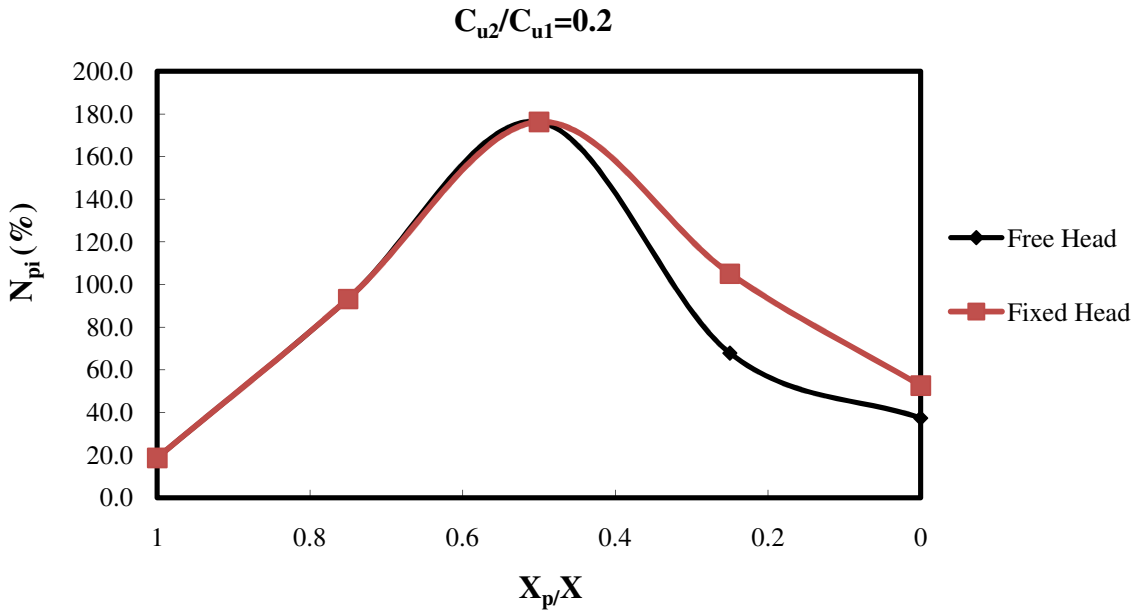


**Figure 7.10 $N_{pi}$ versus $X_p/X$ ($C_{u2}/C_{u1}$=0.2)**

### 7.5.2.2 $C_{u2}/C_{u1}$=0.4

In the case of $C_{u2}/C_{u1}$=0.4, Figure 7.11 shows the factor of safety of the slope stability of piled slope increases at the toe is the lowest, 1.06 for free pile head condition, and 1.1 for fixed pile head condition. The highest factor of safety occurs in the middle portion of the slope**,** which are 2.23 for free head condition and 2.44 for fixed head condition, respectively. The corresponding improvement rate, ($N_{pi}$) at the toe is 2.91% for free head pile and 6.80 % for fixed pile head condition. The highest value of $N_{pi}$ is 116.5% and 136.89% for free and fixed pile head condition, respectively when the pile is placed in the middle portion of the slope which is shown in Figure 7.12.

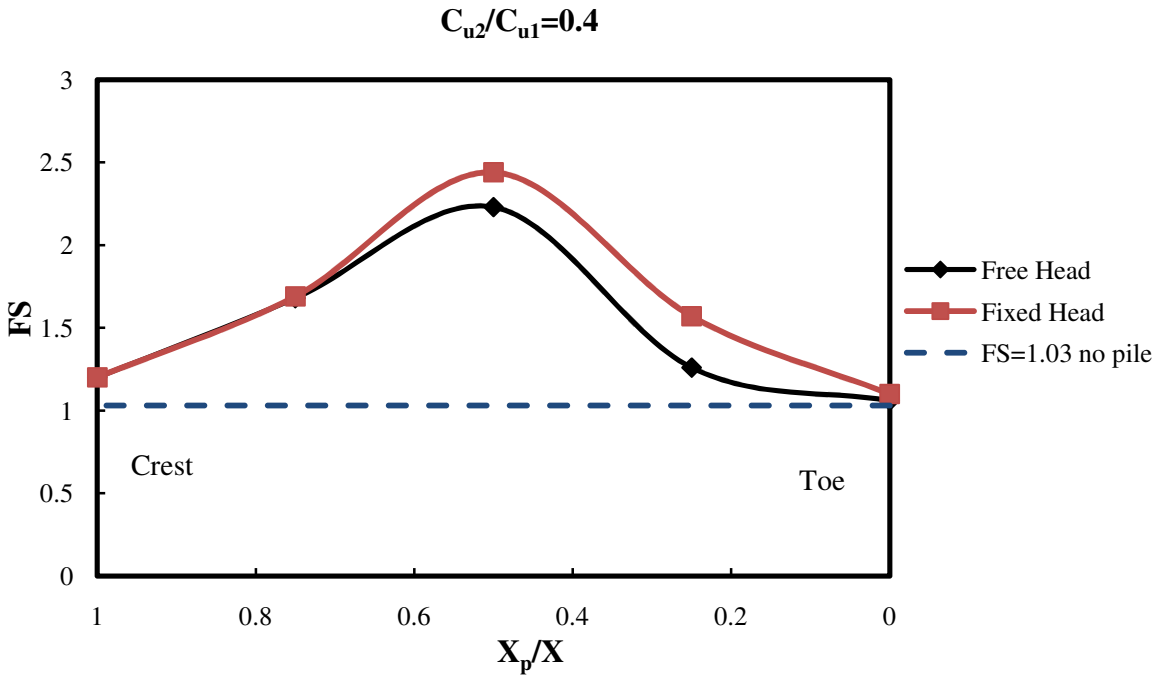


**Figure 7.11 Factor of safety versus $X_p/X$ ($C_{u2}/C_{u1}$=0.4)**

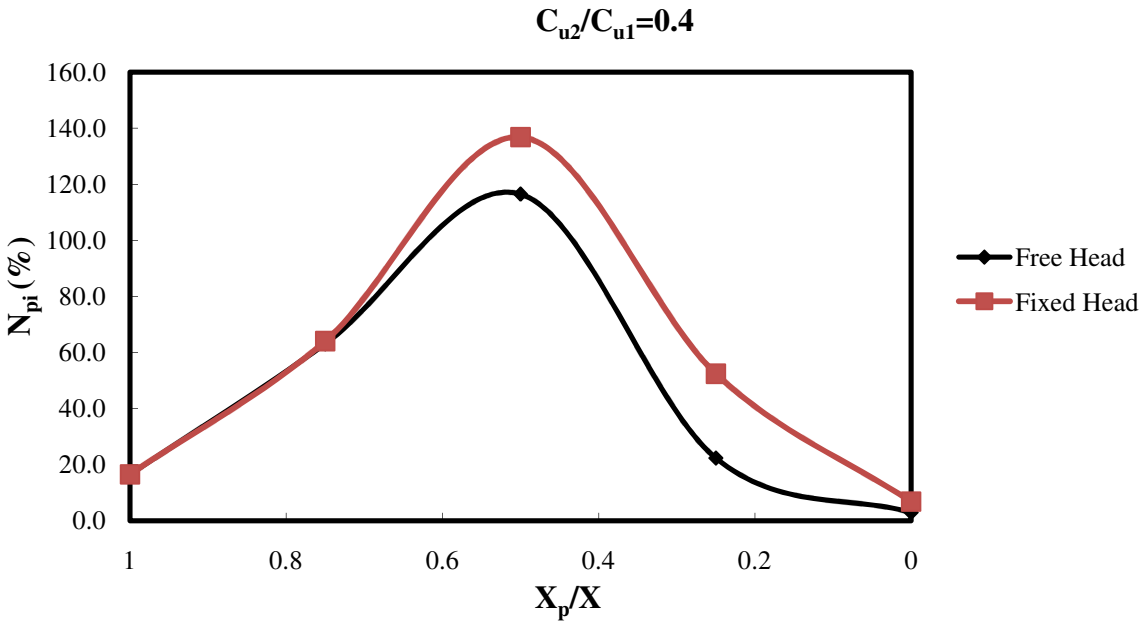


**Figure 7.12 $N_{pi}$ versus $X_p/X$ ($C_{u2}/C_{u1}$=0.4)**

#### 7.5.2.3 $C_{u2}/C_{u1}=0.6$

In the case of $C_{u2}/C_{u1}=0.6$, the lowest factor of safety of the piled slope still occurs when the pile is placed at the toe, 1.46 for free pile head condition, and 1.48 for fixed pile head condition applied. The highest factor of safety is also reached when the pile is placed in the middle portion of the slope, which are 2.13 for free pile head condition and 2.6 for fixed pile head condition. When the pile is placed at the crest, both free and fixed conditions lead to a similar factor of safety. Compared to the factor of safety when the pile is placed at the toe, the factor of safety is slightly higher when the pile is placed at the crest. Figure 7.13 shows the factors of safety distribution along the slope in different positions and Figure 7.14 shows the rate of improvement on slope stability along the slope. The highest improvement rate $N_{pi}$ is 52% for free pile head condition and 85.7% for fixed pile head condition.

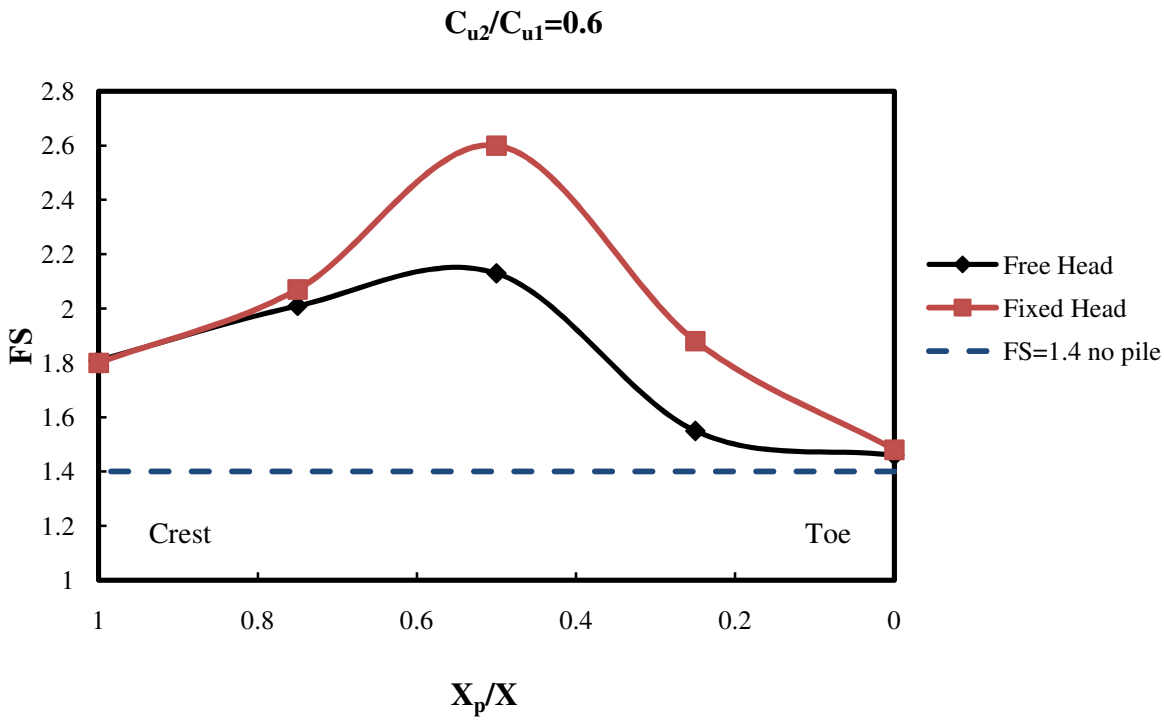


**Figure 7.13 Factor of safety versus $X_p/X$ ($C_{u2}/C_{u1}$=0.6)**

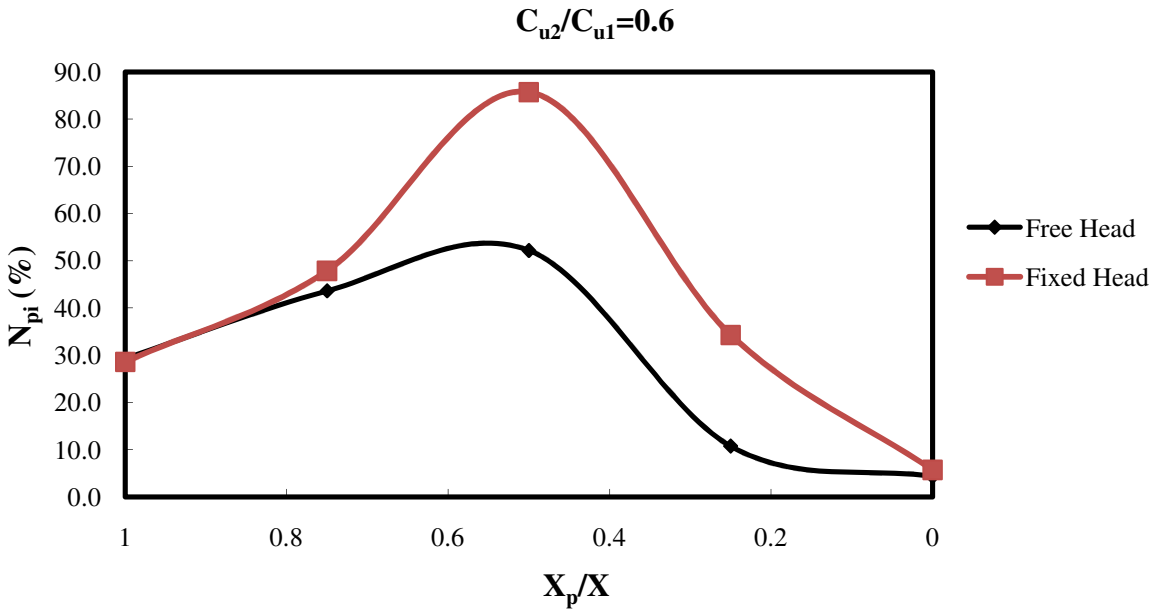


**Figure 7.14 $N_{pi}$ versus $X_p/X$ ($C_{u2}/C_{u1}$=0.6)**

### 7.5.2.4 $C_{u2}/C_{u1}=0.8$

In the case of $C_{u2}/C_{u1}=0.8$, the lowest factor of safety still occurs when the pile is placed at the toe, 1.56 for free pile head condition, and 1.62 for fixed pile head condition, respectively. Very little difference in factor of safety occurs due to the presence of the stabilizing pile. The highest factor of safety due to the presence of pile is also in the middle portion of the slope, 2.19 for free head condition and 2.68 on fixed head condition, respectively. At the crest, both conditions lead to a similar factor of safety which is slightly higher than the value at the toe. Figure 7.15 shows the distribution of the factor of safety due to the different location where the pile is placed and Figure 7.16 shows the rate of improvement ($N_{pi}$) on the slope stability in different location where the pile is installed. When the pile moves toward the crest, the factor of safety resulted from the fixed head pile approaches to the value comes from the free head pile. In both crest and toe, fixed pile head condition makes very little difference on factor of safety and improvement ratio than free head pile condition.

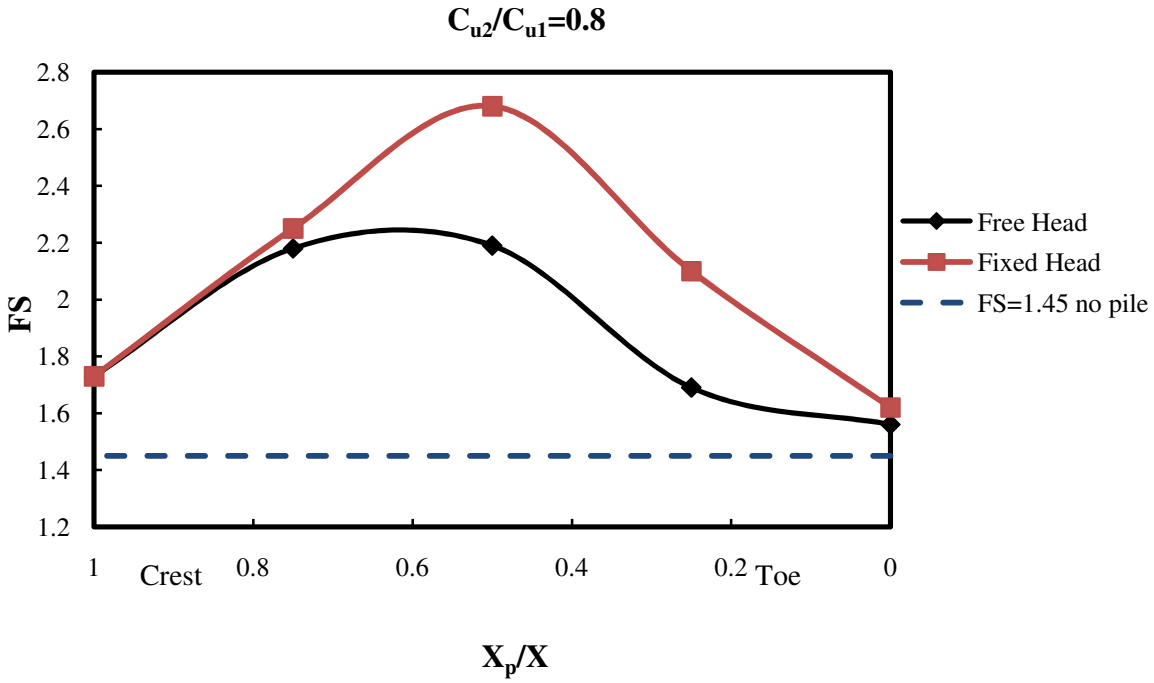


**Figure 7.15 Factor of safety versus $X_p/X$ ($C_{u2}/C_{u1}$=0.8)**

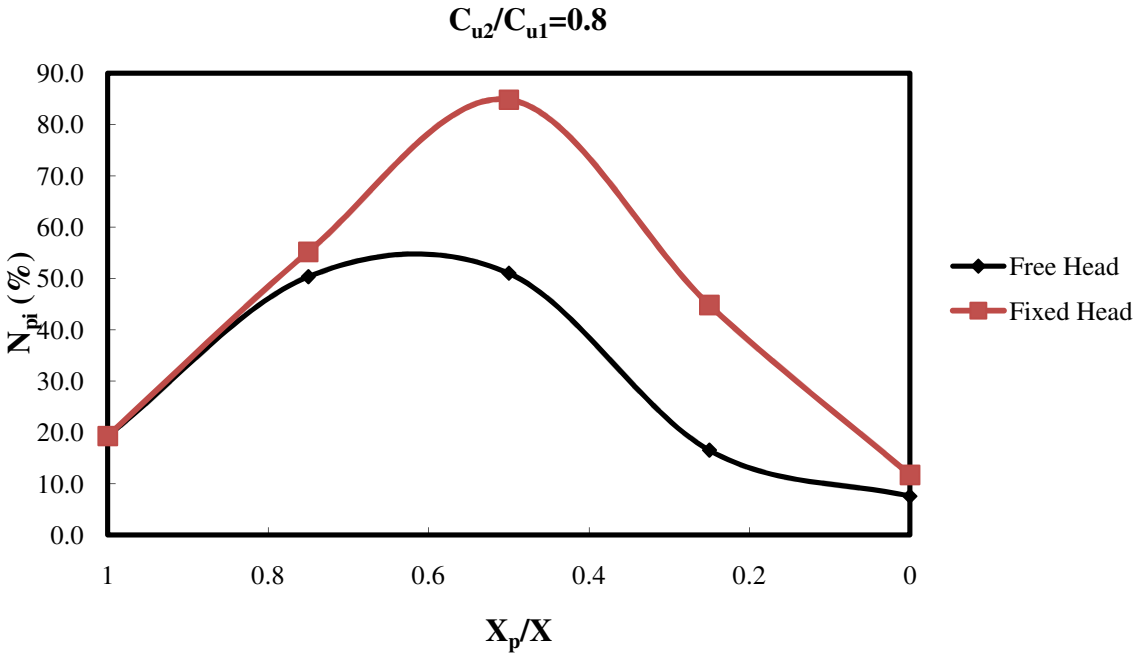


**Figure 7.16 $N_{pi}$ versus $X_p/X$ ($C_{u2}/C_{u1}$=0.8)**

### 7.5.2.5 $C_{u2}/C_{u1}$=1.0

The case of $C_{u2}/C_{u1}$=1.0 is the special case of a "non-homogeneous" slope, and it is actually a homogeneous slope. The lowest factor of safety still occurs when the pile is placed at the toe, 1.59 for free pile head condition, and 1.65 for fixed pile head condition, respectively. The highest factor of safety is also in the middle portion of the slope where the pile is placed, 2.15 for free pile head condition and 2.75 for fixed pile head condition, respectively. At the crest, both conditions lead to a similar factor of safety which is slightly higher than the value at the toe. The results are quite similar to the case with $C_{u2}/C_{u1}$=0.8. Figure 7.17 shows the distribution of the factor of safety along the slope between the toe and the crest and Figure 7.18 shows the rate of improvement ($N_{pi}$) on the slope stability due to the different location of pile installed.

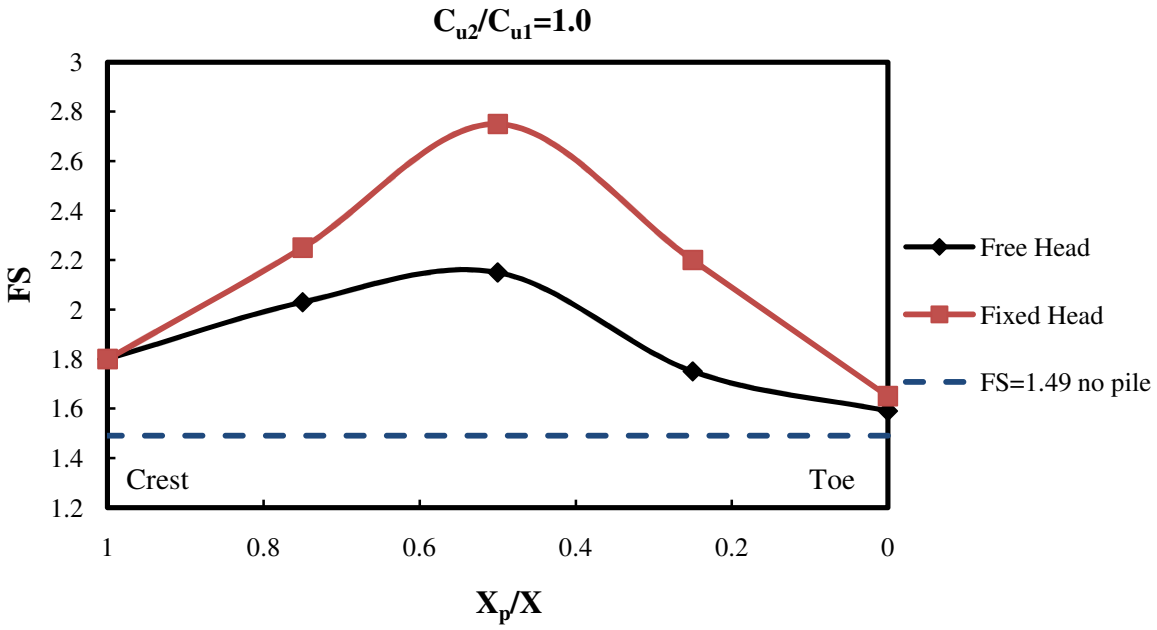


**Figure 7.17 Factor of safety versus $X_p/X$ ($C_{u2}/C_{u1}$=1.0)**

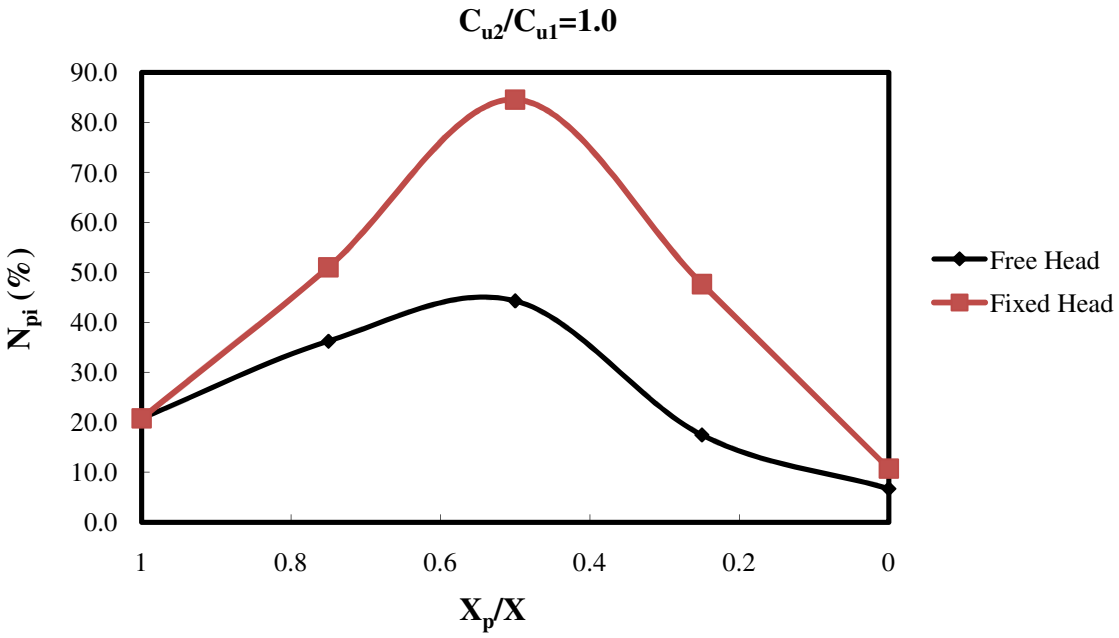


**Figure 7.18 $N_{pi}$ versus $X_p/X$ ($C_{u2}/C_{u1}$=1.0)**

Figure 7.19 shows the comparisons of all five cases with the $C_{u2}/C_{u1}$=0.2, 0.4, 0.6, 0.8 and 1.0 for free pile head condition applied. In this figure, the factor of safety basically increases along with the increase of the strength ratio $C_{u2}/C_{u1}$. However, the largest factor of safety occurs when the pile is placed in the middle portion of the slope and the largest value of the factor of safety occurs when the ratio $C_{u2}/C_{u1}$=0.4 for free head pile cases. In terms of improvement ratio, $N_{pi}$, pile makes the greatest contribution on the slope stability when the slope with the strength ratio, $C_{u2}/C_{u1}$=0.2. The resulting $N_{pi}$ is as high as 176.3%. Figure 7.20 shows the results in terms of the improvement ratio, $N_{pi}$, according to different strength ratios $C_{u2}/C_{u1}$ for the free pile head condition.

In Figure 7.21, the curves are uniform as the bell shape if the fixed head conditions applied on the pile. The maximum values of factor of safety occur if the stabilizing pile is placed in the middle portion of slopes regardless of the strength ratio, $C_{u2}/C_{u1}$. The factor of safety basically increases with the increase of $C_{u2}/C_{u1}$. In terms of the improvement ratio, $N_{pi}$ as shown in Figure 7.21, the strength ratio $C_{u2}/C_{u1}$=0.2 is improved the highest rate in slope stability due to the presence of the pile. The strength ratio, $C_{u2}/C_{u1}$=0.4 is the case which is improved the second highest improvement ratio, $N_{pi}$. The strength rations from $C_{u2}/C_{u1}$=0.6

to 1.0, the improvement ratio, $N_{pi}$ are nearly consistent. The highest improvement ratio, $N_{pi}$ is about 85% in the middle portion of the slopes which is shown in Figure 7.22.

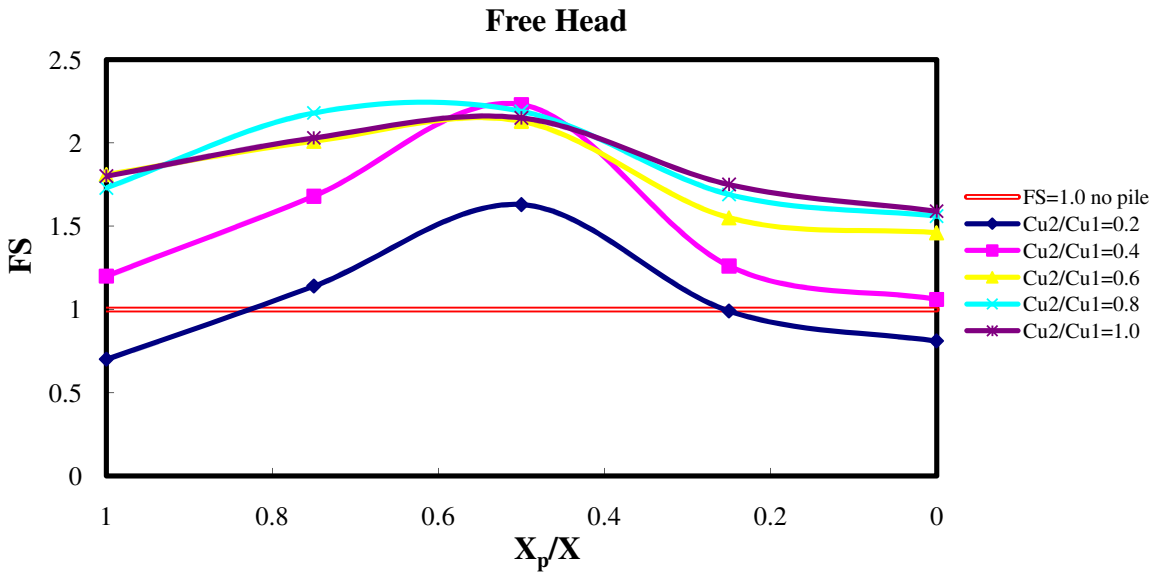


**Figure 7.19 Factor of safety versus $X_p/X$, free head**

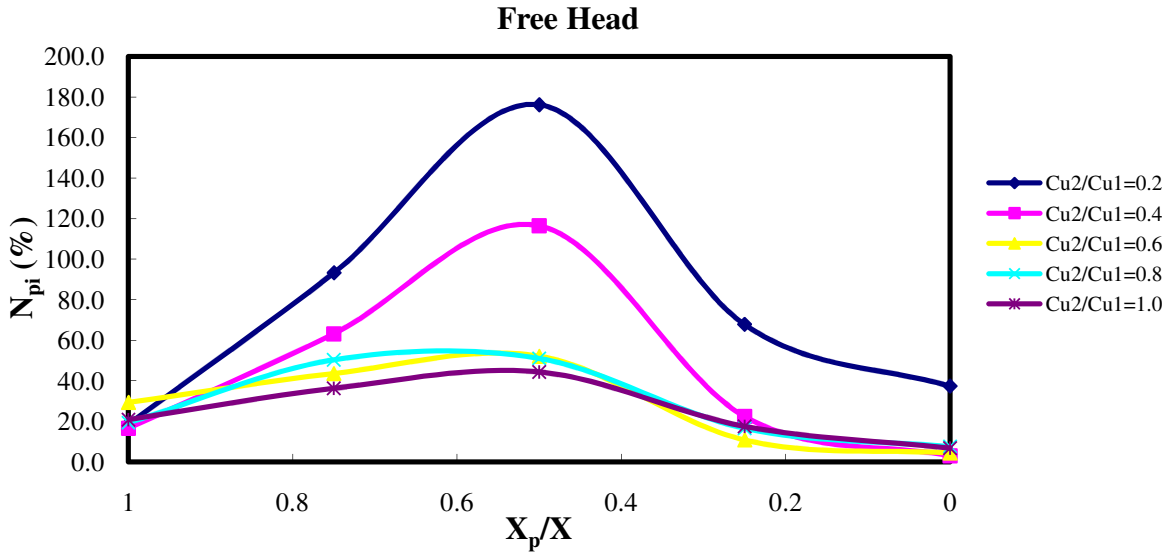


**Figure 7.20 $N_{pi}$ versus $X_p/X$, free head**

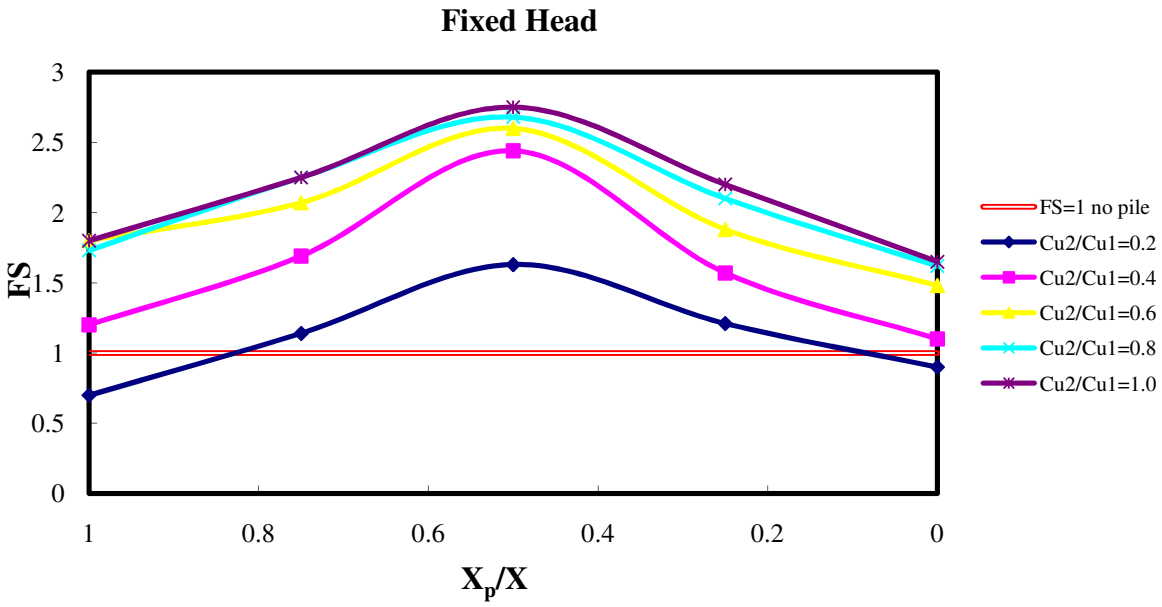


**Figure 7.21 Factor of safety versus $X_p/X$, fixed head**

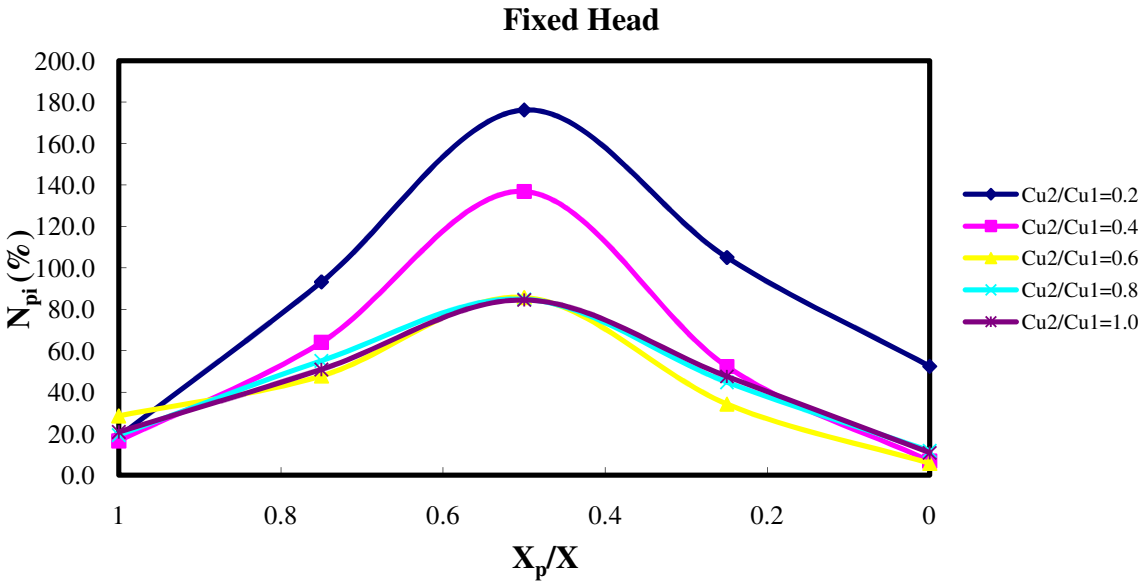


**Figure 7.22 $N_{pi}$ versus $X_p/X$, fixed head**

### 7.5.3 Length of Pile

The results of the finite element analysis of the piled slope using ABAQUS based on the length of pile are summarized in Tables 7.3 to 7.7. The results of the numerical analysis are also plotted in Figures 7.23 to 7.31. The length pile ranges from 16 to 24m with a 2 m increment to investigate the effect of the pile length on slope stability of piled-slope system. The thin weak layer is regarded as the potential slip surface at low strength ratio ($C_{u2}/C_{u1}$) cases which have been regarded as the governing factor of failure mechanism in the unreinforced slope. Therefore, the middle point of the thin weak layer is defined as the depth of the potential slip surface, take the symbol $L_z$ to represent the depth of the slip surface or so called the length of pile above the potential slip surface. L is the true length of the pile and variable. The improvement on slope stability of piled-slope system is discussed case by case depends upon the five different strength rations, $C_{u2}/C_{u1,}$ in the following.

**Table 7.3 Results of numerical analysis using ABAQUS, $C_{u2}/C_{u1}$=0.2**

| $C_{u2}/C_{u1}$=0.2 | | | | | | FS=0.88 | |
|---|---|---|---|---|---|---|---|
| Boundary Conditions | | Failure Mechanism | | | | $N_{pi}$ (%) | |
| Length | Factor of Safety | | Pile | Slope | $L_z/L$ | | |
| | Free | Fixed | | | | Free | Fixed |
| 16 | 1.66 | 1.63 | stiff | planar | 0.78 | 181.36 | 176.27 |
| 18 | 1.61 | 1.63 | stiff | planar | 0.69 | 172.88 | 176.27 |
| 19 | 1.63 | 1.63 | stiff | planar | 0.66 | 176.27 | 176.27 |
| 20 | 1.63 | 1.64 | stiff | planar | 0.63 | 176.27 | 177.97 |
| 22 | 1.59 | 1.64 | stiff | planar | 0.57 | 169.49 | 177.97 |
| 24 | 1.39 | 1.63 | flexible | planar | 0.52 | 135.59 | 176.27 |
| 26 | 1.33 | 1.66 | flexible | planar | 0.48 | 125.42 | 181.36 |

**Table 7.4 Results of numerical analysis using ABAQUS, $C_{u2}/C_{u1}$=0.4**

| $C_{u2}/C_{u1}$=0.4 | | | | | | FS=1.03 | |
|---|---|---|---|---|---|---|---|
| Boundary Conditions | | Failure Mechanism | | | | $N_{pi}$ (%) | |
| Length | Factor of Safety | | Pile | Slope | $L_z/L$ | | |
| | Free | Fixed | | | | Free | Fixed |
| 16 | 2.13 | 2.2 | flexible | planar | 0.78 | 106.80 | 113.59 |
| 18 | 2.19 | 2.33 | flexible | planar | 0.69 | 112.62 | 126.21 |
| 19 | 2.24 | 2.45 | flexible | planar | 0.66 | 117.48 | 137.86 |
| 20 | 2.19 | 2.45 | flexible | planar | 0.63 | 112.62 | 137.86 |
| 22 | 2.1 | 2.46 | flexible | planar | 0.57 | 103.88 | 138.83 |
| 24 | 1.91 | 2.37 | flexible | planar | 0.52 | 85.44 | 130.10 |
| 26 | 1.81 | 2.32 | flexible | planar | 0.48 | 75.73 | 125.24 |

**Table 7.5 Results of numerical analysis using ABAQUS, $C_{u2}/C_{u1}$=0.6**

| $C_{u2}/C_{u1}$=0.6 | | | | | | FS=1.40 | |
|---|---|---|---|---|---|---|---|
| Boundary Conditions | | Failure Mechanism | | | | $N_{pi}$ (%) | |
| Length | Factor of Safety | | Pile | Slope | $L_z/L$ | | |
| | Free | Fixed | | | | Free | Fixed |
| 16 | 2.24 | 2.29 | flexible | planar | 0.78 | 60.00 | 63.57 |
| 18 | 2.13 | 2.44 | flexible | planar | 0.69 | 52.14 | 74.29 |
| 19 | 2.13 | 2.6 | flexible | planar | 0.66 | 52.14 | 85.71 |
| 20 | 2.4 | 2.65 | flexible | planar | 0.63 | 71.43 | 89.29 |
| 22 | 2.15 | 2.83 | flexible | planar | 0.57 | 53.57 | 102.14 |
| 24 | 2.24 | 2.72 | flexible | planar | 0.52 | 60.00 | 94.29 |
| 26 | 2.16 | 2.65 | flexible | planar | 0.48 | 54.29 | 89.29 |

**Table 7.6 Results of numerical analysis using ABAQUS, $C_{u2}/C_{u1}$=0.8**

| $C_{u2}/C_{u1}$=0.8 | | | | | | FS=1.45 | |
|---|---|---|---|---|---|---|---|
| Boundary Conditions | | Failure Mechanism | | | | $N_{pi}$ (%) | |
| Length | Factor of Safety | | Pile | Slope | $L_z/L$ | | |
| | Free | Fixed | | | | Free | Fixed |
| 16 | 2.31 | 2.37 | flexible | planar | 0.78 | 59.31 | 63.45 |
| 18 | 2.15 | 2.52 | flexible | planar | 0.69 | 48.28 | 73.79 |
| 19 | 2.19 | 2.68 | flexible | planar | 0.66 | 51.03 | 84.83 |
| 20 | 2.25 | 2.72 | flexible | planar | 0.63 | 55.17 | 87.59 |
| 22 | 2.2 | 3 | flexible | planar | 0.57 | 51.72 | 106.90 |
| 24 | 2.26 | 2.87 | flexible | planar | 0.52 | 55.86 | 97.93 |
| 26 | 2.31 | 2.77 | flexible | planar | 0.48 | 59.31 | 91.03 |

**Table 7.7 Results of numerical analysis using ABAQUS, $C_{u2}/C_{u1}$=1.0**

| $C_{u2}/C_{u1}$=1.0 | | | | | | | FS=1.49 |
|---|---|---|---|---|---|---|---|
| | Boundary Conditions | | Failure Mechanism | | | $N_{pi}$ (%) | |
| Length | Factor of Safety | | Pile | Slope | $L_z/L$ | | |
| | Free | Fixed | | | | Free | Fixed |
| 16 | 2.35 | 2.41 | Flexible | planar | 0.78 | 62.07 | 66.21 |
| 18 | 2.17 | 2.57 | Flexible | planar | 0.69 | 49.66 | 77.24 |
| 19 | 2.15 | 2.75 | Flexible | planar | 0.66 | 48.28 | 89.66 |
| 20 | 2.13 | 2.77 | Flexible | planar | 0.63 | 46.90 | 91.03 |
| 22 | 2.24 | 3.03 | Flexible | planar | 0.57 | 54.48 | 108.97 |
| 24 | 2.31 | 2.91 | Flexible | planar | 0.52 | 59.31 | 100.69 |
| 26 | 2.37 | 2.79 | Flexible | planar | 0.48 | 63.45 | 92.41 |

**Table 7.8 Factor of safety versus $C_{u2}/C_{u1}$ with free pile head condition**

| Pile | | $C_{u2}/C_{u1}$ vs. FS (Free Head) | | | | |
|---|---|---|---|---|---|---|
| Length (m) | Ratio ($L_z/L$) | 0.2 | 0.4 | 0.6 | 0.8 | 1.0 |
| 16 | 0.78 | 1.66 | 2.13 | 2.24 | 2.31 | 2.35 |
| 18 | 0.69 | 1.61 | 2.19 | 2.13 | 2.15 | 2.17 |
| 19 | 0.66 | 1.63 | 2.23 | 2.13 | 2.19 | 2.15 |
| 20 | 0.63 | 1.63 | 2.19 | 2.40 | 2.25 | 2.13 |
| 22 | 0.57 | 1.59 | 2.10 | 2.15 | 2.20 | 2.24 |
| 24 | 0.52 | 1.39 | 1.91 | 2.24 | 2.26 | 2.31 |
| 26 | 0.48 | 1.33 | 1.81 | 2.16 | 2.31 | 2.37 |

**Table 7.9 Factor of safety versus $C_{u2}/C_{u1}$ with fixed pile head condition**

| Pile | | $C_{u2}/C_{u1}$ vs. FS (Fixed Head) | | | | |
|---|---|---|---|---|---|---|
| **Length (m)** | **Ratio ($L_z/L$)** | **0.2** | **0.4** | **0.6** | **0.8** | **1.0** |
| 16 | 0.78 | 1.63 | 2.20 | 2.29 | 2.37 | 2.41 |
| 18 | 0.69 | 1.63 | 2.33 | 2.44 | 2.52 | 2.57 |
| 19 | 0.66 | 1.63 | 2.44 | 2.60 | 2.68 | 2.75 |
| 20 | 0.63 | 1.64 | 2.45 | 2.65 | 2.72 | 2.77 |
| 22 | 0.57 | 1.64 | 2.46 | 2.83 | 3.00 | 3.03 |
| 24 | 0.52 | 1.63 | 2.37 | 2.72 | 2.87 | 2.91 |
| 26 | 0.48 | 1.66 | 2.32 | 2.65 | 2.77 | 2.79 |

#### 7.5.3.1 $C_{u2}/C_{u1}$=0.2

In this case, the thin weak layer is relatively much weaker than the surrounding soil in the slope. The thin weak layer dominates the slope failure mechanism in the slope stability analysis. The results shown in Figure 7.25 indicates the lowest factor of safety occurs when $L_z/L$=0.48, the corresponding improvement ratio, $N_{pi}$ is 125.4% for free pile head condition. When $L_z/L$ is above 0.57, the factor of safety nearly keeps constantly at 1.60, and the corresponding improvement ratio, $N_{pi}$ is nearly 170%. However, if the pile head condition is fixed, the factor of safety and the improvement ratio are about 1.64 and 176 %, respectively. There is no big change in slope stability with the change of the pile length for fixed pile head

condition cases. The relationship between improvement ratio, $N_{pi}$ and length ratio $L_z/L$ for both pile head conditions is shown in Figure 7.26.

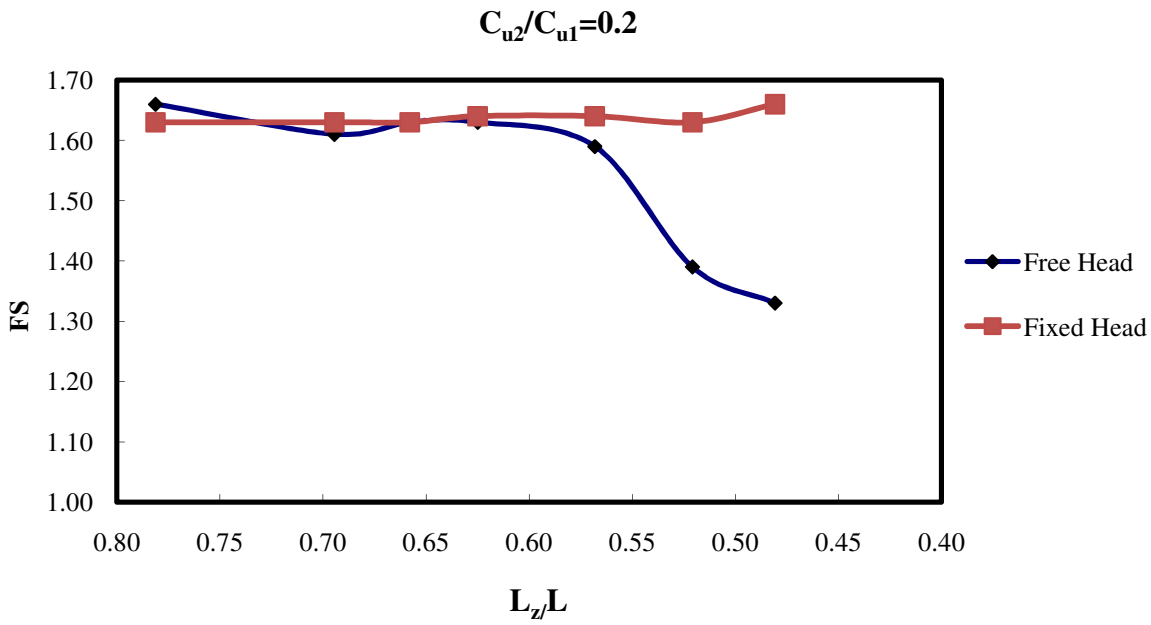


**Figure 7.23 Factor of safety versus $L_z/L$, $C_{u2}/C_{u1}=0.2$**

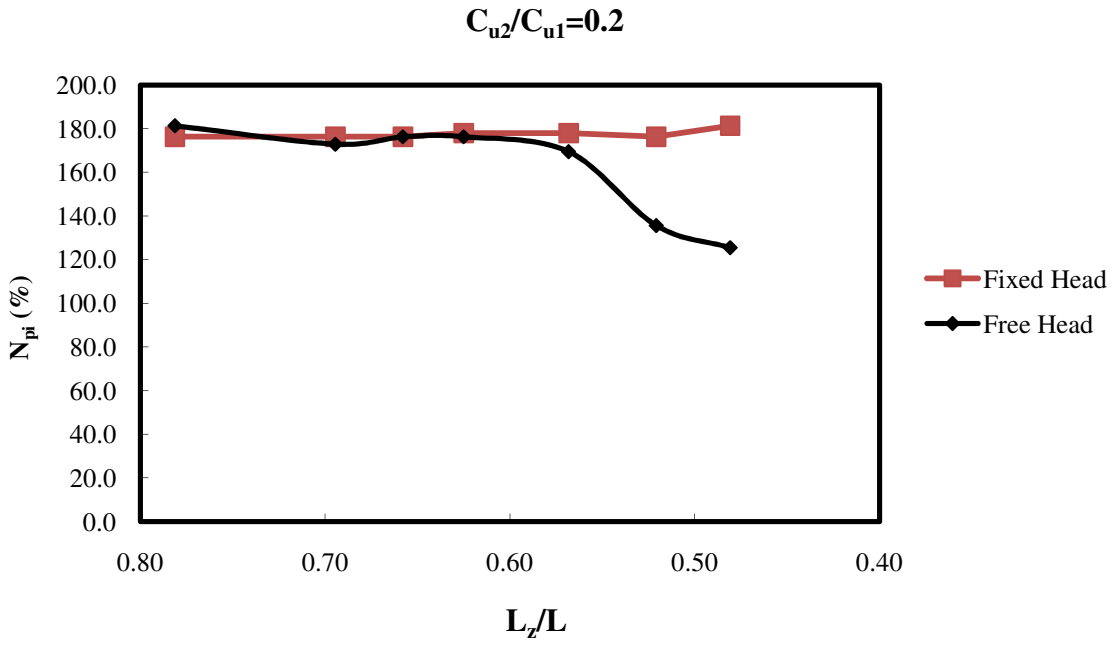


**Figure 7.24 $N_{pi}$ versus $L_z/L$, $C_{u2}/C_{u1}$=0.2**

### 7.5.3.2 $C_{u2}/C_{u1}$=0.4

The strength of thin weak layer in this case is 40% of the surrounding soil. The trend of improvement on slope stability due to the installation of stabilizing pile goes up to a peak value, the factor of safety is 2.23 and $N_{pi}$= 116.5% when $L_z/L$=0.66, then decreases to factor of safety is 1.81, and $N_{pi}$=73% when $L_z/L$=0.48. This value is the lowest in free pile head case. However, in fixed pile head cases, the lowest values of the factor of safety and $N_{pi}$ are 2.2 and 106.8%, respectively when $L_z/L$=0.78. The $L_z/L$ between 0.57 and 0.66, the factor of

safety is at around 2.45. When $L_z/L$ is above 0.66, the factor of safety starts to decrease. The numerical results are summarized in Table 7.4. The results are plotted in Figures 7.27 and 7.28.

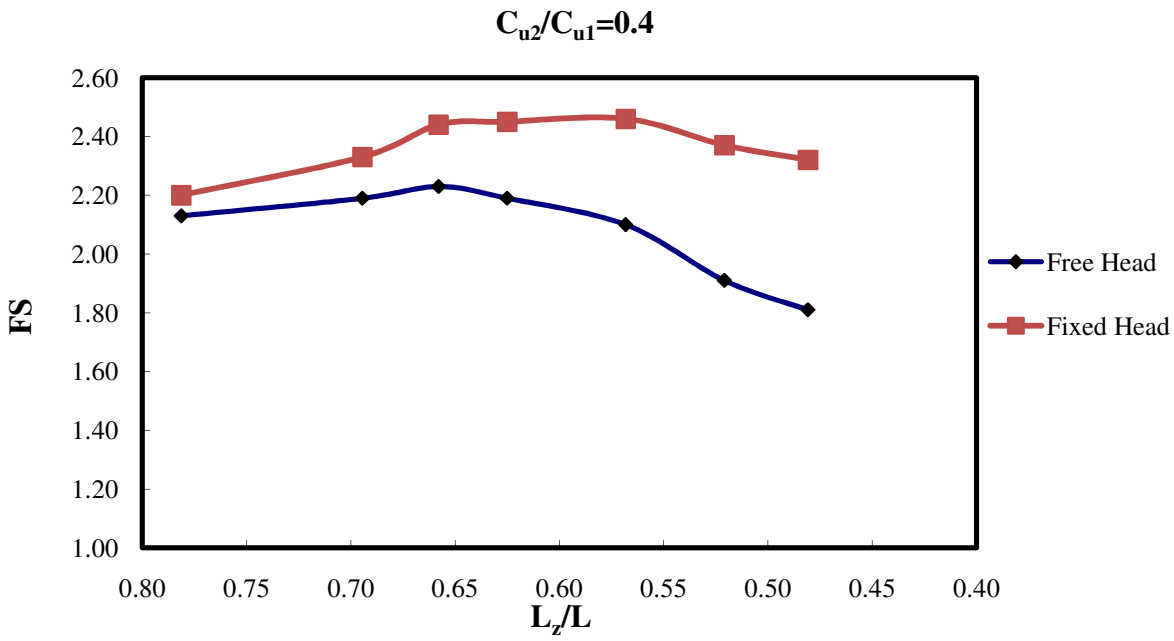


**Figure 7.25 Factor of safety versus $L_z/L$, $C_{u2}/C_{u1}$=0.4**

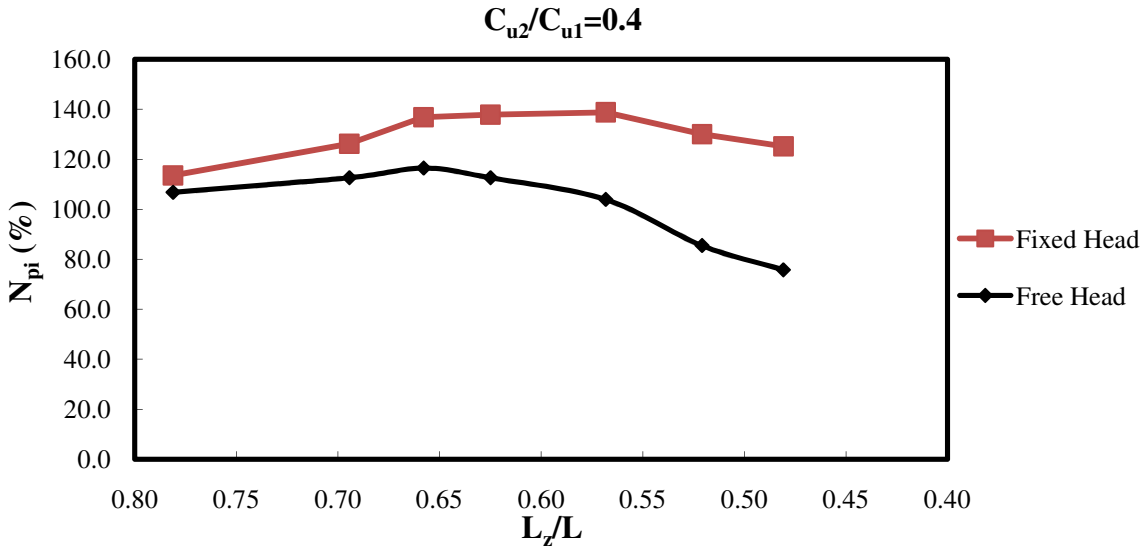


**Figure 7.26 $N_{pi}$ versus $L_z/L$, $C_{u2}/C_{u1}$=0.4**

### 7.5.3.3 $C_{u2}/C_{u1}$=0.6

In the unreinforced slope stability analysis, the failure mechanism is governed by both noncircular failure due to thin weak layer and base circular failure. Therefore, the strength ratio, $C_{u2}/C_{u1}$ =0.6 can be regarded as a critical strength ratio of this case since the failure mechanisms are different when the strength ratio above and below 0.6. The trends of improvement on slope stability due to the presence of the pile are shown in Figures 7.27 and 7.28, respectively. If the pile head condition is free, the factor of safety is quite stable regardless of the length of the pile, the maximum value of the factor of safety is 2.40 which occurs at the length ratio $L_z/L$=0.63. In other length of pile, the factors of safety range

between 2.1 and 2.2. But in the fixed pile head condition, the highest factor of safety is 2.84 when the length ratio, $L_z/L$ is 0.57. The lowest value of the factor of safety is 2.29 when the length ratio, $L_z/L$ =0.78. The factor of safety of the slope stability due to the installation of the pile has no large difference if the pile length is relatively short.

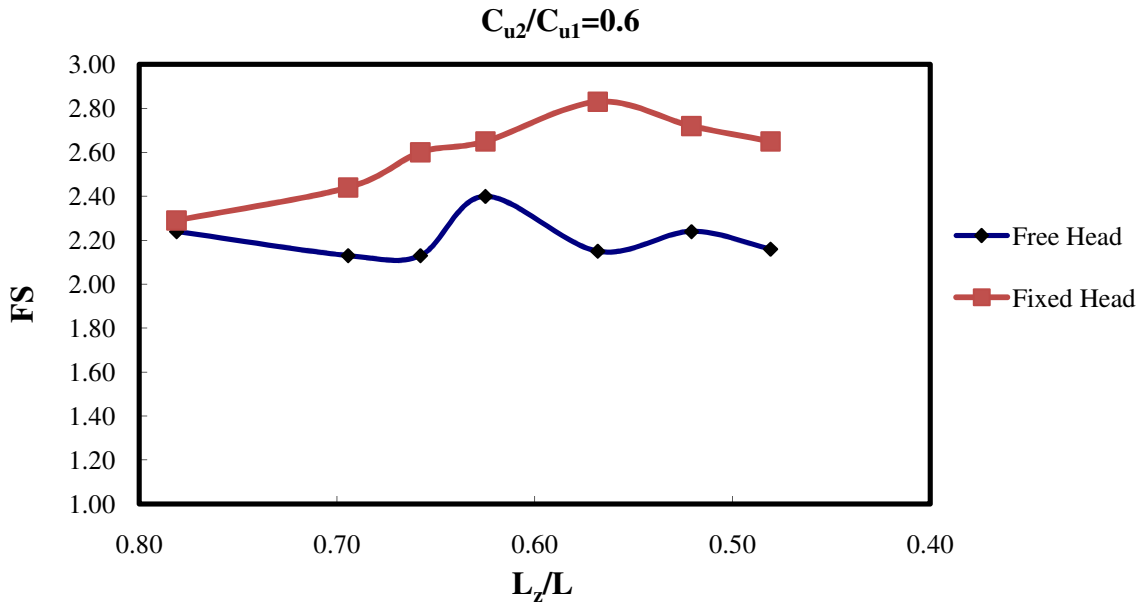


**Figure 7.27 Factor of safety versus $L_z/L$, $C_{u2}/C_{u1}$=0.6**

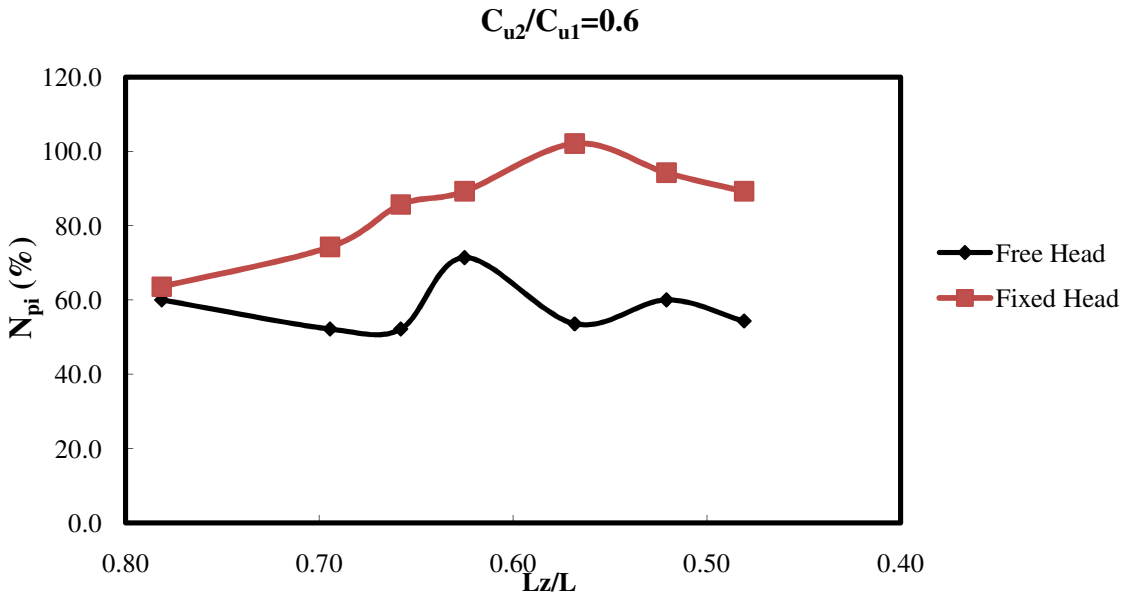


**Figure 7.28 $N_{pi}$ versus $L_z/L$, $C_{u2}/C_{u1}$=0.6**

### 7.5.3.4 $C_{u2}/C_{u1}$=0.8

In this case of $C_{u2}/C_{u1}$=0.8, the undrained shear strength of the soil in this weak layer is 20% lower than the surrounding soil of the slope. From the conclusion made in Griffiths and Lane's study (1999) and validated herein, when the ratio of the strength $C_{u2}/C_{u1}$ is greater than 0.6, the failure mechanism will transit to base circular failure, which is not governed by thin weak layer and it is the failure mechanism can be seen in the slope stability analysis of homogeneous slope. The factor of safety of the piled-slope system with free head pile has the lowest value 2.15 which occurs at the length ratio $L_z/L$=0.69. The highest value of the factor of safety is 2.31 which occurs in both $L_z/L$=0.48 and 0.78. If the pile head condition is fixed,

the peak value of the factor of safety is 3.0 at $L_z/L$=0.57. The lowest value of the factor of safety is 2.37 at $L_z/L$=0.78. The comparisons of factor of safety and improvement ratio, $N_{pi}$ between two different pile head conditions can be seen in Figures 7.29 and 7.30.

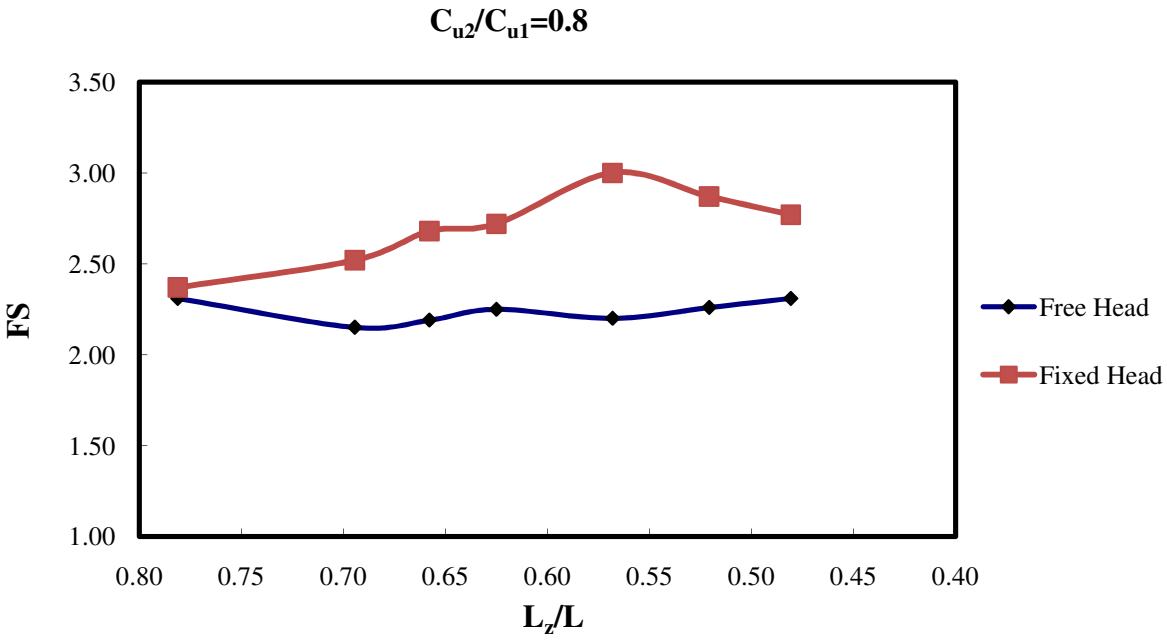


**Figure 7.29 Factor of safety versus $L_z/L$, $C_{u2}/C_{u1}$=0.8**

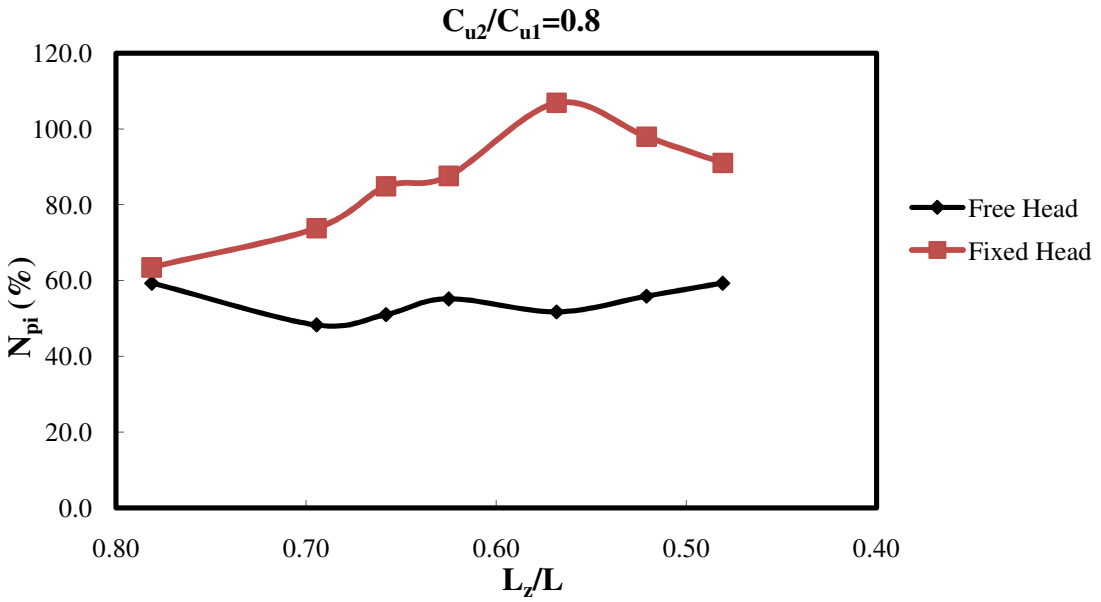


**Figure 7.30 $N_{pi}$ versus $L_z/L$, $C_{u2}/C_{u1}$=0.8**

### 7.5.3.5 $C_{u2}/C_{u1}$=1.0

This slope is homogeneous when the strength ratio $C_{u2}/C_{u1}$=1.0. As previous chapter discussed, the failure mechanism is governed by the base circular failure. Figures 7.31 and 7.32 compare the results of the finite element analysis and the numerical data are summarized in Table 7.7. The pile with free head has the lowest factor of safety 2.13 at the length ratio $L_z/L$=0.63 and largest and second largest values occur at $L_z/L$=0.48 and 0.78, respectively. Comparing the results in Figures 7.27 to 7.32, these figures show the similar results and curve shape if the pile head is restricted as fixed when the strength ratio $C_{u2}/C_{u1}$ is

above 0.6. The highest factor of safety is 3.03 at $L_z/L$=0.57, and the lowest value is 2.41 at $L_z/L$=0.78 in this case with $C_{u2}/C_{u1}$=1.0

The overall numerical results of the factor of safety based on these five cases are summarized in Tables 7.8 and 7.9 on free and fixed pile head respectively. The improvement ratios, $N_{pi}$, of each case are summarized in Tables 7.10 and 7.11, respectively.

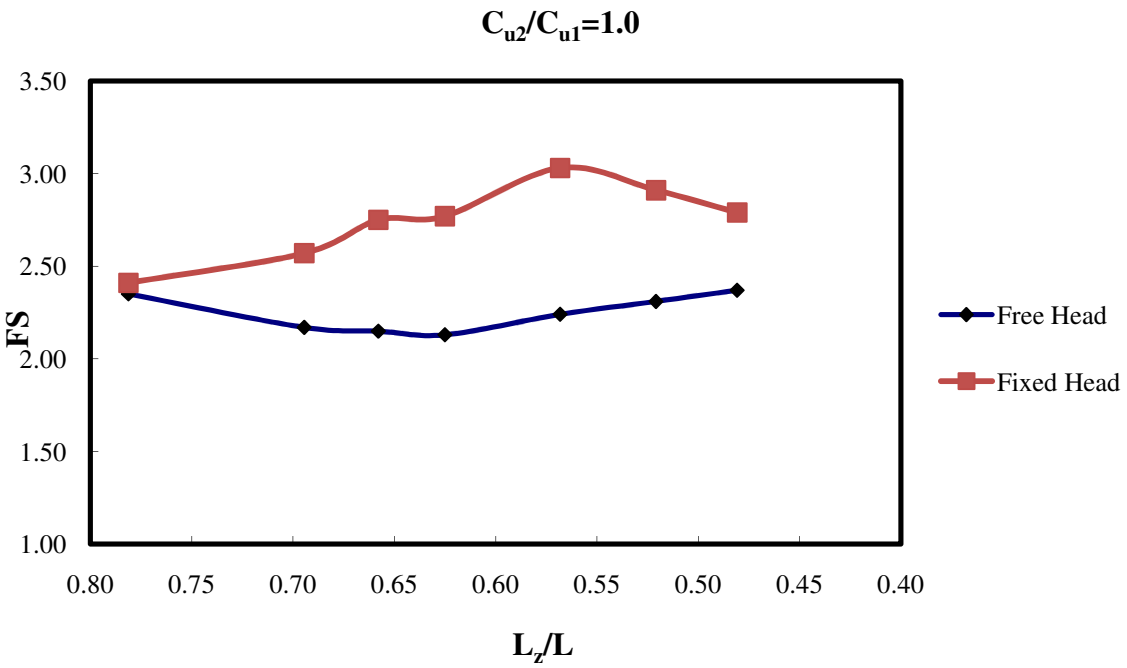


**Figure 7.31 Factor of safety versus $L_z/L$, $C_{u2}/C_{u1}$=1.0**

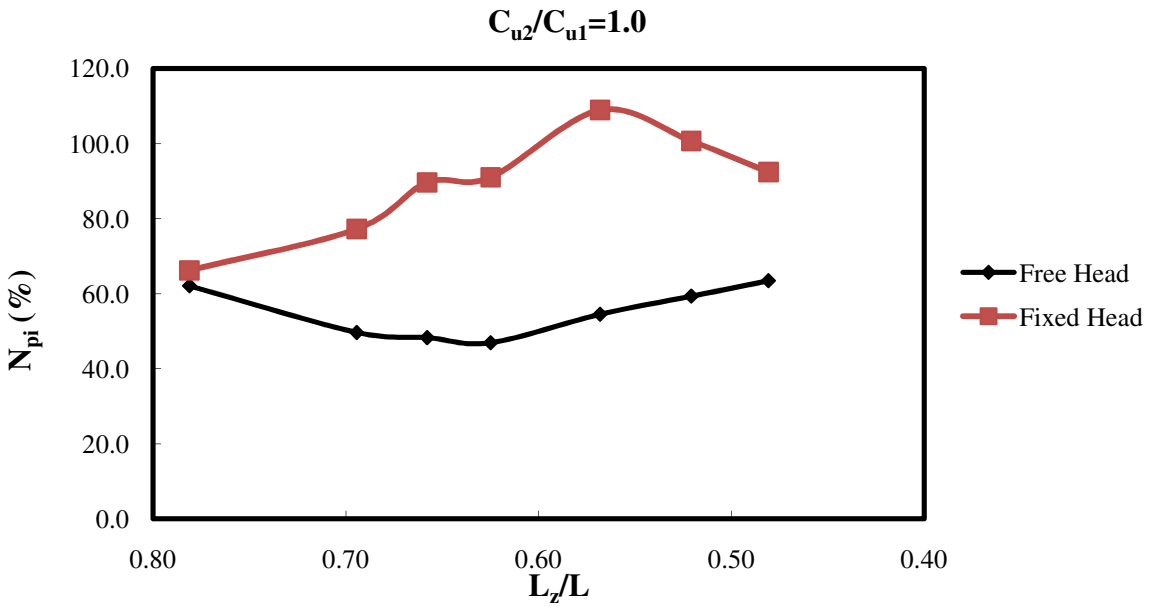


**Figure 7.32 $N_{pi}$ versus $L_z/L$, $C_{u2}/C_{u1}$=1.0**

**Table 7.10 $C_{u2}/C_{u1}$ versus $N_{pi}$ with free pile head condition**

| Pile | | $C_{u2}/C_{u1}$ vs. $N_{pi}$ (%) (Free Head) | | | | |
|---|---|---|---|---|---|---|
| Length (m) | Ratio ($L_z/L$) | 0.2 | 0.4 | 0.6 | 0.8 | 1.0 |
| 16 | 0.78 | 181.36 | 106.80 | 60.00 | 59.31 | 62.07 |
| 18 | 0.69 | 172.88 | 112.62 | 52.14 | 48.28 | 49.66 |
| 19 | 0.66 | 176.27 | 116.50 | 52.14 | 51.03 | 48.28 |
| 20 | 0.63 | 176.27 | 112.62 | 71.43 | 55.17 | 46.90 |
| 22 | 0.57 | 169.49 | 103.88 | 53.57 | 51.72 | 54.48 |
| 24 | 0.52 | 135.59 | 85.44 | 60.00 | 55.86 | 59.31 |
| 26 | 0.48 | 125.42 | 75.73 | 54.29 | 59.31 | 63.45 |

**Table 7.11 $C_{u2}/C_{u1}$ versus $N_{pi}$ with fixed pile head condition**

| Pile | | $C_{u2}/C_{u1}$ vs. $N_{pi}$ (%) (Fixed Head) | | | | |
|---|---|---|---|---|---|---|
| **Length (m)** | **Ratio ($L_z/L$)** | **0.2** | **0.4** | **0.6** | **0.8** | **1.0** |
| 16 | 0.78 | 176.27 | 113.59 | 63.57 | 63.45 | 66.21 |
| 18 | 0.69 | 176.27 | 126.21 | 74.29 | 73.79 | 77.24 |
| 19 | 0.66 | 176.27 | 136.89 | 85.71 | 84.83 | 89.66 |
| 20 | 0.63 | 177.97 | 137.86 | 89.29 | 87.59 | 91.03 |
| 22 | 0.57 | 177.97 | 138.83 | 102.14 | 106.90 | 108.97 |
| 24 | 0.52 | 176.27 | 130.10 | 94.29 | 97.93 | 100.69 |
| 26 | 0.48 | 181.36 | 125.24 | 89.29 | 91.03 | 92.41 |

### 7.5.4 Pile Head Condition

The pile head condition can be applied in two conditions, which are free pile head and fixed pile head, respectively. The relationships between the factor of safety and the location of pile inserted, the factor of safety and the pile length based on these two types of pile head conditions applied are shown and analyzed previously. In terms of the pile location, the fixed pile head condition always makes greater contribution on slope stability than free head does regardless of the strength ratio, $C_{u2}/C_{u1}$. When $C_{u2}/C_{u1}$=0.2, the stabilizing pile with fixed head only contributes a little more when pile is place at toe and at the position, $X_p/X$ =0.25.

When the pile is placed in the middle portion of the slope and the upslope portion to the crest of the slope, the factors of safety due to the presence of stabilizing pile with both pile conditions are almost consistent. Other cases with the strength ratios, $C_{u2}/C_{u1}$=0.4 to 1.0, the results show that the fixed pile condition lead to larger factors of safety of the slope stability more or less except the pile placed at the crest. In overall results, the factor of safety with fixed pile head cannot be promoted larger if the pile is placed at the crest.

Based on the pile length, except $C_{u2}/C_{u1}$=0.2, the fixed pile head contributes the larger factor of safety due to the presence of the stabilizing pile than free pile head does regardless of the strength ratio $C_{u2}/C_{u1}$ and the pile length. While the strength ratio $C_{u2}/C_{u1}$=0.2, the factor of safety of slope reinforced with the pile developed very close on both pile head conditions if pile length is at the ratio $L_z/L$ or above 0.63. If the length ratio, $L_z/L$ less than 0.63, the fixed pile head condition still shows higher factor of safety resulted on the slope stability.

**7.6 Discussion of Results**

In Figure 7.6, the relationship between the factor of safety and the strength ratio $C_{u2}/C_{u1}$ of the slope stability showing the factor of safety is lower if the strength ratio $C_{u2}/C_{u1}$ is lower. This is because the low strength ratio $C_{u2}/C_{u1}$ gives rise to the slope failure to be governed by

this thin weak layer. If the thin layer is unstable (lower than $C_{u2}/C_{u1}$ less than 0.6), the failure will occur from there. That is why the factor of safety is lower in this case. Along with the increase of $C_{u2}/C_{u1}$, the failure mechanism will transit the failure surface from the thin weak layer to the base failure. The factor of safety therefore rises with the increase of $C_{u2}/C_{u1}$.

Comparing the results in Figures 7.09 to 7.18, when the pile is placed from toe toward the crest, all five cases ($C_{u2}/C_{u1}$=0.2, 0.4, 0.6 0.8 and 1.0) indicate that the fixed pile head does not contribute more stability than free pile head does when the pile is placed close to the crest and at the crest. The reason is when the pile is placed close to the toe or at the toe, even the free pile head pile does not move a lot or a large deformation occurs in the pile to resist the movement of the soil. Meanwhile, failure mechanism does not change due to the change of pile head condition. But in the middle portion of the slope, the pile head restricted as fixed can increase more stability on the slope compared to the pile with free head. The results of the finite element analysis in this study are similar to the results presented by Cai and Ugai (2000). In their study, finite element method was used to analyze a homogeneous slope with 1V:1.5H slope. The optimal pile location is in the middle portion of the slope regardless of the pile head condition. However, the fixed pile head condition brought more stability to the slope than free pile head does. The results indicate when the pile is placed in the middle

portion or lower in the slope, the pressures applied on the pile is large due to the large relative displacement between pile and soil so that the shear strength of pile-soil interface can be sufficiently mobilized. However, if the pile is placed in an upper portion, the pressure is not sufficiently mobilized (Cai and Ugai, 2000).

The other interesting phenomenon is when the thin layer fully controls the failure mechanism ($C_{u2}/C_{u1}$=0.2), the improvement ratio, $N_{pi}$ at the toe is higher than that on the crest regardless of pile head condition. The failure mechanism due to the pile placed at toe and crest are shown in Figures 7.33 and 7.34. In the finite element analysis using ABAQUS, the pile placed at the toe carries higher stress than pile at crest does. When the strength ratio, $C_{u2}/C_{u1}$ increases, the failure mechanism switch gradually from the thin weak layer to the base circular failure, the improvement ratios (and factors of safety) on both sides (crest and toe) become very close with each other when $C_{u2}/C_{u1}$=0.4. When the $C_{u2}/C_{u1}$ =0.6 or greater, the thin weak layer does not control the failure mechanism, the improvement ratio of the piled-slope system is higher at crest than at the toe. This is because the two different failure mechanisms are presented and are shown in Figures 7.35 and 7.36, respectively. As can be seen in the figures, the improvement ratio $N_{pi}$ increases as the $C_{u2}/C_{u1}$ decreases, indicating that the piles have more stabilizing effects when the thin layer of soil is relatively weaker.

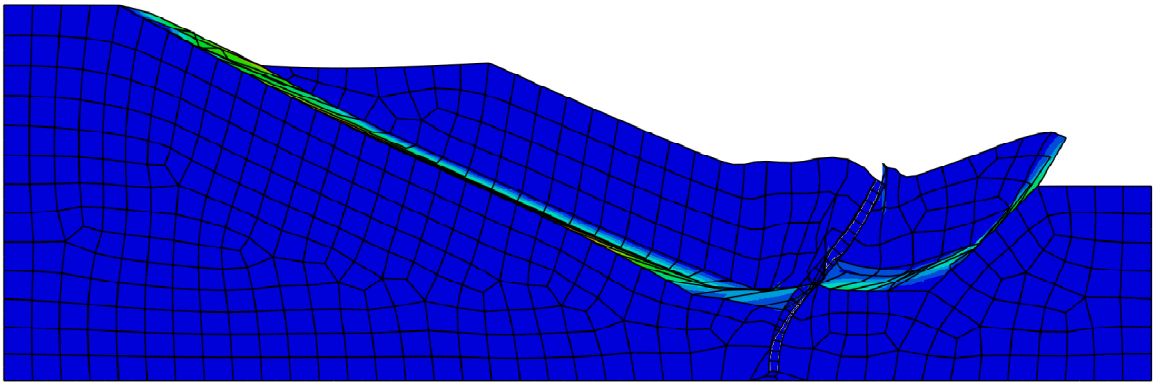

**Figure 7.33 Failure mechanism when pile placed at the toe ($C_{u2}/C_{u1}$=0.2)**

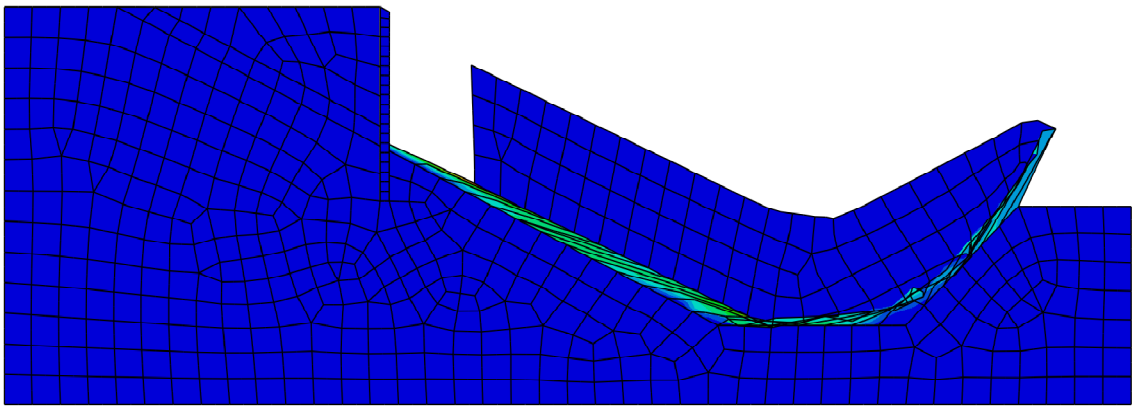

**Figure 7.34 Failure mechanism when pile placed at the crest ($C_{u2}/C_{u1}$=0.2)**

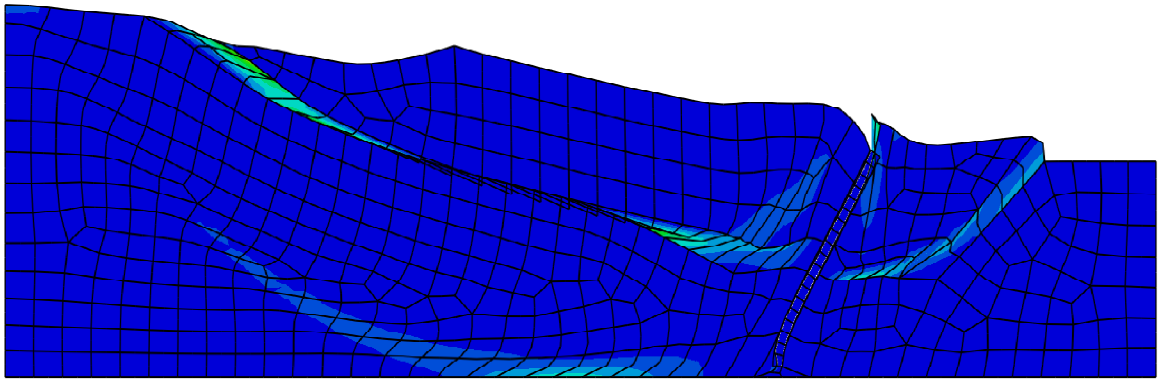

**Figure 7.35 Failure type when pile placed at the toe ($C_{u2}/C_{u1}$=0.6)**

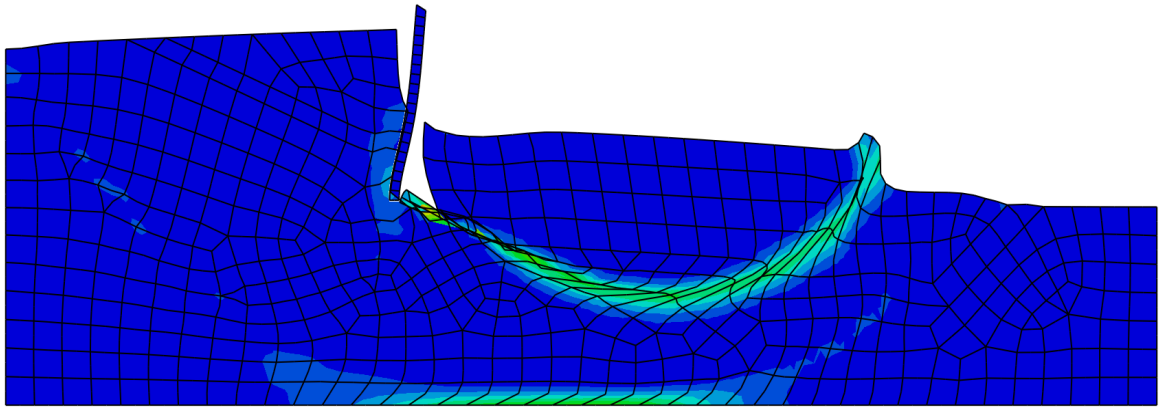

**Figure 7.36 Failure type when pile placed at the crest ($C_{u2}/C_{u1}$=0.6)**

The pile length effect is investigated by changing the length of pile. Because the optimal pile location has been determined as the middle portion of the slope, therefore, the length varies at the same location is reasonable to see the change of factor of safety due to the different pile length. The results indicate the pile with fixed head condition always provides a higher factor of safety of slope stability analysis. Compared to the pile with free head regardless of

strength ratio $C_{u2}/C_{u1}$ except $C_{u2}/C_{u1}=0.2$, the results of the strength ratio, $C_{u2}/C_{u1}=0.2$, show the factor of safety contributed by the fixed head pile is almost constant with the change of the pile length. While the factor of safety remains constant with the pile length increases until the length ratio, $L_z/L=0.63$ then drops when the ratio $L_z/L$ is greater. This is also because the failure mechanism is controlled by the thin weak layer. The pile head with fixed condition thus can hold the soil of the upper portion but cannot reduce the soil movement of lower portion of the slope if the layer is weak.

If the pile with free head condition is shorter, and the tip of the pile is slightly below the weak layer, the stiffness of the pile can reduce the movement of the upper part soil of the slope, the mechanism is quite similar to the pile with fixed head condition. In other words, in this situation, the failure of the slope depends upon the soil in lower portion. Once the soil below the pile is unstable, the slope fails no matter the soil above the pile is still in stable condition. Therefore, the factor of safety resulted from the presence of shorter pile will lead to the close value to pile with fixed head condition with the similar pile response. However, if the pile is longer, the bending stiffness, EI/L of pile will reduce, the pile deform larger due to the movement of the soil. So the slope failure mechanism depends on the entire soil mass

sliding along the weak layer of soil. The factor of safety resulted due to the presence of the longer pile with free head therefore reduced.

Based on the results, the fixed head condition is recommended to be used in reinforcing the slope because the pile with fixed head will result in a higher factor of safety than free head pile does on the slope stability. The best location to place the fixed head pile is at the ratio $L_z/L$ around 0.57 on these cases with different strength ratios except $C_{u2}/C_{u1}$=0.2 which is shown in Figure 7.40. In the strength ratio, $C_{u2}/C_{u1}$=0.2, the shorter pile with free head condition can result in a similar factor of safety as the fixed head pile does as stated above.

The free head pile is also regarded to result in very good improvement in the slope stability of piled-slope system. Particularly if the $C_{u2}/C_{u1}$ is at a lower value, a peak value can be found at the ratio of $L_z/L$ between 0.6 and 0.7, which are presented in Figures 7.23 and 7.24. This is because the weak layer plays an important role in governing the failure mechanism and the failure may still occur at this weak thin layer and the appropriate length beyond the depth of potential slip surface is required. However, for the cases with a higher strength ratios, $C_{u2}/C_{u1}$=0.8, and 1.0, the slope is close to the homogeneous slope. In these cases, the pile length plays an important role on slope stability of piled slope system and the depth of

slip surface may change because the pile presents with the different length. That's why the free pile head cases do not exhibit a particular higher peak value of factor of safety at the middle value of length ratio $L_z/L$. On the contrary, the higher values of factor of safety occur at the maximum and minimum $L_z/L$ defined in this chapter as shown in Figure 7.37. Figure 7.38 present the overall results of the relationship between the factor of safety and the length ratio ($L_z/L$) qhen the pile head condition is fixed. This figure shows the resulting factors of safety increase with the strength ratio ($C_{u2}/C_{u1}$) rises. Except for the case of $C_{u2}/C_{u1}$=0.2, each curve shows the peak value occurs at the $L_z/L$=0.57 in the rest of four cases. Figures 7.39 and 7.40 present the correlation of the improvement ratios ($N_{pi}$) and the length ratios ($L_z/L$) based on the different strength ratios ($C_{u2}/C_{u1}$). In the case of the lowest strength ratio, $C_{u2}/C_{u1}$=0.2, the stabilizing pile results in the largest improvement ratios in the slope stability for both pile head conditions.

Figure 7.41 compares the results of the slope stability analysis of the unreinforced case using different finite element methods and the cases with the pile presence at the toe, middle and the crest, respectively. The cases without being reinforced with pile have been discussed previously in terms of slope stability. In Figure 7.41, the results indicate that the pile placed in the middle leads to largest factor of safety, and the pile placed at the toe seems give rise to

the least stabilization on slope stability analysis of piled slope system which has been proved previously as well. The curve show that the factor of safety increases linearly when the strength ratio $C_{u2}/C_{u1}$ >=0.4 if the pile is placed at the position of the $X_p/X$=0.5. For the pile placed either at toe or the crest, the curves become flat when the strength ratio, $C_{u2}/C_{u1}$>=0.6.

As noted previously, the pile head conditions do not make much difference on the case of $C_{u2}/C_{u1}$ = 0.2. For the higher strength ratios, the improvement ratios resulted are higher for the fixed pile head condition compared to the free pile head condition. The results are similar to those found by Cai and Ugai (2000). For all three cases resented in the paper, the improvement ratio (and factors of safety) resulted are the highest when the piles are placed in the middle third of the slope. As piles are placed near the crest and the toe there is little increase on the improvement ratio and the factor of safety of the slope stability, except for the case of the toe. In this study, one interesting point has to be mentioned and noticed in design. In Figure 7.21, it shows the factors of safety are still below 1.0 if the stabilizing pile is installed both at the toe and the crest if $C_{u2}/C_{u1}$=0.2. That means if the strength ratio, $C_{u2}/C_{u1}$=0.2, the pile placed at both the toe and the crest still insufficient to stop the failure.

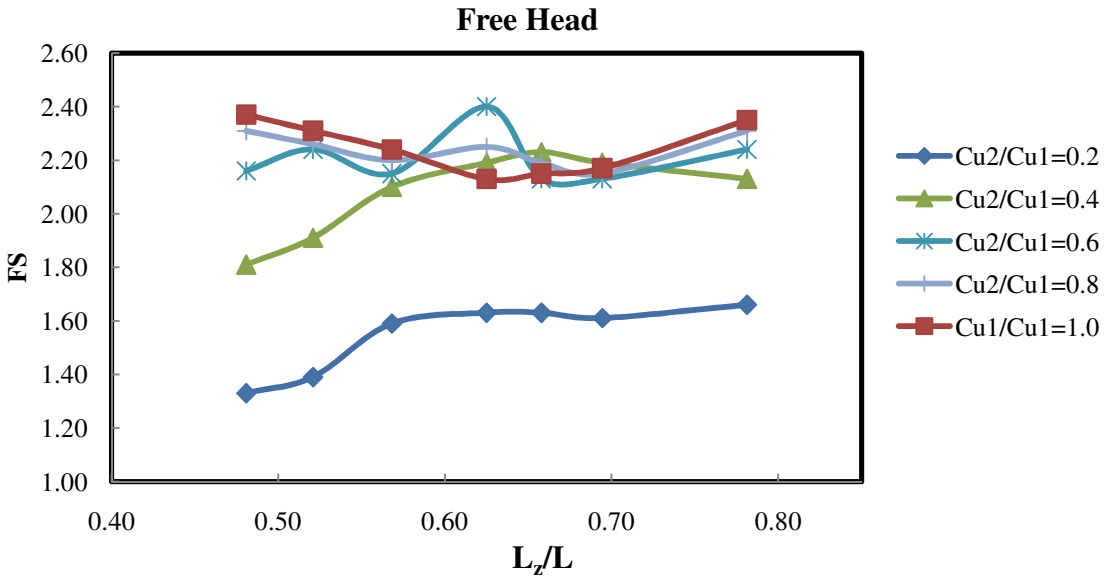


**Figure 7.37 Factor of safety versus $L_z/L$, free head**

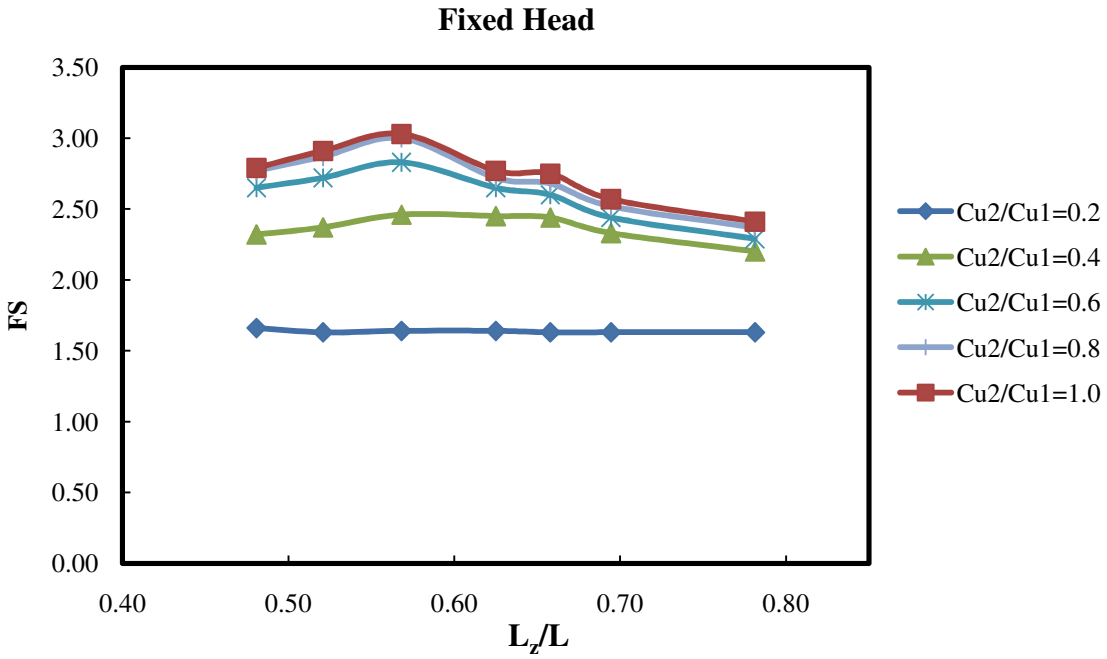


**Figure 7.38 Factor of safety versus $L_z/L$, fixed head**

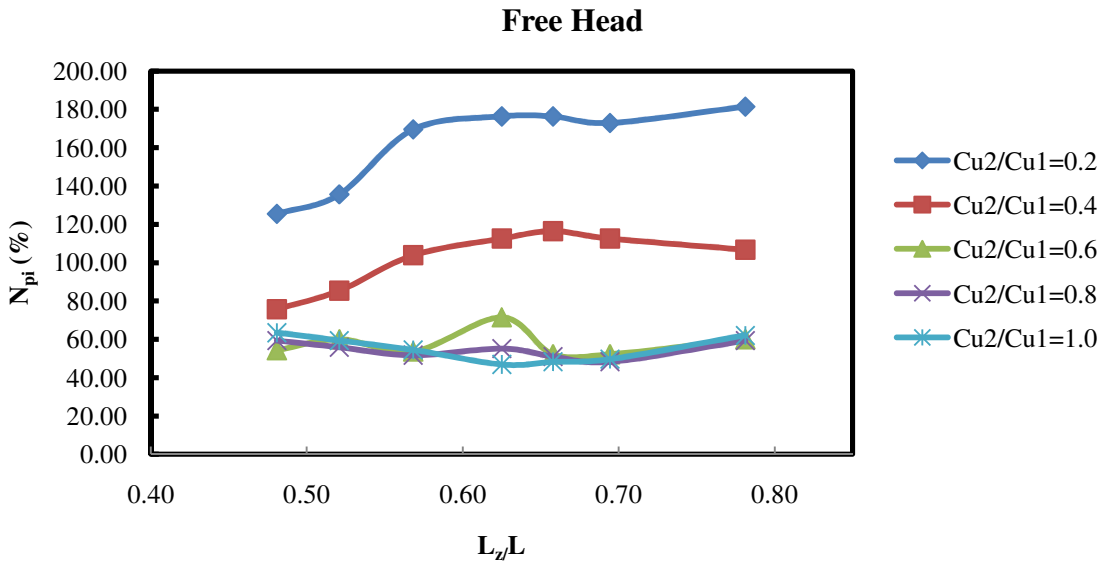


**Figure 7.39 $N_{pi}$ versus $L_z/L$, free head**

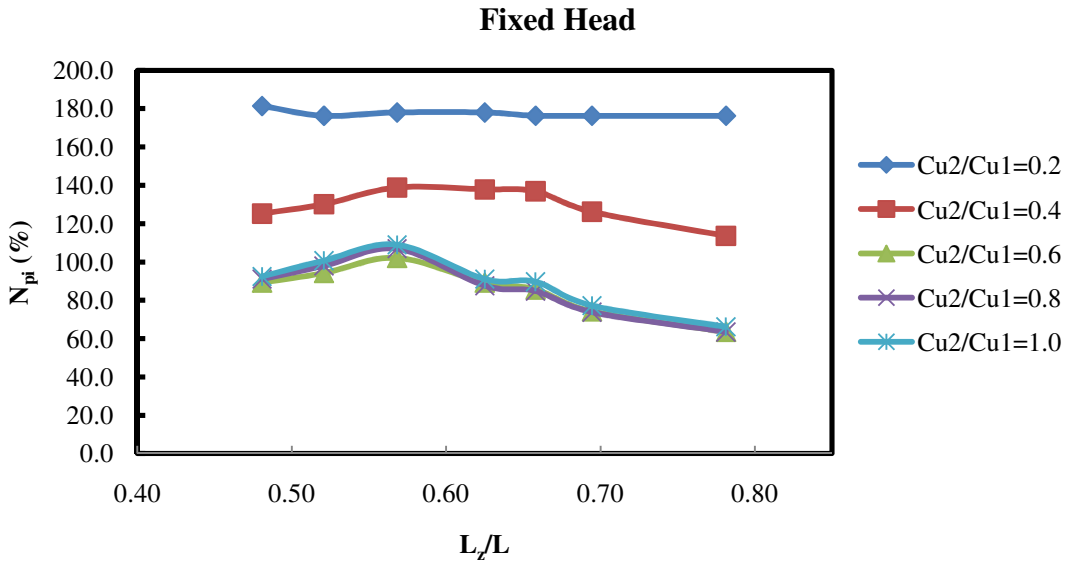


**Figure 7.40 $N_{pi}$ versus $L_z/L$, fixed head**

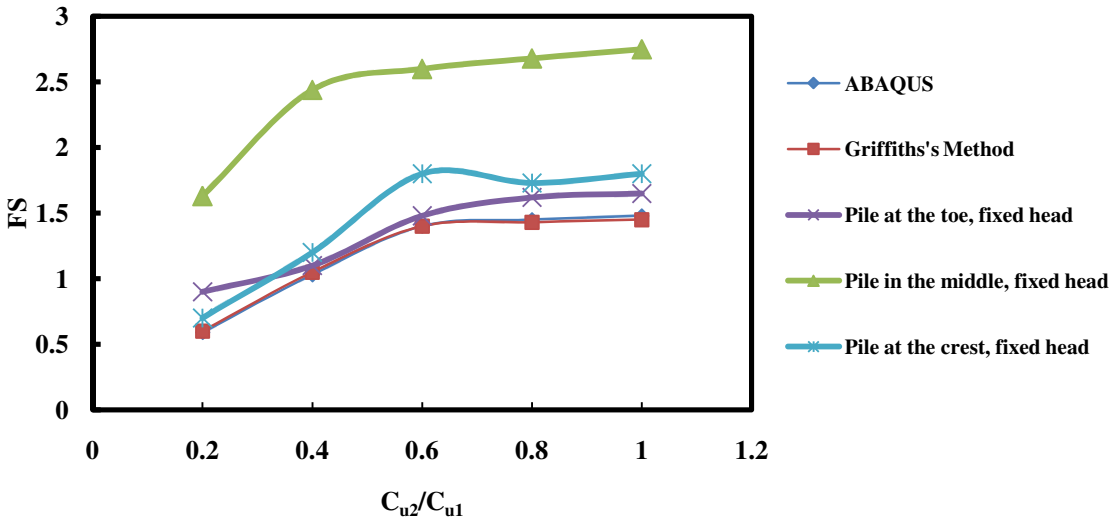


**Figure 7.41 Factor of safety versus $C_{u2}/C_{u1}$**

As can be seen the failure mechanism is changed by the pile installation if Figures 7.42 to 7.51 are compared. In the unreinforced case, as the strength ratio $C_{u2}/C_{u1}$ increases, the failure mechanism changed from the planar to a base circular failure at a $C_{u2}/C_{u1}$ values above 0.6. At the strength ratio, $C_{u2}/C_{u1}$ =0.6 the planar failure mechanism and the base circular failure mechanism were both evident. The installation of piles did not affect the failure mechanism of planar failure when $C_{u2}/C_{u1}$ =0.2, however, the soil only fails below the pile and not above it. The installation of piles changed the nature of the failure mechanism for $C_{u2}/C_{u1}$ =0.6 to one of a clear base circular failure. The $C_{u2}/C_{u1}$ =1.0 shows a failure mechanism similar to the $C_{u2}/C_{u1}$ =0.6 case of the pile head condition is fixed.

The failure mechanism of strength ratios $C_{u2}/C_{u1}$=0.2 and 0.4 are similar which shown in Figures 7.42 to 7.45. In these soils with these two soil strength ratios, the fixed pile head condition applied does not change the failure mechanism from free pile head condition. The factors of safety are actually dominated by the soil failure downslope of the pile regardless of pile head condition. In the strength ratio at $C_{u2}/C_{u1}$=0.6, if the pile head condition is free, the failure mechanism is similar to the unreinforced case that failure mechanism is governed by both planar failure and base circular failure. However, the pile head condition restricted as fixed changes the failure mechanism to the circular base failure as shown in Figure 7.47. In the strength ratio $C_{u2}/C_{u1}$ above 0.6, if the pile head condition is fixed, the failure mechanism is only dominated by circular base failure which as shown in Figures 7.47, 49 and 51, respectively.

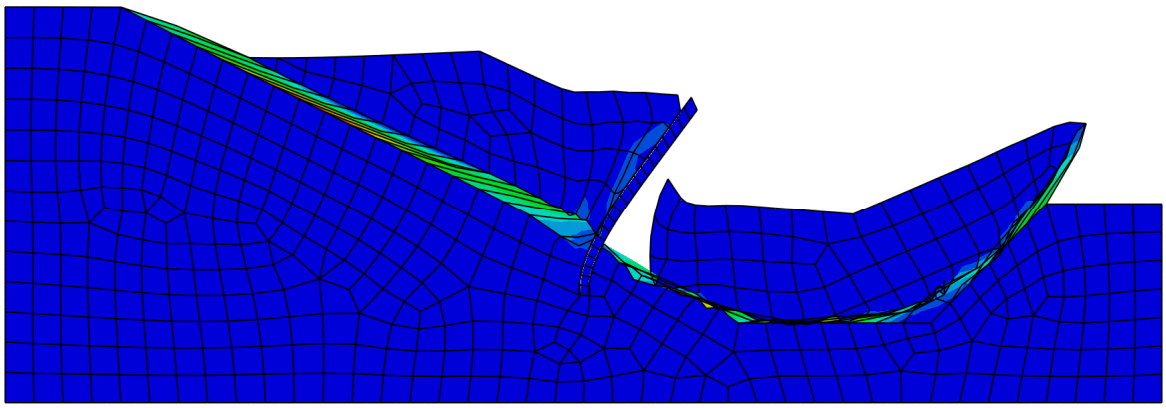

**Figure 7.42 Failure mechanism for free head condition and $C_{u2}/C_{u1}$=0.2.**

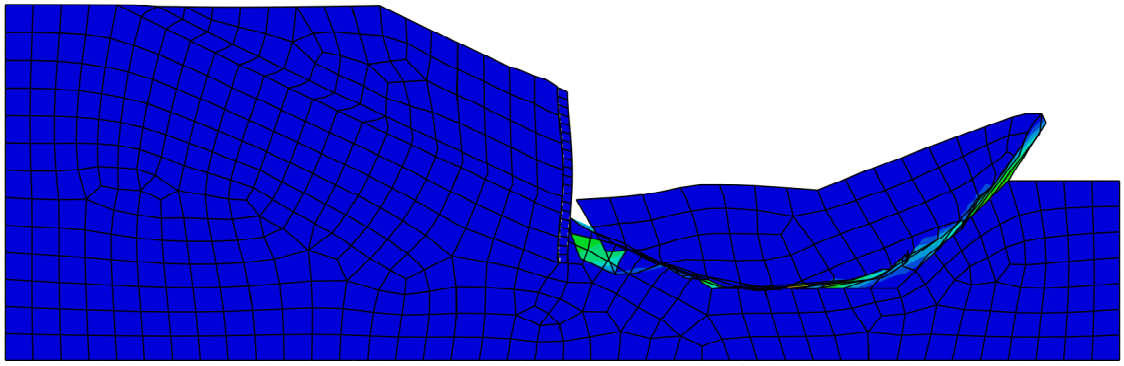

**Figure 7.43 Failure mechanism for fixed head condition and $C_{u2}/C_{u1}$=0.2.**

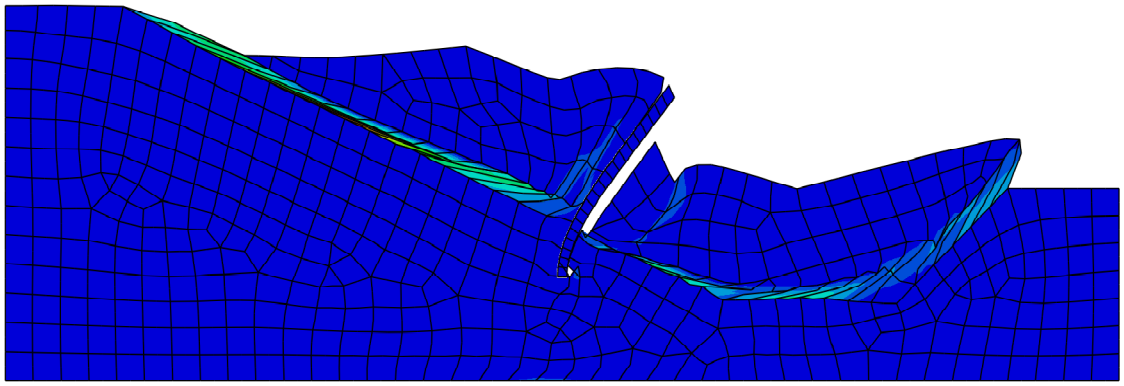

**Figure 7.44 Failure mechanism for free head condition and $C_{u2}/C_{u1}$=0.4.**

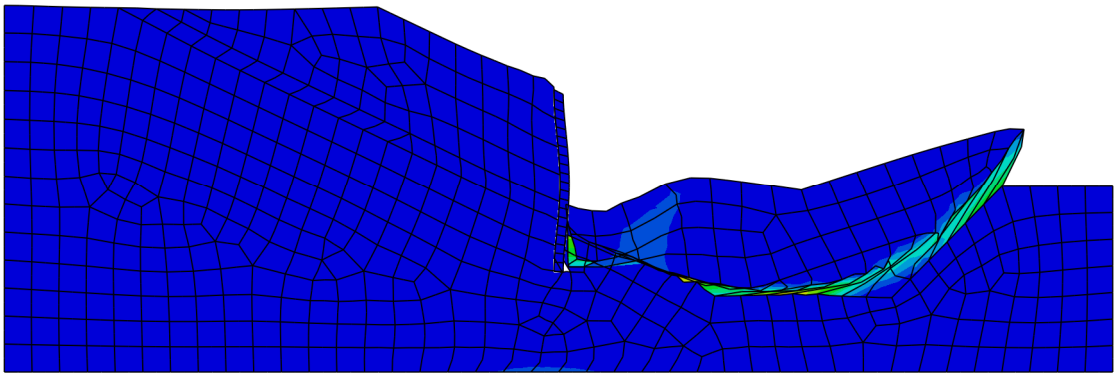

**Figure 7.45 Failure mechanism for fixed head condition and $C_{u2}/C_{u1}$=0.4.**

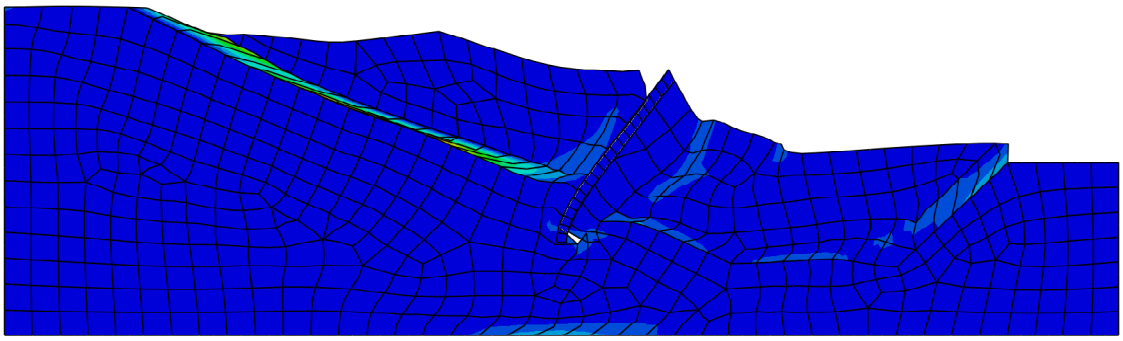

**Figure 7.46 Failure mechanism for free head condition and $C_{u2}/C_{u1}$=0.6.**

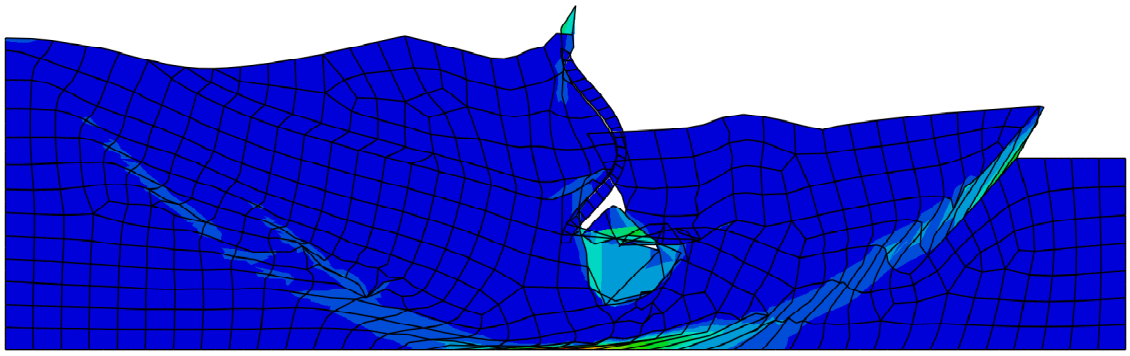

**Figure 7.47 Failure mechanism for fixed head condition and $C_{u2}/C_{u1}$=0.6.**

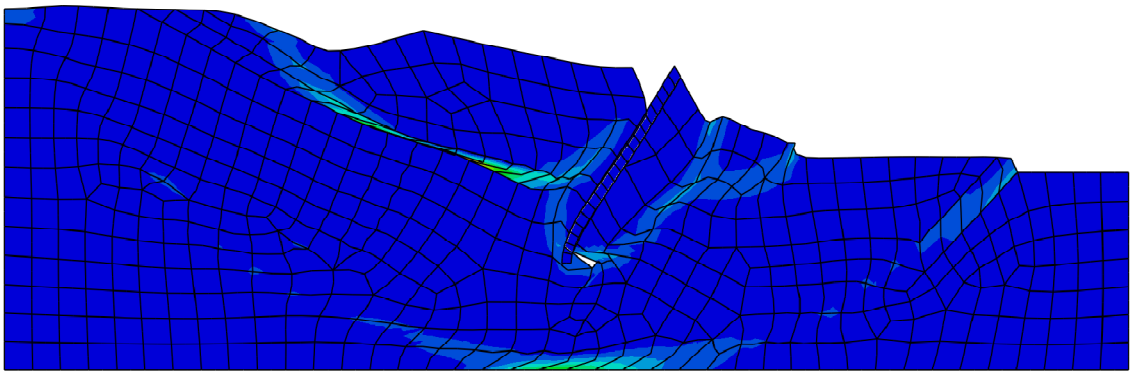

**Figure 7.48 Failure mechanism for free head condition and $C_{u2}/C_{u1}$=0.8.**

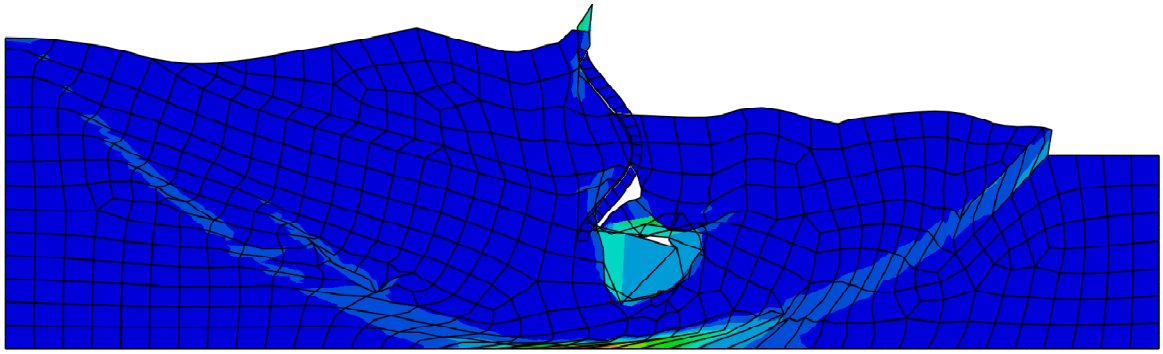

**Figure 7.49 Failure mechanism for fixed head condition and $C_{u2}/C_{u1}$=0.8.**

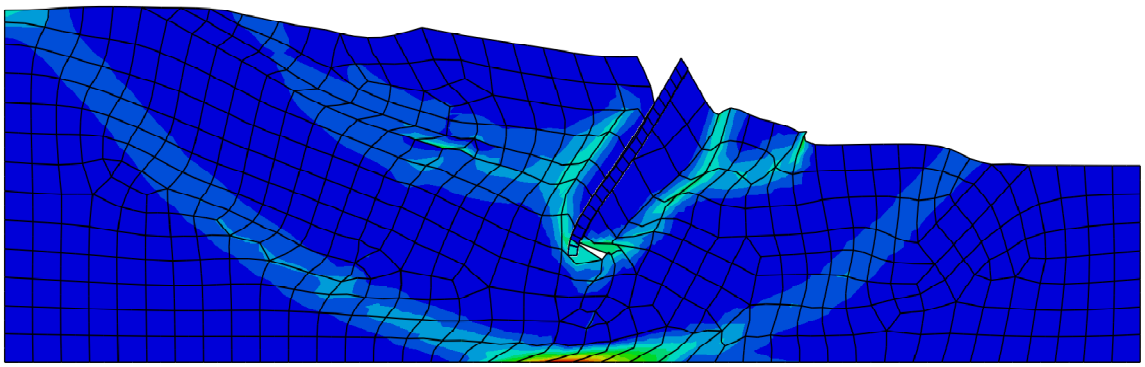

**Figure 7.50 Failure mechanism for free head condition and $C_{u2}/C_{u1}$=1.0.**

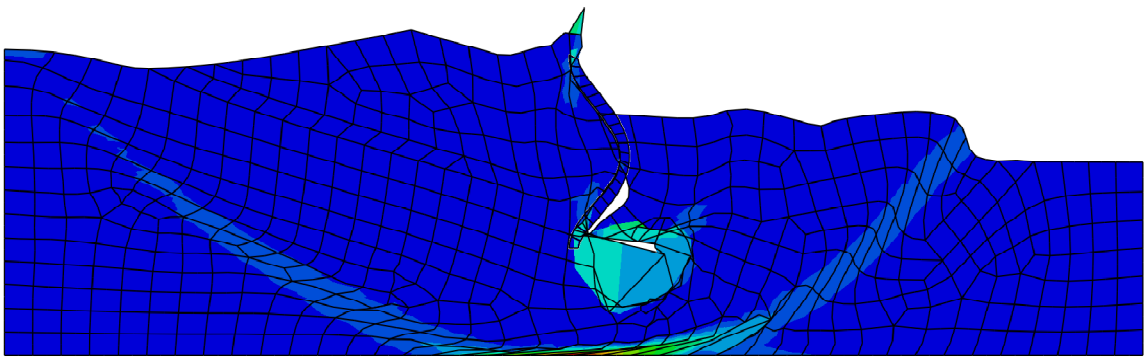

**Figure 7.51 Failure mechanism for fixed head condition and $C_{u2}/C_{u1}$=1.0.**

## 7.7 Three-Dimensional Finite Element Model

In this section, a three-dimensional finite element technique is employed to extend the analysis from two dimensions to three dimensions. The soil properties and dimensions of the slope are summarized in Table.7.1 as well. The geometry of the three dimensional slope is shown in Figure 7.52 and the mesh of this model is shown in Figure 7.53.

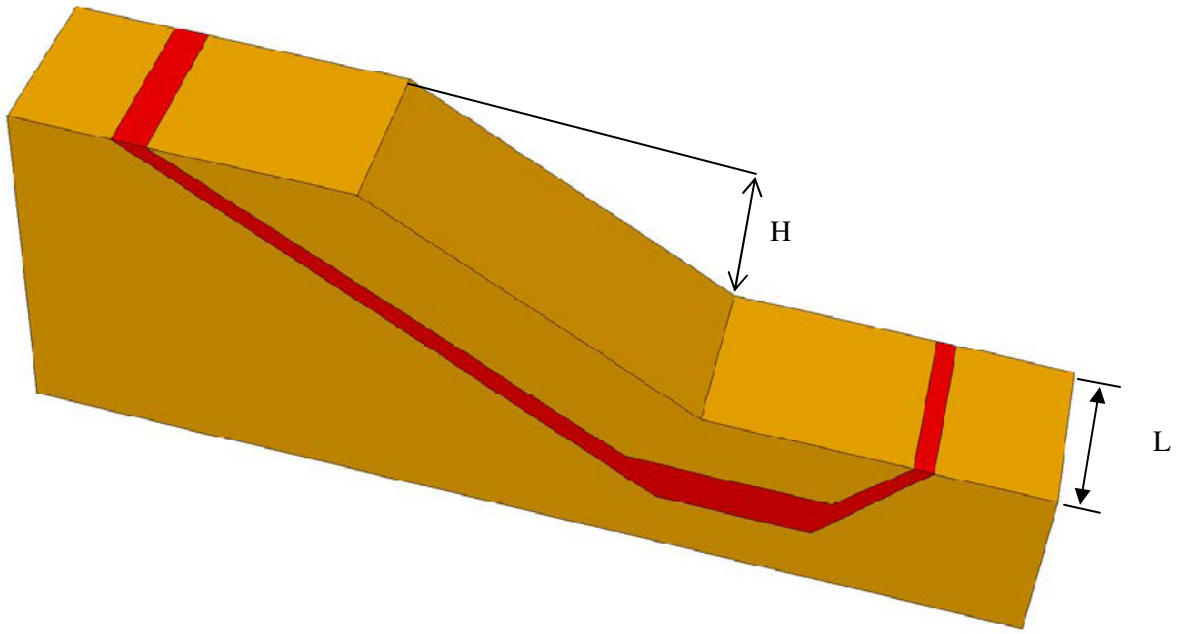


**Figure 7.52 Non-homogeneous slope with thin layer-3-D (ABAQUS)**

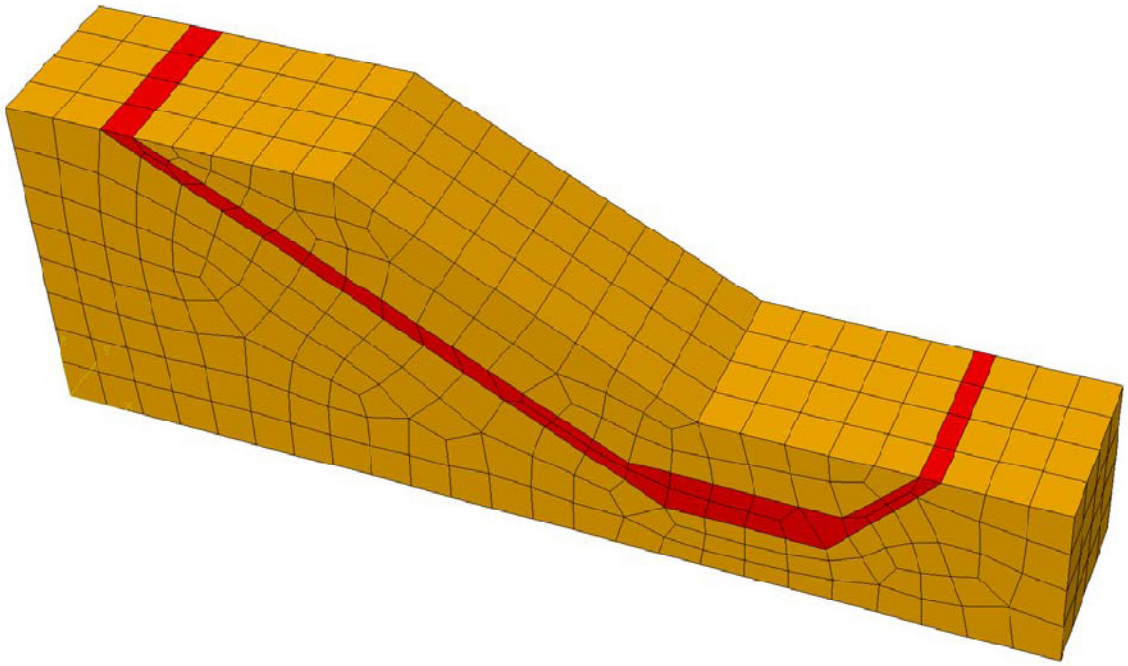

**Figure 7.53 Mesh of the non-homogeneous with thin layer in 3-D model (ABAQUS)**

### 7.7.1 Slope Model

In the cases of three-dimensional slope stability analysis, the strength ratios $C_{u2}/C_{u1}$ =1.0, 0.6 and 0.2 are analyzed using finite element method in ABAQUS with 3-D stress element with 8 node linearly with reduced integration. The Young's modulus (E) and Poisson's ratio (υ) of both soils are defaulted as $10^5$ kPa and 0.4, respectively. The same parameters are used in the 2-D finite element models. The elastic-perfectly plastic Mohr-Coulomb failure criterion is also applied to be the constitutive model of the soil. The factors of safety based on these three strength ratios (0.2, 0.6 and 1.0) are discussed herein. The mesh type and element shape are

shown in Figure 7.53. The dilation angle in this model is assumed as zero, therefore, the plastic potential in non-associated flow. The boundary conditions on both sides in the third dimension are regarded an important influencing factors in three dimensional slope analysis. According to Griffiths and Marquez (2007), the boundary can be assumed as three typical types, which are smooth-smooth, rough-smooth and rough-rough, respectively. In this study, the boundary conditions of both sides are assumed fixed, and that is the so called rough-rough in Griffiths and Marquez's study. The effect of the width to height ratio, L/H was studied by analyses of L/H=1.0 to 12. Here, H means the height of the slope excluding foundation beneath and the L is the width of the slope model in the third dimension. The relationship of factor of safety and L/H is shown in Figure 7.54.

### 7.7.2 Analysis Result

The results of the slope stability analysis based on the factor of safety using three-dimensional models are summarized in Table 7.12. A higher factor of safety is presented if compared to two dimensional finite element analyses with the same material and boundary conditions. In terms of percentage, the factor of safety difference is about 30~40% for this case if L/H of all cases set as 1.0. Compared to 2-D finite element analysis, factor of

safety was found to decrease if L/H increases. When the ratio, L/H is over 10, the factors of safety from both 3-D and 2-D analyses are very close. This results show the impact of the boundary conditions of two sides are decreasing with the increase of L/H. The solutions get close to the plane strain solutions which obtained in 2-D model. The contours of slope deformation with different soil strength ratios which are 0.2, 0.6 and 1.0 are shown in Figures 7.55, 56 and 57, respectively. The soil mechanisms shown in these figures are very similar to the results in two dimensional finite element models discussed above.

**Table 7.12 Factor of Safety versus $C_{u2}/C_{u1}$, L/H=1.0**

| $C_{u2}/C_{u1}$ | 0.2 | 0.6 | 1.0 |
|---|---|---|---|
| ABAQUS 2-D | 0.59 | 1.40 | 1.49 |
| ABAQUS 3-D | 0.85 | 1.78 | 1.95 |

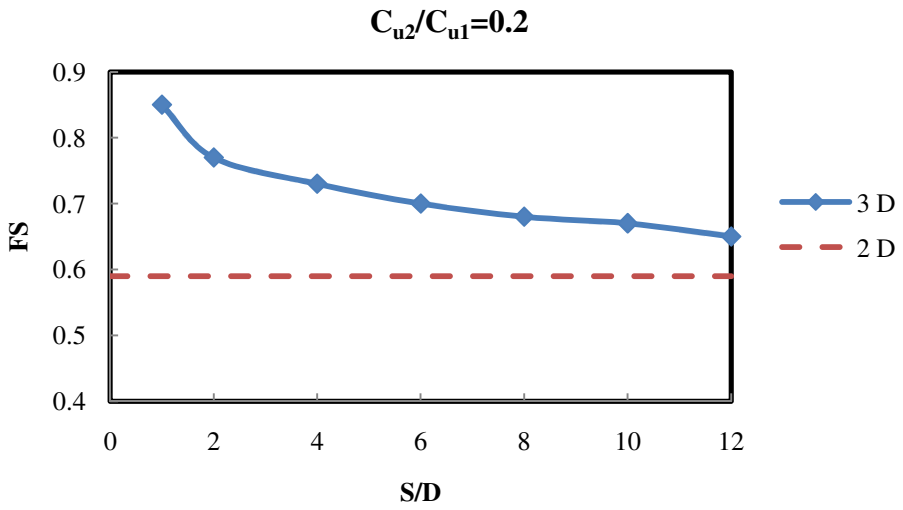


**Figure 7.54 Comparison of 3-D and 2-D finite element analysis, $C_{u2}/C_{u1}$=0.2**

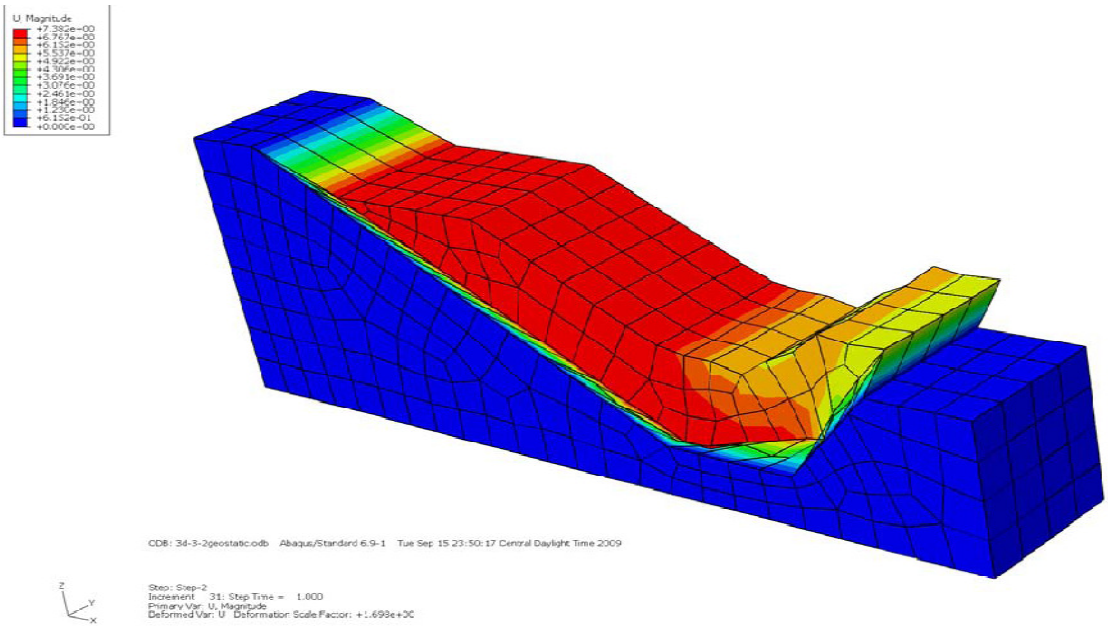


**Figure 7.55 Slope failure mechanism in 3-D model, $C_{u2}/C_{u1}$=0.2**

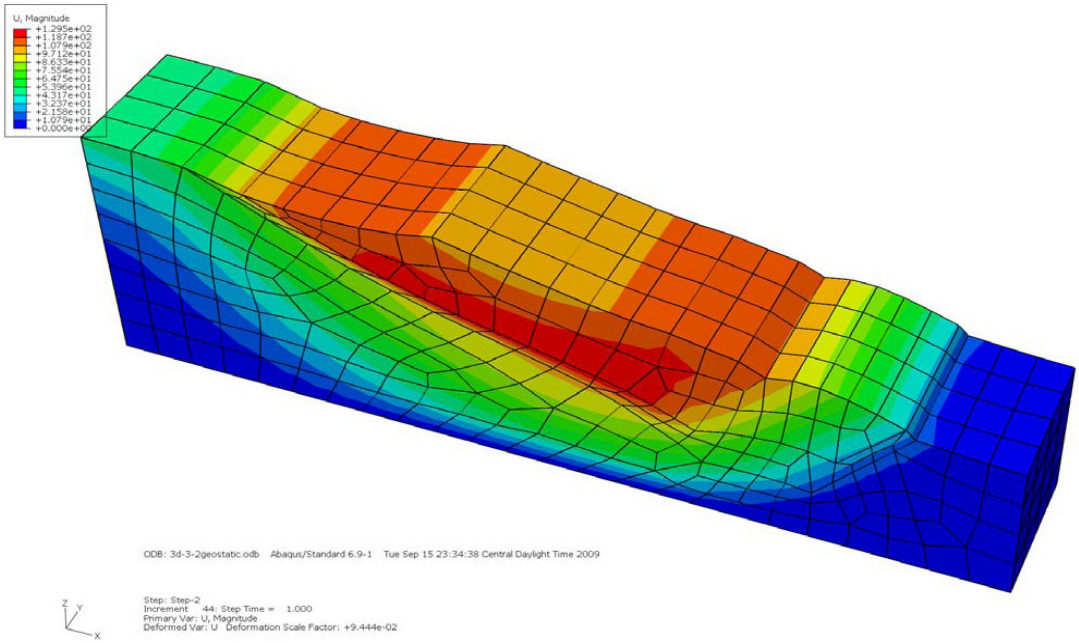


**Figure 7.56 Slope failure mechanism in 3-D model, $C_{u2}/C_{u1}$=0.6**

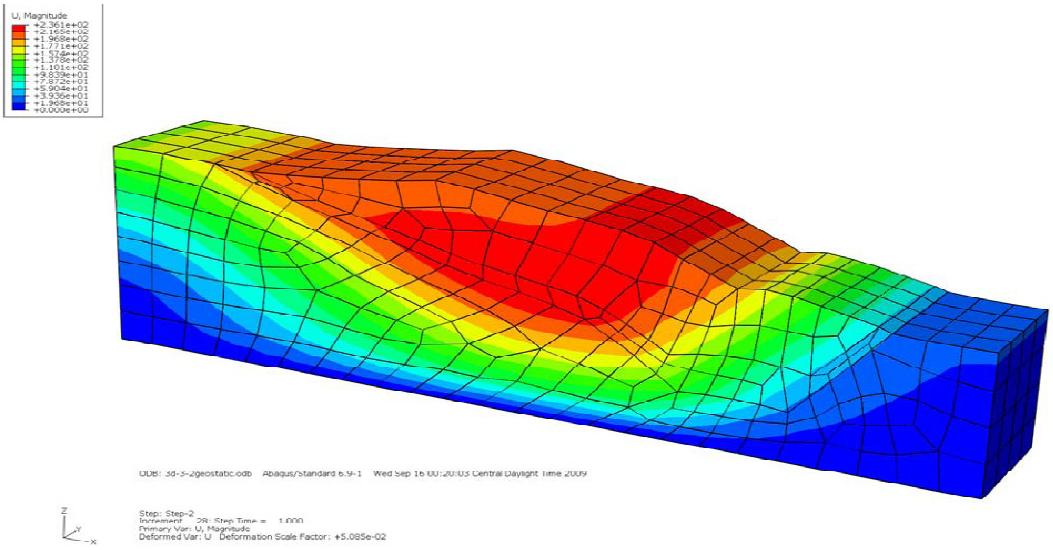


**Figure 7.57 Slope failure mechanism in 3-D model, $C_{u2}/C_{u1}$=1.0**

## 7.8 Three-Dimensional Model of Pile-Reinforced Slope

To further verify the impact of pile stabilization on slope stability, a three-dimensional slope model reinforced with piles is used thereafter. As shown in Figure 7.58, a 3-D slope with two piles with symmetric position in the slope is analyzed. The top view of piled slope system is as shown as Figure 7.59. The side width of slope is set at 10 m in this case. The factor of safety is identified as independent on the width of the slope in the slope stability analysis. The soil properties and failure criteria are the same to the slope stability analysis cases used above. However, for accurate mesh the entire model, a 4-node linear tetrahedron element is selected in pile-stabilized slope models due to some limitation of mesh in the finite element model using ABAQUS. The properties of the pile is still the same to the 2-D case used previously which is an elastic media, but the element is selected as the structural shell element with 4 node, reduced integration as shown in Figure 7.60. As for the dimension of pile assumed in this case is 2.5 meter in diameter, 25 meter long with 10 mm thickness placed in the middle portion of the slope. The pile head condition applied is free in this case and the slope with strength ratio $C_{u2}/C_{u1}$=0.2 reinforced with pile is analyzed and discussed herein.

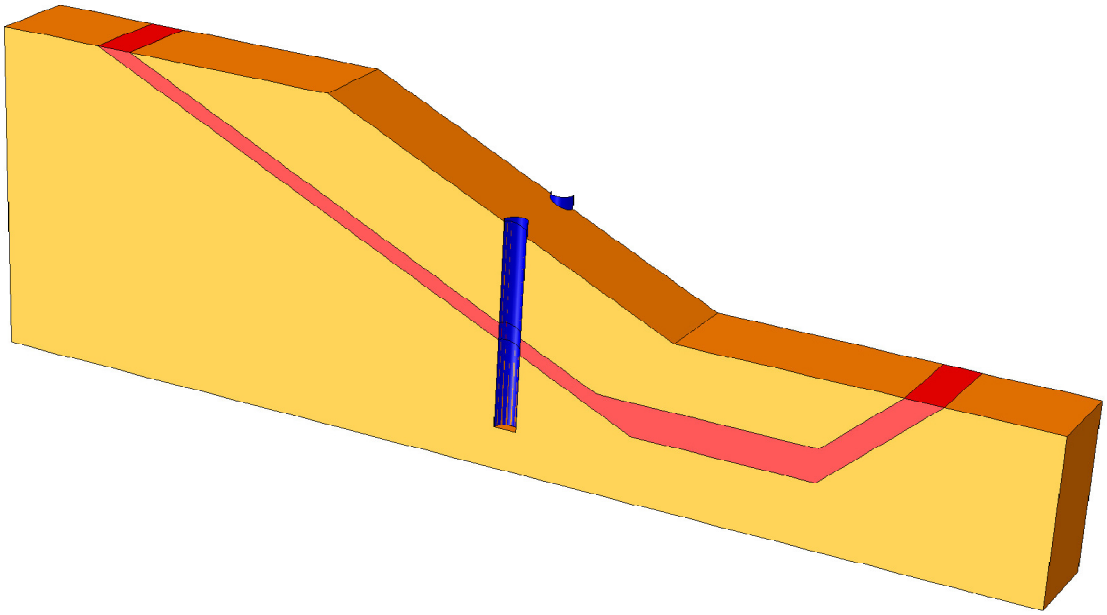

**Figure 7.58 Geometry of slope reinforced with piles in 3-D model**

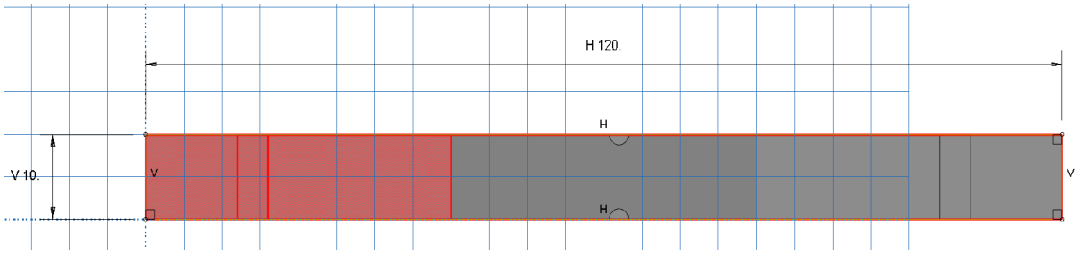


**Figure 7.59 Top view of piled slope system in 3-D model**

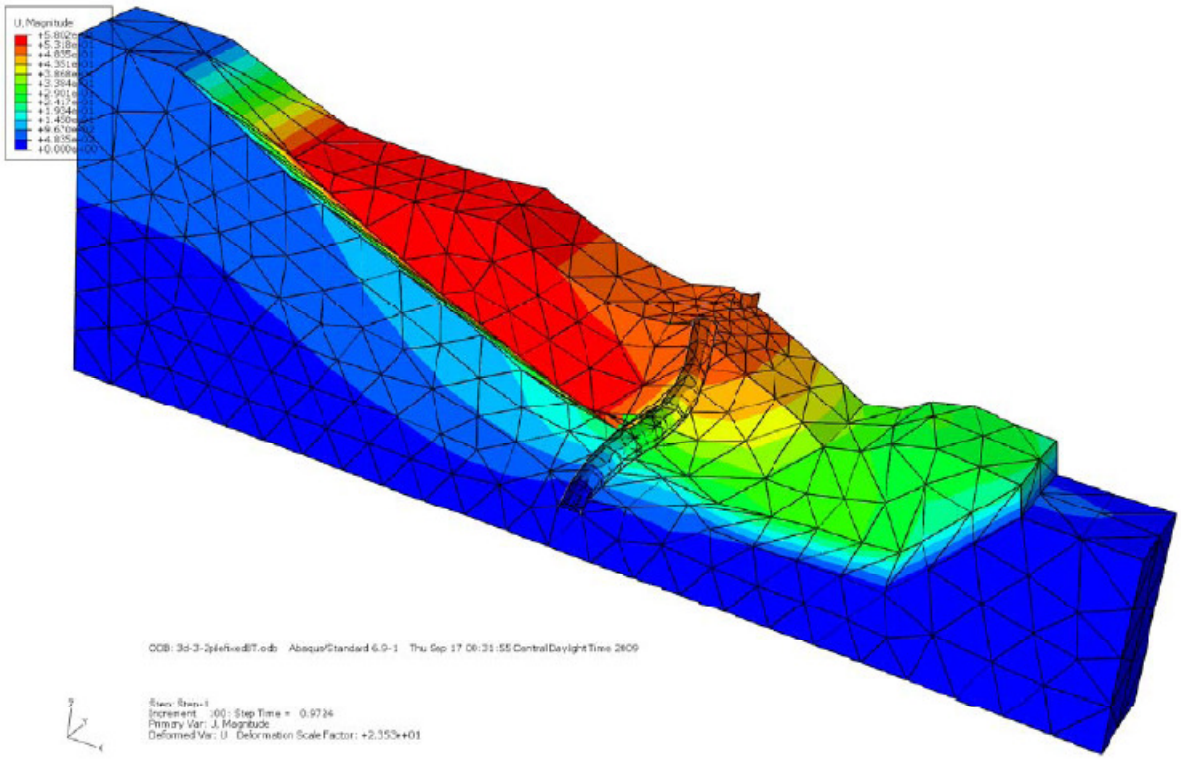


**Figure 7.60 Slope reinforced with piles in 3-D model, S/D=4.0, FS=1.52**

### 7.8.1 Results of Analysis

To study the effect of pile spacing, the ratios of S/D from 2 to 12 are investigated and the results are shown in Figure 7.61. Compared to the 2-D cases, the factor of safety in 2-D case is about 1.6 when pile is placed in the middle portion of the slope. In the results of 3-D finite element analysis, the spacing of pile (S/D) below 4 was found to lead to a higher factor of safety than 2-D pile-stabilized slope does. The factor of safety decreases sharply from

S/D=2.0 to 8.0, after S/D greater 8.0, the factor of safety in pile-stabilized slope is very close to the factor of safety of a unreinforced slope. The results of the finite element analysis in terms of pile response are also shown in Figure 7.62 based on the deformation of pile, moment distribution, shear distribution and soil resistance.

From the pile displacement curve, the lateral pile displacement increases with the increase of strength reduction factor, the pile head movement reaches the maximum 0.5m when the piled slope fails. The shear force has a maximum value at the depth of 17.5 m which corresponds to the bottom of thin weak layer. Due to the flexibility of pile, the different deformation of pile in the slope depends on the pile-soil interaction mechanism. Therefore, the moment distribution along the pile is different on each case with different strength reduction factor (SRF) as shown in Figure 7.62.

The soil resistance also depends on the deformation of the pile and the relative movement between the pile and the soil, the pile displacement increases due to the increase of soil strength reduction factor, when the pile has a larger movement than the soil, the soil provides opposite direction of resistance. The portion under the thin weak layer is relatively stable and always provides the resistance against the pile movement. The maximum strength reduction

factor or the so called factor of safety is 1.52, compared to the case without stabilizing piles, the resulting factor of safety of the finite element analysis is 0.85. The pile presence does provide stabilization and increase the factor of safety of the slope stability. Comparing the impact of the pile installed in terms of the soil displacement, the maximum soil movement in the sliding mass is 7 meters in the unreinforced slope, however, when the pile is installed and the same strength reduction factor 0.85 is used, the maximum soil movement in the sliding mass is reduced to 0.08 m in the finite element analysis.

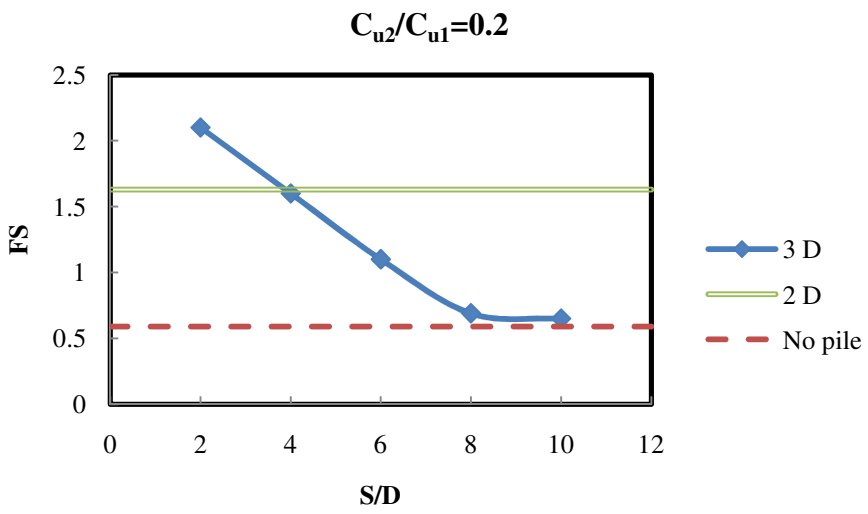


**Figure 7.61 Effect of pile spacing on factor of safety in pile-stabilized slope**

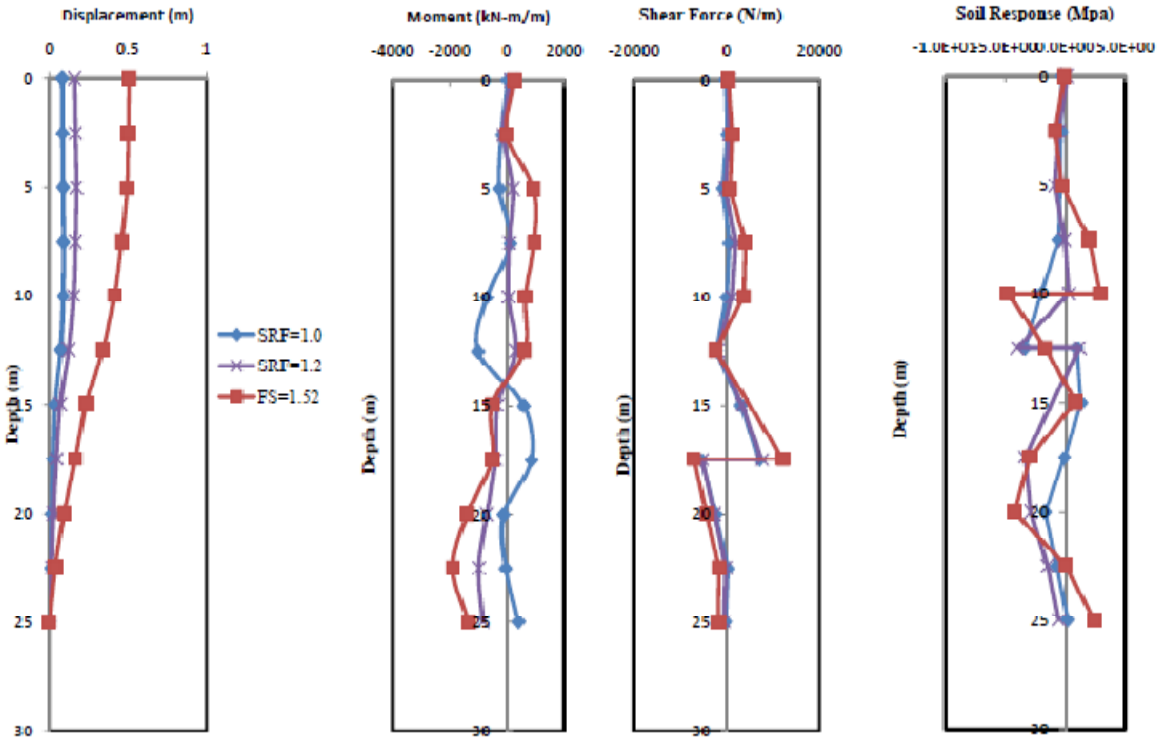


**Figure 7.62 Displacement, moment, shear, soil response for non-homogeneous slope with thin weak layer ($C_{u2}/C_{u1}$=0.2, L=25m)**

## 7.9 Summary and Conclusions

The results presented show that the pile installation may change the failure mechanism in this type of slope with weak thin layer. Based on the analyses on five cases with different strength ratios ($C_{u2}/C_{u1}$=0.2, 0.4, 0.6, 0.8 and 1.0), several conclusions on slope stability, pile position, pile length and pile head condition for stabilizing slopes using 2-D finite element method and the spacing effect of pile in 3-D finite element model can be made.

### 7.9.1 Conclusions

(1) As shown in Figure 7.6, the factor of safety varies due to different ratios of $C_{u2}/C_{u1}$. In the early portion of the curve, the factor of safety increase sharply until $C_{u2}/C_{u1}$=0.6, after $C_{u2}/C_{u1}$=0.6, the factor of safety increases smoothly with the increase of $C_{u2}/C_{u1}$.

(2) The optimal location of the stabilizing pile is in the middle portion of the slope regardless of the strength ratio and the pile head condition. The results of the factor of safety and the improvement ratio in terms of pile head conditions are summarized in Tables 7.8,7.9 7.10 and 7.11, respectively. The pile makes the greatest contribution to stability of a slope at the lower ratios.

(3) The appropriate length of pile in terms of $L_z/L$ can be concluded base on pile head condition. If the pile head condition is fixed, $L_z/L$=0.57 can result in the maximum value of the factor of safety except for $C_{u2}/C_{u1}$=0.2. When the strength ratio, $C_{u2}/C_{u1}$=0.2, the factor of safety resulted is constant regardless of the pile length.

(4) If the pile head condition is free, the ratio of $L_z/L$ between 0.6 and 0.7 is acceptable on the cases with the strength ratios, $C_{u2}/C_{u1}$=0.2, 0.4 and 0.6. However, when the

ratio, $C_{u2}/C_{u1}$=0.8 and 1.0, the $L_z/L$ should be selected either minimum or maximum on the scale built in Figure 7.33 to result in a higher value of the factor of safety.

(5) In the more critical case where $C_{u2}/C_{u1}$ = 0.2, there is little difference between the fixed and free head condition of the pile, indicating that either can be used to stabilized a slope containing a weak zone as long as the pile is placed in the center third of the slope. If $C_{u2}/C_{u1}$=0.4, 0.6, 0.8 and 1.0, the fixed pile head can more or less provide a higher stability on the slope in any other locations except at the crest.

(6) The fixed head pile always provides the higher stability than the free pile head does regardless of the pile length except for $C_{u2}/C_{u1}$=0.2. When $C_{u2}/C_{u1}$=0.2, the improvement ratios of the pile with either condition are very close if the ratio, $L_z/L$ greater than 0.63 as shown in Figures 7.23 and 7.24. Only when the length ratio is below 0.63, the fixed pile head condition exhibits the advantages.

(7) At $C_{u2}/C_{u1}$ ratio of 0.2, the presence of the pile at the toe or crest does not provide sufficient resistance to increase the factor of safety above one. Thus for slopes with weak layers, pile placement near the toe or crest will not improve the stability.

(8) Piles installation reduces the soil movement in the potential sliding mass at the same factor of safety if compared to the unreinforced slope.

(9) The three dimensional finite element model exhibits higher factors of safety than two-dimensional model does. In the three-dimensional model, more influencing factors such as pile spacing effect, arching effect, group pile effect, type of piles, stiffness of piles and soil anisotropy can be investigated further.

(10) The three-dimensional model simulation is more close to the reality, the results are more helpful to the practical design in stabilizing piles to avoid over-conservative design.

### 7.9.2 Recommendations

(1) In design, if the ratio, $C_{u2}/C_{u1}$=0.2, the pile has to be placed in the middle portion of the slope, the appropriate length of pile is at $L_z/L$=0.63 to 0.78. Either pile head condition is suitable for use.

(2) At $C_{u2}/C_{u1}$=0.4, 0.6, 0.8 and 1.0, pile also recommended to be placed in the middle portion with the fixed pile head, the acceptable length ratio of $L_z/L$ is 0.57 to 0.6.

(3) In the three dimensional finite element model, the further research based on the pile spacing effect, the effect of soil anisotropy, soil arching, effect of the pile stiffness can be done, respectively in the future research.

# CHAPTER 8: SUMMARY, CONCLUSIONS AND RECOMMENDATIONS

## 8.1 Overview

This chapter includes the overall summary, conclusions and the recommendations for the analytical method and design methodology drawn in this dissertation.

## 8.2 Analytical Method

The finite element method with strength reduction technique is used in this study. The pile incorporated in the finite element model using coupled analysis is used. This analysis method considers the slope stability and pile response simultaneously. The advantages of this method can be summarized in the following.

(1) For slope stability analysis, well known advantages are (1) no slip surface has to be preassumed in advance, (2) the stress is not the same along the entire failure surface, and (3) the stress and strain in the slope can be evaluated.

(2) Using limit equilibrium methods, the location and type of failure surface assumed for analysis will bias the results of the factor of safety. In some cases, the differences will be large and the failure surface assumed cannot represent the real failure mechanism.

In the case analyzed in Chapter 7, for the relatively low shear strength in the thin layer, if the failure surface is assumed as the base failure, the error in the analysis will be large.

(3) In the stability analysis of the piled slope system, coupled analysis can eliminate the error that could be made in the assumption of the potential slip surface. Also, due to the presence of the stabilizing pile, the slip surface may change and different failure mechanisms will be presented based on the location of the pile inserted, the length of the pile and the pile head conditions. Thus, the uncoupled analysis may not be able to estimate the real stress-strain relationship between the pile and the soil.

(4) In the slope stability using 3-D limit equilibrium methods, more complex computation needs to be conducted and the limitations including the assumption of failure surface, the normal and shear forces applied on the surfaces of each “column” have to be overcome. However, in the 3-D finite element model, the stress-strain relationship can be considered, and the slip surface can be determined as the location with the maximum plastic strain whatever any elastic-plastic soil model is employed.

(5) The analysis and the solution using 3-D finite element method are rigorous, and more influencing factors such as spacing of pile, arching effect and group effect can be investigated instead of using 2-D model. However, the boundary conditions in three-dimensional model have to be assumed reasonably, otherwise, the solution could be mispresented. In addition, it takes more time to complete a computation in 3-D finite element model than in 2-D finite element model. The results still show the 2-D finite element model still provides acceptable results in the analysis of piled-slope system.

### 8.3 Design Methodology for Slope Stabilization Using Piles

Due to the parametric study and the analytical work conducted in the problems of slope stabilization using the pile in the numerical method, a design methodology can be proposed herein based on the results of the finite element analysis.

(1) In the overall results, the middle portion of the slope is the optimal location to insert a stabilizing pile regardless of a homogeneous slope with or without an underlying foundation, non-homogeneous with an underlying foundation or a thin weak layer.

(2) The appropriate pile length base on the length ratio, $L_z/L$, has to be lower than 0.5, it means the pile length is twice of the depth of the slip surface determined in the unreinforced slope stability analysis regardless of the type of the slope analyzed in this study.

(3) For the pile head condition, even the pile with fixed head condition usually can make more contribution on the stability of the piled slope, however, the pile length factor has also be taken into consideration because the fixed head pile will only show more advantage when the length of pile reaches a certain value. Thus, based on economical design or workability design of a stabilizing pile, the fixed head pile is not always recommended.

(4) Based on the results of finite element analysis using 3-D model, to improve the stability of the pile-stabilized slope, the spacing ratio, S/D less than 4.0 is recommended to take the advantage of using group pile over the single pile. Because the group effect and arching effect which are regarded as beneficial in design of stabilizing pile usually require the S/D at around 3.0 to 5.0.

## 8.4 Recommendations

The author would like to propose the following recommendations as the additional studies to enhance the analytical work.

(1) In 2-D and 3-D finite element analysis, the likely influential factors in the stability of piled-slope such as soil constitutive model, pile type and material, soil-pile interface property can be verified.

(2) In 3-D finite element model, the arching effect occurs between piles can be investigated and the benefits can be quantified.

(3) Other factors such as anisotropy of soil, ground water table effect and overconsolidated ratio soil can also be verified in the finite element analysis.

# REFERENCES

Abramson, L.W., Lee, T.S., Sharma, S, and Boyce, G.M. (2002). “Slope stability and stabilization methods.” 2nd ed. John Wiley.

ABAQUS, ABAQUS Documentation Version 6.8: Abaqus /CAE User’s manual. Simlulia,Providence, RI., 2008.

Ang, E.C. (2005). “Numerical investigation of load transfer mechanism in slopes reinforced with piles.” PhD. Thesis, University of Missouri-Columbia.

Ausilio, E., Conte, E., and Dente, G. (2001). “Stability analysis of slopes reinforced with piles.” Computers and Geotechnics, Vol. 28, No. 8, 591-611.

Bishop, A.W. (1954). "The use of pore pressure coefficients in practice." Geotechnique, Vol. IV, No. 4, 148-152.

Broms, B. B. (1964a). “Lateral resistance of piles in cohesive soils.” Journal of Soil Mechanics and Foundations Division, ASCE, Vol. 90, No. 2, 27-63.

Broms, B. B. (1964b). “Lateral resistance of piles in cohesionless soils.” Journal of Soil Mechanics and Foundations Division, ASCE, Vol. 90, No.3, 123-156.

Byrne, P. M., Anderson, D. L., and Janzen, W. (1984). “Response of pile and casings to horizontal free-field soil displacements.” Canadian Geotechnical Journal, Vol. 21, 720-725.

Cai F, and Ugai K.(2000). “ Numerical analysis of the stability of a slope reinforced with piles.” Soils Found, Japan Geotech Society, Vol. 40(1), 73–84.

Cai, F., and Ugai, K., (2003). “Response of flexible piles under laterally linear movement of the sliding layer in landslides.” Canadian Geotechnical Journal, Vol. 40, 46-53.

Chen W.F., Saleeb, A.F. (1982). “Constitutive equations for engineering materials: plasticity and modeling.” Vol.1, John Wiley & Sons.

Chen, L.T. and Poulos, H.G. (1997). “Piles subjected to lateral soil movements.” Journal of Geotechnical and Geoenvironmental Engineering, ASCE, Vol. 123(9), 802-811.

Chen, C.Y. and Martin, G.R. (2002). “Soil-strauctureinteraction for landslide stabilizing piles.” Computers and Geotechnics, Vol. 29, 363-386.

Chow, Y. K. (1996). “Analysis of piles used for slope stabilization.” International Journal for Numerical and Analytical Methods in Geomechanics, Vol. 20, 635-646.

Clough, R.W. and Woodward, R.J. III (1967) "Analysis of embankment stresses and Deformations." Journal of the Soil Mechanics and Foundations Division, ASCE, Vol. 93, No. SM4, 529-550.

Cook, R.D., Malkus, D.S., Plesha, M. E. and Witt, R.J. (2001). “Concepts and applications of finite element analysis.” Wiely, 4th edition, 2001.

Duncan, J.M. and Dunlop, P. (1969). “Slopes in stiff –fissured clay and shales.” Journal of Soil Mechanics and Foundation Division, ASCE, Vol. 95, No.2, 467 – 492.

Duncan, J.M. (1996). “State of the art: limit equilibrium and finite-element analysis of slopes.” Journal of Geotechnical Engineering, Vol. 122, No. 7, 577-596.

Duncan, J.M. and Wright, S.G. (2005). Soil Strength and Slope Stability, Wiley, New Jersey.

Fukumoto, Y. (1972). “Study on the behavior of stabilizing piles for landslides.” Soils and Foundations, Vol. 12, 61-73.

Fukumoto, Y. (1976). “The behavior of piles for preventing landslide.” Soils and Foundations, Vol. 16, 91-103.

Fukumoto, Y., and Tyo, T. (2000). “Stress distribution, behavior and subgrade reaction of landslide prevention piles.” Journal of Japanese Landslide Society, Vol. 16, 25-34.

Fukuoka, M. (1977) “The effects of horizontal loads on piles due to landslide.” In Proceedings of the Specialty Session 10, the 9th International Conference on Soil Mechanics and Foundation Engineering, Tokyo, The Japanese Society of Soil Mechanics and Foundation Engineering, Tokyo, 27-42.

Goh A.T.C, Wong, K.S. (1997). “Analysis of piles subjected to embankment induced lateral soil movements. “ Journal of Geotech and Geoenvironmental Eng. ASCE, Vol. 123, 312-323.

Griffiths, D.V., and Lane, P.A. (1999). “Slope stability analysis by finite elements.” Géotechnique, Vol. 49, 387-403.

Hassiotis, S., Chameau, J.L, Gunaratne, M. (1997). “Design method for stabilization of slopes with piles.” Journal of Geotechnical and Geoenvironmental Engineering, Vol. 123 No.4, 314–23.

Hetenyi, M. (1946). Beam on Elastic Foundation, The University of Michigan Press, Ann Arbor, Michigan.

Hull, T.S., Lee, C.Y., and Poulos, H.G. (1992). “Behavior of fixed and free head piles in a laterally sliding soil.” New Zealand Geomechanics Society, Christchurch, New Zealand, 151-156.

Ito, T., and Matsui, T. (1975). “Methods to estimate lateral force acting on stabilizing piles.” Soils and Foundations, Vol. 15, No.4, 43-59.

Ito, T., Matsui, T., and Hong, W.P. (1981), “Design method for stabilizing piles against landslide – one row of piles.” Soils and Foundations, Vol. 21, No. 1, 21-37.

Janbu, N. (1973). “Slope stability computations in embankment-dam engineering.” Wiley, New York, pp 47–86.

Jeong, S., Kim, B., Won, J. and Lee, J. (2003). “Uncoupled analysis of stabilizing piles in weathered slopes.” Computers and Geotechnics, Vol.30, 671-82.

Lee, C. Y., Poulos, H. G., and Hull, T. S. (1991). “Effect of seafloor instability on offshore pile foundations.” Canadian Geotechnical Journal, Vol. 28, No.5, 729-737.

Lee, C.Y., Hull, T.S., and Poulos, H.G. (2006). “Simplified pile-slope stability analysis.” Computers and Geotechnics, Vol. 17, No. 1, 1-16.

Matsui, T., and San, K. C., 1992, “Finite element slope stability analysis by shear strength reduction technique.” Soils and Foundations, Vol. 32, No. 1, 59-70.

Morgenstern, N. R., and Price, V.E. (1965). "The analysis of the stability of general slip surfaces." Geotechnique, Great Britain, Vol. 15, No. 1, Mar., 79-93.

Nian, T.K., Chen, G.Q., Luan, M.T., and Zheng, D.F. (2008). “Limit analysis of the stability of slopes reinforced with piles against landslide in non-homogeneous and anisotropic soils.” Can. Geotech. J. Vol.45, 1092-1103.

Poulos, H. G. (1995). “Design of reinforcing piles to increase slope stability.” Canadian Geotechnical Journal, Vol 32, 808-818.

Poulos, H. G. (1973). “Analysis of piles in soil undergoing lateral movement.” Journal of the Soil Mechanics and Foundations Division, SM5, 391-406.

Reese, L.C., and Van Impe, W.F. (2001). Single Piles and Pile Groups Under Lateral Loading, A.A. Balkema, Rotterdam, Netherlands.

Reese, L. C., Wang, S. T., Isenhower, W., M., and Arrellaga, J. A. (2004). LPILE Plus 5.0 for Windows, Technical and User Manuals, ENSOFT, Inc., Austin, Texas.

Pan, J.L., Goh, A.T.C., Wong, K.S., and The, C.I. (2002). "Ultimate soil pressures for piles subjected to lateral soil movements." Journal of Geotechnical and Geoenvironmental Engineering, Vol. 128, No. 6, 530-535.

Pan, J.L., Goh, A.T.C., Wong, K.S., and Selby, A.R. (2002). "Three-dimensional analysis of single pile response to lateral soil movement." Int. J. Numer. Anal. Meth. Geomech., Vol 26, 747-758.

Potts, M.D., and Zdravkovic, L. (2001). " Finite element analysis in geotechnical engineering; analysis." Vol. 1, Thomas Telford.

Potts, M.D., and Zdravkovic, L. (2001). " Finite element analysis in geotechnical engineering; application." Vol. 2, Thomas Telford.

Shibata, T., Yashima, A. and Kimura, M. (1989). "Model tests and analysis of laterally loaded pile groups." Soils and Foundations, Vol. 29, No. 1, JSSMFE.

Snibhan, N., and Chen, W.F. (1976). "Elastic-plastic large deformation analysis of soil slopes." ComputStruc, Vol 9, 567-577.

Thompson, M.J. (2004), "Slope reinforcement using soil displacement grouted micropiles." Master thesis, Iowa State University.

Tien, H.J. (1990). “A literature study of the arching effect.” Master thesis, Massachusetts Institute of Technology.

Ugai, K. (1989). “A method of calculation of total factor of safety of slopes by elasto-plastic FEM.” Soils and Foundations, Vol. 29, No. 2, 190-195.

Viggiani, C. (1981). “Ultimate lateral load on piles used to stabilize landslides.” Proceedings, 10th International Conference on Soil Mechanics and Foundation Engineering, Stockholm, Vol. 3, 555-560.

Wei, W.B., and Cheng, Y.M. (2009). “Strength reduction analysis for slope reinforced with one row of piles.” Computers and Geotechnics, Vol. 36, 1176-1185.

Xu, K.J., and Poulos, H.G. (2001). “3-D elastic analysis of vertical piles subjected to passive loadings.” Computers and Geotechnics, Vol. 28, 349-375.

Zienkiewicz, O. C., Humpheson, C., and Lewis, R. W. (1975). “Associated and non-associated visco-plasticity and plasticity in soil mechanics,” Geotechnique, Vol. 25, No. 4, 671-689.

Zienkiewicz, O.C., and Taylor, R. L. (1989). “The finite element method.” Vol. I. McGraw-Hill, London, New York, 4th edition, 1989.

# ACKNOWLEDGEMENTS

I wish to express my deepest gratitude to my major advisor Dr. Vernon Schaefer, for his guidance, expertise and comments on the completion of my research and this dissertation. In addition to his professionalism and enthusiasm for geotechnical engineering research, Dr. Schaefer is also a mentor in these years and the rest of my life.

I would like to thank the committee members, Dr. Christopher Williams, Jeramy Ashlock, Dr. David White and Dr. Thomas Rudolphi for their comments and contribution for the research, as well as Mr. Don Davidson's assistance in the lab.

I am also grateful to all my friends, Mr. Sheng Tang, Mr. Weixi Zeng, and Mr. Caleb Douglas at Iowa State University, as well as my previous classmate Mr. Longjie Hong, for their unselfish assistance.

Additionally, I would like to express my greatest appreciation to this grand country, the USA for providing me the opportunity and resources to be educated here.

Finally, I am grateful to my grandparents and parents in Taiwan for their love, encouragement, and support to complete my studies in the USA.